Max-Planck-Institut für molekulare
Pflanzenphysiologie

Arbeitsgruppe Stitt

Metabolic interactions in leaf development in *Arabidopsis thaliana*.

Dissertation

zur Erlangung des akademischen Grades “doctor rerum naturalium“

(Dr. rer.nat.)

in der Wissenschaftsdisziplin „Molekulare Pflanzenphysiologie“

eingereicht an der

Mathematisch-Naturwissenschaftlichen Fakultät

der Universität Potsdam

von

Alexander Ivakov

Potsdam, den 04.10.2011

Published online at the
Institutional Repository of the University of Potsdam:
URL http://opus.kobv.de/ubp/volltexte/2012/5973/
URN urn:nbn:de:kobv:517-opus-59730
http://nbn-resolving.de/urn:nbn:de:kobv:517-opus-59730

Eidesstattliche Erklärung

Die vorliegende Dissertationsschrift ist das Ergebnis meiner eigenen praktischen Arbeit. Sie wurde von Januar 2008 bis Juli 2011, am Max-Planck-Institut für molekulare Pflanzenphysiologie in Potsdam, in der Arbeitsgruppe von Prof. Dr. Mark Stitt durchgeführt. Ich erkläre, dass ich die vorliegende Arbeit selbstständig und ohne unerlaubte Hilfe angefertigt habe. Es wurden keine anderen als die angegebenen Quellen und Hilfsmittel benutzt. Die verwendeten Quellen sind als solche im Text kenntlich gemacht. Die Arbeit wurde zuvor noch an keiner anderen Stelle eingereicht.

Potsdam, den 03.09.2011

Alexander Ivakov

Table of Contents.

Summary.

Plant growth and survival depend on photosynthesis in the leaves. This involves the uptake of carbon dioxide from the atmosphere and the simultaneous capture of light energy to produce organic molecules, which enter metabolism and are converted to many other compounds which then serve as building blocks for biomass growth. Leaves are organs specialised for photosynthetic carbon dioxide fixation. The function of leaves involves many trade-offs which must be optimised in order to achieve effective use of resources and maximum photosynthesis. It is known that the morphology of leaves adjusts to the growth environment of plants and this is important for optimising their function for photosynthesis. However, it is unclear how this adjustment is regulated.

The general aim of the work presented in this thesis is to understand how leaf growth and morphology are regulated in the model species *Arabidopsis thaliana*. Special attention was dedicated to the possibility that there might be internal metabolic signals within the plant which affect the growth and development of leaves. In order to investigate this question, leaf growth and development must be considered beyond the level of the single organ and in the context of the whole plant because leaves do not grow autonomously but depend on resources and regulatory influences delivered by the rest of the plant.

Due to the complexity of this question, three complementary approaches were taken. In the first and most specific approach it was asked whether a proposed down-stream component of sucrose signalling, trehalose-6-phosphate (Tre-6-P), might influence leaf development and growth. To investigate this question, transgenic Arabidopsis lines with perturbed levels of Tre-6-P were generated using the constitutive 35S promoter to express bacterial enzymes involved in trehalose metabolism. The plants were grown under standard experimental conditions on soil and their metabolic function and leaf morphology analysed. Analogous plants were also created in the phosphoglucomutase mutant (*pgm*) background. The results confirmed the proposed role of Tre-6-P as a signal of sucrose status and a feedback regulator of starch biosynthesis and degradation. In addition, it was found that Tre-6-P may also be involved in regulating sucrose synthesis. The effects of perturbed Tre-6-P levels on plant and leaf growth were inconsistent with a function of Tre-6-P as a regulator of leaf development in response to sugar supply. High Tre-6-P consistently inhibited biomass growth. The results of morphological analysis of leaves in the plants suggest that Tre-6-P may regulate leaf size by controlling cell size through cell expansion. It is concluded that clear effects of Tre-6-P on leaf development are difficult to resolve using an ectopic over-expression approach.

These experiments also led to an unanticipated project concerning a possible role for Tre-6-P in stomatal function, which is another very important function in leaves. The levels of Tre-6-P were specifically perturbed in stomatal guard cells using the guard cell-specific MYB60 promoter. The results of this approach indicate that Tre-6-P may be involved in starch metabolism in guard cells, and may promote starch degradation there. This is the opposite of its function in leaf mesophyll cells. Analysis of stomatal function using gas exchange and dry matter carbon isotope fractionation revealed some impairment in stomatal opening. The results suggested that trehalose, and not Tre-6-P, may be responsible for altered stomatal function in these plants. Plants with altered Tre-6-P levels in guard cells did not show improved growth under controlled mild drought. It is concluded that altering Tre-6-P specifically in guard cells affects starch metabolism in these cells and has a small but discernable effect on stomatal function.

In a second and more general approach it was investigated whether changes in sugar levels in plants affect the morphogenesis of leaves in response to light. For this, a series of metabolic mutants impaired in central metabolism were grown in one light environment and their leaf morphology was analysed. The results indicate that phenotypes resembling high-light-adapted leaves are present in some metabolic mutants with high sugar levels. This phenotype appears not to be caused by high sugar levels and was only observed in mutants which lack starch. A possible interaction of altered metabolism with a known plastid redox signal (plastoquinone) in these starchless mutants was investigated. Using chlorophyll fluorescence measurements, it was found that this also cannot explain the observed morphological phenotype, as no alteration in plastoquinone redox state was observed.

In a third and even more general approach the natural variation in leaf and rosette morphological traits was investigated in a panel of wild Arabidopsis accessions with the aim of understanding how leaf morphology affects leaf function and whole plant growth and how different traits relate to each other. The analysis included measurements of leaf morphological traits as well as the number of leaves in the plant to put leaf morphology in a whole plant context. The variance in plant growth could not be explained by variation in photosynthetic rates and only to a small degree by variation in rates of dark respiration. There were four key axes of variation in rosette and leaf morphology – leaf area growth, leaf thickness, cell expansion and leaf number. These four processes were integrated in the context of whole plant growth by models that employed a multiple linear regression approach. The relationships between the parameters were then explored further in order to partition the variance in leaf size, cell size, leaf thickness and plant size between their components and to identify further relationships between traits. The relationship of leaf number to whole plant growth and leaf size was further investigated by normalising leaf number on rosette fresh weight to estimate a parameter termed leafing intensity. Leafing intensity integrates leaf number, leaf size and whole rosette growth in a series of trade-off interactions, which seem to result in a growth benefit when plants make fewer but larger leaves per unit biomass. This led to a theoretical approach in which a simple allometric mathematical model was constructed, linking leaf number, leaf size and plant growth rate together in a whole plant context in Arabidopsis.

Zusammenfassung.

Das Wachstum und Überleben von Pflanzen basiert auf der Photosynthese in den Blättern. Diese beinhaltet die Aufnahme von Kohlenstoffdioxid aus der Atmosphäre und das simultane Einfangen von Lichtenergie zur Bildung organischer Moleküle. Diese werden nach dem Eintritt in den Metabolismus in viele andere Komponenten umgewandelt, welche die Grundlage für die Zunahme der Biomasse bilden. Blätter sind Organe, die auf die Fixierung von Kohlenstoffdioxid spezialisiert sind. Die Funktionen der Blätter beinhalten vor allem die Optimierung und Feinregulierung vieler Prozesse, um eine effektive Nutzung von Ressourcen und eine maximale Photosynthese zu gewährleisten. Es ist bekannt, dass sich die Morphologie der Blätter den Wachstumsbedingungen der Pflanze anpasst und eine wichtige Rolle bei der Optimierung der Photosynthese spielt. Trotzdem ist die Regulation dieser Art der Anpassung bisher nicht verstanden.

Die allgemeine Zielsetzung dieser vorliegenden Arbeit ist das Verständnis wie das Wachstum und die Morphologie der Blätter im Modellorganismus *Arabidopsis thaliana* reguliert werden. Besondere Aufmerksamkeit wurde hierbei der Möglichkeit geschenkt, dass es interne metabolische Signale in der Pflanze geben könnte, die das Wachstum und die Entwicklung von Blättern beeinflussen. Um diese Fragestellung zu untersuchen, muss das Wachstum und die Entwicklung von Blättern oberhalb des Levels des einzelnen Organs und im Kontext der gesamten Pflanze betrachtet werden, weil Blätter nicht eigenständig wachsen, sondern von Ressourcen und regulatorischen Einflüssen der ganzen Pflanze abhängig sind.

Aufgrund der Komplexität dieser Fragestellung wurden drei komplementäre Ansätze durchgeführt. Im ersten und spezifischsten Ansatz wurde untersucht ob eine flussabwärts liegende Komponente des Zucker-Signalwegs, Trehalose-6-Phosphat (Tre-6-P), das Blattwachstum und die Blattentwicklung beinflussen kann. Um diese Frage zu beantworten wurden transgene Arabidopsis-Linien mit einem gestörten Gehalt von Tre-6-P durch die Expression von bakteriellen Proteinen die in dem metabolismus von trehalose beteiligt sind. Die Pflanzen-Linien wurden unter Standard-Bendingungen in Erde angebaut und ihr Metabolismus und ihre Blattmorphologie untersucht. Des Weiteren wurden analoge Pflanzen im Hintergrund der Phosphoglucomutase-Mutante (*pgm*) generiert, der keine Fähigkeit besitzt Stärke zu aufbauen. Die Ergebnisse bestätigen die vermutete Rolle von Tre-6-P als Signal des Sucrose-Status und Feedback-Regulators der Stärkebiosynthese und -degradation. Weiterhin wurde gefunden, dass Tre-6-P auch in der Regulation der Sucrose-Synthese involviert ist. Die Effekte des gestörten Tre-6-P Gehalts auf Pflanzen- und Blattwachstum waren inkonsistent mit der aufgestellten Funktion von Tre-6-P als ein Regulator der Blattentwicklung als Antwort auf den Gehalt von Zucker. Die Ergebnisse der morphologischen Analyse von Blättern in den Pflanzen deuten darauf hin, dass Tre-6-P die Blattgröße regulieren könnte durch die Kontrolle der Zellgröße. Aus diesen Befunden wurde geschlossen, dass eindeutige Effekte von Tre-6-P auf die Blätterentwicklung mittels eines ektopischen Überexpressionsansatzes nicht einfach nachzuweisen sind.

Diese Experimente führten auch zu einem unerwarteten Projekt hinsichtlich einer möglichen Rolle von Tre-6-P in der Regulation der Stomata**.** Die Funktion der Stomata ist eine weitere wichtige Komponente der Funktion der Blätter. Durch einen Schließzellen-spezifischen MYB60-Promotor wurde der Gehalt von Tre-6-P spezifisch in Schließzellen der Stomata gestört. Die Ergebnisse dieses Ansatzes deuten darauf hin, dass Tre-6-P im Stärkemetabolismus der Schließzellen involviert sein könnte und dort die Degradation von Stärke fördert. Dies ist das Gegenteil der Funktion von Tre-6-P in Blatt-Mesophyllzellen. Die Analyse der Funktion von Stomata mittels Gasaustausch-Messungen und Kohlenstoff-Isotopenfraktionierung offenbarte Beeinträchtigungen in der Öffnung der Stomata

und deutet darauf hin, dass Trehalose, und nicht Tre-6-P, für die veränderte Funktion der Stomata in diesent Pflanzen verantwortlich sein könnte. Pflanzen mit verändertem Tre-6-P-Gehalt in den Schließzellen zeigten kein verbessertes Wachstum unter kontrollierten milden Trockenbedingungen. Aus diesen Befunden wurde geschlossen, dass ein veränderter Tre-6-P-Gehalt geringe Auswirkungen auf die Funktion der Stomata ausübt.

In einem zweiten, allgemeineren Ansatz wurde untersucht, ob Änderungen im Zucker-Gehalt der Pflanzen die Morphogenese der Blätter als Antwort auf Licht beeinflussen. Dazu wurden eine Reihe von Mutanten, die im Zentralmetabolismus beeinträchtigt sind, in derselben Lichtbedingung angezogen und bezüglich ihrer Blattmorphologie analysiert. Die Analyse ergab, dass die Phänotypen einiger Mutanten mit hohem Zuckergehalt denen von Starklicht adaptierten Blättern ähneln. Trotzdem basieren die Phänotypen scheinbar nicht auf dem Zucker-Gehalt und wurden nur in Stärkemangelnden Mutanten beobachtet. Eine mögliche Interaktion des veränderten Metabolismus mit einem bekannten plastidären Redox-Signal (pastoquinon) in diesen Stärkemangelnden Mutanten wurde mittels Chlorophyll-Fluoreszenz untersucht und konnte nicht den beobachteten morphologischen Phänotyp erklären.

In einem dritten noch allgemeineren Ansatz wurde die natürliche Variation von morphologischen Ausprägungen der Blätter und Rosette anhand von wilden Arabidopsis Ökotypen untersucht, um zu verstehen wie sich die Blattmorphologie auf die Blattfunktion und das gesamte Pflanzenwachstum auswirkt und wie unterschiedliche Eigenschaften miteinander verknüpft sind. Die Analyse beinhaltete sowohl Messungen von morphologischen Eigenschaften des Blattes als auch die Anzahl der Blätter einer Pflanze um die Blattmorphologie in den Kontext der gesamten Pflanze zu bringen. Die Variation im Pflanzenwachstum zwischen den Ökotypen konnte nicht durch Variationen in der Photosyntheserate erklärt werden und nur zu einem kleinen Teil durch Variation in der Rate der Nachtrespiration. Es gab vier Hauptaxen für die Variation der Rosetten- und Blattmorphologie – Blattflächenwachstum, Blattdicke, Zellwachstum und Blattanzahl. Mithilfe von Modellen, die auf multiplen linearen Regressionsansätzen beruhen, wurden diese vier Prozesse in den Kontext des Gesamtwachstums der Pflanze integriert. Die Beziehungen zwischen diesen Parametern wurden weiterhin untersucht um Variationen in der Blattgröße, Zellgröße, Blattdicke und Pflanzengröße zwischen ihren Komponenten weiter zu unterteilen und weitere Beziehungen der morphologische Eigenschaften zu identifizieren.

Das Verhältnis der Blattanzahl zum Gesamtwachstum der Pflanze und Blattgröße wurde gesondert weiter untersucht mittels Normalisierung der Blattanzahl auf das Frischgewicht der Rosette, um den Parameter „leafing Intensity“ abzuschätzen. Leafing Intensity integriert Blattanzahl, Blattgröße und gesamtes Rosettenwachstum in einer Reihe von Kompromiss-Interaktionen, die in einem Wachstumsvorteil resultieren, wenn Pflanzen weniger, aber größere Blätter pro Einheit Biomasse ausbilden. Dies führte zu einem theoretischen Ansatz in dem ein einfaches allometrisch mathematisches Modell konstruiert wurde, um Blattanzahl, Blattgröße und Pflanzenwachstum im Kontext der gesamten Pflanze Arabidopsis zu verknüpfen.

Acknowledgements.

I am deeply indebted -

To Prof. Mark Stitt for giving me an opportunity to work at the MPI-MP and for his never-waning enthusiasm for science and fascination with plants which has been a great inspiration for me. To Dr. John Lunn for his supervision and support during the three and a half years of my work here. To Ola Bąbała (Biedrzycka) and Ezgi Sarikaya, my student assistants who have helped me a lot with my scientific work. To past and present members of AG Stitt for providing a nice working environment and their help and assistance in times of need. To Ursula Krause and the AG Stitt technicians for their valuable technical assistance in the lab. To Dr. Vanessa Wahl for teaching me cloning techniques. To Regina Feil for measuring metabolites. To Dr. Ronan Sulpice for valuable discussions and assistance. To Eugenia Maximova for assistance with microscopy. To Dr. Francesco Licausi for inspiration and for his valuable friendship. To Hendrik Poorter for valuable discussions and inspiration to do good science. To the Greenteam for taking care of my plants.

To Anna Flis for her support, care and friendship. To my friends Francesco, Daan, Federico, Benjamin, Lilian, Marek, Marta and Marion for their valuable friendship. To Hiro and Mark for being great flatmates. To Fara and all the people at Salsa Libre Potsdam for the great time we spent dancing. To my parents for bringing me up and letting me be here now. To my brother Roma for inspiration as a great musician.

List of abbreviations.

Abbreviation	Definition	Unit or range (where appropriate)
A_{area}	rate of net CO_2 assimilation on a leaf area basis	µmol CO_2 m^{-2} s^{-1}
A_{mass}	rate of net CO2 assimilation on a rosette fresh weight basis	µmol CO_2 g^{-1} FW d^{-1}
AGPase	ADP-glucose pyrophosphorylase	
ANOVA	analysis of variance	
Cell area	surface area of cells	μm^2
CellNo	number of cells per leaf	cells
CO_2	carbon dioxide	parts per million
df	degrees of freedom	
DW	dry weight	g or mg
EpiAb	density of epidermal pavement cells per area of leaf on the abaxial (lower) side	cells mm^{-2}
EpiAd	density of epidermal pavement cells per area of leaf on the adaxial (upper) side	cells mm^{-2}
F	variance ratio	
F6P	fructose-6-phosphate	nmol g^{-1} FW
FBP	fructose-1,6-bisphosphate	nmol g^{-1} FW
FW	fresh weight	g or mg
g	stomatal conductance	mmol m^{-2} s^{-1}
G6P	glucose-6-phosphate	nmol g^{-1} FW
HXK	hexokinase	
INV	invertase	
LA	leaf area	mm^2
Layers	number of cell layers in a leaf cross section	
LC/MS-MS	liquid chromatography coupled to tandem mass spectrometry	
LDMC	leaf dry matter content	g DW g^{-1} FW
LI	leafing intensity	leaves g^{-1} FW
LN	leaf number	leaves
LT	leaf thickness	µm
MD	density of mesophyll cells per area of leaf	cells mm^{-2}
$NADP^+$	nicotinamide adenine dinucleotide phosphate	
NADPH	reduced nicotinamide adenine dinucleotide phosphate	
NAR	net assimilation rate	
PCA	principal components analysis	
PCR	polymerase chain reaction	
PGI	glucose phosphate isomerase	
PGM	phosphoglucomutase	
ppm	parts per million	
PQ	plastoquinone	
PSI	photosystem I	
PSII	photosystem II	
qL	photochemical quenching assuming a lake model of light-harvesting complex connectivity	0 to 1
qRT-PCR	quantitative reverse-transriptase polymerase chain reaction	
r	Pearson correlation coefficient	0 to 1
r^2	coefficient of determination	0 to 1
R_{area}	rate of dark respiration (CO_2 release) on a leaf area basis	µmol CO_2 m^{-2} s^{-1}
R_{mass}	rate of dark respiration (CO_2 release) on a rosette fresh weight basis	µmol CO_2 g^{-1} FW s^{-1}

RGR	relative growth rate	$g\ g^{-1}\ d^{-1}$
RLI	rate of leaf initiation	leaves day^{-1}
RT-PCR	reverse transcriptase polymerase chain reaction	
SLA	specific leaf area	$m^2\ kg^{-1}$ DW
SPP	sucrose phosphatase	
SPS	sucrose-6-phosphate synthase	
StAb	density of stomata per area of leaf on the abaxial (lower) side	stomata mm^{-2}
StAd	density of stomata per area of leaf on the adaxial (upper) side	stomata mm^{-2}
StIndAb	stomatal index on the abaxial (lower) side of the leaf	
StIndAd	stomatal index on the adaxial (upper) side of the leaf	
Suc-6-P	sucrose-6-phosphate	nmol g^{-1} FW
t	variance ratio	
TPP	trehalose-phosphatase	
TPS	trehalose-6-phosphate synthase	
Tre-6-P	trehalose-6-phosphate	nmol g^{-1} FW
$\delta^{13}C$	carbon isotope composition relative to Pee Dee Belemnite standard	per mil (‰)
φNPQ	quantum yield of regulated thermal energy dissipation at PSII	0 to 1
φPSII	quantum yield of electron tranport at PSII in the light	0 to 1

Chapter 1. General Introduction

1.1. Introduction.

Plant growth and survival depend on the photosynthetic assimilation of carbon dioxide from the atmosphere. Photosynthesis occurs primarily in the leaves and results in the production of carbohydrates. The carbohydrates can be used to provide energy through respiration in the leaves or can be exported as sucrose to other plant parts e.g. the roots, where they drive the uptake and assimilation of inorganic nutrients to produce other compounds such as amino acids and nucleotides. Carbohydrates and many other metabolites are then used as building blocks to allow growth and the formation of new leaves, roots and reproductive organs.

Growth depends on the supply and efficient use of these metabolic resources within the plant. The supply of these resources depends on the efficient absorption of CO_2 and light during photosynthesis in the leaves and the efficient uptake of nutrients in the roots. The effectiveness of these processes obviously depends, among other things, on the structure of the cells and organs which perform them – on their morphology. The efficient absorption of light requires extensive leaf area and absorption capacity for carbon dioxide while at the same time avoiding shading from other leaves and minimising the loss of water through transpiration.

Furthermore, different plants grow in different environments, and these environments are often changing. The morphology allowing the most efficient resource acquisition is different depending on the availability of these resources in the environment. Therefore plants have evolved to adjust their morphology in response to the environment in order to acquire resources efficiently and achieve more growth (Terashima et al., 2001; Oguchi et al., 2003).

1.2. Leaves.

Leaves are specialised lateral appendages produced by the vast majority of land plants. Strictly speaking, leaves of various shapes and sizes serve a diverse array of functions in different plants. However, the main function of the vast majority of plant leaves is photosynthesis. Leaves evolved by developmental modification of lateral branches in the simple body plan of early land plants (Beerling, 2005). The majority of photosynthetic leaves have a flat laminar structure, which allows efficient interception of light. The internal structure of leaves is specialised for maximal gas exchange, with a network of intercellular air spaces that are connected to the outside atmosphere through adjustable stomatal pores. This increases the internal cell surface area in contact with air and facilitates the absorption of CO_2 (Syvertsen et al., 1995). Another very important constraint on terrestrial leaves is the loss of water to transpiration (Yoo et al., 2009). This must be tightly controlled as water is often scarce and, given the high surface area of leaves, plants would rapidly desiccate if water loss were not controlled. Leaves thus have an impermeable cuticle barrier, which is punctuated by stomatal pores that open and close to regulate water loss.

Leaves must achieve efficient use of resources while performing their photosynthetic function. The optimisation of leaves for photosynthesis involves a fundamental trade-off between the modes of acquisition of the two resources involved – light and CO_2, while also minimising the loss of water through transpiration. The trade-off arises because the modes of acquisition of the two resources are largely incompatible, one requiring high leaf area to intercept more light, the other needing a high internal surface area for gas absorption, for which expensive thick leaves are required (Roderick et al., 1999). Leaf morphology serves to fine-tune the properties of leaves in order to optimise their

photosynthetic function for their environment.Morphogenesis is the process through which organs acquire their morphology during growth and development. Morphogenesis is a result of differential growth (Fleming, 2007). It may be assumed that the morphology displayed by a population growing in a particular environment is an evolved characteristic which maximises the functional utility of the leaf in the particular environment which has shaped its selection. The growth and efficient function of leaves is essential in order for plants to obtain the resources that they require to grow. In addition, most plants are not mobile and growth is also the process through which plants explore and make use of their environment. Growth thus has its own benefits and allows plants to acquire more resources and continue growing.

1.3. Plant Growth.

Growth has been extensively used as an indicator of plant performance. The growth of plants as photosynthetic organisms carries with it a return on investment akin to compound interest in finance. The production of more biomass creates the capacity for more photosynthetic carbon fixation, nutrient absorption etc and therefore more growth. The absolute growth rate thus increases with the size of the plant, resulting in exponential growth. The rate of plant growth is therefore normalised relative to existing biomass and expressed as relative growth rate (RGR; g biomass per g existing biomass per day, where the measure of biomass can be fresh weight (FW), dry weight (DW), or leaf area).

There is a large body of literature addressing the methodology of measuring relative growth rates (Evans, 1972; Hunt, 1982; Poorter and Garnier, 1996; Hoffmann and Poorter, 2002). The methods can broadly be divided into two approaches. In the classical approach RGR is calculated by dividing the difference in log-transformed biomass at two harvests by the time interval in which growth had occurred. This gives an average RGR across the time period. Other approaches attempt to resolve variations in RGR with time by fitting more complicated growth curves to biomass data from many harvests (e.g. sigmoidal functions or polynomial curves).

In order to understand the variation in growth rates between species, genotypes of a given species or between different conditions, relative growth rate (RGR) is often factorised into physiological, morphological and allocation components according to the following equation:

$$RGR = NAR * SLA * LMR$$

where NAR (net assimilation rate) is total biomass growth per unit leaf area, SLA (specific leaf area) is the leaf area displayed per unit leaf biomass and LMR (leaf mass ratio) is the proportion of plant biomass in leaves (Hunt, 1982). Several equivalent factorisations exist, one of them is: RGR=NAR*LAR, where LAR (leaf area ratio) is leaf area per plant biomass. Much research has been dedicated to the question, which component of these equations determines relative growth rate among and within species.

SLA is a morphological parameter which essentially expresses the amount of light that a unit of leaf biomass will intercept and therefore, potentially, the amount of photosynthesis and the return on biomass investment. SLA has been found to be the best predictor of RGR across many species, functional types, ecosystems and biomes (Poorter and Remkes, 1990; Reich et al., 1997; Reich et al., 1998; Wright and Westoby, 2000; Wright and Westoby, 2001; Rees et al., 2010). Its relative importance increases in low light environments (Poorter and Nagel, 2000; Shipley, 2006). SLA is also one of a set of inter-correlated traits forming the so-called ‘leaf economics spectrum’ and influences many leaf traits, including photosynthetic rates, leaf longevity and leaf nitrogen content (Wright et al., 2005; Wright et al., 2005).

LMR is an allocation parameter which reflects the plants investment strategy in leaves. The contribution of LMR to growth rates has usually been found to be low in cross-species studies. Reich et al. (1998) found almost no variation in LMR in seedlings of a set of tree species and little contribution to RGR, with similar results in a much broader range of species by Wright and Westoby (2001). Poorter and Nagel (2000) found LMR to be relatively constant in different light environments and to contribute little to RGR, with similar results by Shipley (2006). LMR does depend on the nutrient supply with plants growing in a limiting nutrient (e.g., N, P) supply typically having a lower LMR, and having a larger root system (Poorter and Nagel, 2000).

NAR has been interpreted as a physiological parameter related to photosynthesis on a leaf area basis. In contrast to SLA and LMR, NAR is not directly measured during growth analysis; instead, it is inferred from measurements of biomass growth and leaf area at different time points. NAR from growth analysis should not be confused with rates of net assimilation measured by gas exchange analysis. Nevertheless, NAR has often been interpreted as a "physiological" variable (Loveys et al., 2002) and assumed to be broadly comparable with net daily CO_2 exchange rates. Various factorisations of NAR are possible, revealing NAR to be a complex variable, related not only to photosynthesis and respiration but also to chemical composition parameters and resource use efficiencies (Poorter and van der Werf, 1998; Wright and Westoby, 2000). Variation in NAR can be seen, in a way, as the residual variation not directly explained by SLA and LMR and is therefore not always easy to interpret. Although SLA has usually been found to be the major factor determining RGR, studies have shown NAR to also be a good determinant of variation in RGR, its importance increasing in high irradiance environments, as well as under CO_2 enrichment (Li et al., 1998; Poorter and Nagel, 2000; Shipley, 2006).

1.4. Genetic analysis of leaf growth.

Much research has been conducted on the molecular mechanisms behind the growth and development of leaves. Leaves arise at the shoot apical meristem as microscopic leaf primordia. The initiation of leaf primordia at the shoot apical meristem involves pattern-forming processes, which include the spatial patterning of gene expression (Gordon et al., 2007) and localised accumulation of auxin (Heisler et al., 2005).

Leaf primordia are produced at the shoot apex in a highly ordered spatial pattern, which is called phyllotaxy. This is thought to be driven by the asymmetric localisation of auxin transport proteins and the subsequent development of localised auxin sinks at sites of primordium initiation (Reinhardt et al., 2003). This redistributes the auxin concentration and automatically leads to new primordia being formed at sites of auxin minima, which are most distal to existing primordia on the meristem (Fleming, 2005). This results in a very defined and very conserved spatial organisation of leaf primordia and, as a consequence leaves, in a given species (Adler et al., 1997). Phyllotaxy is a self-organised process which resembles physical processes where order and organisation arise out of a self-stabilising requirement for energy minimisation in dynamic systems (Douady and Couder, 1992). Phyllotaxy is evident in purely physical systems such as in growing crystals, where it arises out of an energetic requirement for efficient spatial packing of atoms (Hauck and Mika, 2003). It has been suggested that phyllotaxy is important in plants for similar reasons – it increases the efficiency with which plants can use available space by optimising the packing of organs on the cylindrically-symmetric primary axis (Ridley, 1982).

The subsequent outgrowth of the leaf primordium from the meristem depends on a tight coordination between the rates and orientations of cell division (Reddy et al., 2004) as well as cell expansion, with a strong involvement of cell-wall and cytoskeleton-related processes (Fleming et al., 1997; Hamant et

al., 2008). After initiation, the growth of leaf primordia follows a temporal progression of stages culminating in maturity. During the early stages the primordium expands through purely cell-division-driven growth, which is later followed by a progressive arrest in cell division and a transition to cell expansion (Beemster et al., 2005). This gradual arrest in cell division activity to give way to cell expansion occurs in the form of a front originating at the tip of the leaf and gradually moving towards the base (Donnelly et al., 1999). The subsequent expansion of cells is associated with endo-reduplication, an alternative cell cycle resulting in endo-polyploidy, the degree of which has been associated with final cell size (Inzé and De Veylder, 2006).

How these processes are related to one another and how they regulate leaf size is much investigated but still poorly understood. Recent genetic studies reveal that the regulation of leaf size is complex and involves many genes, the genetic factors are somewhat redundant and affect leaf size in different ways and at different developmental stages (Gonzalez et al., 2010; Johnson and Lenhard, 2011). The early processes of leaf development are largely correlated with one another and with the final cell number in the leaf, as well as with leaf size, indicating that leaf size is determined early through the control of cell division (Cookson et al., 2005). Consequently, genetic alterations in the temporal and spatial pattern of cell-division arrest in growing leaves often lead to changes in leaf size and leaf shape, for example in the *jaw* mutant, where proliferation arrest is delayed and this results in substantially larger leaves (Palatnik et al., 2003; Efroni et al., 2008). AINTEGUMENTA, an E2F/AP2 transcription factor, has been shown to be involved in maintaining cells in a proliferative state and also regulates leaf size (Mizukami and Fischer, 2000). Genetic manipulation of cell cycle genes to alter cell division rates often, but not always, results in compensation for altered cell number by reciprocal changes in final cell size, which can keep leaf size unaltered within some limits, although this compensation is not always total, and changes in leaf size also often result (Tsukaya, 2003; Horiguchi et al., 2006; Tsukaya and Beemster, 2006). It has been suggested that this phenomenon may be brought about by compensatory variation in the duration of leaf expansion at the later stages of leaf growth (Cookson et al., 2005).

An involvement of so-called cytoplasmic growth in leaf size control has been proposed based on observations of altered leaf size and developmental patterning in mutants of genes encoding cytosolic ribosomal proteins (Byrne, 2009; Szakonyi and Byrne, 2011). Ribosomes are, ultimately, essential for cell growth as they constitute the biosynthetic machinery which produces new proteins. Factors affecting leaf size have been shown to affect the expression and/or regulation of ribosomal proteins e.g. *TARGET OF RAPAMYCIN (TOR)* (Deprost et al., 2007; Ren et al., 2011) as well as the processing and abundance of ribosomal RNA, for example *nucleolin-1* (Kojima et al., 2007). Cytoplasmic growth must be coordinated to cell division and cell expansion. The TCP20 protein may be involved in co-ordinating ribosome biogenesis with cell cycle progression, thus linking ribosome biogenesis with cell division (Li et al., 2005) while TOR may coordinate ribosome abundance with cell wall synthesis (Leiber et al., 2010), thus linking it with cell expansion.

Phytohormones have a strong involvement in leaf growth control. Auxin, apart from its role in the spatial patterning processes of leaf initiation at the meristem (Heisler et al., 2005), also promotes leaf expansion through increased cell division and cell expansion, mediated by AUXIN RESPONSE FACTOR2 (Okushima et al., 2005; Horiguchi et al., 2006). This protein also integrates an input from brassinosteroids (Vert et al., 2008), another hormone which promotes leaf growth. Brassinosteroids have been shown to control both cell division (Nakaya et al., 2002) and cell expansion in leaves (Azpiroz et al., 1998). Cytokinin is known to promote cell division through activation of *CyclinD* expression (Riou-Khamlichi et al., 1999; Devvitte et al., 2007) and cytokinin-deficient plants show decreased cell proliferation in leaf primordia and smaller leaves (Werner et al., 2003). Gibberellin is

also a growth-promoting hormone and regulates leaf size through DELLA proteins (Harberd et al., 2009).

1.5. Genetic analysis of leaf morphology.

1.5.1. Specific leaf area.

Leaf morphological traits have attracted much less attention in molecular studies and the genetic analysis of leaf morphology is much less comprehensive than that of leaf size. There have been various attempts to identify genetic bases for morphological traits such as specific leaf area (SLA) in crop species using quantitative genetic methods (Yin et al., 1999; Jiang et al., 2000) however few molecular mechanisms have been elucidated. SLA is a complex trait which responds to many environmental conditions (Poorter et al., 2009). In particular it plays an important part in the optimisation of leaves to the prevailing irradiance regime (Evans and Poorter, 2001). It may be hypothesised that SLA may be related to cell expansion, however it is not routinely analysed in molecular studies of leaf development and little is known about how it may vary in various leaf development mutants. SLA is altered in gibberellin-deficient mutants (Nagel and Lambers, 2002) supporting a role for cell expansion. SLA is also altered in plants with severe photosynthetic impairments (Stitt and Schulze, 1994), pointing to a possible metabolic input.

1.5.2. Leaf thickness.

Very little is currently known about the molecular mechanisms regulating leaf thickness. The difficulty inherent in measuring leaf thickness has precluded attempts to identify QTL's for this trait. Arabidopsis phytochrome B over-expressors and cytosolic invertase mutants in *Lotus japonicus* exhibit thicker leaves suggesting that light and metabolic signalling may be involved in its regulation (Thiele et al., 1999; Welham et al., 2009). Leaf thickness is a major component of developmental acclimation of leaves to the light environment and leaves developed in high light are thicker and have more cell layers within the leaf (Terashima et al., 2001; Oguchi et al., 2003). The regulatory basis for this acclimation is poorly understood. Its adjustment in response to light seems to involve a systemic signal from mature leaves (Yano and Terashima, 2001). It has been suggested that the delivery of sugars to developing leaves may be a metabolic signal involved in regulating leaf thickness indirectly in response to light (Coupe et al., 2006; Terashima et al., 2006). Increased leaf thickness has also been associated with genetic factors which increase water use efficiency (Masle et al., 2005; Karaba et al., 2007).

1.5.3. Stomata.

The formation of the stomata in the leaf upper and lower epidermis is a special case. The development of the stomatal lineage is well investigated and involves meristematic cells undergoing a progressive differentiation process of asymmetric cell divisions and cell-to-cell signalling to generate a one-cell spacing rule between stomata (Bergmann and Sack, 2007). As stomata are essential in regulating water use, there have been many efforts to identify genetic factors regulating stomatal numbers and various mutants have been identified which show improved water use efficiency, most of which have been determinants of stomatal numbers (Yoo et al., 2009)

1.5.4. Genetic and molecular regulation of leaf number.

While the pattern-forming processes determining the initiation of single leaf primordia at the shoot apical meristem are well understood, less is known about what regulates the speed with which the meristem initiates these leaf primordia. This will determine one potentially important axis of variation in plant growth – the rate of leaf production and the number of leaves.

The rate of cell division at the shoot apical meristem has been implicated as a gross determinant of the rate of leaf production (Cockcroft et al., 2000; Poethig, 2003). Other factors act on this to regulate this rate. Cytokinin has been shown to accelerate leaf production through effects on cell division activity (Riou-Khamlichi et al., 1999) while cytokinin-deficient plants produce fewer leaves (Werner et al., 2003). Evidence exists for regulation of leaf initiation rates by plant age through the interaction of miR156 with SPL genes (Wu and Poethig, 2006; Wang et al., 2008). Studies have shown changes in leaf initiation in response to environmental factors - irradiance (Cookson and Granier, 2006), daylength (Cookson et al., 2007; Clerget et al., 2008) and temperature (Granier et al., 2002) in *Arabidopsis*.

A regulatory input from nutrition and metabolism appears plausible as the meristem is essentially a heterotrophic sink while the subsequent growth of initiated leaf primordia requires considerable metabolic resources. Leaf initiation rates are decreased under low nitrogen nutrition (Steer and Hocking, 1983) and in the starchless *pgm* mutant (Caspar et al., 1985). A number of possible metabolic factors in the organogenesis of leaves at the shoot apical meristem have been identified (Fleming, 2006). The interaction of cytokinin with sucrose in controlling the cell cycle is a promising mechanism (Richard et al., 2002). Incidentally, the rate of leaf initiation is not only important for biomass formation during vegetative growth. It may also affect developmental processes. In *Arabidopsis* the time taken until flowering correlates strongly with the number of leaves at bolting and genetic bases affecting flowering time also affect the rates of leaf production (Koornneef et al., 1991; Pouteau et al., 2004; Méndez-Vigo et al., 2010). An example is phytochrome B, which is involved in photoperiod sensing (Koornneef et al., 1995).

It appears plausible that there may be an interdependency between the rate of leaf initiation and the subsequent growth of leaf primordia. On the one hand, the meristem is very small. The growth that is required in the process of initiating new primordia presumably requires only a very small proportion of the total resources that are invested in growth. On the other hand, subsequent growth of initiated leaf primordia requires considerable metabolic resources, i.e., each leaf primordium represents a *future* demand, which must be balanced with supply. It can be hypothesised that the control of the rate of leaf initiation at the meristem must play a part in this balance, however little is known about how this is achieved, especially on a whole plant level. Unlike roots, which develop in an indeterminate manner, leaves are formed and grow in a determinate fashion. This means that they must stop growing at some stage and new leaves must be produced in order for growth to continue. We know little about how resources are partitioned between growth of the meristem to initiate new leaves, and growth of the existing primordia and leaves.

1.6. Metabolic effects on plant growth.

While much research has been dedicated to the molecular and genetic mechanisms regulating leaf growth and morphogenesis, less attention has been given to carbon status as an input in the regulation of growth and development. As already mentioned, plants are autotrophic organisms and their rate of growth ultimately depends on carbohydrates, which are formed during photosynthesis in the light in leaves, and nutrients that are acquired by the roots. Environmental conditions in nature are highly variable and plants may find themselves with more or less available carbon (or nutrients) at different times if, for example, changes in the light environment or temperature affect the rate of photosynthesis. In many conditions, the supply of carbohydrate or nutrients will restrict growth (Gibon et al., 2009). Growth is subject to tight regulation in response to available carbon supply (Smith and Stitt, 2007). Plants respond to conditions of low carbon availability by decreasing growth in order to conserve resources and avoid starvation (Stitt et al., 2007; Gibon et al., 2009). In high carbon and high sugar situations growth rates increase (Walter et al., 2009; Yazdanbakhsh and Fisahn, 2009, 2011).

Further, the life history of plants as autotrophic organisms is punctuated on a daily basis by interruptions in carbon supply during the night. In order to maintain growth and metabolic function during the night, plants must ensure that they store enough carbon reserves during the day. For this they synthesise starch during the day and break it down at night (Smith and Stitt, 2007; Zeeman et al., 2007). During the day photosynthate in leaves must be partitioned between sucrose export for growth and starch synthesis for storage, ensuring that enough starch is produced in order to avoid resource exhaustion during the night (Stitt, 1990; Stitt et al., 2007). The use of stored reserves for growth and metabolism at night must also be precisely regulated and timed in order to ensure that the reserves are not exhausted prematurely (Smith and Stitt, 2007; Stitt et al., 2007). On the other hand, stored reserves must also be used efficiently to generate growth, as maintaining un-used pools of reserves is an inefficient use of resources (Cross et al., 2006; Sulpice et al., 2009). Plants which are impaired in the ability to synthesise starch during the day exhaust their carbon at night and this leads to starvation and decreased growth (Caspar et al., 1985; Gibon et al., 2004; Wiese et al., 2007). Plants which are unable to mobilise their starch reserves are also strongly inhibited in growth (Zeeman and Rees, 1999; Rasse and Tocquin, 2006). The degradation of starch and its use for growth must be precisely timed so as not to run out of reserves prematurely and the rate of starch degradation is tightly adjusted depending on the length of the night (Gibon et al., 2004; Zeeman et al., 2007). Starch degradation exhibits anticipatory behaviour and is immediately adjusted when plants are placed in a premature night or if the day is extended (Gibon et al., 2004; Lu et al., 2005). This precise timing of starch degradation is linked to the circadian clock (Graf et al., 2010). The circadian clock has also been implicated in the regulation of plant growth as growth rates exhibit diurnal rhythms (Walter et al., 2009). The diurnal rhythms of plant growth can be modified by metabolic status (Wiese et al., 2007; Yazdanbakhsh and Fisahn, 2011), suggesting that metabolism also has regulatory inputs into the regulation of growth along with the clock.

In order to coordinate the use of available sugar and other metabolites with growth and development plants must be able to sense the metabolic resources at their disposal (Smeekens et al., 2010). We have only a poor understanding of the molecular mechanisms that plants use to sense sucrose or other sugars. Addition of sucrose to starved seedlings elicits changes in the expression of 1700 genes within three hours (Osuna et al., 2007) There is mounting evidence that TOR may regulate metabolism and cellular growth in response to the resource status of the plant (see above). Work by Smeekens and colleagues has implicated translation regulation of ATB2, a bZIP transcription factor, as one element of the sucrose-signalling pathway (Rook et al., 1998; Wiese et al., 2004). Hexokinase has been

implicated as a sensor of glucose levels in plants and in Arabidopsis *hxk1* and *gin2* hexokinase mutants are inhibited in growth (Moore et al., 2003; Cho et al., 2006). Trehalose-6-phosphate (Tre-6-P) is a novel signalling metabolite which has a proposed function as a specific signal of sucrose status in plants (Yadav, 2009; Lunn et al., 2006)., Current evidence indicates strongly that Tre-6-P is synthesised by trehalose-phosphate-synthase 1 (TPS1) (Vandesteene et al., 2010). There are extended gene families of TPS-like proteins in plants that probably lack catalytic functions and have another unknown function, and trehalose phosphate phosphatases (Lunn, 2007). The basic evidence for the importance of Tre-6-P in the regulation of plant metabolism and growth comes from the finding that *tps1* mutants are embryo lethal (Eastmond et al., 2002; Gómez et al., 2010). Furthermore, over-expression of heterologous *TPS* and *TPP* in plants leads to a marked and opposing phenotype that affects starch levels, leaf size and morphology, flowering time and branching of the inflorescence stem (Schluepmann et al., 2003; Pellny et al., 2004; Raines and Paul, 2006; Paul, 2007). This makes it an attractive candidate for a link between metabolism and development, however its effects on development beyond the level of leaf size are still quite unclear, as only superficial descriptions of plants have been presented. Furthermore, Tre-6-P has been widely implicated as a regulator of whole plant growth, which may be due to its demonstrated effect of inhibiting SnRK1 (Zhang et al., 2009), an AMP-activated kinase which functions as a metabolic sensor and a central transcriptional regulator of multiple metabolic pathways and serves to conserve energy in carbon-limited conditions by decreasing growth (Ghillebert et al., 2011).

Tre-6-P is also known to induce tolerance to various stresses, including drought stress (Almeida et al., 2007). It is also a known feedback regulator of starch metabolism (Kolbe et al., 2005). Apart from being vitally important for plant growth in diurnal cycles, starch metabolism is also vital for stomatal function (Lasceve et al., 1997). This leads to the question whether Tre-6-P is also involved in the regulation of stomatal function. This regulation is crucial to the function of terrestrial plants, as photosynthesis is subject to a trade-off with the loss of water through transpiration. Up to 1000 molecules of water are lost to fix just one molecule of CO_2 in photosynthesis. An optimal function of stomata is thus a vitally important component of the overall function of leaves.

Aims of the thesis.

The general question investigated in this thesis is how leaf growth and morphology are regulated in Arabidopsis. There has been considerable research into how leaf size is regulated at the organ level by regulation of cell division and cell expansion. It is also well known that environmental treatments e.g. irradiance, exert a morphogenetic influence on leaf development. In this thesis, special attention was dedicated to the possibility that there might be internal metabolic or physiological signals that regulate leaf growth and development. In order to investigate this question, leaf growth and development must be considered beyond the level of the single organ and in the context of the whole plant, because leaves do not grow in an autonomous manner, but depend on resources and regulatory influences that are delivered by the rest of the plant, at least during their early growth and development when many morphogenetic decisions are made.

Due to the complexity of this question, three complementary approaches were taken. In the first and most specific approach it was asked whether a proposed down-stream component of sucrose signalling, namely Tre-6-P, might influence leaf development and growth. This would be the most direct way to establish a link between metabolic status and leaf development and growth, but is also the most risky, if the initial hypothesis is not true. These experiments also led to an unanticipated project concerning a possible role for this metabolite in stomatal function, which is another very important process in the function of leaves. In a second and more general approach, it was attempted to manipulate sugar levels at the whole plant level using environmental or genetic treatments and

asked whether this affected leaf morphology and growth. In the third and even more general approach, the variation of many traits associated with leaf development and growth was investigated in a panel of 20 wild Arabidopsis accessions. Multivariate approaches and mathematical modelling was then used to search for dependencies between different leaf traits, leaf growth and whole plant growth and understand how they are interrelated how variation in leaf morphology contributes to leaf function and plant growth.

The specific aims of this thesis are:

1) To gain a further understanding of the effects of Tre-6-P on the development of leaves by examining in more detail the leaf developmental phenotypes of plants with constitutively altered Tre-6-P levels, which have been described previously

2) To investigate whether modulation of Tre-6-P levels in guard cells has effects on stomatal starch metabolism and stomatal physiology

3) To investigate the hypothesis that endogenous sugar levels regulate the developmental program of the leaf during developmental light acclimation

4) To investigate leaf morphology and leaf function in a whole plant context and establish relationships between morphological traits, leaf functional indicators and whole plant growth

5) To gain a mathematical understanding of variation in leaf number as whole organism process influencing the growth and development of leaves and whole plant growth

Chapter 2. Materials and methods.

2.1. Plant material.

Arabidopsis thaliana (L.) Heynh accession Col-0 seeds were obtained from common institute Col-0 seed stock of Dr. Karin Köhl (MPI for Molecular Plant Physiology, Golm). Starchless *pgm* mutant was obtained from Dr. Yves Gibon. Starchless *adg1* mutant was obtained from Dr. John Lunn. *f2kp-1* and *f2kp-2* mutants were a gift from Dr. Tom Hamborg-Nielsen (Copenhagen University). The *cinv1cinv2* double mutant was obtained from Prof. Alison Smith (John Innes Centre). The list of mutants used in this thesis is presented in Table. 2.1.

Mutant	Type	Line	Construct
pgm	EMS		
adg1	EMS		
f2kp-1	T-DNA	SALK_028529	pR0K2
f2kp-2	T-DNA	SALK_016314	pR0K2
cinv1cinv2	T-DNA	SALK_095807, SAIL_518_D02	pR0K2, pDAP101

Table 2.1. List of mutants used in the thesis.

The list of wild Arabdopsis accessions used in this study is presented in Table 2.2.

Accession	Country	City	altitude	latitude	longitude
Ang0	Belgium	Angleur	1-100	50.37	5.35
Bla11	Spain	Blanes/Gerona	1-100	41.41	2.48
Bsch2	Germany	Buchschlag/FFM	1-100	50.01	8.40
Bu2	Germany	Burghaun/Rhon	260	50.42	9.43
C24	Unknown	Unknown			
Col0	USA	Columbia	unknown		
Cvi0	Cape Verde Islands	Cape Verdi Islands	1100-1200	16.00	-24.00
Da0	Germany	Darmstadt	100-200	49.52	8.38
Ei4	Germany	Eifel	400-500	50.15	6.45
Hi3	Germany	Holtensen	200-300	51.50	09.50
Kl0	Germany	Koeln?	1-100	50.55	6.57
Kn0	Lithuania	Kaunas	1-100	54.54	23.54
Ler1	Germany	Landsberg			
Lip0	Poland	Lipowiec/Chrzanow	400-500	50.09	19.24
Mh1	Poland	M?en (OstPr)	100-200	53.31	20.12
Old1	Germany	Oldenburg	1-100	53.1	8.10
Petergof	Russia	Petergof	100-200	59.53	29.53
RRS7	USA	North Liberty (Midwest - Indiana)	221	41.32	86.25
Van0	Canada	U. of British Columbia	1-100	49.16	-123.07
Wei1	Switzerland	Weiningen	400-500	47.25	8.25

Table 2.2. List of wild accessions of Arabidopsis used in this study.

2.2. Plant culture.

Seeds were germinated on soil in 10cm diameter (500cm^3) pots in controlled environment growth chambers (Percival Scientific Inc., Perry, IA). Seedlings were pricked after 14 days to individual 6cm diameter pots (140cm^3). Plants grown for whole-plant gas exchange analysis were grown in long RLC4 Cone-tainer pots which had a volume of 115cm^3 (Hummert International, Earth City, MO,USA). The plants were grown in controlled environment growth chambers with different daylengths (as stated in the text). The chambers were equipped with dimmable fluorescent lighting. The output of the lamps was adjusted for a photon irradiance of 160 μE m^{-2} s^{-1} at plant level, unless otherwise stated. Photosynthetically-active irradiance was determined using an LI-250A spectroradiometer (Li-Cor, Lincoln, NE). Plants were watered daily from above with tap water.

2.2.1 Irradiance treatments.

Irradiance regimes were imposed by 1) adjusting the light output of the fluorescent lamps (allowing two light levels per chamber) and 2) using four layers of white shade-cloth placed over the trays of plants, supported approx. 6cm above the plants by plastic supports (allowing two more light levels).

2.2.2. Drought treatments.

Pots with soil were prepared and weighed. The dry weight of soil in the pots was determined by drying a representative sample of pots in an oven at 70°C. Soil field capacity was determined by weighing saturated soil. Field capacity was 2.05 g water g^{-1} dry soil. Plants were pricked into the pots at field capacity. Drought-treatment pots were not watered and were allowed to dry to 30% of field capacity. This level was maintained by daily gravimetric watering on a balance until harvest. Control pots were watered every few days but were not at field capacity all the time.

2.2.3. Sampling.

The plants used for combined metabolite and morphological analysis were pricked 5 plants to one 10cm pot. Four plants were harvested for metabolite analysis at the age of 25-28 days. Rosettes were cut at ground level, placed in plastic scintillation vials and frozen in liquid nitrogen for metabolite analysis. End of day (ED) samples were collected in the last half-hour of the light period while in the light. End of night (EN) samples were collected in the last half-hour of the dark period in the presence of low-intensity green light. Plants were sampled and pooled in such a way that five rosettes coming from different, randomly-picked pots were collected in one vial. One plant was left in each pot and was allowed to grow until subsequent harvest for leaf morphology analysis, which was typically at the age of 35-39 days, and longer in some conditions where growth was very slow, e.g. very short days.

2.4. Gas exchange and chlorophyll fluorescence measurements

Rates of photosynthesis and dark respiration were measured using the LI-6400XT Photosynthesis System fitted with the 6400-40 Leaf Chamber Fluorometer (Li-Cor, Lincoln, NE).

Chlorophyll fluorescence was measured using the PAM-2100 Portable Chlorophyll Fluorometer (Walz GmbH, Effeltrich, Germany). For dark-adapted measurements specially-designed leaf-clips were applied at the end of the day and kept on the leaf until measurement the next day to maintain a dark-adapted state. φNPQ, the fraction of excitation energy absorbed by PSII antennae and dissipated

through regulated thermal dissipation was assessed as derived in (Hendrickson et al., 2004) using the formula:

$$\varphi NPQ = \frac{F_S}{F'_m} - \frac{F_s}{F_m}$$

where F_s – chlorophyll fluorescence yield under actinic illumination, F'_m - maximal fluorescence yield under actinic illumination, F_m – maximal fluorescence yield in a dark adapted leaf. Photochemical quenching assuming a lake model of light-harvesting antenna connectivity (equivalent to the fraction of open PSII centres and the redox state of Q_A) was assessed as derived in (Kramer et al., 2004) using the formula:

$$q_L = \frac{F'_m - F_s}{F'_m - F'_o} \cdot \frac{F'_o}{F_s}$$

where parameters are as described above and F'_o – minimal fluorescence yield in a light-adapted leaf during a brief dark period in the presence of far-red illumination. The quantum yield of linear electron transport at PSII was determined as derived in (Genty et al., 1989) using the formula:

$$\varphi PSII = \frac{F'_m - F_s}{F_m}$$

2.5. Morphological analysis

2.5.1. Clearing for determination of cell size and number

Sixth leaves were harvested 35-39 days after germination. Leaves were cut along the mid-vein and then into 2mm strips perpendicular to the mid-vein. Leaf strips obtained from the middle-portion of the leaf were placed in 2mL Eppendorf tubes containing a 12.5% solution of glacial acetic acid in ethanol and spun on a rotary shaker until the leaves were cleared of chlorophyll (approx. 1h). Strips were washed with 50% ethanol for 20 mins followed by water. The strips were re-suspended in 1M KOH solution and stored until observation. Leaf strips suspended in 1M KOH were placed under a cover-slip and observed under a light microscope with differential interference contrast optics fitted with a digital camera. Stomata were counted in 10 random locations on the leaf for both sides of the leaf in fields of view which were 0.168mm^2 in area. Images were taken in random portions of the leaf strip, staying in the middle portion of the leaf. Five images per sample were taken of epidermal layers and the palisade mesophyll layer. Five images per leaf sample were taken 168mm^2. Cells were later counted and measured in the images using ImageJ.

2.5.2. Fixation and embedding

Leaf strips were placed in 2mL Eppendorf tubes containing fixative solution (4% paraformaldehyde, 0.25% glutaraldehyde, 10 mM phosphate buffer, pH 7.4). Samples were vacuum infiltrated at 100mbar for 4-6 hours until the strips sank to the bottom of the tube. All handling and wash steps were performed using thin glass Pasteur pipettes to avoid damaging the strips. Samples were washed in 1X phosphate buffer 3 times for 15 minutes. Samples were de-hydrated in the ethanol series: 30%, 50%, 70%, 80%, 90% and 4-times 100% for 40 minutes at each step, using freshly-opened 100% ethanol for the final steps. Samples were infiltrated with a 50% Technovit 7100 resin:ethanol mixture for 4 hours and then in 100% Technovit 7100 (Heraeus-Kulzer GmbH, Wehrheim, Germany) for 24 hours.

Samples were polymerised to hardness in Technovit 7100 resin with 1g hardener I/100mL and 0.5mL hardener II/7 mL in conical plastic moulds. The resin blocks were cut to 3µm thickness on a microtome (Leica, Wetzlar, Germany) and collected on poly-lysine-coated glass slides (Sigma Aldrich). Once a set of sections was collected, a 100µm depth of sections was cut through and discarded before collecting a second set of sections. Slides were stained with 0.1% Toluidine Blue in Tris-Borate buffer and observed under a light microscope at 200X magnification. Images were taken for subsequent analysis.

2.5.3. Leaf thickness and the number of cell layers.

Images of leaf cross sections were rotated in ImageJ to display the cross section vertically. The screen was obscured by a piece of cardboard. Random perpendicular transects were drawn across the leaf by hand. There were twenty transects drawn on four different sections for each leaf sample. Leaf thickness was measured directly. The number of cell walls crossing each transect was counted. The number of cell layers was determined as half the number of cell walls.

2.5.4. Specific Leaf Area and Dry Matter Content.

After sampling leaf 6 for morphological analysis, between four and six mature leaves on the rosette were sampled, weighed and photographed. Leaves were placed in paper bags and dried in an oven at 70°C for three days and the dried leaves weighed. Leaf area was calculated in ImageJ from images calibrated with a ruler. Specific leaf area was calculated as the leaf area per unit dry weight in m^2 kg^{-1}. Dry matter content was calculated as dry weight per unit fresh weight as g DW g^{-1} FW.

2.5.5. Leaf number determination

Visibly emerged leaves were counted on multiple occasions during growth.

2.6. Metabolite analysis.

2.6.1. Sample preparation

Frozen rosettes were homogenised at very low temperature by vigorous shaking in plastic vials with steel balls using the Cryogenic Grinder System (Labman Automation, Stokesley, UK) or in a ball mill (Retsch, Haan, Germany).

2.6.2. Soluble sugars.

Frozen tissue powder was weighed and aliquoted (18-22mg) into 1.5mL srew-cap Eppedorf tubes. Samples were mixed with 250µL ice-cold 80% ethanol in water (v/v), shaken vigorously and incubated for 20 minutes at 80°C. Samples were centrifuged and the supernatant was transferred to a cold 96-deep-well plate. The pellets were extracted a second time by re-suspending and heating with 150µL 80% ethanol (v/v) and a third time with 250µL ice-cold 50% ethanol (v/v) and the supernatants added to the same 96-deep-well plate.

50µL aliquots of the extracts were used for soluble sugar determination. Soluble sugars (glucose, fructose and sucrose) were determined using a previously published method (Stitt et al., 1989) relying

on the quantitative enzymatic reduction of nicotinamide adenine dinucleotide phosphate ($NADP^+$) and spectrophotometric detection of NADPH by absroptance at 340nm. Extracts were added to 160µL of determination solution containing 100 mM Hepes/KOH pH 7.0, 3mM MgCl2, 1mM $NADP^+$, 2.5mM ATP and 0.5U glucose-6-phosphate dehydrogenase (G6PDH, Grade II, Roche GmbH) in 96-well plates. Absorption at 340nm was measured every 60 seconds in a robotised plate reader. 1 µL of the enzymes hexokinase (HXK, 1U, Roche GmbH), phosphoglucoisomerase (PGI, 0.2U, Roche GmbH) and invertase (INV, 10U, Roche GmbH) were added to each well successively after a stable absorptance was reached.

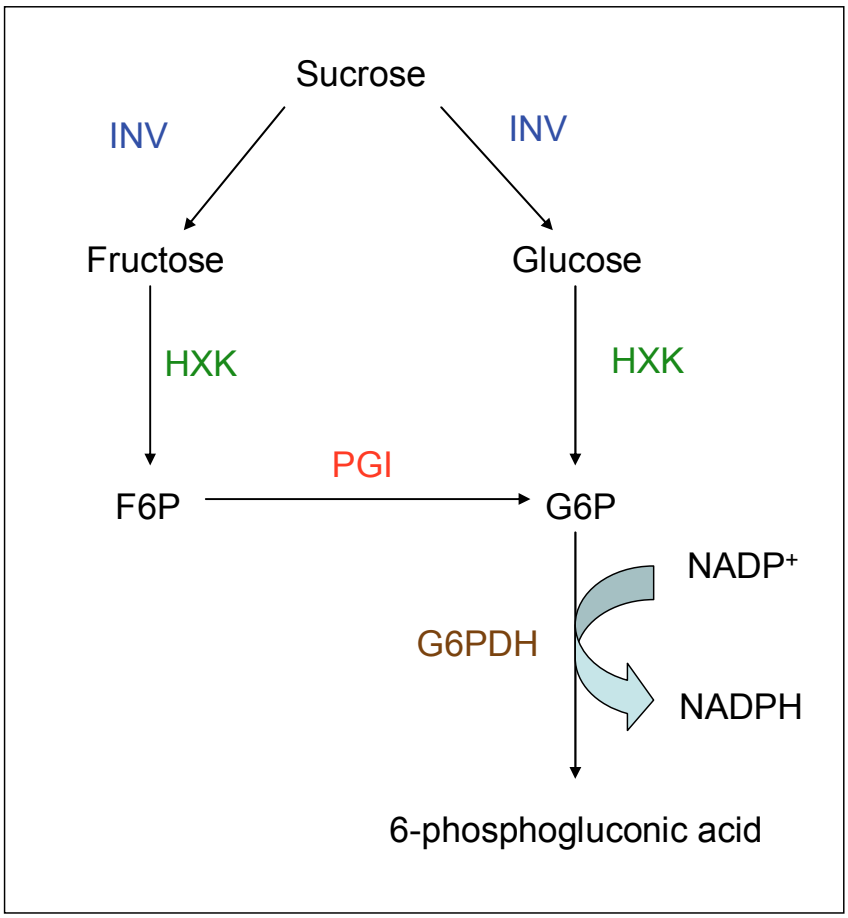

Fig 2.1 Determination of glucose, fructose and sucrose by enzymatic $NADP^+$ reduction. (F6P-fructose-6-phosphate, G6P – glucose-6-phosphate, G6PDH – glucose-6-phosphate dehydrogenase, HXK – hexokinase, PGI – phosphoglucose isomerase, INV – invertase, $NADP^+$ – oxidised nicotinamide adenine dinucleotide phosphate, NADPH – reduced nicotinamide adenine dinucleotide phosphate).

2.6.3. Starch.

The pellets from ethanolic extraction (above) were re-suspended in 400 µL 0.1M NaOH and heated at 95°C for 30 minutes. The samples were neutralised with 65µL neutralisation solution containing 0.5M HCl and 0.1M acetate buffered to pH 4.9 with NaOH. 40µL aliquots of the neutralised suspension were transferred to 96-well plates and mixed with 60µL starch degradation mix containing 50mM acetate/NaOH buffer pH 4.9 and α-amyloglucosidase (6U, Roche GmbH) and α-amylase (0.5U, Roche GmbH) and incubated at 37°C for 16 hours. Plates were centrifuged at 1200g for 5 minutes. Aliquots of 50µL were taken for glucose determination using hexokinase as described above.

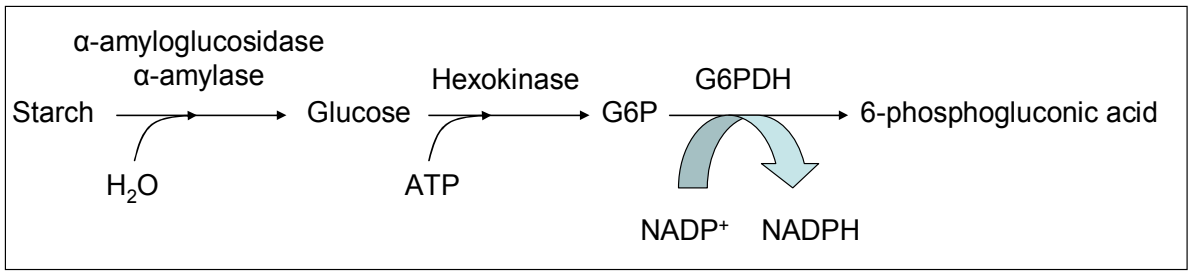

Fig 2.2 Enzymatic determination of starch.

2.6.4. Visualisation of guard cell starch.

Epidermal peels were prepared from the abaxial side of mature leaves by making a small incision in the adaxial side, attaching tape to the leaf and peeling off the epidermis. Epidermis was quenched in 80% ethanol (v/v) and heated briefly to 80°C. Epidermal pieces were washed with 50% ethanol (v/v) and then re-suspended in water. To visualise, the epidermal pieces were placed in Lugol iodine solution for 2 minutes and placed on a microscope slide under a cover slip (in Lugol solution). Strips were photographed at 100X magnification.

2.6.5. Trehalose-6-phosphate.

Aliquots of ground tissue powder (18-20mg) were transferred to pre-cooled 2mL Safe-lock microcentrifuge tubes. Frozen samples were quenched with 350µL ice-cold chloroform/methanol mixture (3:7, v/v) and incubated at -20°C for 2 hours. Samples were mixed with 300µL ice-cold de-ionised water and shaken vigorously. Samples were centrifuged at 14000 rpm for 5 min at 4°C. The upper aqueous phase was removed and retained at 4°C. The chloroform phase was re-extracted with 300µL ice-cold water and the aqueous phase added to the first. The aqueous extract was evaporated to dryness in a centrifugal vacuum lyophiliser. The dry pellets were re-suspended in 350µL de-ionised water. High-molecular weight compounds were removed from the extracts by centrifugation through Multiscreen Ultracel-10 (Millipore).

Tre-6-P was determined in the extracts as described in Lunn et al., (2006). Tre6P was determined in plant extracts as described in Lunn et al. (2006), using anion-exchange liquid chromatography (LC) coupled to triple quadruple mass spectrometry (MS-Q3). Samples (100 µl) of the extract, spiked with deuterated Tre6P as internal standard, were injected on to a 2×50 mm AG11-HC pre-column (Dionex, Sunnyvale, CA, USA), before separation of anionic compounds on a 2×250 mm Ion Pac AS11-HC column (Dionex) at 25°C, connected to a Dionex HPLC system. The column was equilibrated with a mixture of 95% solution A [5% (v/v) methanol] and 5% solution B [100 mM NaOH in 5% (v/v) methanol] for 15 min before each sample run. Solutions were gassed with helium. Anionic compounds were eluted with a multi-step gradient as follows: 0-5 min, 5% B; 5- 25 min, 5-29% B; 25-26 min, 29-100% B; 26-31 min, 100% B; 31-32 min, 5% B, at a flow rate of 0.2 ml·min-1. Peak detection in the eluate from the Dionex system was made with suppressed conductivity (ASRS-Ultra, 2 mm, 50 mA, external water mode), after which the eluate entered directly into a Finnigan TSQ Quantum triple quadrupole mass spectrometer (Thermo Finnigan, Waltham, MA, USA). The MS-Q3 was operated in multiple reactions monitoring mode, with an electrospray ionization source in negative ionization mode, and centroid data acquisition. Nitrogen was used as a sheath and auxiliary gas, and the second quadrupole (Q2) collision gas (argon) was set to 1.1 mTorr. The capillary voltage ranged from -1 to -56 V, the capillary temperature was 320 °C and the scan time was 0.2 ms. The Q1 and Q3 peak widths were 0.5 and 0.7 m/z, respectively. Tre-6-P was selected using a parent ion of 421.1 m/z in the first quadrupole, a collision energy of 46 eV, and a product ion of 79 m/z (metaphosphate PO_3^-) in the third quadrupole. Metabolites were quantified by comparison of the integrated MS-Q3 signal peak area with

a calibration curve obtained using authentic standards. The concentration of Tre6P in the standard stock solution was determined enzymatically using phosphotrehalase as described in Lunn et al. (2006). The internal standard, deuterated Tre-6-P, was used to correct for matrix and ion suppression effects in the LC-MS/MS analysis. Other metabolites, including - organic acids and hexose phosphates, were determined in parallel with Tre-6-P by LC-MS/MS, but in most cases their quantification has not yet been validated by corresponding internal standards, therefore the values obtained for these other metabolites must be regarded as estimates.

2.6.6. Dry matter carbon isotope analysis.

Plants were grown in a greenhouse away from artificial CO_2 sources and harvested after 35 days. Mature leaves were taken and dried in an oven at 70°C in paper bags. Samples were ground to a fine powder using mortar and pestle. Samples were sent to Cornell University Isotope Laboratory for measurements ^{12}C and ^{13}C abundance using isotope-ratio mass spectrometry (IR-MS).

2.7. Gene expression analysis.

2.7.1. RNA Extraction.

Total RNA was extracted from ground tissue powder using 1mL TriZol reagent (Invitrogen). RNA was precipitated with isopropanol and the pellet was washed with 70% ethanol. The pellet was resuspended in 50µL distilled water and re-precipitated with 3M sodium acetate and 100% ethanol. After re-suspension in 30µL distilled water, RNA concentration was determined spectrophotometrically by measuring absorbance at 260nm using NanoDrop ND-1000 spectrophotometer (NanoDrop Technologies). RNA was stored at -80°C in all cases 0.5µg RNA was separated on a 1% agarose non-denaturing gel to assess RNA integrity.

2.7.2. cDNA Synthesis.

RNA concentration was adjusted to 100 µg/mL by dilution. RNA was treated for 30mins using the Turbo DNA-free Kit (Ambion) to remove residual genomic DNA. First strand cDNA was synthesised from 0.5µg DNA'se treated total RNA with SuperScript III (Invitrogen) reverse transcriptase using a mixture of random hexamer and oligo-dT primers.

2.7.3. RT-PCR.

cDNA was diluted 1:12.5 with distilled water. 5µL of template cDNA was used in 20 µL PCR reactions containing 2.5mM Mg^{2+} and 0.1µL HotStar Taq polymerase (Qiagen). Gene-specific primer-pairs were designed using Primer3 software to achieve primer melting temperatures of 60±2°C and a length of 20-24bp. Primers were present at 500nM per reaction. Reactions were started with 15min at 95ºC to activate the hot-start Taq polymerase. Primer annealing was 58ºC for 10 seconds. PCR products were separated on 1.5% agarose gels in TAE buffer at 60V. Gels were imaged using GelRed fluorescence.

2.7.4. qRT-PCR.

Table. 2.3 lists al primer sequences used for gene expression analysis using RT-PCR and qRT-PCR.

Gene	Forward primer 5' - 3'	Reverse primer 5' - 3'
OtsA	CGGGATGAACCTGGTAGCAAA	CTCCCGCAAATTGCGAAAG
OtsB	TGCATTATCGTCAGGCTCC	TCTCGACAACACACTTTCCCT
ABF4	AACAACTTAGGAGGTGGTGGTC	CTTCAGGAGTTCATCCATGTTC
Rab18	CAGCAGCAGTATGACGAGTA	CAGTTCCAAAGCCTTCAGTC
ABI1	AGAGTGTGCCTTTGTATGGTTTTA	CATCCTCTCTCTACAATAGTTCGCT
ABI2	GATGGAAGATTCTGTCTCAACGATT	GTTTCTCCTTCACTATCTCCTCCG
ABI4	GGGCAGGAACAAGGAGGAAGTG	ACGGCGGTGGATGAGTTATTGAT
ABI5	CAATAAGAGAGGGATAGCGAACGAG	CGTCCATTGCTGTCTCCTCCA
OST1	ACGATAACACGATGAC	TCCTGTGAGGTAATGG
Actin	GGTAACATTGTGCTCAGTGGTGG	AACGACCTTAATCTTCATGCTGC

Table 2.3. List of primer sequences used for RT-PCR and qRT-PCR.

Real-time quantitative reverse-transcriptase PCR was performed on a ABIPRISM® 7900 HT Sequence Detection System (Applied Biosystems, USA), using SYBR® Green fluorescence to monitor double-stranded product synthesis. Each reaction contained 2.5µL 2x Power SYBR Green PCR Master Mix (Applied Biosystems), 5ng cDNA and 50 nM of each primer in a reaction volume of 5µL. Reactions were dispensed into optical 384-well plates using a Janus pipetting robot (Perkin-Elmer, Zaventem, Belgium). Fluorescence traces were analysed using SDS v2.2.1 software (Applied Biosystems). The cycle threshold (C_t) is the value at which the fluorescence signal in a reaction rises above the background. The background threshold was automatically determined in SDS software using log-slope optimisation (the minimum intensity where there was a linear increase in log-transformed fluorescence intensity in PCR reactions). C_t values were the cycle numbers where the fluorescence crossed the threshold. C_t data were analysed using the Relative Expression Software Tool-384 (Pfaffl et al., 2002). In this method gene expression ratios relative to control samples, normalised relative to the expression of a reference gene (Actin) are derived using the formula:

$$R = \frac{E_{gene}^{(Ct_{control} - Ct_{sample})}}{E_{Actin}^{(Ct_{control} - Ct_{sample})}}$$

where R is the expression ratio of the gene of interest between treatment and control samples, E is the primer efficiency, gene – gene of interest-specific primers. Actin-specific primers (Actin10) were used as a reference gene for normalisation. Primer efficiencies were not determined and were assumed to be 1.8 for all calculations. Standard errors were derived using Taylor series with statistical analysis using Pairwise Fixed Reallocation Randomisation Test, a non-parametric probability model relying on random re-sampling and re-allocation to derive p-values.

2.8. Isolation of transgenic plants.

2.8.1. Cloning of constructs.

The MYB60 promoter was obtained in a plasmid vector from Prof. Massimo Galbiati. The MYB60 promoter was excised from the plasmid at flanking HindIII and BamHI restriction endonuclease sites, generating a 1291 base-pair fragment. The promoter fragment was ligated into a modified pGreen Gateway™ destination vector obtained from Dr Vanessa Wahl. The transgenes *OtsA*, encoding E.coli

trehalose-6-phosphate synthase (*TPS*), *OtsB*, encoding E.coli trehalose phosphatase (*TPP*) and *nptII* encoding E. coli β-glucoronidase (Gus reporter) were recombined into AttR sites downstream of the MYB60 promoter in the pGreen vector using Gateway™ LR Clonase (Invitrogen) from pJLBlue entry vectors obtained from Dr. Vanessa Wahl. Positive recombinants were selected in Gateway-incompatible E. coli DH5α cells on spectinomycin medium. The presence of the trans-genes in the recombinant plasmids was confirmed by the observation of gene-specific restriction fragment patterns. The recombinant pGreen vectors were electroporated into competent *Agrobacterium tumefaciens* strain GV3101 in the presence of pSOUP helper plasmid. The cells were selected on YEB medium containing spectinomycin, gentamycin and rifampicin. Presence of recombinant plasmids in colonies was confirmed by PCR. In this approach one primer was designed within the gene of interest and a second primer within the promoter. A product could only be produced when the right promoter-gene fusion was present.

2.8.2. Plant transformation.

The recombinant *Agrobacterium* strains were inoculated from a pre-culture grown for 48 hours into 400mL YEB medium with spectinomycin (100mg/L), gentamycin (25mg/L) and rifampicin (50mg/L) and grown overnight. Cultures were centrifuged at 4000rpm in a Beckman centrifuge for 30 minutes. Cells were re-suspended in inflitration medium containing 5% sucrose (w/v), 0.22% MS Salts (Sigma Aldrich, w/v), 0.005% MES (w/v) and 10µL benzylaminopurine in DMSO per litre of medium. *Arabidopsis thaliana* wild type Col-0 was transformed by floral dip transformation.

2.8.3. Screening of transformants.

The seeds from transformed plants were germinated on soil and screened by spraying with BASTA solution five times every two days. Large numbers of PPT-resistant transformants were obtained and 20 were kept from each of the OtsA, OtsB and Gus constructs. Lines were screened by segregation of progeny for the selectable marker on Murashige and Skoog (MS) agar plates containing phosphinothricin (25mg/L). The plants were selected on the basis of Mendelian segregation of progeny with a 3:1 ratio of resistant:susceptible plants. Lines with a single segregating locus were retained to T_2 generation. The seeds of T_2 plants were screened for homozygosity (100% resistant progeny). Three MYB60:OtsA and two MYB60:OtsB lines were brought to homozygosity.

2.8.4. Histochemical Gus staining.

Tissues (leaves) were immersed in staining solution, which contained the following ingredients: 0.1 M Na_3PO_4 pH 7.0, 10 mM EDTA, 0.1% Triton X-100 (v/v), 1 mM $K_3Fe(CN)_6$, 2 mM 5-bromo-4-chloro-3-indolyl glucuronide (X-Gluc). Tissues were infiltrated under low vacuum (100 kPa) for 1 hour and transferred to an incubation room at 37°C. Staining was stopped and leaves were cleared of chlorophyll using successive washes in 50% ethanol (v/v).

2.9. Western Blotting.

Protein expression was detected in transgenic lines using immunoblotting. Protein was extracted from aliquots (20mg) of ground tissue powder by mixing with 400µL sample buffer (65mM Tris-HCl, 10% glycerol (v/v), 2% SDS, 0.01% bromophenol blue (w/v) and 5% β-mercaptoethanol (v/v)). Samples were heated at 95°C for 5 minutes, centrifuged at 14000rpm for 1 minute and kept on ice.

10% polyacrylamide gels were prepared as follows: 4.1 ml H_2O, 2.5ml 1.5 M Tris-HCl pH 8.8, 3.3 ml 30% Rotiphorese30 (Carl-Roth GmbH, Karlsruhe), 0.1ml 10% SDS in water (w/v), 50µl 10% ammonium persulphate in water (w/v, Sigma Aldrich), 5 µl N,N,N',N'-tetramethylethylenediamine (TEMED, Carl-Roth). Gels were cast to 1mm thickness between glass plates in a BioRad SDS-PAGE electrophoresis module (Bio-Rad, Hercules, CA, USA). A stacking gel (4% acrylamide) was prepared as follows: 6.1ml H_2O, 2.5 ml 0.5M Tris-HCl pH 6.8, 1.3 ml Rotiphorese30 (Carl-Roth), 0.1ml 10% SDS in water (w/v), 50µl 10 % ammonium persulphate in water (w/v), 10 µl TEMED. The stacking gel was cast on top of the gel and a well-comb inserted.

10µL was loaded onto the polyacrylamide gels and separated at 200V for 45 minutes. The gels were transferred onto PVDF membranes by electro-blotting at 100V for 1h in 25mM Tris 192mM glycine with 20% methanol (v/v). Membranes were blocked for 1h in blocking buffer (25mM Tris pH 7.5, 150mM NaCl, 0.2% Tween-20 (v/v, Sigma-Aldrich), 0.2% fat-free milk powder (w/v)). Membranes were incubated for 1h with primary antibody (against OtsA or OtsB) diluted 1:40000 in blocking buffer. Membranes were washed four times for 20 minutes with blocking buffer. Membranes were incubated with secondary antibody (goat anit-rabbit alkaline-phosphatase IgG, Promega) diluted 1:5000. Membranes were washed 5 times for 20 minutes with blocking buffer. Membranes were developed with alkaline-phosphatase buffer (100mM Tris-HCl, pH 9.8, 4mM $MgCl_2$) containing 130µM nitroblue tetrazolium (Sigma Aldrich) and 160µM bromochloroindolyl phosphate (Sigma Aldrich).

2.10. Statistical analysis.

2.10.1. Analysis of Variance.

Analysis of variance was performed in SigmaPlot for Windows version 11.0 (Systat Software Inc). Adjusted means (LS Means) were derived from the ANOVA output in Sigma Plot.

2.10.2. Multiple comparisons.

Differences between ANOVA groups were tested using the sequentially rejective Holm-Sidak procedure in Sigma Plot. This method controls for Type I error in multiple comparisons. Type I error is the conditional probability of finding a significant difference when none exists, and is therefore the probability of finding a false positive result by chance (0.05 in most tests with 5% significance threshold). Type I errors add up in multiple tests and increase the probability of false positive results. The test is based on the Holm-Bonferroni test (Holm, 1979). It begins by computing p-values using pairwise T-tests and then adjusts the significance threshold α sequentially according to the number of tests n using the formula α/n. It also adjusts the p-value according to the Sidak correction for p-values using the formula $1-(1-\text{unadjusted p-value})^n$ (Sidak, 1967). The test is thus more conservative than the Student's T-test and is less likely to find spurious differences.

2.10.3. Linear regression.

Ordinary least squares linear and multiple linear regression was performed using the lm() function in R version 2.13.0 (The R Foundation for Statistical Computing) and using the LINEST function in Excel 2003 (Microsoft Corporation).

2.10.4. Testing regressions.

Regression fits (r^2) were tested for statistical significance by computing the F variance-ratio between the mean square of the regression and the error mean square. The F statistic was tested on F distributions using the FDIST function in Excel 2003 with degrees of freedom n-df-1 and df, where df is the degrees of freedom of the regression and n is the number of samples. Regression coefficients were tested for significanct differences from 0 by computing the t variance-ratio between the coefficient estimate and the coefficient standard error. The t-statistic was tested for significance on a T-distribution using the TDIST function in Excel 2003 with the degrees of freedom of the regression.

2.10.5. Testing differences between slopes.

Differences between regression slope coefficients were tested by computing the difference between the coefficients, adding the standard errors of the coefficients using the formula $(SE_1^2+SE_2^2)^{0.5}$ and computing the t-statistic as the ratio of the difference in slopes to the summed standard error. The t-statistic was tested on a t-distribution using TDIST in Excel 2003 with degrees of freedom df_1+df_2 where df_1 is the degrees of freedom of regression 1 and df_2 the degrees of freedom of regression 2.

2.10.6. Robust regression.

Least squares regression is prone to being influenced by irregular data, e.g. by outliers. Robust regression was performed to control for this. Robust regression using fitting criteria based on M-estimation (Huber, 1964) was conducted using the rlm() function in the MASS package in R (Venables and Ripley, 2002).

2.10.7. Cross validation.

Regression models were tested for their performance on an independent dataset using 5-fold cross validation, performed using the cv.lm() function in the DAAG package in R (John Maindonald, Australian National University).

2.10.8. Re-sampling statistics.

Regression coefficients were validated by non-parametric bootstrap re-sampling (1000 times) using the boot() function in the boot package in R. 95% confidence intervals were derived using boot.ci().

2.10.9. Relative importance.

The variance in a dependent variable explained by predictor variables was assessed using five methods. Marginal effects were computed as correlation coefficients (r^2) of bivariate associations. The "Importance" metric was from (Rees et al., 2010). It is a variance decomposition method which partitions the variance in a variable into variance and covariance components of component variables according to the formula: var(a) = var(b) + var(c) + 2cov(bc) and taking the absolute values of all covariances The method was extended to five component variables by computing covariance matrices. The importance of a variable was the sum of its variance and its covariances with all other variables, divided by the sum of absolute values of all variances and covariances. η^2 (Eta-square) is the ANOVA effect size. It was computed from multiple linear regression fits by obtaining the sums of squares of

each regression coefficient and of the error variance using the anova() function on linear regression fits in R. η^2 was each predictor's explained percentage of the total sum of squares. The lmg statistic was computed using the calc.relimp() function in the relaimpo package in R (Grömping, 2006). It is an application of the hierarchical partitioning technique (Chevan and Sutherland, 1991). It computes the average η^2 for all possible permutations of sequential parameter ordering in multiple regression models. Log-log scaling slope analysis was performed on log-transformed data in Excel 2003. The slopes of regressions between a log-transformed variable and its log-transformed components are the variances explained by each component (Renton and Poorter, 2011).

2.10.10. Principal Components Analysis.

Datasets were standardised for principal components analysis by subtracting the grand mean of a trait from each sample and dividing it by the standard deviation. Principal component analysis was performed on the correlation matrix using the prcomp() function in R. Rescaled coefficients were obtained using loadings(). Principal component scores of each sample were obtained using scores(). Biplots were generated using biplot().

2.10.11. Exploratory factor analysis.

Principal components were rotated by Varimax rotation (Kaiser, 1958) using principal() in the psych package in R.

2.10.12. Similarity and hierarchical clustering.

Multivariate Euclidean distance matrices were calculated from standardised data using the dist() function in R. Hierarchical clustering was performed on Euclidean distance matrices using the Ward criterion with bootstrap re-sampling (1000 times) using the pvclust() function in the pvclust package in R.

Chapter 3. Transgenic modulation of trehalose-6-phosphate levels and its effect on leaf development and function

3.1. Introduction.

Trehalose is a neutral sugar which is involved in the remarkable ability of some species to survive severe desiccation and functions by stabilising membranes, preventing protein denaturation and as a compatible solute (Ingram and Bartels, 1996; Wingler, 2002). Trehalose is synthesised in two steps (Fig 3.1), first trehalose-6-phosphate (Tre-6-P) is synthesised from glucose-6-phosphate and UDP-glucose by the enzyme trehalose 6-phosphate synthase (TPS), which is then broken down to trehalose by trehalose phosphatase (TPP). Trehalose itself can be broken down to glucose by trehalase. The levels of trehalose normally found in higher plants are very low and often undetectable (Goddijn et al., 1997; Almeida et al., 2007; Miranda et al., 2007) and not consistent with a role as a compatible solute, although it may participate in osmotic adjustment as part of a combination of substances with compatible-solute properties (Kaplan et al., 2004).

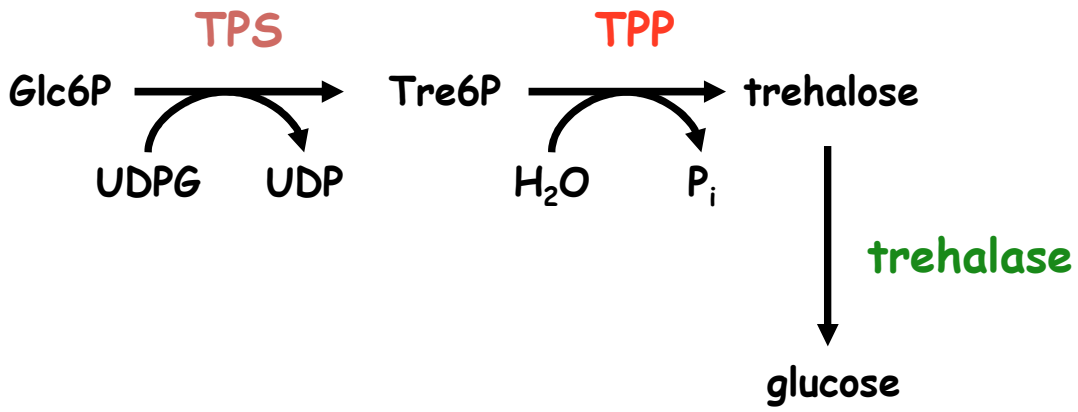

Fig 3.1 Trehalose biosynthesis pathway in plants.

Plants contain a multitude of genes encoding TPS and TPP enzymes (Lunn, 2007). Arabidopsis has been found to contain 11 *TPS* and *10* TPP genes. The 11 TPS genes have been sub-divided into two phylogenetic classes (Leyman et al., 2001), one of which may be specific to Brassicacea only (Lunn, 2007). Only one of the TPS proteins (TPS1) encoded by Arabidopsis has been shown to have catalytic activity (Blázquez et al., 1998; Vandesteene et al., 2010). The remaining TPS genes lack catalytic activity and show extensive expression regulation and tissue specificity (Ramon et al., 2009). Interestingly, plant TPS enzymes possess N-terminal domains with high sequence similarity to TPP which have no known catalytic activity (Vogel et al., 2001) and also exhibit high sequence relatedness to sucrose phosphatase (Lunn et al., 2000). The function of the non-catalytic TPS proteins as well as the TPP-like domains that they possess is unclear, however they have been proposed to have regulatory functions and may be involved in Tre-6-P binding (Lunn, 2007). At least some *Arabidopsis* TPP iso-forms have been shown to have catalytic activity (Vogel et al., 1998) and conservation of active site residues suggests that all the TPP enzymes may be active (Lunn, 2007).

Trehalose-6-phosphate is a metabolic regulator in yeast, where it regulates the entry of carbon into glycolysis by inhibiting hexokinase (Blazquez et al., 1993). Hexokinase is also involved in sugar sensing in plants (Moore et al., 2003). However, in contrast to yeast, plant hexokinases are not

inhibited by Tre-6-P (Gonzali et al., 2002), however there is evidence that Tre-6-P modulation in plants has effects on sugar utilisation and glycolytic activity analogous to those in yeast (Schluepmann et al., 2003). Much broader metabolic control by Tre-6-P has been suggested (Paul, 2007) due to its demonstrated role in regulating the Snf1-related protein kinase 1 (SNRK1), a central transcriptional regulator of multiple metabolic pathways (Zhang et al., 2009). It was subsequently shown that plants with high Tre-6-P show extensive coordinated up-regulation of anabolic pathways and downregulation of catabolic ones which is consistent with an effect of Tre-6-P on SNRK1 (Paul et al., 2010).

The tissue localisation pattern of the only active TPS enzyme in *Arabidopsis* (TPS1) suggests that the capacity to produce Tre-6-P may not be present throughout the plant (Bae et al., 2009; Vandesteene et al., 2010). The expression patterns of most TPS genes exhibit strong specificity to shoot and root apical regions, with localisation to the shoot apical meristem or developing leaf primordia as well as the meristematic zones of roots, suggesting functions in the regulation of meristem growth and morphogenesis (Ramon et al., 2009; Vandesteene et al., 2010). Similar patterns of expression have been found for *TPP* genes (Lopez, 2010).The expression patterns of many of the genes are consistent with a possible role in responses to abiotic stress (Iordachescu and Imai, 2008; Li et al., 2008) and trehalose accumulation is also triggered by stress (Fernandez et al., 2010), for example under drought stress in wheat (El-Bashiti et al., 2005). Many of the genes are strongly sugar-responsive, in fact the genes encoding *TPS7* and *TPS9* show some of the strongest expression responses to sugar of all *Arabidopsis* genes (Bläsing et al., 2005).

Tre-6-P has been shown to regulate starch synthesis during the day through effects on both the expression and the redox regulation of chloroplast AGPase (Kolbe et al., 2005; Lunn et al., 2006). In particular, it was shown to stimulate the redox-activation of AGPase in isolated chloroplasts and also correlates with AGPase activation in intact seedlings. It has thus been suggested that it may function in a negative feedback loop regulating the metabolism of starch according to downstream sucrose demand (Stitt et al., 2007). Further evidence suggests that it may also regulate starch degradation at night in accordance with sucrose demand downstream (Martins, 2011).

Levels of Tre-6-P correlate strongly and specifically with the sugar status of plants (Lunn et al., 2006) and there is further evidence that trehalose-6-phosphate is a specific signal of the availability of sucrose in the cell (Yadav, 2010). According to this hypothesis, plants with artificially-perturbed Tre-6-P levels may thus experience a false sugar signal, which is inappropriate to their actual sugar status. Plants with increased Tre-6-P levels show increased growth on high sugar media and this has been interpreted as an increased ability to utilise sugars, while plants with low Tre-6-P grew slower (Schluepmann et al., 2003; Paul et al., 2010). The situation is reversed when the plants are grown on soil – plants with high Tre-6-P grow very slowly while plants with low Tre-6-P grow faster (Schluepmann et al., 2003). The results suggest that Tre-6-P may coordinate carbon supply and plant growth.

As mentioned above, another proposed role of Tre-6-P is as a developmental regulator. Knockout of the *TPS1* gene in *Arabidopsis* results in embryo arrest at the torpedo stage (Eastmond et al., 2002; Gomez et al., 2005). The developmental arrest can be overcome by dexamethasone-inducible expression of *TPS1*, making it possible to obtain homozygous seeds. The resulting plants show stunted growth and vegetative development and fail to flower unless *TPS1* is induced (van Dijken et al., 2004). In maize, the *ramosa3* mutation has been shown to be in an active *TPP* gene and to be involved in the regulation of inflorescence branching (Satoh-Nagasawa et al., 2006). In *Arabidopsis* overexpression of TPS and TPP enzymes also has effects on flowering time and inflorescence architecture (Schluepmann et al., 2003).

There have also been implications for regulation of leaf development. Early attempts to perturb trehalose levels in plants for biotechnological purposes often yielded "undesirable" and "pleiotropic" developmental effects on plant and leaf development (Romero et al., 1997; Pilon-Smits et al., 1998; Cortina and Culiáñez-Macià, 2005). Plants with artificially-elevated Tre-6-P levels in various species produce small leaves with alterations in leaf shape while plants with low Tre-6-P have been shown to have larger leaves (Schluepmann et al., 2003; Pellny et al., 2004). A mutation affecting pavement cell shape in *Arabidopsis* leaves has been mapped to the TPS6 gene, which encodes a catalytically-inactive TPS (Chary et al., 2008). Over expressing TPS and TPP in tobacco also led to altered leaf photosynthetic rates, which led to suggestions that Tre-6-P may also regulate leaf function (Paul et al., 2001; Pellny et al., 2004). In spite of many reports of altered leaf morphology in plants with altered Tre-6-P levels (Romero et al., 1997; Schluepmann et al., 2003), the descriptions have been scant and often limited only to pictures. There is yet no information about the cellular and morphological changes underlying the developmental and growth phenotypes of plants with altered Tre-6-P levels and thus little understanding of what drives them.

Previous reports indicate that plants with increased Tre-6-P levels exhibit stunted growth on soil but grow faster than the wild type on sugar-containing media. Based on the hypothesis that Tre-6-P is a signal of sugar status, such plants are proposed to experience a continuous high-sugar signal, regardless of their actual sugar status. The observation of increased growth on high sugar suggests that the effects of the perturbed Tre-6-P signal may be alleviated in conditions which are more appropriate to the endogenous Tre-6-P signal they experience. On the other hand, the phenotype may become more severe when the actual sugar status is very different from the Tre-6-P signal the plants experience. Variation in the length of the day is a manipulation which affects the amount of carbon plants are able to fix during the diurnal cycle and thus directly affects the availability of carbon (Gibon et al., 2004). Varying the length of the day allows the above hypothesis to be tested.

As pointed out in the introductory chapter, sugar levels have also been implicated as developmental signals regulating the morphogenesis of leaves in response to the light environment. As Tre-6-P is a proposed sugar signalling metabolite and is implicated in the regulation of leaf development, it is an attractive candidate for this possible link between sugar and developmental light acclimation. Analysis of leaf morphology in plants with perturbed Tre-6-P levels should reveal whether Tre-6-P is involved.

3.1.1. Aims of the chapter.

In this chapter, it will be attempted to obtain a deeper understanding of these phenotypes by examining the leaf morphology in plants with constitutively altered Tre-6-P levels in more detail. The processes behind the growth, developmental and metabolic alterations in these lines will also be investigated by using a series of daylength conditions to induce variation in metabolic and developmental traits.

3.2. Results.

3.2.1. Isolation and characterisation of lines.

Arabidopsis thaliana wild type Col-0 and the starchless *pgm* mutant were transformed by floral dipping with *Agrobacterium tumefaciens* carrying a pGreen binary vector containing bacterial *OtsA* or *OtsB* genes downstream of the constitutive 35S promoter and a *bar* selectable marker conferring resistance to phosphinothricin (PPT). *OtsA* encodes a TPS enzyme cloned from E. coli and is expected to have high Tre-6-P levels. *OtsB* encodes a TPP enzyme cloned from E. coli and is expected to have lower Tre-6-P levels. T_0 seed was screened by germination on soil and spraying with a BASTA solution. Resistant T_1-transformants were screened by western blotting of OtsA and OtsB proteins in leaves. Lines found to express the foreign proteins were retained for seed production. The progeny (T_2) of the expressing lines was screened by segregation for PPT resistance on sterile MS-agar plates containing 2% sucrose and 25 mg/L phosphinothricin (PPT). Lines exhibiting Mendelian segregation consistent with the presence of one or two transgenic loci (3:1 and 15:1 of resistant:susceptible plants respectively) were retained for seed production. The progeny (70-120 seedlings) were screened for PPT resistance in a similar way. T_2 lines whose progeny were 100% PPT-resistant were judged to be homozygous for the transgenic locus. Lines with two-locus segregation were screened several times to confirm no susceptible progeny.

No 35S:OtsA lines in the wild type background could be established by direct transformation of wild-type Col-0 due to poor seed yields and viability of primary transformants. The problem was overcome by back-crossing a *pgm* 35S:OtsA line (line #4) to the wild type and isolating the homozygous expressor by screening for PPT resistance. The presence of starch was then confirmed by iodine staining (not shown), demonstrating the loss of the null *pgm* allele.

Fig. 3.1 shows the visual phenotype of the 35S over-expressing lines in the wild type and the starchless *pgm* backgrounds, grown in 16-hour days for 35 days. The 35S:OtsA line in the wild type background was isolated subsequently and is shown separately with a wild type plant (Fig. 3.1b), grown in the same conditions as the remaining lines. The phenotypes were essentially the same as those published previously by Schluepmann et al. (2003). 35S:OtsA plants were severely stunted and flowered early. 35S:TPP plants were larger than wild type and flowered late. Expression in the *pgm* background gave similar phenotypes as those seen in the wild type background.

a)

b)

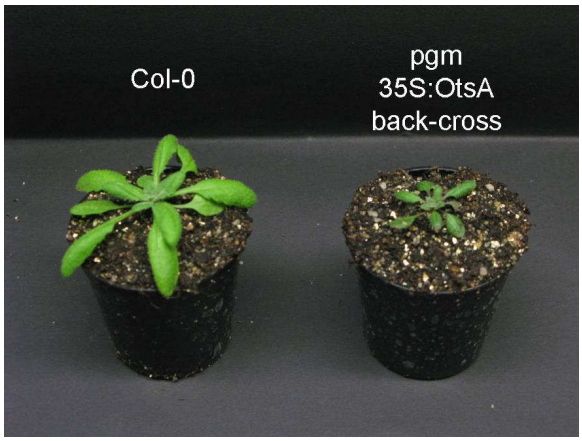

Fig 3.1. Effect of constitutive modulation of trehalose-6-phosphate levels on plant growth and development.
Phenotypes of plants over-expressing trehalose-metabolism genes under the 35S promoter grown in 16-hour days at a irradiance of 160 µE m^{-2} s^{-1} and a constant temperature of 20°C. In b) the phenotype of the *pgm* 35S:OtsA line back-crossed into wild type is shown in plants grown separately in identical conditions to the plants in a).

OtsA or OtsB protein expression in the 100%-resistant lines was re-confirmed by western blotting (Fig. 3.2)

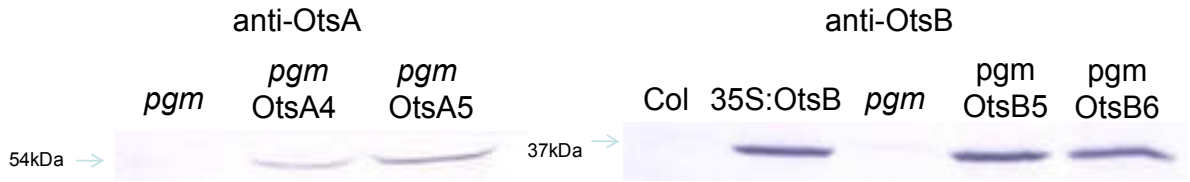

Fig. 3.2 Western blotting of bacterial OtsA and OtsB proteins in transgenic *Arabidopsis thaliana* wild type Col-0 and starchless *pgm* mutant expressing these proteins under the control of the constitutive 35S promoter.

Tre-6-P levels were measured in the lines using anion-exchange chromatography and mass-spectrometric detection. Fig. 3.3 shows the content of Tre-6-P in the lines grown in parallel in 16-hour days, sampled at the end of the day after 21 days of growth. Tre-6-P levels in the wild type were 0.294 nmol g^{-1} FW. The *pgm* mutant had double the Tre-6-P levels of the wild type, with 0.585 nmol g^{-1} FW, however this was not significantly higher than wild type (P=0.126, Holm-Sidak Test).

35S:OtsA plants in the *pgm* background had highly elevated levels of Tre-6-P. The level of Tre-6-P was somewhat dependent on the number of transgenic loci in the genome. Line #4 (one transgenic locus) had 78% higher Tre-6P levels than the *pgm* mutant (P=0.029) while line #5 (two transgenic loci) had almost 4-fold higher levels of Tre-6-P than the *pgm* mutant control (P<0.001).

35S:OtsB plants in the wild type background did not have significantly altered levels of Tre-6-P (P=0.834). In the *pgm* mutant background 35S:OtsB plants had slightly lower Tre-6-P levels than the *pgm* control, however the differences were not significant. Line #5 (single transgenics locus) had 28% lower levels (P=0.411) while in line #6 (single trangenic locus) it was reduced by 31% (P=0.329).

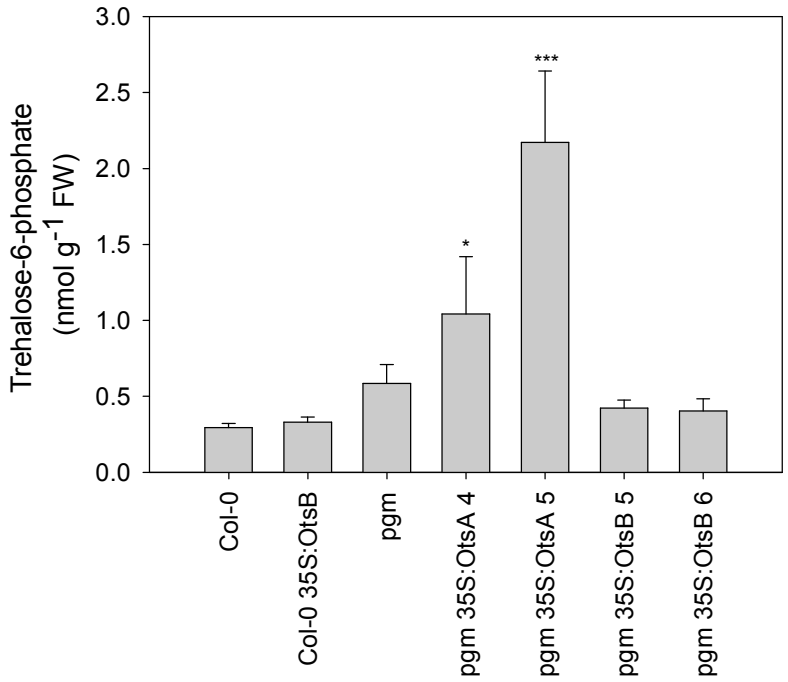

Fig. 3.3. Trehalose-6-phosphate levels in transgenic lines expressing OtsA and OtsB proteins driven by the constitutive 35S promoter in wild type Col-0 and starchless *pgm* background. Levels of trehalose-6-phosphate in rosettes of transgenic *Arabidopsis thaliana* wild type Col-0 and starchless *pgm* mutant expressing bacterial OtsA and OtsB proteins under the control of the constitutive 35S promoter, grown in 16-hour days at a irradiance of 160 µE m^{-2} s^{-1} and a constant temperature of 20°C and sampled at the end of the day. N=5. Bars are standard deviations. Significant differences (t-test with Holm-Sidak correction) from the relevant control are shown as * P < 0.05, ** P < 0.01, *** P < 0.001.

3.2.2. Leaf morphology.

In order to examine the growth phenotypes of the 35S over-expressing lines in more detail, an investigation of cellular and leaf morphological properties was undertaken in the 35S lines in the wild type and the starchless *pgm* background grown in 16-hour days. The 35S:OtsA line in the wild type background was not available at the time and was grown in a separate experiment at a later date and in identical conditions. It is presented separately, with its own wild type control, which was grown in parallel. Leaf 6 was chosen as a representative leaf and was sampled when the plants were 35 days old, at which stage leaf 6 was mature and assumed to be fully expanded. Data of both datasets were analysed using analysis of variance with multiple comparisons using the Holm-Sidak step-down method. Comparisons are presented relative to the relevant background.

The changes in rosette size were reflected in the size of individual leaves (Fig. 3.4). 35S:OtsA plants had much smaller leaves in both backgrounds. In the wild type background the 35S:OtsB plants had larger leaves in the wild type background (P=0.016) but when expressed in the *pgm* mutant background, the 35S:OtsB plants had smaller leaves than the *pgm* mutant (P=0.003).

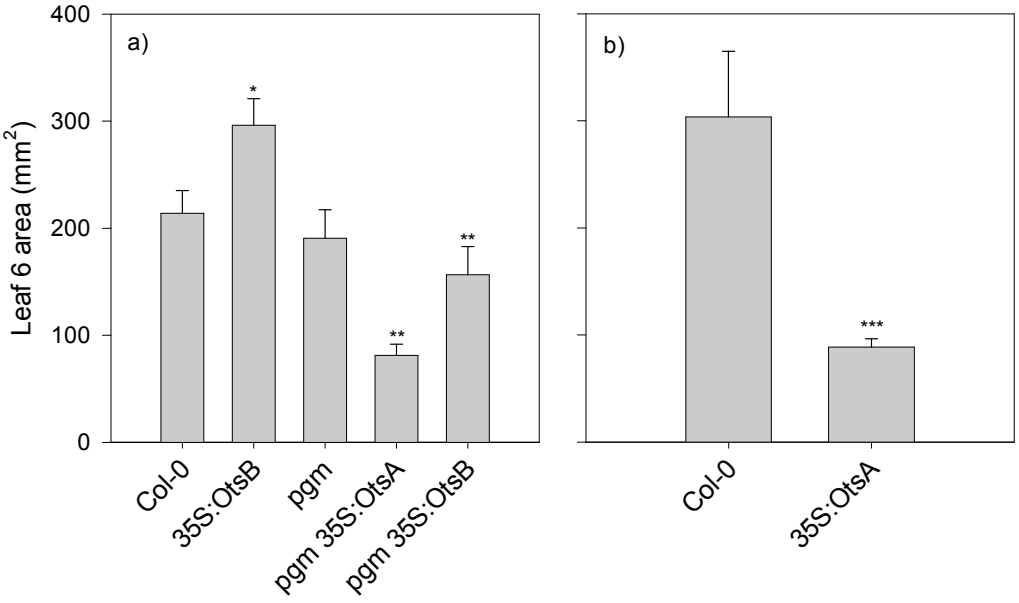

Fig 3.4 Effects of constitutive modulation of trehalose-6-phosphate levels on the area of leaf 6. Leaf 6 area in transgenic *Arabidopsis thaliana* wild type Col-0 and starchless *pgm* mutant expressing bacterial OtsA and OtsB proteins under the control of the constitutive 35S promoter, grown in 16-hour days at a irradiance of 160 μE m^{-2} s^{-1} and a constant temperature of 20°C and sampled after 35 days of growth. In b) the phenotype of the *pgm* 35S:OtsA line back-crossed into wild type is shown, in plants grown separately in identical conditions to the plants in a). Bars are standard deviations. Significant differences (t-test with Holm-Sidak correction) from the relevant control are shown as * P < 0.05, ** P < 0.01, *** P < 0.001. N=5 leaves.

A comprehensive morphological analysis was carried out to investigate cellular changes underlying the alterations in leaf size in the lines. The growth of a leaf is determined by the combined action of cell division and cell expansion. Thus the number and the sizes of cells in a mature, fully expanded leaf are indicators of the relative contribution of these two factors to leaf growth, integrated over the whole duration of leaf expansion.

The density of cells in the leaf (cells per leaf area, inversely proportional to cell size) exhibited coordinated changes in the over-expression lines depending on the gene being over expressed (Fig. 3.5). 35S:OtsB plants had significantly fewer cells per unit area, and therefore larger cells, compared to the wild type. The density of adaxial epidermal cells was reduced by 35% relative to wild type (P=0.002), with an almost identical reduction in the palisade mesophyll cells (P<0.001). 35S:OtsA plants in the wild type background had almost double the cell density of the wild type, and therefore much smaller cells. The differences were highly significant for both adaxial epidermis and palisade mesophyll (P<0.001). In the starchless *pgm* background the phenotypes were less severe. The 35S:OtsA (*pgm*) plants had 36% more epidermal cells per area relative to the *pgm* mutant (P=0.006), however mesophyll cells were not significantly different. The 35S:OtsB (*pgm*) plants did not differ significantly from the *pgm* mutant in cell densities.

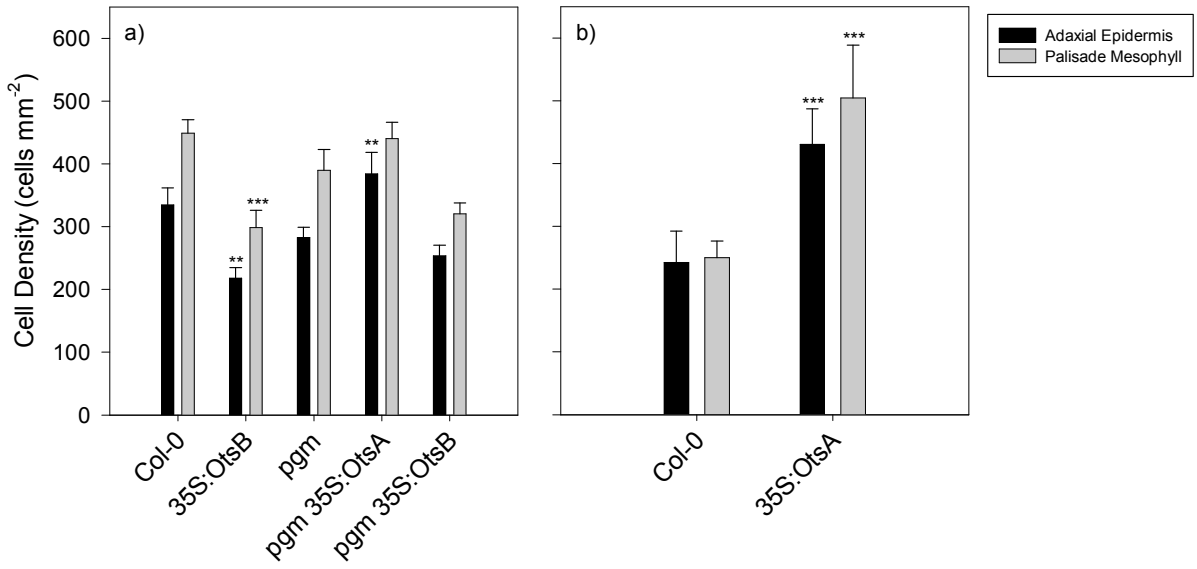

Fig. 3.5 Effects of constitutive modulation of trehalose-6-phosphate levels on leaf cell densities. Densities of cells (in cells per mm^2) of adaxial epidermis and palisade mesophyll cells in transgenic *Arabidopsis thaliana* wild type Col-0 and starchless *pgm* mutant expressing bacterial OtsA and OtsB proteins under the control of the constitutive 35S promoter, grown in 16-hour days at a irradiance of 160 µE m^{-2} s^{-1} and a constant temperature of 20°C and sampled after 35 days of growth. In b) the phenotype of the *pgm* 35S:OtsA line back-crossed into wild type is shown, in plants grown separately in identical conditions to the plants in a). Bars are standard deviations. Significant differences (t-test with Holm-Sidak correction) from the relevant control are shown as * P<0.05, ** P<0.01, *** P<0.001. N=5 leaves.

Knowing the number of cells per unit area, the total number of cells in the leaf can be calculated by multiplying by leaf area, assuming a constant density of cells throughout the leaf. Fig. 3.6 shows the number of palisade mesophyll cells in the sixth leaf of the over-expressing lines. While the 35S:OtsB plants had larger leaves than the Col-0 wild type, the number of cells per leaf was not significantly altered (P=0.564). 35S:OtsA plants had 40% fewer cells in the leaf than the Col-0 wild type (P=0.001). In the *pgm* background 35S:OtsA plants also had half the number of cells in leaf 6 than the *pgm* mutant (P=0.008). The *pgm* 35S:OtsB plants had fewer cells in the leaf than the *pgm* mutant, however this was not significant (P=0.112).

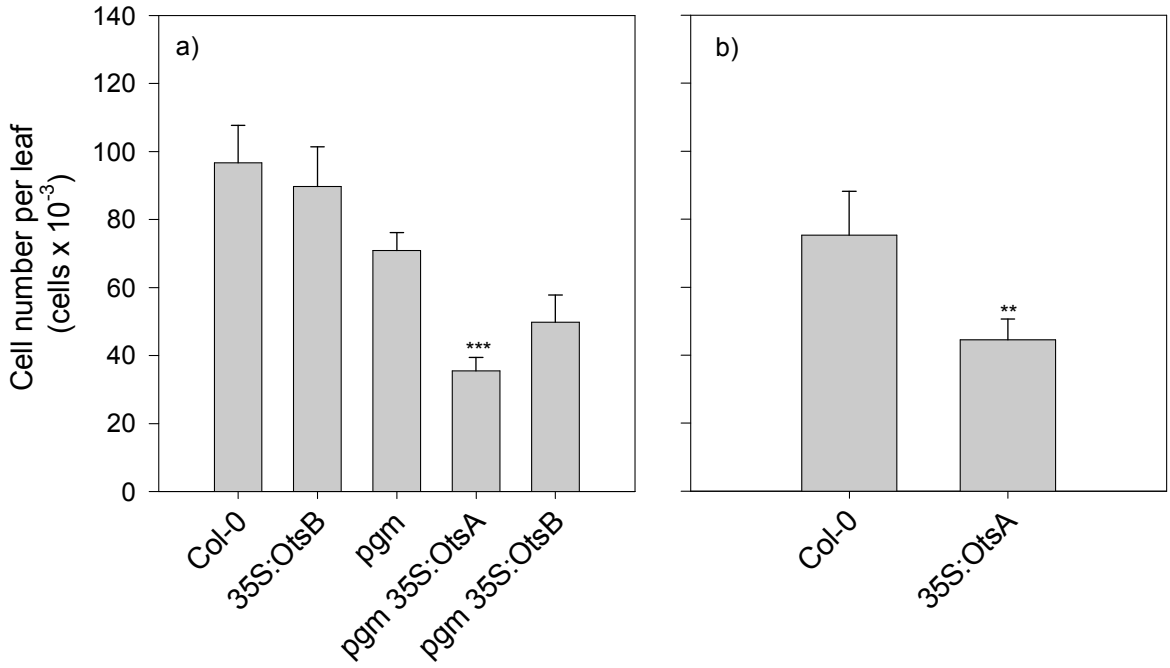

Fig. 3.6. Effects of constitutive modulation of trehalose-6-phosphate levels on cell number per leaf.
Cell number per leaf in the sixth leaf of transgenic *Arabidopsis thaliana* wild type Col-0 and starchless *pgm* mutant expressing bacterial OtsA and OtsB proteins under the control of the constitutive 35S promoter, grown in 16-hour days at a irradiance of 160 μE m^{-2} s^{-1} and a constant temperature of 20°C and sampled after 35 days of growth. In b) the phenotype of the *pgm* 35S:OtsA line back-crossed into wild type is shown, in plants grown separately in identical conditions to the plants in a). Bars are standard deviations. Significant differences (t-test with Holm-Sidak correction) from the relevant control are shown as * $P < 0.05$, ** $P < 0.01$, *** $P < 0.001$. N=5 leaves.

Segments of leaf 6 were fixed and embedded for histological analysis. Thin transverse sections were cut on a microtome and observed under a light microscope. Leaf thickness and the number of cell layers in the leaf were determined by drawing perpendicular transects across the leaf cross sections along the abaxial/adaxial axis. Leaf thickness in the transgenic genotypes is presented in Fig. 3.7. Genotypic differences in leaf thickness were driven chiefly by the *pgm* background rather than the trans-genes. Leaves in the *pgm* mutant were 58% thicker than the Col-0 wild type (P=0.001). Leaf thickness was not significantly different from control in 35S:OtsA and 35S:OtsB plants in both the wild type and the *pgm* background.

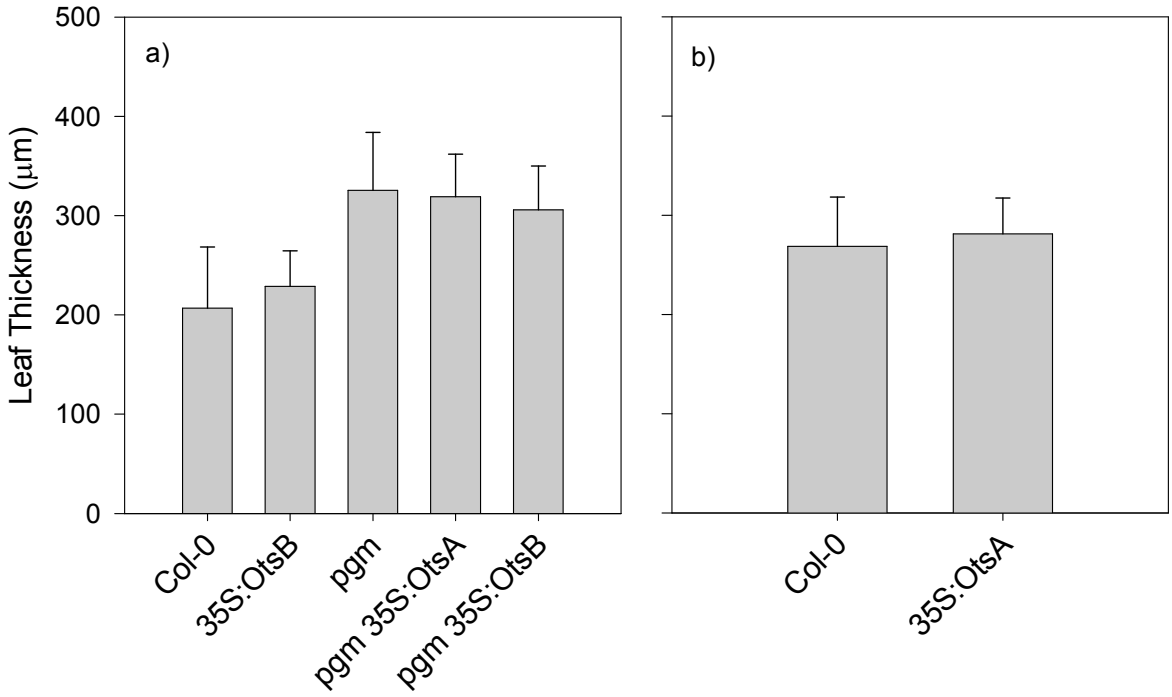

Fig. 3.7. Effects of constitutive modulation of trehalose-6-phosphate levels on leaf thickness. Leaf thickness of the sixth leaf in *Arabidopsis thaliana* wild type Col-0 and starchless *pgm* mutant expressing bacterial OtsA and OtsB proteins under the control of the constitutive 35S promoter, grown in 16-hour days at a irradiance of 160 μE m^{-2} s^{-1} and a constant temperature of 20°C and sampled after 35 days of growth. In b) the phenotype of the *pgm* 35S:OtsA line back-crossed into wild type is shown, in plants grown separately in identical conditions to the plants in a). Bars are standard deviations. Significant differences (t-test with Holm-Sidak correction) from the relevant control are shown as * $P < 0.05$, ** $P < 0.01$, *** $P < 0.001$. N=5 leaves.

The number of cell layers in the leaf, which includes all mesophyll cells and two layers of epidermal cells, is presented in Fig. 3.8. Similar to the results of leaf thickness, the *pgm* background rather than the expressed trans-genes, drove most of the variation in the number of cell layers, however there was also an effect of OtsA over-expression. Leaves in the *pgm* mutant had an average of 6.24 layers, compared to the wild type average of 5.3 (P=0.009). On average, 35S:OtsA in the wild type background had approximately one extra layer of cells in the leaf (P=0.034). The 35S:OtsA plants in the *pgm* background also had more cell layers than the *pgm* mutant control, however this was not significant (P=0.054). The 35S:OtsB plants did not differ from controls in both the wild type (P=0.395) and the *pgm* backgrounds (P=0.499).

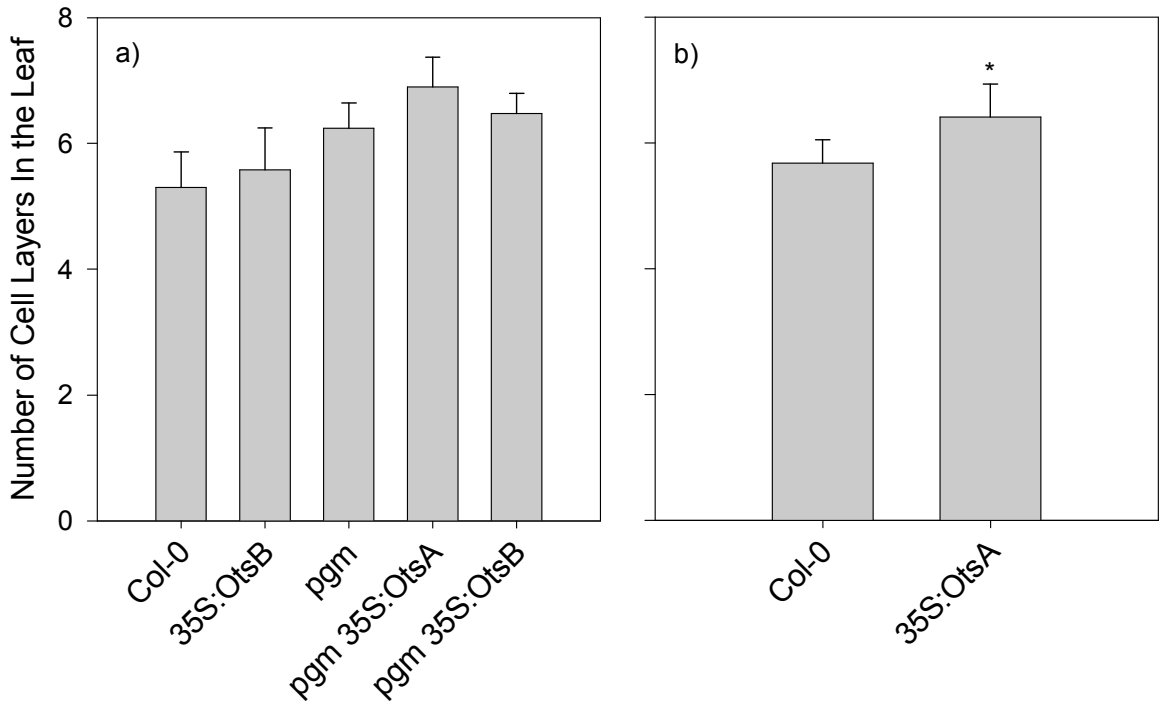

Fig. 3.8 Effects of constitutive modulation of trehalose-6-phosphate levels on the number of cell layers in the leaf.
Number of cell layers in the leaf in *Arabidopsis thaliana* wild type Col-0 and starchless *pgm* mutant expressing bacterial OtsA and OtsB proteins under the control of the constitutive 35S promoter, grown in 16-hour days at a irradiance of 160 μE m^{-2} s^{-1} and a constant temperature of 20°C and sampled after 35 days of growth. In b) the phenotype of the *pgm* 35S:OtsA line back-crossed into wild type is shown, in plants grown separately in identical conditions to the plants in a). Significant differences (t-test with Holm-Sidak correction) from the relevant control are shown as * $P < 0.05$, ** $P < 0.01$, *** $P < 0.001$. N=5 leaves.

Numbers of stomata were counted on both adaxial and abaxial sides of the leaf. The density of stomata per unit leaf area is shown in Fig. 3.9. Stomata were present on both sides of leaves, with higher numbers on the abaxial side. The 35S:OtsA plants in the wild type background had 80% more stomata per unit leaf area on the adaxial side ($P<0.001$) and 64% more on the abaxial side ($P<0.001$) compared to the wild type. The 35S:OtsB in the wild type background showed a contrasting phenotype, with half the stomatal density of wild type on the adaxial side ($P<0.001$) and 34% lower density on the abaxial side ($P=0.003$). Over-expression of OtsA and OtsB in the *pgm* mutant background produced similar but weaker effects on stomatal densities, which were not significant.

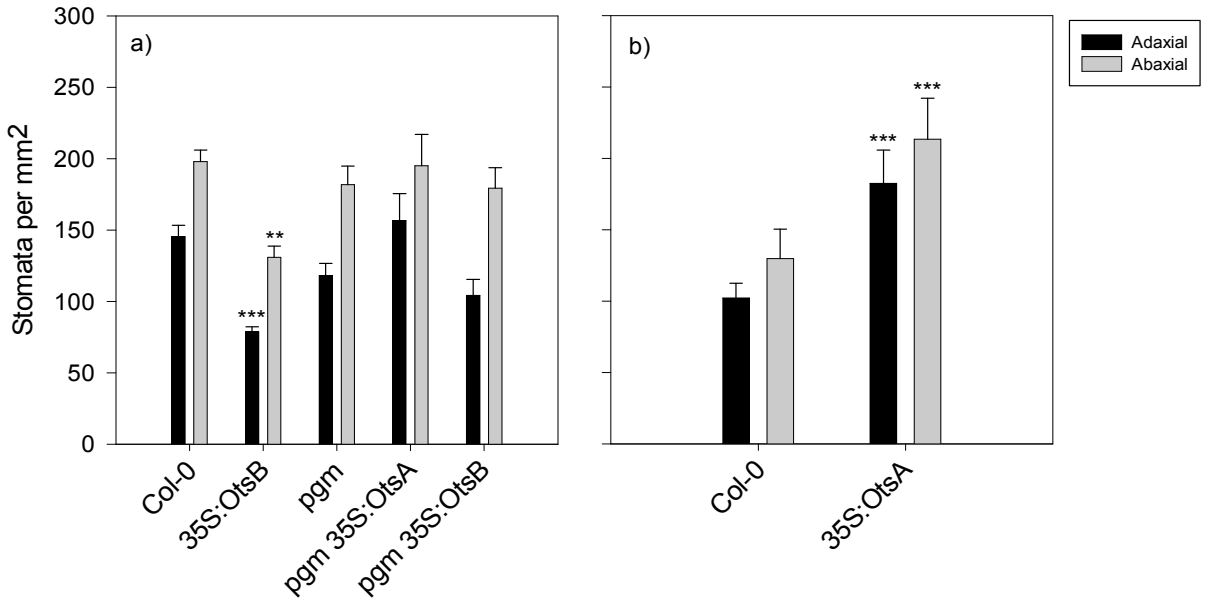

Fig. 3.9. Effects of constitutive modulation of trehalose-6-phosphate levels on stomatal densities. Stomatal densities on the adaxial (black bars) and abaxial (grey bars) sides of the leaf in *Arabidopsis thaliana* wild type Col-0 and starchless *pgm* mutant expressing bacterial OtsA and OtsB proteins under the control of the constitutive 35S promoter, grown in 16-hour days at a irradiance of 160 μE m^{-2} s^{-1} and a constant temperature of 20°C and sampled after 35 days of growth. In b) the phenotype of the *pgm* 35S:OtsA line back-crossed into wild type is shown, in plants grown separately in identical conditions to the plants in a). Significant differences (t-test with Holm-Sidak correction) from the relevant control are shown as * $P < 0.05$, ** $P < 0.01$, *** $P < 0.001$. N=5 leaves.

While the density of stomata on an area basis varied between genotypes, this parameter does not reflect the true number of stomata, which is determined by epidermal patterning processes. The stomatal index is a parameter representing the proportion of all epidermal cells which are stomata. It is thus a more appropriate indicator of actual stomatal numbers. Fig. 3.10 shows the stomatal index of the transgenic lines. In contrast to the large variation in stomatal density, there was no significant change in stomal index in any of the lines. The change in stomatal densities is thus caused not by an increase in the number of cells differentiating into guard cells but rather due to the differential expansion of leaf cells (Fig. 2.5), with stomata being pushed farther apart in 35S:OtsB lines with larger epidermal cells and closer together in 35S:OtsA lines with smaller epidermal cells.

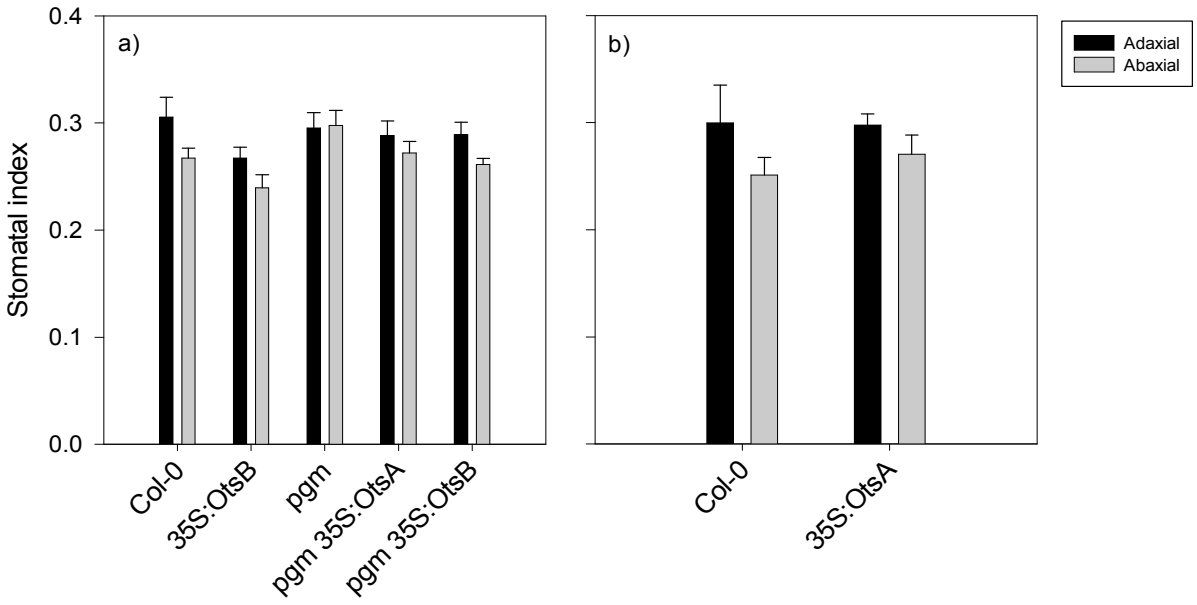

Fig. 3.10 Effects of constitutive modulation of trehalose-6-phosphate levels on stomatal index. Stomatal index on the adaxial (black bars) and abaxial (grey bars) sides of the leaf in *Arabidopsis thaliana* wild type Col-0 and starchless *pgm* mutant expressing bacterial OtsA and OtsB proteins under the control of the constitutive 35S promoter, grown in 16-hour days at a irradiance of 160 µE m^{-2} s^{-1} and a constant temperature of 20°C and sampled after 35 days of growth. In b) the phenotype of the *pgm* 35S:OtsA line back-crossed into wild type is shown, in plants grown separately in identical conditions to the plants in a). Bars are standard deviations. Significant differences (t-test with Holm-Sidak correction) from the relevant control are shown as * $P < 0.05$, ** $P < 0.01$, *** $P < 0.001$. N=5 leaves.

3.2.3. Correlations between morphological traits.

Table 3.1 shows the correlation matrix of the morphological dataset which includes the five genotypes presented in section (a) of the above graphs and does not include 35S:OtsA in the wild type background. Leaf area was strongly positively correlated with cell number per leaf (r=0.86) and less strongly and negatively with cell and stomatal densities as well as leaf thickness and the number of cell layers in the leaf. The densities of cells and stomata were strongly inter-correlated. The densities of cells in the two epidermal cell layers (adaxial and abaxial) were strongly correlated with each other (r=0.67). The density of palisade mesophyll cells was strongly related to adaxial epidermal cells (r=0.83) and less strongly to those on the abaxial side (r=0.54). Adaxial and abaxial stomatal densities were strongly correlated with each other (r=0.89) as well as with epidermal and mesophyll densities. Stomatal index on both sides of leaves was correlated with stomatal densities but not with any other parameters. Leaf thickness was strongly determined by the number of cell layers in the leaf (r=0.86) and both parameters were somewhat negatively related to leaf size and cell number per leaf.

To aid the interpretation of the multivariate data, principal components analysis was performed on the correlation matrix and the results plotted on a biplot (Fig 3.11). On a biplot both the samples and the variables are visualised at the same time (Gabriel, 1971). Samples (individual leaves) are shown as points and variables are shown as vectors. The lengths of the vectors are proportional to the variation in the variable and the angle between two vectors represents the correlation between the two variables (smaller angle corresponding to a high correlation, 90° representing no correlation and angles >90° representing negative correlations, with a perfect negative correlation being an angle of 180°). The

				Cell Density cells mm^{-2}			Stomatal Density mm^{-2}		Stomatal Index		Leaf Thickness	
		Leaf Area mm^2	Cell No. Leaf^{-1}	Adaxial Epidermis	Abaxial Epidermis	Mesophyll	Adaxial	Abaxial	Adaxial	Abaxial	Thickness µm	Cell Layers
	Leaf Area mm^2	1.00	**0.86**	**-0.52**	-0.30	**-0.43**	**-0.55**	**-0.48**	-0.27	-0.29	**-0.46**	**-0.58**
	Cell Number Leaf^{-1}		1.00	-0.17	-0.01	0.04	-0.24	-0.21	-0.22	-0.27	**-0.56**	**-0.65**
Cell Density cells mm^{-2}	Adaxial Epidermis			1.00	**0.67**	**0.83**	**0.87**	**0.70**	0.02	0.11	0.05	0.17
	Abaxial Epidermis				1.00	**0.54**	**0.67**	**0.74**	0.21	-0.26	-0.01	0.14
	Mesophyll					1.00	**0.68**	**0.51**	-0.04	0.01	-0.05	0.01
Stomatal Density mm^{-2}	Adaxial						1.00	**0.89**	**0.51**	**0.37**	0.11	0.23
	Abaxial							1.00	**0.59**	**0.45**	0.18	0.27
Stomatal Index	Adaxial								1.00	**0.57**	0.16	0.18
	Abaxial									1.00	0.30	0.21
Leaf Thickness	Thickness µm										1.00	**0.86**
	Cell Layers											1.00

Table. 3.1 Correlation matrix (Pearson r) between morphological parameters in the sixth leaf of *Arabidopsis thaliana* wild type Col-0 and starchless *pgm* mutant expressing bacterial OtsA and OtsB proteins under the control of the constitutive 35S promoter. grown in 16-hour days and sampled after 35 days of growth. 35S:OtsA in the wild type background is not included (it was a separate experiment). Slopes were tested for significance on a two-tailed t-tistribution with 24 degrees of freedom. Correlations with significant slopes at $P < 0.05$ are highlighted in blue (positive correlations) and red (negative correlations).

relative position of the points to each other represents the similarity between them and their position along the vectors reflects their differentiation by each morphological variable.

The first two principal components summarised 67% of the total variance in the dataset. The first principal component (44% of total variance) was dominated by cell density variables as well as leaf size. The densities of epidermal and mesophyll cells as well as stomata were all strong components of the first principal component axis, along with leaf area. The first principal component axis primarily separated 35S:OtsA and 35S:OtsB genotypes from their controls (the wild type or *pgm* mutant), chiefly on the basis of its components, the cell densities and therefore cell size. The second principal component (24% of total variance) was driven by variation in leaf thickness and the number of cell layers on the one hand and by cell number in the leaf on the other. The second principal component chiefly separated the wild type and *pgm* mutant backgrounds.

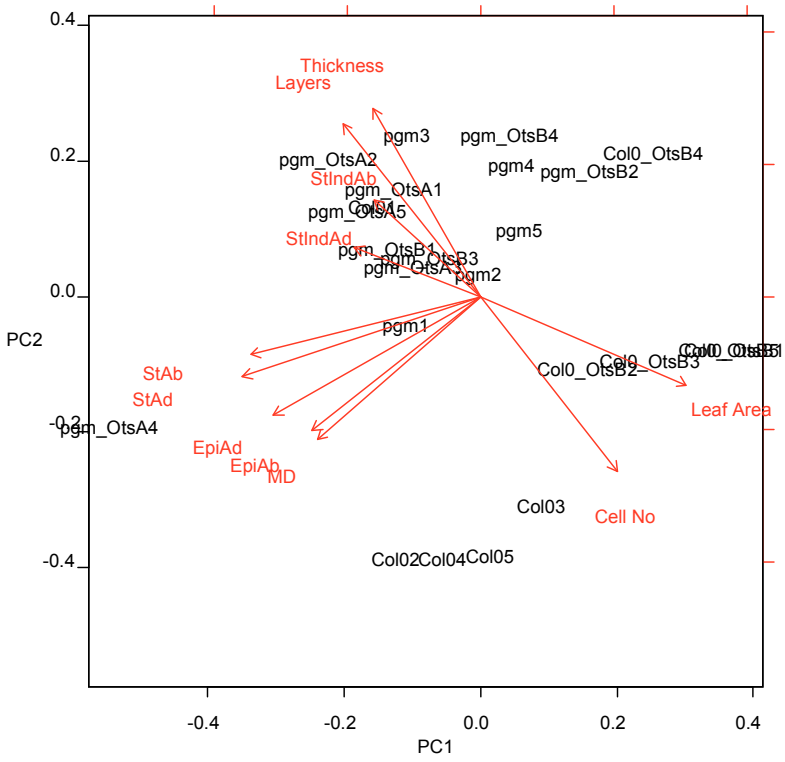

Fig. 3.11. Effects of constitutive modulation of trehalose-6-phosphate levels on leaf morphology, summarised by principal components analysis.
Biplot of principal component analysis on the correlation matrix of leaf morphological parameters determined from the sixth leaves of *Arabidopsis thaliana* wild type Col-0 and starchless *pgm* mutant expressing bacterial OtsA and OtsB proteins under the control of the constitutive 35S promoter, grown in 16-hour days and sampled after 35 days of growth. Labels of variables: Leaf Area – area of leaf 6 in mm^2, Cell number – number of mesophyll cells per leaf, EpiAd – density of epidermal cells on the adaxial side, in cells mm^{-2}, EpiAb – density of epidermal cells on the abaxial side, in cells mm^{-2}, MD – density of palisade mesophyll cells in cells mm^{-2}, StAd – density of stomata on the adaxial side in stomata mm^{-2}, StAb – density of stomata on the abaxial side in stomata mm^{-2}, StIndAd – stomatal index on the adaxial side, StIndAb – stomatal index on the abaxial side, Thickness – leaf thickness in µm, Layers – number of cell layers in the leaf.

3.2.4. Growth in different daylengths.

In order to induce variation in both metabolic function and growth and examine the effect of altered Tre-6-P levels on them, the OtsA and OtsB over-expressing lines in the wild type background were grown in three daylengths ranging from short days (8 hours of light), through an intermediate daylength (12 hours) to long days (16 hours). Fig. 3.12 shows the plants at the time of harvest. Plants grown in 12-hour and 16-hour days were harvested after 35 days of growth, plants grown in 8-hour days were harvested after 46 days. Growth and the leaf morphology parameters specific leaf area (SLA) and leaf dry matter content (LDMC) were measured. The latter two parameters allow an estimate of leaf thickness to be calculated based on the methodology of Vile (2005). Data was analysed using analysis of variance in a two-way factorial design with interactions, and multiple comparisons using the Holm-Sidak step-down method.

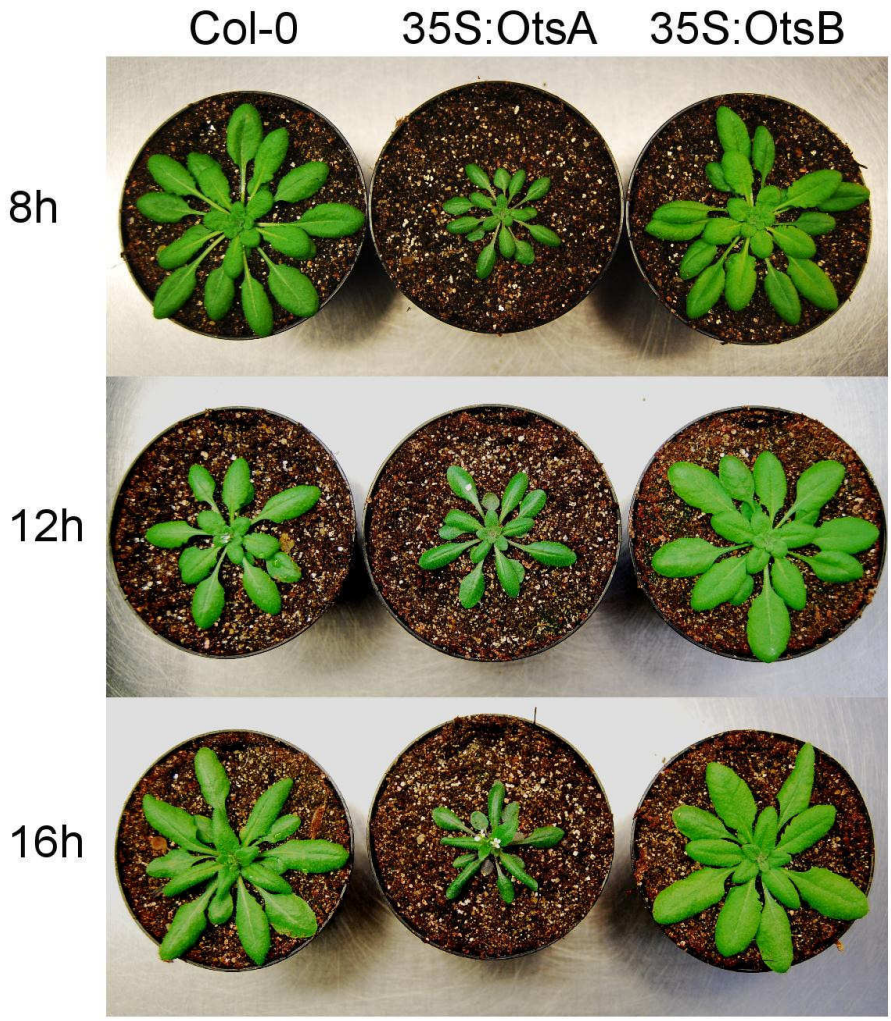

Fig. 3.12 Effects of constitutive modulation of trehalose-6-phosphate levels on growth and development in three daylength regimes.
Arabidopsis thaliana transgenic lines over-expressing bacterial OtsA and OtsB proteins under the control of the constitutive 35S promoter grown in three daylengths (labelled on left) at a irradiance of 160 µE m^{-2} s^{-1} and a constant temperature of 20°C. Plants grown in 12-hour and 16-hour days are 35 days old, 8 hour-day-grown plants are 46 days old. Pots are 10cm in diameter.

35S:OtsA plants were stunted in growth in all three daylengths and were much smaller than wild type plants. 35S:OtsB did not appear different from the wild type except in 16-hour days, where they were 32% bigger on a rosette fresh weight basis (fresh weights are not shown).

Relative growth rates (RGR) were calculated from fresh weight biomass data (Fig. 3.13a). There were significant effects of both daylength ($P<0.001$) and genotype ($P<0.001$) on RGR while the daylength:genotype interaction was not significant ($P=0.106$). In wild type plants, relative growth rates increased between 8 and 12 hours ($P<0.001$) but became saturated and did not increase further between 12 and 16 hours ($P=0.367$). The relative growth rate of 35S:OtsA plants was reduced in all daylengths by an almost constant 25%, which was highly significant in all daylengths ($P<0.001$). 35S:OtsB plants did not differ from the wild type in either daylength. The observed 32% increase in rosette fresh weight in 16-hour days translated to an increase in RGR of 0.014 d^{-1}, or 4.6% relative to wild type, which was not significant ($P=0.062$).

Specific leaf area (SLA, Fig. 3.13b), the amount of leaf area displayed per unit dry weight biomass, was significantly affected by both daylength ($P<0.001$) and genotype ($P<0.001$), with no significant genotype:daylength interaction ($P=0.352$). SLA decreased with increasing daylength in all three genotypes, this was significant in 35S:OtsA ($P<0.001$) and 35S:OtsB ($P=0.003$) but not in the wild type ($P=0.05$). 35S:OtsA plants had lower SLA than wild type in all three daylengths ($P<0.001$), with reductions between 28% and 40% in 8h and 16h respectively. 35S:OtsB plants had marginally higher SLA in 12h days and no differences in other daylengths ($P=0.034$).

The dry matter content of leaves (LDMC, Fig. 3.13c), determined by drying the leaves in an oven, was significantly affected by daylength ($P<0.001$) and genotype ($P<0.001$), with a significant genotype:daylength interaction ($P<0.001$). LDMC did not vary significantly with daylength in the wild type. 35S:OtsA plants had highly elevated LDMC levels in all three daylengths compared to wild type, with a 67% increase in 16-hour days ($P<0.001$). 35S:OtsB plants did not differ from wild type.

Leaf thickness, calculated from SLA and LDMC as in Vile et al (2005), is presented in Fig. 3.13d. Leaf thickness varied significantly with daylength ($P<0.001$) but not genotype ($P=0.234$). In the wild type, leaf thickness increased with increasing daylength by 15% between 8h and 12h ($P<0.001$) but did not increase further in 16-hours ($P=0.199$). There were no significant differences from the wild type in any genotype in any daylength.

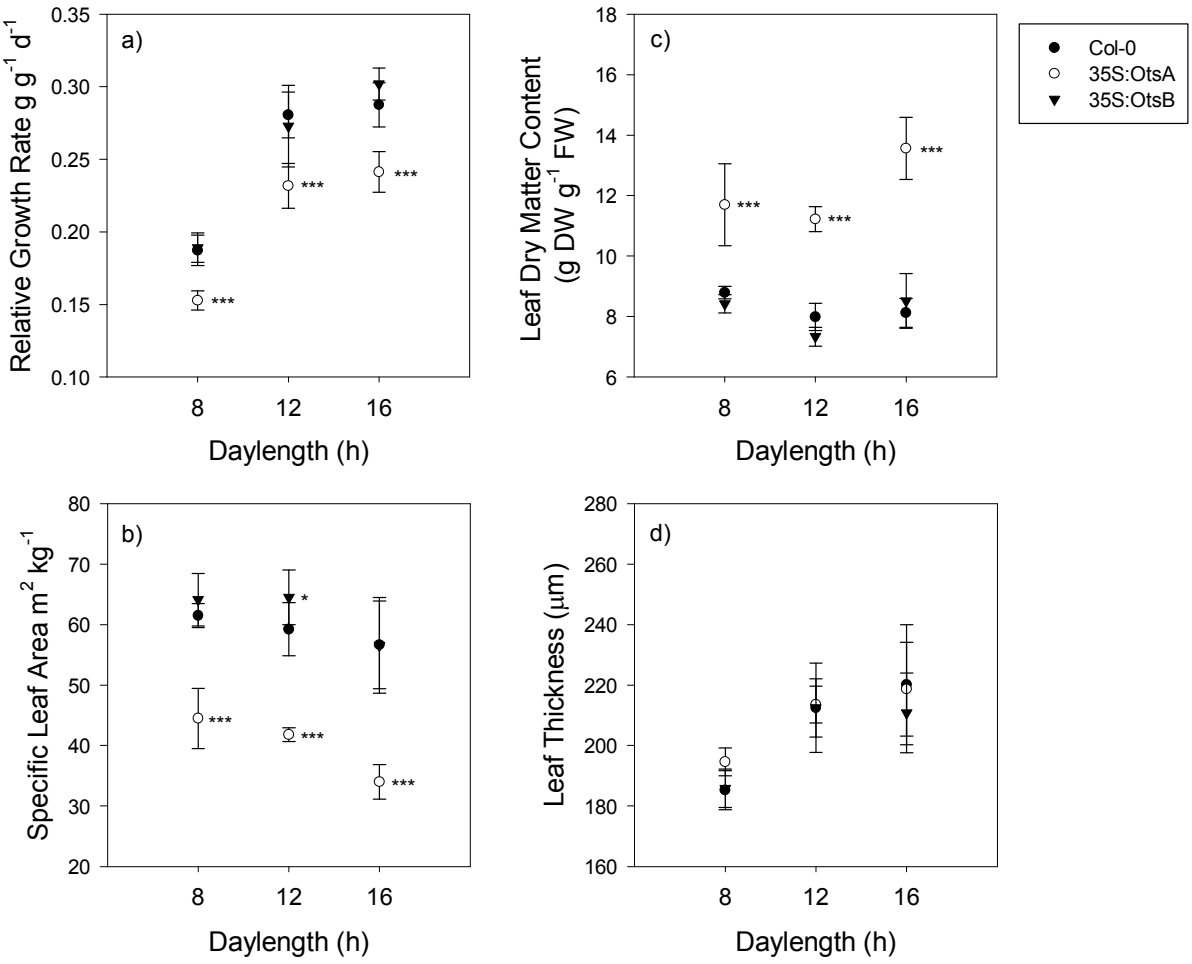

Fig. 3.13. Effects of constitutive modulation of trehalose-6-phosphate levels on relative growth rate (a), specific leaf area (b), leaf dry matter content (c) and leaf thickness (d) in three daylength regimes.
Arabidopsis thaliana over-expressing bacterial OtsA and OtsB proteins under the control of the constitutive 35S promoter were grown in three daylength regimes at a irradiance of 160 µE m^{-2} s^{-1} and a constant temperature of 20°C. Significant differences (t-test with Holm-Sidak correction) from the wild type are shown as * $P < 0.05$, ** $P < 0.01$, *** $P < 0.001$. N= 8 plants, bars are standard deviations.

3.2.5. Trehalose-6-phosphate.

Plants were grown in parallel with the plants presented above and rosettes were harvested at the end of the day and end of the night for metabolite measurements. Metabolite data was analysed using a three-way analysis of variance design with genotype, daylength and timepoint as effects. Pairwise multiple comparisons were performed using the Holm-Sidak step-down method.

Fig. 3.14 shows the patterns of Tre-6-P accumulation in plants sampled at the end of the day (a) and the end of the night (b) Tre-6-P levels increased with increasing daylength in all genotypes, however this was only significant in 35S:OtsA plants, both at the end of the day and the end of the night. OtsA over-expression strongly increased Tre-6-P levels in the plants with high significance in all three daylengths and in both timepoints ($P<0.001$ in all cases). Values were 4-5-fold higher than wild type at the end of the day and 6-10-fold higher at the end of the night. Tre-6-P levels were marginally lower in 35S:OtsB over-expressors, however this was not significant in any daylength or timepoint.

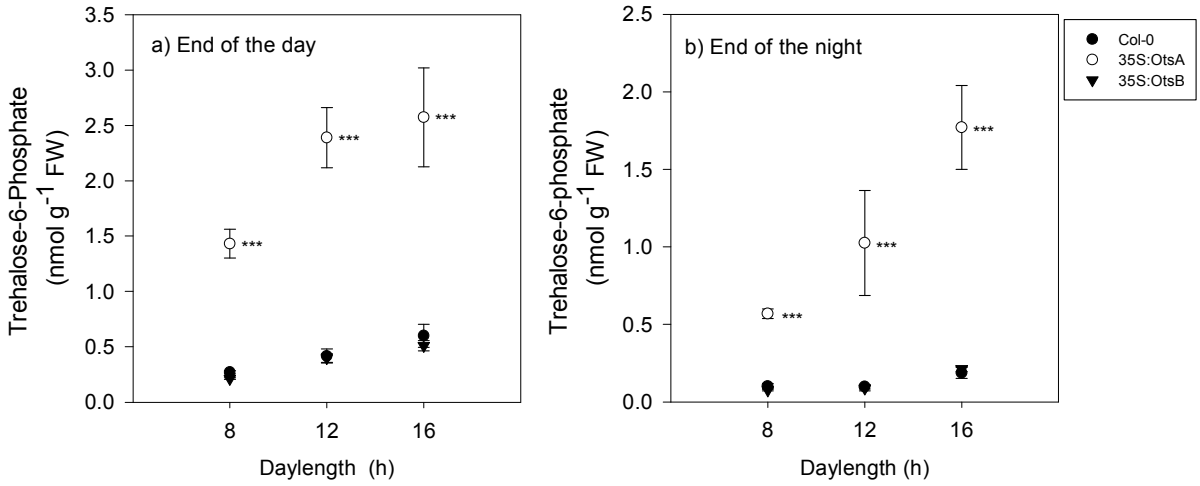

Fig. 3.14. Trehalose-6-phosphate levels at the end of the day (a) and end of the night (b) in transgenic lines expressing OtsA and OtsB proteins driven by the constitutive 35S promoter in the wild type Col-0 background grown in three daylength regimes.
Arabidopsis thaliana wild type Col-0 and transgenic lines over-expressing bacterial OtsA and OtsB proteins under the control of the constitutive 35S promoter grown in three daylength regimes at a irradiance of 160 µE m^{-2} s^{-1} and a constant temperature of 20°C and harvested at the end of the day and end of the night. Tre-6-P was determined by LC-MS/MS. Significant differences (t-test with Holm-Sidak correction) from the wild type are shown as * < 0.05, ** <0.01, *** <0.001. N= 5, bars are standard deviations.

3.2.6. Metabolic Phenotype.

A multivariate approach was taken in order to assess the impact of altered Tre-6-P levels on the metabolism of the plants. A dataset of 27 metabolites was collected from the daylength experiment. The dataset was normalised as standard deviates and principal components analysis was performed. Fig. 3.15 plots the first and second principal component scores of individual samples from the two transgenic genotypes and the wild type in each daylength/timepoint combination. This was done in order to investigate whether metabolic changes were more or less pronounced in particular conditions and particular genotypes. Over-expression of OtsA and OtsB led to reciprocal alterations in metabolism in the transgenic lines. 35S:OtsA samples were generally well separated from the wild type samples while 35S:OtsB were less so.

The overall degree of metabolic perturbation of the transgenic genotypes was assessed quantitatively using a multivariate approach and tested for statistical significance. For this, multivariate Euclidean distance was used as a similarity measure. Euclidean distance is the simplest and most commonly-used of all distance measures used in statistics. It is based on Euclidean geometry where the distance between two points on a plane involves the calculation of the length of the hypotenuse of a right angled-triangle. It can be extended to multi-dimensional spaces to provide a measure of distance in multivariate data. Euclidean distance is a linear distance measure. The Euclidean distance of all data-points from all wild type points was determined and the average taken. Fig. 3.16 shows the mean Euclidean distances of 35S:OtsA and 35S:OtsB samples from wild type samples at the end of the day (Fig 3.16a) and end of the night (Fig. 3.16b). Since the dataset had been standardised prior to analysis, the units of distance are standard deviations of metabolites, enabling comparisons between treatments, timepoints and genotypes. A higher separation (larger distance) corresponds to less similarity to wild type and therefore a more perturbed metabolic state. 35S:OtsA plants were farther separated from wild type than 35S:OtsB plants in all daylengths and both timepoints, indicating that their metabolism was

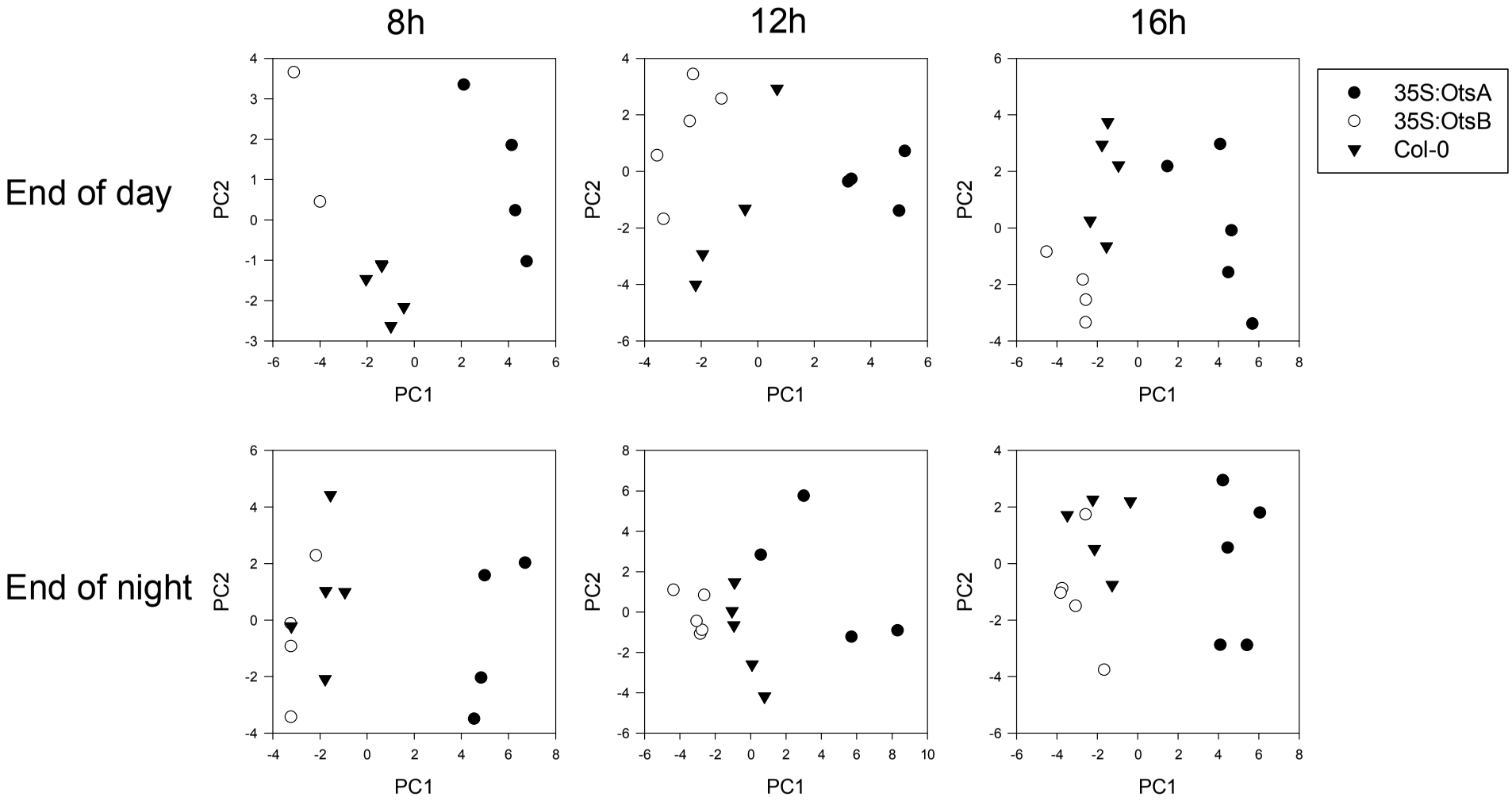

Fig. 3.15. Principal component analysis of metabolic phenotype in transgenic lines of Arabidopsis with altered Tre-6-P levels.
Bivariate plots of first and second principal component scores of biological replicate samples collected from *Arabidopsis thaliana* wild type Col-0 and transgenic lines over-expressing bacterial OtsA and OtsB proteins under the control of the constitutive 35S promoter grown in three daylengths and sampled at the end of the day and end of the night. Principal components analysis was conducted on correlation matrices of 27 metabolites measured on the samples.

more perturbed. The degree of separation was approximately constant between different daylengths. At the end of the night 35:OtsA plants were more dissimilar from wild type than end of day while 35S:OtsB became less separated from the wild type at the end of the night than at the end of the day.

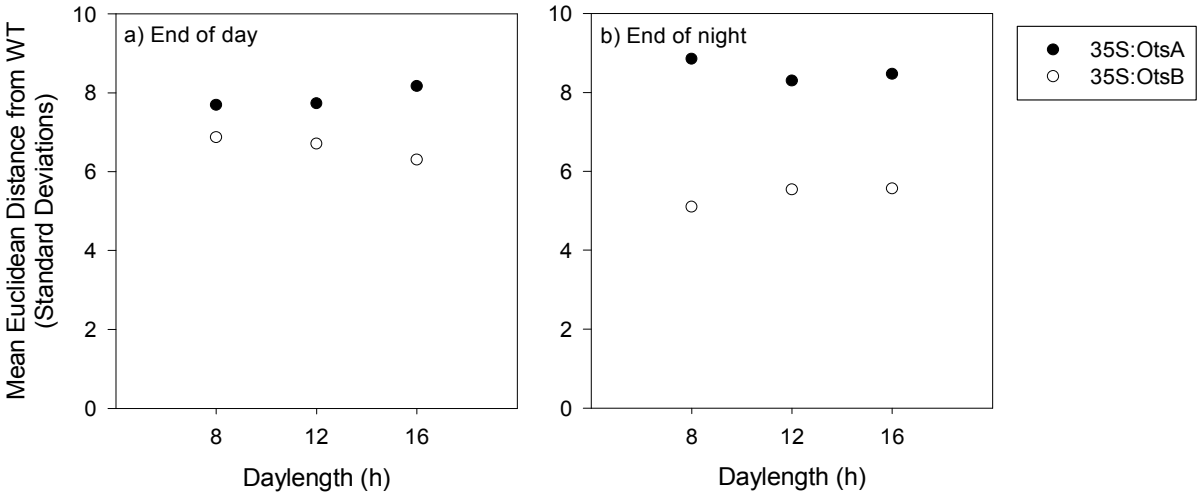

Fig. 3.16. Quantification of perturbation in metabolic phenotype in transgenic lines of Arabidopsis with altered Tre-6-P levels grown in three daylength regimes.
Mean multivariate Euclidean distance of all genotype points from all wild type points of *Arabidopsis thaliana* transgenic lines over-expressing bacterial OtsA and OtsB proteins under the control of the constitutive 35S promoter grown in three daylength regimes at a irradiance of 160 μE m^{-2} s^{-1} and a constant temperature of 20°C and sampled at the end of the day (a) and end of the night (b). Distances were calculated from a dataset of 27 metabolites normalised as standard deviates.

Testing Euclidean distance separation for statistical significance is not straightforward because the variance of this distance is a multivariate variance while simple parametric tests, like the T-test, are only applicable to testing the difference between two means in univariate space. In order to assess the significance of the differences in metabolism in a statistical manner, the Euclidean distance matrices were subjected to hierarchical clustering. It was checked whether all samples of a genotype could be separated from the wild type samples as a single group (branch) on a cluster tree. The cluster trees were then validated using bootstrap re-sampling and bootstrap probabilities were obtained. Table 3.2 shows the bootstrap probabilities of branches separating samples of a genotype from wild type samples. Cluster trees were determined for each daylength and timepoint. The bootstrap probability shows the percentage frequency of occurrence of a particular branch in multiple rounds of random iterative re-sampling of the data. One interpretation of bootstrap probabilities is as a non-parametric p-value, which can be used to test for significant differences. Non-parametric statistics have the advantage of not making assumptions about normal distribution of data, which can be difficult to assess in datasets with few samples and many variables and can strongly affect the results of parametric methods, such as MANOVA.

35S:OtsA samples were consistently separated from wild type samples as a separate branch on cluster trees and these separations were significant in some conditions. 35S:OtsB could not be distinguished as a separate branch from wild type samples in two cases and in most other cases its separation was not significant. In both genotypes, there were more robust separations in 8-hour days than in 12 and 16 hours. The results indicate that 35S:OtsA plants were substantially perturbed in metabolic function while 35S:OtsB plants could hardly be distinguished from the wild type with statistical significance.

Daylength	8h		12h		16h	
Timepoint	End of day	End of night	End of day	End of night	End of day	End of night
35S:OtsA	**96**	**100**	90	71	67	**100**
35S:OtsB	**95**	92	Not separated	93	91	Not separated

Table. 3.2 Statistical testing of perturbation in metabolic phenotype in transgenic lines with altered Tre-6-P levels grown in three daylength regimes.
Bootstrap probabilities of branches separating samples of the listed genotypes as a single group from wild type samples on Ward-hierarchical clustering trees computed from a dataset of 27 metabolites profiled in *Arabidopsis thaliana* wild type Col-0 and transgenic lines over-expressing bacterial OtsA and OtsB proteins under the control of the constitutive 35S promoter grown in three daylengths. Hierarchical clustering was performed using Euclidean distance as a distance measure. Significant separations from wild type (at a 5% threshold) are highlighted in boldface.

The metabolites strongly associated with the first two principal component axes and the ones driving the Euclidean distance separation most strongly were Tre-6-P, starch, soluble sugars and organic acids (data are not shown). These key primary metabolites are explored in more detail below.

3.2.7. Soluble Sugars.

The over-expression of OtsA and OtsB was associated with strong and reciprocal effects on the levels of soluble sugars in *Arabidopsis thaliana* rosettes (Fig. 3.17). The 35S:OtsA generally had lower levels of glucose, fructose and sucrose than the wild type both at the end of the day and end of the night, which was more pronounced in 16-hour days. The 35S:OtsB plants generally had higher sugar levels.

There were mild changes in glucose content in the transgenic lines compared to wild type. The 35S:OtsA plants tended to have more glucose than wild type at the end of the day and end of the night, particularly in longer days. The 35S:OtsB plants also displayed higher levels of glucose in longer daylengths at the end of the day ($P=0.044$ in 12h and $P=0.01$ in 16h) and at the end of the night in 16-hour days ($P=0.011$).

There was a clearly opposing pattern of fructose accumulation in the transgenic genotypes with respect to the wild type. The 35S:OtsA plants had lower levels of fructose at the end of the day, which was significant in 16-hour days ($P<0.001$). The pattern was similar at the end of the night, with significantly lower fructose in 12-hour days ($P=0.005$). The 35S:OtsB plants, in contrast, had significantly higher levels of fructose at the end of the day in 12 hour ($P<0.001$) and 16-hour days ($P<0.001$), with almost double the levels of wild type in 16-hour days.

Sucrose followed a similar reciprocal pattern in the transgenic lines. The 35S:OtsA plants had significantly lower sucrose levels in all daylengths both at the end of the day and the end of the night. Levels of sucrose in this genotype were approximately half of that found in the wild type in the same conditions. The 35S:OtsB plants had significantly higher levels of sucrose in 12-hour and 16-hour days, both at the end of the day and the end of the night. Levels of sucrose were more-than double the wild type values in equivalent conditions.

Since trehalose-6-phosphate amount is a proposed signal of sucrose availability, the relationship between Tre-6-P and sucrose was examined. Fig. 3.18 plots the level of Tre-6-P against sucrose levels in the three genotypes. Tre-6-P was strongly linearly related to sucrose levels in all genotypes and in both timepoints. However, in parallel with the alterations in sucrose levels in the transgenic lines, the slopes of the relationships with Tre-6-P were altered. The 35S:OtsA plants had a very steep slope of Tre-6-P increase with increasing sucrose while 35S:OtsB plants had a lower slope. The regression

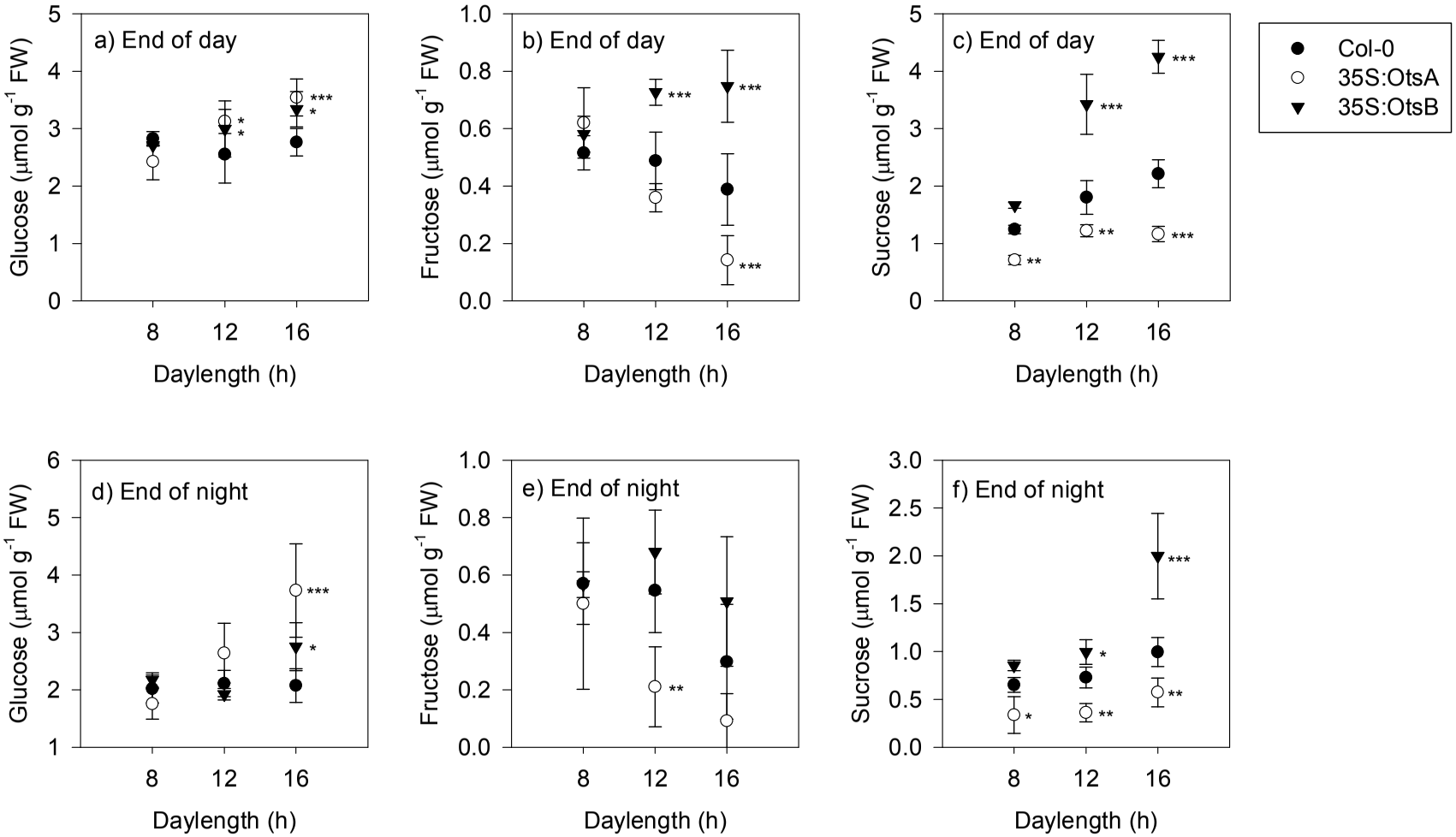

Fig. 3.17. Effects of constitutive modulation of trehalose-6-phosphate levels on soluble sugar content in three daylength regimes.
Soluble sugar content in *Arabidopsis thaliana* wild type Col-0 and transgenic lines over-expressing bacterial OtsA and OtsB proteins under the control of the constitutive 35S promoter grown in three daylengths. Glucose (a, d), fructose (b, e) and sucrose (c, f) were measured in rosettes sampled at the end of the day (a, b, c) and end of the night (d, e, f) when the plants were 25 days old. Significant differences (t-test with Holm-Sidak correction) from the wild type are shown as * $P < 0.05$, ** $P < 0.01$, *** $P < 0.001$. $N = 5$, bars are standard deviations.

slope coefficients were tested for significant differences from the wild-type (details of the test in the methods section). The slopes in the 35S:OtsA and 35S:OtsB samples were significantly different from wild type at the end of the day (both P<0.001) and the end of the night (P<0.001 in 35S:OtsA and P=0.001 in 35S:OtsB).

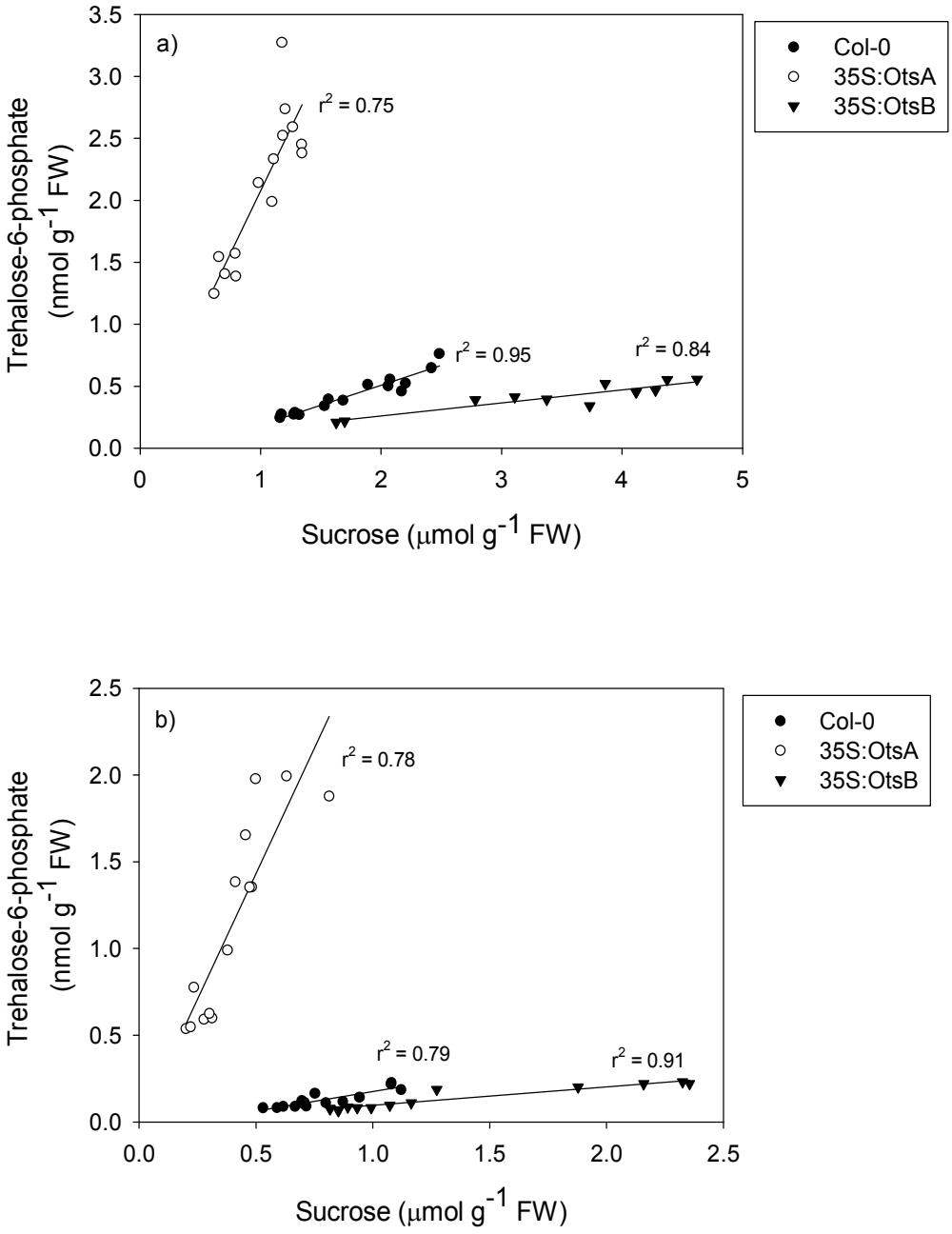

Fig. 3.18. Effects of constitutive modulation of trehalose-6-phosphate levels on the relationship between Tre-6-P and sucrose.
Lines are linear regressions.

The relationship of Tre-6-P with glucose and fructose was also investigated. Table. 3.3 shows regression slopes of Tre-6-P as the dependent variable in linear models against the three soluble sugars and the strengths of their correlations. The slopes were tested for significant differences from zero. In the wild type, Tre-6-P was very weakly related to the levels of hexoses in both timepoints. The

Genotype	Col-0						35S:OtsA						35S:OtsB					
	Slope			r^2			Slope			r^2			Slope			r^2		
Metabolite	Glucose	Fructose	Sucrose	Glucose	Fructose	Sucrose	Glucose	Fructose	Sucrose	Glucose	Fructose	Sucrose	Glucose	Fructose	Sucrose	Glucose	Fructose	Sucrose
End of Day	0,12	-0,61	0,32	0,06	0,21	0,95	0,93	-2,15	2,02	0,76	0,65	0,75	0,16	0,68	0,10	0,34	0,38	0,84
End of Night	0,07	-0,15	0,23	0,12	0,37	0,79	0,51	-1,42	2,89	0,84	0,34	0,78	0,12	-0,15	0,11	0,69	0,14	0,91

Regression Diagnostics	StdErr of Slope			p value of Slope			StdErr of Slope			p value of Slope			StdErr of Slope			p value of Slope		
	Glucose	Fructose	Sucrose	Glucose	Fructose	Sucrose	Glucose	Fructose	Sucrose	Glucose	Fructose	Sucrose	Glucose	Fructose	Sucrose	Glucose	Fructose	Sucrose
End of Day	0,13	0,36	0,03	0,35	0,11	**<0,001**	0,16	0,46	0,34	**<0,001**	**<0,001**	**<0,001**	0,07	0,28	0,01	**0,04**	**0,03**	**<0,001**
End of Night	0,05	0,05	0,03	0,202	**0,016**	**<0,001**	0,06	0,56	0,45	**<0,01**	**0,027**	**<0,001**	0,02	0,11	0,01	**<0,001**	0,192	**<0,001**

Table. 3.3. The relationships of trehalose-6-phosphate levels with the contens of soluble sugars glucose, fructose and sucrose in transgenic lines with altered Tre-6-P levels grown in three daylength regimes.

Slope coefficients (mmol Tre-6-P mol^{-1} sugar), coefficients of determination (r^2) and significance tests of the slope coefficient of linear regression models with trehalose-6-phosphate content as a dependent variable against the contents of the soluble sugars glucose, fructose and sucrose in *Arabidopsis thaliana* wild type Col-0 and transgenic lines over-expressing bacterial OtsA and OtsB proteins under the control of the constitutive 35S promoter grown in three daylengths and sampled at the end of the day and end of the night. Linear regressions were fitted using the LINEST function in Excel 2003. Slopes were tested for significant differences from zero. A t-variance ratio was computed for the slope coefficient and tested on a two-tailed T-distribution using the TDIST function, with the degrees of freedom of the regression (12 in most cases). Significant slopes ($P < 0.05$) are highlighted in boldface.

regression against glucose was not significant. The relationship with fructose had a negative slope which was only significantly different from zero at the end of the night (r^2=0.37, P=0.01). Sucrose was very strongly related to Tre-6-P in both end of day (r^2=0.95, P<0.001) and end of night samples (r^2=0.79, P<0.001).

In 35S:OtsA plants Tre-6-P was strongly and significantly related to all three sugars in both timepoints with very exaggerated slopes compared to wild type. The relationship with fructose was strongly negative while that with glucose and sucrose very strongly positive. While the slope of Tre-6-P against sucrose was decreased in 35S:OtsB plants, this was not the case with glucose and fructose, where the slopes were unchanged or somewhat higher. Tre-6-P was significantly positively related to glucose levels at the end of the day (r^2=0.34, P=0.04) and the end of the night (r^2=0.69, P<0.001). The relationship with fructose was positive and significant only at the end of the day (r^2=0.38, P=0.03).

3.2.8. Starch.

Starch content is shown in Fig. 3.19. All genotypes accumulated starch during the day and broke it down during the night in all daylengths. In the wild type, starch contents at the end of the day were not influenced significantly by daylength. At the end of the night very little starch remained, however this was slightly daylength-dependent. Starch levels at the end of the night showed an increase in 16-hour days compared to 12-hour days (P=0.021).

The 35S:OtsA line had highly elevated levels of starch in all daylengths at the end of the day and the end of the night. At the end of the day the increase in starch in this genotype ranged from 31% over the wild type in 8-hour days (P=0.005), through 67% in 12-hour days (P<0.001) but decreased again in 16-hour days to 50% above wild type levels (P<0.001). At the end of the night, the line retained substantial amounts of its starch reserves, between 42% and 71% of its end-of-day starch. The amount of starch retained at the end of the night increased with daylength and in 16-hour days was up to the levels of the wild type at the end of the day.

Starch levels in 35S:OtsB plants were largely in line with wild type levels at the end of the day, except in 16-hour days, where they were lower by 14% (P=0.044). End of day starch levels in this genotype were daylength dependent, with a tendency toward less starch with increasing daylength. End of night levels did not differ from the wild type.

It was investigated whether the observed changes in starch levels can account for the increased dry matter content in 35S:OtsA leaves (Fig. 3.13c). The dry weight of starch at the end of the day constituted an almost constant 1.2% of fresh weight in the wild type in all three daylengths. The observed increase in starch in 35S:OtsA plants at the end of the day would account for an increase of 0.4-0.8% in the dry matter content in these lines compared to wild type. Thus the extra starch is insufficient to explain the much larger increase in LDMC observed in this line, which was 3-6-% higher than the wild type.

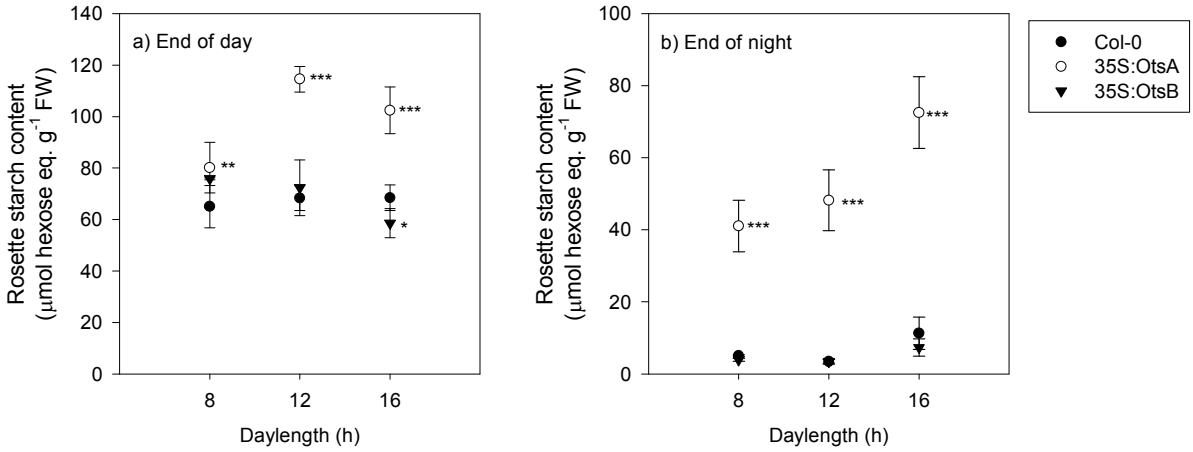

Fig. 3.19. Effects of constitutive modulation of trehalose-6-phosphate levels on rosette starch content at the end of the day (a) and end of the night (b) in three daylength regimes.
Arabidopsis thaliana wild type Col-0 and transgenic lines over-expressing bacterial OtsA and OtsB proteins under the control of the constitutive 35S promoter grown in three daylength regimes at a irradiance of 160 µE m^{-2} s^{-1} and a constant temperature of 20°C and harvested at the end of the day and end of the night. Significant differences (t-test with Holm-Sidak correction) from the wild type are shown as * $P < 0.05$, ** $P < 0.01$, *** $P < 0.001$. N= 5, bars are standard deviations.

3.2.9. Organic acids.

There were substantial alterations in the contents of TCA-cycle organic acids in the transgenic lines (Fig. 3.20). While 35S:OtsB plants had generally unaltered levels of organic acids with respect to the wild type, 35S:OtsA plants had highly elevated levels of malate and fumarate and mildly elevated levels of citrate. The differences were especially pronounced in 12-hour and 16-hour days and could be seen both at the end of the day and the end of the night. End of day malate levels were up to 63% higher than wild type, while fumarate levels were more than double the wild type in some conditions.

3.2.10. Carbon turnover.

The more abundant metabolites described above are present in sufficient amounts to form substantial carbon pools in the plant. Starch was the biggest carbon pool by size. The accumulation of starch during the day is an example of a transient carbon store which is used to fuel metabolism and growth during the night. The abundances of sugars and organic acids were smaller than starch and also exhibited diurnal fluctuations, with accumulation during the day and depletion during the night. The diurnal turnover of these pools, i.e. the difference between the end of the day and end of night values, is an indication of the amount of assimilates stored in these pools during the day and their utilisation at night to fuel metabolism and growth. The diurnal turnover of the metabolites presented above was analysed and is presented in Fig. 3.21. Since the different compounds contain a different number of carbon atoms, the pools are expressed in C-equivalents, allowing a direct comparison of pool sizes to be made.

There were reciprocal effects of altered Tre-6-P on the turnover of soluble sugars (Fig. 3.21a). The 35S:OtsA plants turned over slightly less soluble sugars on a daily basis, with a significant difference from wild type in 16-hour days. 35S:OtsB plants had a substantially higher turnover (66% higher in 16-hour days). The effects in both genotypes were minor in 8-hour days and became more severe with increasing daylength. The turnover of organic acids (Fig. 3.21b) was unaltered compared to wild type.

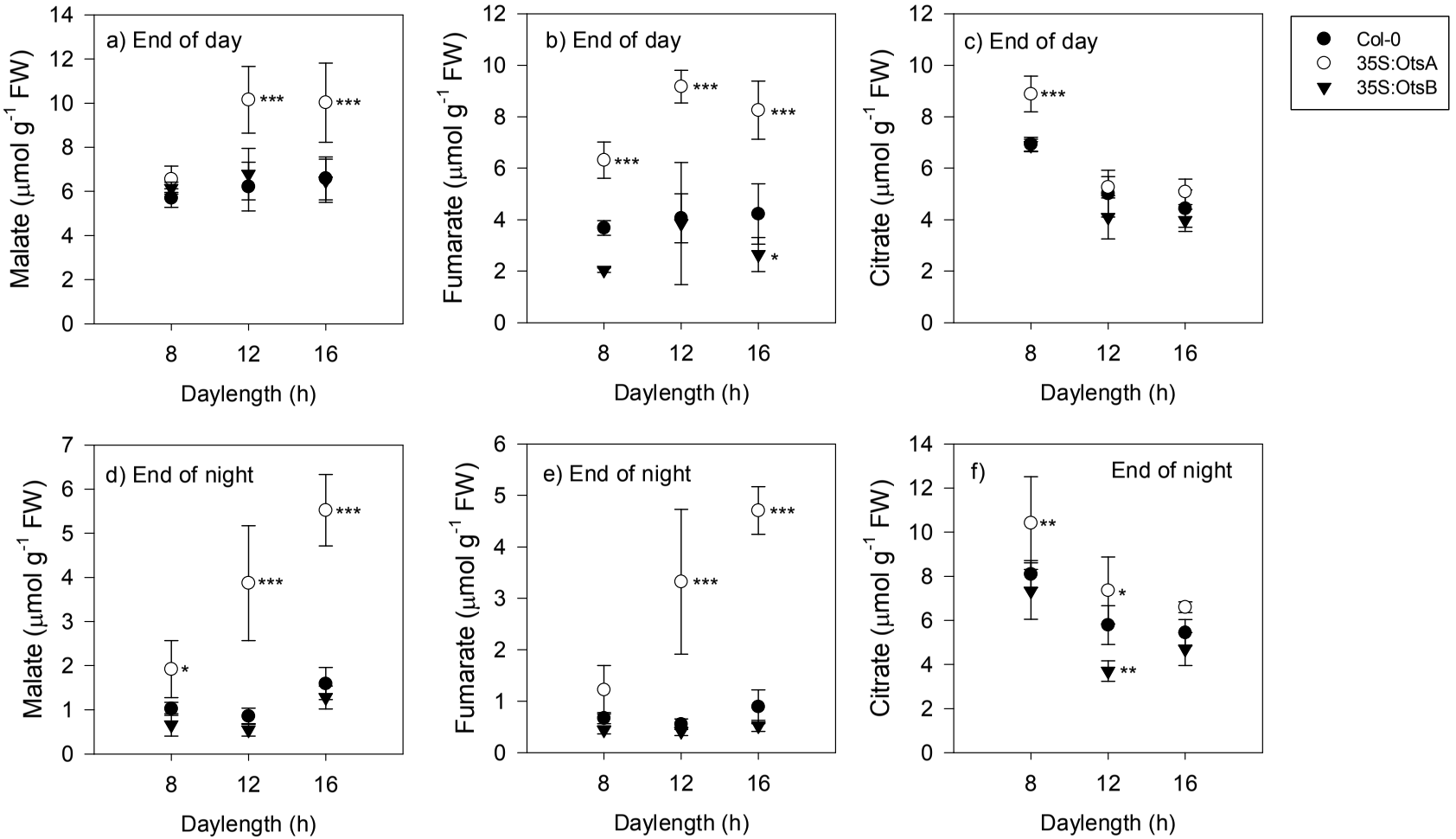

Fig. 3.20. Effects of constitutive modulation of trehalose-6-phosphate levels on organic acid content in three daylength regimes.
Contents of TCA-cycle organic acids malate (a, d), fumarate (b, e) and citrate (c, f) in *Arabidopsis thaliana* wild type Col-0 and transgenic lines over-expressing bacterial OtsA and OtsB proteins under the control of the constitutive 35S promoter grown in three daylengths. Organic acids were measured in rosettes sampled at the end of the day (a, b, c) and end of the night (d, e, f) when the plants were 25 days old. Significant differences (t-test with Holm-Sidak correction) from the wild type are shown as * $P < 0.05$, ** $P < 0.01$, *** $P < 0.001$. N= 5, bars are standard deviations.

Even though there were substantial alterations in the pools sizes of organic acids in 35S:OtsA plants compared to wild type, they turned over equivalent amounts of these compounds on a daily basis as the wild type. Organic acid turnover in 35S:OtsB plants was also unaltered. The turnover of starch (Fig. 3.21c) was strongly inhibited in 35S:OtsA plants, however the difference was only apparent in 8 and 16-hour days, but not 12-hours. Starch turnover was reduced by 35% and 48% in 8 and 16-hour days respectively, both highly significant differences. There were no significant differences in starch turnover in 35S:OtsB plants.

The turnover of these metabolites was summed to give an indication of transient carbon turnover, and is presented in Fig. 3.21d. This summed pool represents a substantial portion of the transient carbon stores in the plants, but is not a complete picture, as other pools of compounds are also present in substantial amounts and turnover at high rates, e.g. amino acids (which were not determined here). Starch, being by far the largest carbon pool, determined the bulk of the variation in the total carbon turnover. Total carbon turnover was reduced in 35S:OtsA plants compared to wild type in 8-hour and 16-hour days by 43% and 46% respectively, while there was no difference in 12-hour days. The 35S:OtsB plants were not significantly affected in any daylength.

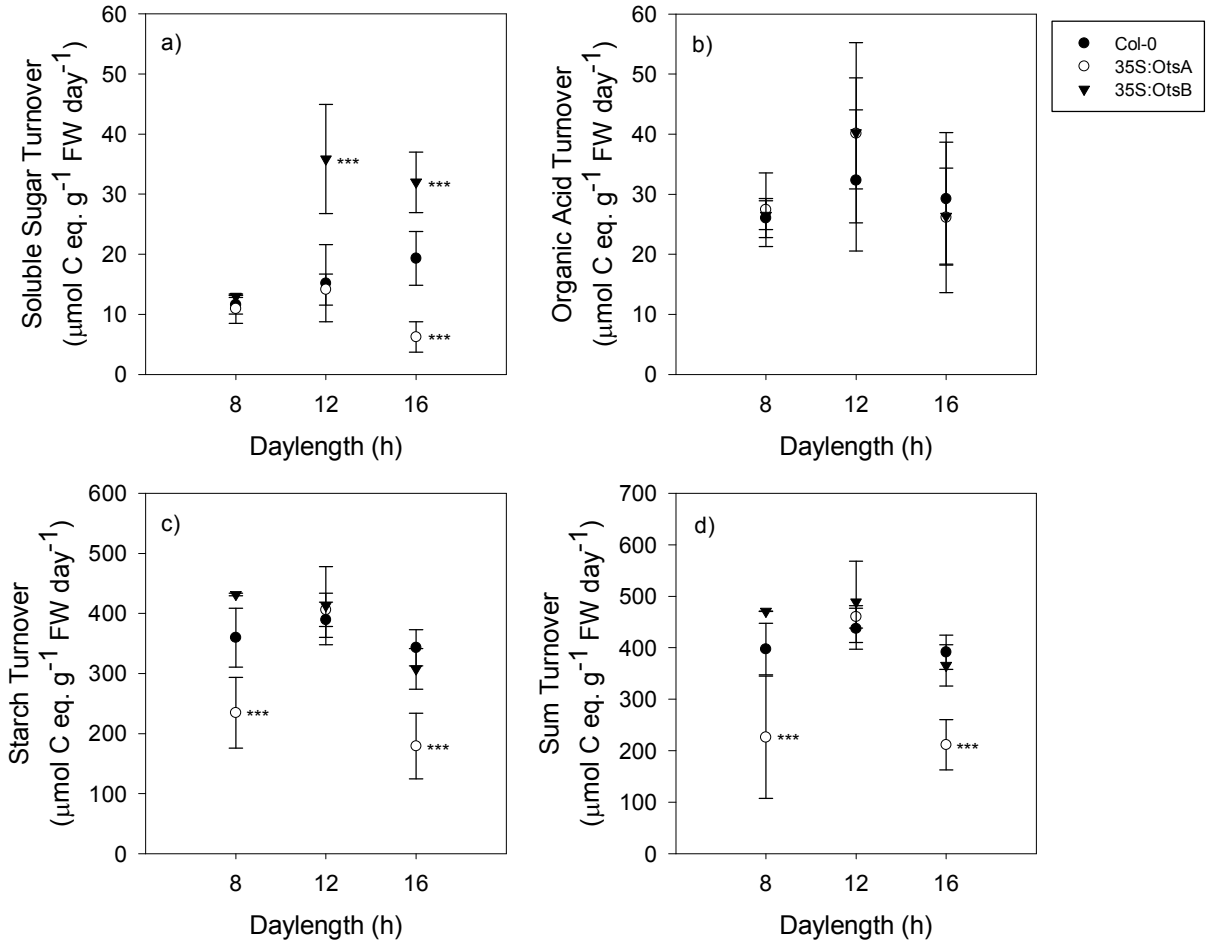

Fig. 3.21. Effects of constitutive modulation of trehalose-6-phosphate levels on diurnal turnover of central metabolite pools in three daylength regimes.
Diurnal turnover of metabolite pools in µmol C equivalents in rosettes of *Arabidopsis thaliana* wild type Col-0 and transgenic lines over-expressing bacterial OtsA and OtsB proteins under the control of the constitutive 35S promoter grown in three daylength regimes at a irradiance of 160 µE m^{-2} s^{-1} and a constant temperature of 20°C and harvested at the end of the day and end of the night. Significant differences (t-test with Holm-Sidak correction) from the wild type are shown as * $P < 0.05$, ** $P < 0.01$, *** $P < 0.001$. N= 5, bars are standard deviations.

3.3. Discussion.

The superficial visual phenotypes observed in the OtsA and OtsB over-expressors resemble those previously reported in analogous over-expressions in *Arabidopsis* (Schluepmann et al., 2003) as well as in other species such as in tobacco (Goddijn et al., 1997; Romero et al., 1997; Pellny et al., 2004). The superficial observation of strong phenotypes upon expression of both enzymes in the Col-0 and starchless *pgm* backgrounds indicate that the developmental effects of Tre-6-P modulation are not downstream of the documented role of Tre-6-P in starch metabolism. This supports a function of Tre-6-P as a specific developmental regulator.

When interpreting phenotypes of over-expressions driven by constitutive promoters the possibility of secondary phenotypes resulting from ectopic expression should not be ignored. The 35S promoter is a strong and ubiquitously expressed promoter (Kay et al., 1987). In addition, the expressed enzymes of bacterial origin presumably lack the regulation that the plant TPS and TPP proteins may be subject to, for example phosphorylation (Glinski and Weckwerth, 2005). When the OtsA enzyme is expressed under the 35S promoter, it may produce super-physiological amounts of Tre-6-P in cells/tissues where it would not normally be present. The constant unregulated flux may also override the normal regulation of Tre-6-P levels in cells which do produce it. The OtsB enzyme, on the other hand, should consume Tre-6-P where it is present and should thus be a more physiological manipulation. Another concern is that Tre-6-P levels are altered throughout the life of the plant, during which the plants may have adapted to the altered Tre-6-P levels and any observed phenotypes may be complex and contain many secondary effects, not directly related to Tre-6-P itself. This generally limits the strength of any conclusions that can be made from the analysis of these plants.

Few robust conclusions can be made from the morphological analysis of the transgenic lines in the wild type and *pgm* backgrounds. Any effect caused by Tre-6-P itself would be expected to drive opposing phenotypes in OtsA and OtsB plants with respect to the wild type. Such an effect could only be observed for cell densities, which are the inverse of cell size. Cell densities were the strongest contributors to the first principal component axis, which means that they account for a large portion of the major axis of morphological variation in the transgenic lines. The densities of both mesophyll and epidermal cells as well as stomata were also altered in a very coordinated way, the densities being highly correlated with each other. On one hand this may be expected as plant cells are immobile and cannot expand independently of their neighbours due to being fixed together. On the other hand, this suggests that Tre-6-P may drive changes in cell size through a general effect on organ size through cell size control. There also do not seem to be specific effects on the morphogenesis of particular cell types. Together these results suggest that Tre-6-P may be involved in organ size regulation, possibly through effects on cell sizes and cell expansion. The latter stages of leaf expansion, after cell division ceases, have been implicated in leaf size control through effects of the duration of leaf expansion on final cell size (Cookson et al., 2005).

Long days (high carbon) did not lead to an alleviation of the phenotype of 35S:OtsA plants and the phenotype was not stronger in short days (low carbon). Instead growth was consistently suppressed in all conditions. Similarly, short days did not lead to more growth in 35S:OtsB plants, which was instead observed in long days. Thus the hypothesis that the severity of phenotype in these plants may be rescued by altering their carbon status to levels more appropriate to their imposed Tre-6-P signal is not supported. Altered Tre-6-P strongly influenced the metabolism of these plants and this was more pronounced in long days in both genotypes. This suggests that the downstream effects of Tre-6-P are also dependent on metabolism.

The hypothesis that Tre-6-P signals the generation of "sun" or "shade" leaf morphology independently of light is not supported as no changes in leaf thickness were observed. The small change in the number of cell layers in the leaves of 35S:OtsA plants may be explained by the greatly decreased cell size in these plants. The number of cell layers in the leaf is not a definitive indicator of extra cell divisions and is not straightforward to assess. It is complicated by the fact that leaf cells, and the spongy mesophyll in particular, are not necessarily arranged as distinct layers. Cell layers were determined by counting the number of cell walls crossing perpendicular transects of leaf cross sections along the adaxial/abaxial axis. If cells are small and closer together the probability of a section passing through a cell may increase and this may be reflected in more cell layers being observed without a change in leaf thickness. The changes in leaf thickness were driven chiefly by the starchless *pgm* background. This is an interesting finding which will be explored in more detail and forms the basis of Chapter 5.

Superficially, high Tre-6-P appeared to strongly inhibit growth and decrease the size of leaves while low Tre-6-P appeared to have a mild inverse effect. This observation appears to be inconsistent with a proposed function of Tre-6-P as a signal of sugar status which regulates growth. As pointed out in the introductory chapter, plant growth is subject to tight regulation in response to available carbon supply (Smith and Stitt, 2007). Plants respond to conditions of low carbon availability by decreasing growth in order to conserve resources and avoid severe starvation (Stitt et al., 2007; Gibon et al., 2009). In high carbon and high sugar situations growth rates increase (Walter et al., 2009; Yazdanbakhsh and Fisahn, 2009, 2011). Thus, if Tre-6-P is a high-sugar signal the observed inhibition of growth would not be expected. Instead, it would be expected to stimulate growth. The results suggest that the effects of sugar status on growth may not be transduced through Tre-6-P. There are a number of other putative sugar sensing systems in plants (Rook et al., 1998; Moore et al., 2003; Smeekens et al., 2010). Moreover, a microarray study of inducible over-expressing lines of OtsA in Arabidopsis has revealed that the massive transcriptional reprogramming associated with manipulation of sucrose is not likely to be mediated by Tre-6-P (Martins, 2011).

The 35S:OtsA plants also retained large amounts of starch reserves instead of mobilising them for growth. The increased level of starch in 35S:OtsA plants is in line with previous studies and with the proposed function of Tre-6-P as an activator of starch synthesis (Kolbe et al., 2005; Lunn et al., 2006) and an inhibitor of starch degradation (Martins, 2011). The results presented here are in support seem to support these functions. The strong starch-excess phenotype at the end of the night suggests an inhibition of starch degradation and its mobilisation for growth. The decreased turnover of starch at night may partly explain the stunted growth phenotype of 35S:OtsA plants, as starch turnover has been shown to be strongly related to growth (Gibon et al., 2009) and starch-excess mutants which are impaired in starch degradation are also stunted in growth (Zeeman and Rees, 1999; Rasse and Tocquin, 2006). A study of a large panel of natural accessions of *Arabidopsis* has shown that slower-growing genotypes contained more starch than faster-growing ones at the end of the day and the end of the night (Sulpice et al., 2009), demonstrating the growth benefits of efficient mobilisation of reserves for growth.

Tre-6-P has been proposed to stimulate sugar utilisation for biosynthetic processes and growth, which stems from observations that plants with high Tre-6-P grow faster than wild type on sugar-containing media (Schluepmann et al., 2003). This may be due to the demonstrated inhibitory effect of Tre-6-P on SnRK1 (Zhang et al., 2009) and subsequent up-regulation of anabolic pathways and down-regulation of catabolic ones, which has been shown in a transcriptomic study (Paul et al., 2010). Under normal conditions high Tre-6-P may signal an abundance of sucrose and promote the conservation of starch reserves while stimulating sucrose utilisation for growth downstream. The 35S:OtsA transgenics are, however, constitutively perturbed in Tre-6-P regulation and, hypothetically, experience a constant high

sucrose signal. When sugar is super-abundant, such as on sugar-containing medium, this may lead to faster growth, as has been published (Schluepmann et al., 2003) but under normal conditions on soil a de-regulated carbohydrate utilisation may become unbalanced from supply and thus lead to exhaustion of carbohydrate pools and inhibition of growth (Smith and Stitt, 2007). This may be an explanation for the observed changes in soluble sugar contents in the lines – sugars are lower in 35S:OtsA plants because of higher consumption and a decreased supply due to a higher allocation to storage. However, the observation of a similar strong growth defect in the starchless *pgm* mutant, which has no starch stores, suggests that the inhibition of growth in these lines may also be due to other factors. For example 35S:OtsA lines had very small cells in both backgrounds, suggesting that cell expansion may be inhibited. The lines in both backgrounds also had much fewer cells in the leaf and may be unable to grow due to effects on cell division.

The daylength treatments may also be thought of as manipulations of carbon status, with carbon limitation in short days and an excess of carbon in long days (since growth did not increase further with daylength above 12h), similar to the previously published experiments on sugar media. However long days did not result in an alleviation of the growth phenotype in the 35S:OtsA line and instead more starch was retained while growth was consistently suppressed. There is however a fundamental difference between sugar treatments and plants grown on soil. When sugars are supplied exogenously, growth can occur independently of starch turnover as the sugars are always present and may overcome the depletion in sugar pools observed in these plants. Plants growing on soil in different daylengths must rely on photosynthesis and starch storage during the day and the mobilisation of reserves for growth at night. This again points to a role of starch storage and mobilisation in the phenotype of these plants.

In 35S:OtsB lines growth was stimulated only in long days, and this was the only condition where starch levels were significantly altered in this genotype, being lower. This suggests a lower allocation of carbohydrates to storage and more towards sugars. The levels of the latter were indeed highly elevated. The suppression of this growth enhancement in the starchless *pgm* mutant also suggests that it may be caused by effects on starch storage and/or mobilisation rather than by Tre-6-P directly. Upon closer investigation of 35S:OtsB plants the observed growth increase turned out to be due to very minor changes in the rate of growth and to be caused by an increase in the final size of leaves, which was due to an increase in cell size but not the number of cells. The high sugar content may exert an osmotic effect, which may explain the increased cell size in this line, however this is unlikely. Although it is impossible to assess the contribution of this change in sucrose content to osmotic pressure in the cell, the 2 μmol g^{-1} FW change in sucrose content translates to a maximum 2 mOsm change in osmolality assuming all the extra sucrose was in the symplast, which is probably not true, and the real value is likely to be lower. This is fairly minute compared to reported osmolalities of 300-400 mOsm in plant cells (Speer and Kaiser, 1991). Is not clear whether this is adequate to cause a sufficient effect on osmotic turgor to drive an increase in cell size.

In addition to decreased mobilisation of carbon due to starch accumulation, the efficiency of carbon use may also be decreased. It is puzzling how an upregulation of anabolic processes should lead to a severe stunting of growth, and not the opposite. The key may lie in the increased dry matter content in the leaves and the observation of very small cells in these plants may be an indication that a high rate of anabolic processes is occuring but the resulting biomass is not being expanded effectively during growth and thus leads to a high LDMC. The high dry matter content could not be explained by increased starch accumulation alone. A lack of cell (and biomass) expansion would decrease the amount of leaf area produced per unit biomass, which is reflected by SLA. The 35S:OtsA plants indeed had a much lower SLA which was not due to increased leaf thickness but to a high LDMC. Leaf area is directly proportional to light interception which drives photosynthesis. SLA, representing the amount of leaf area produced per unit biomass invested, effectively represents the return on

investment in leaf biomass and should be strongly related to growth. This is because when a unit of biomass is invested in extra leaf area, it pays itself off with more photosynthesis and growth, particularly in low-light environments and should clearly be advantageous. On the contrary, when biomass is concentrated in a smaller volume and a smaller leaf area, the same unit of photosynthetic capacity (chlorophyll, Rubisco etc), is exposed to as smaller amount of incident light, and therefore is less effectively used when light is limiting. Indeed, SLA has been shown to be a strong predictor of growth across many species and functional groups (Poorter et al., 1990; Reich et al., 1997; Wright and Westoby, 2000). Taken together, these data suggest that decreased cell expansion leads to less leaf area being produced per unit biomass investment as biomass is instead concentrated in a small volume of leaf. This is an inefficient use of carbon and biomass and results in less light interception per unit biomass. This may be another reason for decreased growth in these plants. The importance of leaf cell and biomass expansion for plant growth is analysed in more detail from a functional perspective in Chapter 5, where similar conclusions were reached.

Available and mobilised carbon may also be lost without being incorporated into biomass. Respiratory CO_2 loss and exudation of organic substances by roots are two ways that carbon can be lost from the plant. Analysis of inducible over-expression lines of OtsA yielded results consistent with altered glycolytic or anapleurotic fluxes, possibly through regulatory effects on pyruvate kinase and/or phosphoenolpyruvate carboxylase (PEPC) (Martins, 2011). Respiratory losses in herbaceous plants are typically 30-60% of gross daily fixed carbon (Poorter and van der Werf, 1998). The shoot alone respired an average of 28% of gross daily photosynthesis in a set of *Arabidopsis* accessions, which will be presented in Chapter 6, making respiratory carbon loss a very significant component of plant carbon balance. Respiration rates were measured in some of the lines. The 35S:OtsA plants in the starchless *pgm* background had a 43% higher rate of dark CO_2 efflux, measured in whole rosettes and expressed on an area basis than the *pgm* control, which is a large increase (data not shown). Such a large increase in respiration would be expected to have a large impact on plant carbon balance and would be expected to significantly affect growth.

PEPC catalyses the anapleurotic conversion of PEP to oxaloacetate, which is converted to malate by malate dehydrogenase (O'Leary, 1982). The 35S:OtsA plants had increased levels of organic acids, including malate. Plants exude organic acids from their roots to aid nutrient acquisition, stimulate soil microbial communities and overcome metal ion toxicities (Ryan et al., 2001). An estimate of carbon loss to rhizodeposition in grasses is 11% of net fixed carbon, a substantial flux (Jones et al., 2009). Since our OtsA over-expression is constitutive, if a similar effect on organic acid synthesis is present in roots, it may cause an increased loss of carbon through this mechanism. A 7-fold increase in organic acid exudation was observed when malate production was increased in roots by over expression of malate dehydrogenase in alfalfa (Tesfaye et al., 2001). It remains to be tested whether alterations in this flux contribute to the slow growth in 35S:OtsA plants.

The organic acids malate and fumarate are involved in many biochemical pathways and accumulate to high levels in the vacuoles of plant cells (Chia et al., 2000; Fahnenstich et al., 2007). Apart from their involvement in mitochondrial respiration, they may also have a function as a transient carbon store (Zell et al., 2010). Malate also accumulates in the vacuoles of plant cells as a counter-ion to balance the assimilation of nitrate (Kirkby and Knight, 1977). Organic acid levels in 35S:OtsA plants were consistently elevated while there was no effect on their diurnal turnover. This suggests that their up-regulation may be acting to compensate for an ion imbalance and is not the result of a decreased utilisation. Thus the accumulation of organic acids in the 35S:OtsA plants points to possible alterations in nitrogen metabolism. This warrants a closer investigation of nitrate metabolism in these lines.

The abundance of a metabolite at steady state is a balance between the rates of its synthesis and degradation. While OtsA over-expression increased Tre-6-P levels to high above wild-type levels, OtsB over-expressors did not have decreased Tre-6-P levels, which was confirmed in two experiments and in three daylengths. Thus Tre-6-P levels seemed to be strongly influenced by increases in its synthesis by OtsA while they seemed to be buffered from increased dephosphorylation by OtsB. An unaltered pool of Tre-6-P in 35S:OtsB plants can be possible if Tre-6-P production increases in parallel with the increased degradation flux. This suggests a negative feedback interaction between Tre-6-P and its biosynthesis. In this scenario, the increased dephosphorylation flux in 35S:OtsB plants would depress Tre-6-P levels, which would feed back to stimulate more Tre-6-P production, keeping the pool size constant. However, the Tre-6-P data from 35S:OtsB plants must be treated with caution, as the bacterial OtsB enzyme has a relatively low affinity for Tre-6-P, with a K_m of 2.5mM (Seo et al., 2000) and may not be very effective at dephosphorylating Tre-6-P at its estimated physiological concentrations in leaf cells of 1-15µM (J. Lunn, pers. comm). The over-expression of OtsB may only affect Tre-6-P levels in cells which contain high Tre-6-P levels. The meristematic regions and young leaf primordia have been shown to contain several-fold higher Tre-6-P levels than leaves (Wahl et al., personal communication), which is consistent with the localisation of TPS1 expression there (Ramon et al., 2009; Vandesteene et al., 2010). It is possible that some of the developmental phenotypes observed in 35S:OtsB lines may be related to decreased Tre-6-P in these regions. This decrease may not be observed in Tre-6-P measurements in whole rosettes as they represent only a small proportion of the total mass of the plant. As an outlook, Tre-6-P levels should be measured in the meristem and leaf primordia of 35S:OtsB lines.

The strong correlations between Tre-6-P and sucrose are in line with the proposed function of Tre-6-P as a sucrose-specific signal and similar correlations have been presented previously (Yadav, 2009). However the observed reciprocal alterations in the sensitivity of Tre-6-P to sucrose in the transgenic lines is a significant new finding. The relationships were altered not only because Tre-6-P levels were higher or lower, but mainly because sugar levels were also altered. This suggests that the sucrose-Tre-6-P interaction is not unidirectional and that Tre-6-P also feeds back to regulate sugar metabolism. In addition, the absolute levels of Tre-6-P were not altered in 35S:OtsB plants while sucrose levels were increased. Thus any effects in this genotype may not be due to Tre-6-P alone as it was not altered (however, see previous paragraph). This leads to a suggestion that Tre-6-P and sucrose act synergistically rather than Tre-6-P acting alone and the relationship (ratio) between the two metabolites may be more relevant than the amount of Tre-6-P itself. Such a scheme can be explained if Tre-6-P and sucrose are both effectors of an enzyme or of different enzymes in a single pathway.

The observed pattern of soluble sugar contents in the transgenic lines, and particularly that of sucrose, may be explained if Tre-6-P is seen as a feedback inhibitor of sucrose synthesis. The pathways for the synthesis of sucrose and trehalose are remarkably similar in plants. In the first step of sucrose synthesis, sucrose-6'-phosphate (Suc-6-P) is synthesised from fructose-6-phosphate and UDP-glucose by sucrose phosphate synthase (SPS). S6P is then dephosphorylated by sucrose phosphatase (SPP) to yield sucrose. SPP and TPP both belong to the haloacid dehalogenase superfamily of hydrolase enzymes and share several structural and mechanistic features (Lunn et al., 2000). Interestingly, SPS has a C-terminal SPP-like domain which is catalytically inactive (Lunn and Ap Rees, 1990) and has some resemblance to TPP enzymes (Lunn et al., 2000; Lunn and MacRae, 2003). A similar situation is seen in TPS, where inactive C-terminal TPP-like domains are present (Lunn et al., 2000; Lunn, 2007). The functions of these domains are still unclear. Lunn et al. (2000) suggested that the SPP-like domains of SPS may facilitate the formation of a complex with SPP. Class II TPS proteins, which have catalytically inactive TPS and TPP-like domains, have been suggested to function as regulatory subunits in a complex with TPS1 (Lunn, 2007), similar to what is seen in yeast (Bell et al., 1998) and possibly as Tre-6-P binding proteins (Lunn, 2007) although Tre-6-P binding has not been

demonstrated. Tre-6-P and Suc-6-P are structurally similar, which invites the possibility that they may have similar steric properties and binding kinetics. One possibility may be Tre-6-P binding to the SPP-like domain of SPS, which is very similar to TPP, to feedback-regulate sucrose synthesis in response to the Tre-6-P signal. Analogously, Suc-6-P, which is strongly linked to sucrose levels, may bind to the TPP-like domains of TPS and regulate Tre-6-P synthesis in response to sucrose. These are speculative, but exciting possibilities which may explain the observed two-way interaction between Tre-6-P and sucrose. These may be interesting directions for future research.

A second possibility for how Tre-6-P may regulate sucrose synthesis may be through SPP. This enzyme has been shown to be inhibited by sucrose in a competitive or partially-competitive manner (Hawker, 1967; Lunn et al., 2000). If Tre-6-P and sucrose act synergistically to inhibit this enzyme, the observed effects of altered Tre-6-P/sucrose ratio rather than Tre-6-P itself may be explained. In addition, SPP is strongly inhibited by trehalose, the inhibition being stronger than that by sucrose itself (Fieulaine et al., 2007). Trehalose may thus be an alternative feedback link between the trehalose pathway and sucrose synthesis.

3.4. Chapter summary.

In summary, a set of transgenic lines over-expressing enzymes of trehalose metabolism were created in *Arabidopsis* with the aim of altering the levels of Tre-6-P in the plants. Plants with highly elevated levels of Tre-6-P could be obtained by over-expression of OtsA. Over-expression of OtsB failed to produce an appreciable decrease in Tre-6-P levels, however these plants nevertheless exhibited phenotypic and metabolic alterations. In addition to the wild type background, over-expression lines in the starchless *pgm* mutant were also generated in order to distinguish starch-related and starch-unrelated phenotypes. Gross morphological phenotypes in the transgenic lines were similar to those published previously. Plants with high Tre-6-P were severely stunted and had small leaves while plants with low Tre-6-P were slightly larger and had larger leaves. Closer morphological examination of leaves in the lines found cell size to vary in a manner consistent with Tre-6-P being a regulator of cell size. Plants with high Tre-6-P had very small leaves with a decrease in cell number and very small cells. Plants with low Tre-6-P had larger leaves, which was driven by increased cell size only. The phenotypes of OtsA over-expressors were largely conserved in the starchless *pgm* background while there were differences in the phenotypes of OtsB plants depending on the background, suggesting that some of the effects are related to starch metabolism. An analysis of over-expression lines grown in three different daylengths found alterations in sugar metabolism consistent with a role of Tre-6-P as a feed back regulator of sucrose synthesis. Growth of 35S:OtsA plants was equally suppressed in all daylengths while the growth enhancement of 35S:OtsB plants was very mild and only evident in long days. Possible reasons for the growth suppression in 35S:OtsA plants are: i) lack of cell expansion suppresses leaf area production from biomass, negating the pay-back benefits of leaf area and light interception and ii) increased CO_2 losses due to de-regulated respiratory flux.

Chapter 4. Transgenic modulation of Tre-6-P in guard cells affects stomatal function

4.1. Introduction.

Stomata are pores on the surface of leaves which mediate the counter-current exchange of carbon dioxide and water vapour between the leaf and the atmosphere. The stomata consist of a pair of guard cells and their subtending subsidiary epidermal cells and form an adjustable pore through the epidermis of the leaf connecting the internal airspaces to the outside atmosphere. The guard cell wall is very specialised in structure and causes a change in cell shape when turgor pressure builds up inside the cell, and this results in a change in the size of the stomatal pore (Sharpe et al., 1987). The size of the pore determines its conductance to gases and is instrumental in regulating gas exchange.

Guard cells are a very specialised cell type adapted to sense and integrate multiple signals and regulate leaf function with great precision. Stomata open in response to light, low CO_2 concentration and high humidity as well as responding to changes in plant water status (Outlaw, 2003; Ache et al., 2010). The drought and stress-related hormone abscisic acid (ABA) is a strong modulator of stomatal function, causing rapid closing (Raschke, 1987). Red and blue light elicit two different signalling pathways in guard cells and result in different physiological responses.

The multiple signals sensed by stomata are integrated by a complex system of regulatory interactions. There is much evidence that the different signals are not processed by single transduction pathways and stomatal regulation has been modelled as a network (Li et al., 2006). There have been unverified suggestions that the regulatory network has scale-free properties (Hetherington and Woodward, 2003; Assmann, 2010) and exhibits a high degree of connectivity as well as the emergent properties of a high degree of redundancy and the ability to acclimate to external signals on a whole-network level. The latter conclusion originally stems from observations of different stomatal behaviour in response to the same stimuli in plants grown in different conditions (Talbott and Zeiger, 1996; Frechilla et al., 2002, 2004).

4.1.1. Stomatal movements.

Stomatal opening is driven by turgor buildup inside stomatal guard cells, which is brought about by the accumulation of large amounts of solute and the osmotic accumulation of water. During stomatal opening protons are actively extruded from the guard cell, hyper-polarising the plasma membrane and causing the inflow of K^+ ions through an inward-rectifying potassium channel which is specific to guard cells, KAT1 (Latorre et al., 2003). The ion buildup causes the osmotic inflow of water, building turgor within the cell. The large accumulation of positive ions in the cell requires anions to balance charges in order to maintain the membrane potential. The availability of inorganic anions in plants may be insufficient to maintain a charge balance in guard cells (Speer and Kaiser, 1991).

4.1.2. Metabolism in guard cells.

4.1.2.1. Malate.

Metabolism plays a crucial role both in the signalling aspect of stomatal regulation and in the mechanism of stomatal movements. A number of organic anions accumulate in guard cells during stomatal opening, presumably to be involved in charge balancing. Malate is the most abundant species

but citrate, aspartate and glutamate have all been demonstrated to be present and to increase in isolated stomata during opening (Allaway, 1973; Outlaw and Lowry, 1977). Guard cell malate concentration in open stomata on intact leaves of *Vicia faba* has been measured to be up to 10-fold higher than in closed stomata (Humble and Raschke, 1971; Assmann and Zeiger, 1987). Epidermal malate content correlates with stomatal aperture in isolated epidermis (Van Kirk and Raschke, 1978; Allaway, 1981). Guard cells can take up labelled malate from external solutions (Dittrich and Raschke, 1977) and it has been proposed that the leaf mesophyll and subsidiary epidermal cells are a source of malate during stomatal opening (Araújo et al., 2011).

Malate accumulation can also occur independently of the mesophyll in isolated epidermal strips with no external source of malate (Raschke and Schnabl, 1978) and fixation of $^{14}CO_2$ into malate by individual guard cells is well documented (Dittrich and Raschke, 1977; Willmer and Rutter, 1977). Malate accumulated by guard cells during stomatal opening in the absence of the mesophyll thus seems to be of mainly endogenous origin. The malate seems to originate from carbon skeletons derived from starch breakdown in the guard cell chloroplast and formed through the PEP carboxylase pathway (Outlaw and Manchester, 1979; Vavasseur and Raghavendra, 2005). There is evidence that decreasing leaf malate content by over-expression of a malate-consuming enzyme impairs stomatal function (Laporte et al., 2002). The role of malate is stomatal opening is somewhat redundant, as inorganic ions can substitute for it when they are available (Raschke and Schnabl, 1978; Van Kirk and Raschke, 1978).

During stomatal closing malate is removed from the guard cell mainly through rapid export (Dittrich and Raschke, 1977), although some flux from malate to starch has been demonstrated in closing stomata (Willmer and Rutter, 1977). Modulation of ion channel activity by external malate in guard cells has been implicated in guard cell CO_2 sensing (Assmann, 1999; Hedrich et al., 2001; Hanstein and Felle, 2002).

4.1.2.2. Sucrose.

Neutral sugars also accumulate as osmolytes in guard cells during stomatal opening. It has been suggested that inorganic cations and sugars have distinct functions as osmolytes in guard cell turgor regulation has been suggested (Lu et al., 1995; Talbott and Zeiger, 1998). In a study of *Vicia* faba stomatal opening in the morning was shown to be driven by potassium uptake balanced by malate while after midday there is a switch to sucrose as the main osmoticum (Talbott and Zeiger, 1996, 1998). Starch breakdown and guard cell photosynthesis can contribute to the formation of sucrose in guard cells (Talbott and Zeiger, 1993) but do not appear to be sufficient to produce the amount of sucrose needed to support stomatal opening (Reckmann et al., 1990; Lu et al., 1997; Outlaw and De Vlieghere-He, 2001). Sucrose accumulating in guard cells has been shown to originate from carbon fixed in the mesophyll in labelling studies (Lu et al., 1997). The import of sugars from the apoplast into the guard cell has the capacity to support stomatal opening (Ritte et al., 1999) and may be an alternative solute to the potassium malate model of guard cell turgor generation.

4.1.2.3. Starch.

Guard cells are also highly specialised with respect to starch metabolism. In contrast to the pattern normally seen in leaves, guard cells have a reversed diurnal starch cycle and accumulate starch at night and break it down during the day (Outlaw and Manchester, 1979; Talbott and Zeiger, 1993). The mechanism of activation of starch synthesis at night is poorly understood in guard cells, however its breakdown in the light is brought about by two mechanisms: starch is broken down in the light by a

guard cell specific β-amylase (BAM1) which is redox activated in the light by thioredoxin *f* (Sparla et al., 2006; Valerio et al., 2011). The malate formed from starch breakdown is converted to malate in a series of reactions with the penultimate step catalysed by PEPC. This enzyme is activated through regulatory phosphorylation in response to blue light (Du et al., 1997; Outlaw et al., 2002), which alters its allosteric regulation properties and increases the flux to malate (Zhang et al., 1994). Malate formation seems to be the only destination of carbohydrates released from starch during light-stimulated stomatal opening. The starchless *pgm* mutant shows impaired stomatal opening in epidermal strips which can be restored by supplying chloride (Lasceve et al., 1997). Inhibition of starch degradation in a knockout mutant of the guard cell BAM1 was also shown to affect stomatal opening (Valerio et al., 2011).

4.1.3. Stomatal light response.

Stomata open in response to light. The stomatal response to light consists of two separate but possibly interacting mechanisms: the red-light and blue-light responses. The opening response elicited by red light requires high intensity light and is driven by accumulation of sucrose as the osmoticum and does not lead to malate production or starch degradation (Talbott and Zeiger, 1993). There have been many suggestions that photosynthesis mediates the sensing of red light either directly (Poffenroth et al., 1992; Olsen et al., 2002; Zeiger et al., 2002) or through its effects on leaf CO_2 concentrations (Roelfsema et al., 2002; Messinger et al., 2006) – see next section. The role of photosynthesis has been challenged by studies on plants with severely impaired photosynthesis, which show normal stomatal function and red-light responses (von Caemmerer et al., 2004; Baroli et al., 2008), suggesting a different sensing mechanism and that photosynthetic sucrose production is not absolutely necessary for stomatal opening.

The blue light response, in contrast, is mediated by the phototropin blue-light photoreceptors (Kinoshita et al., 2001; Talbott et al., 2003), is activated at very low fluence rates of blue light and specifically stimulates starch breakdown and malate production but not sucrose accumulation (Poffenroth et al., 1992; Talbott and Zeiger, 1993).

4.1.4. Stomatal CO_2 response.

Another environmental parameters strongly influencing stomatal movements is carbon dioxide concentration. Stomata open in response to low CO_2 concentration in order to let more CO_2 into the leaf for photosynthesis. High CO_2 concentrations elicit stomatal closure. The sensing and signalling mechanisms behind the stomatal response to CO_2 are distinct from the responses to light. The sensing of CO_2 in guard cells seems to involve the catalytic activity of carbonic anhydrase (Hu et al., 2010) and cytosolic Ca^{2+} transients (Schroeder et al., 2001; Young et al., 2006). An involvement of malate as a second messenger in stomatal CO_2-sensing has long been proposed (Hedrich and Marten, 1993; Hedrich et al., 2001; Vavasseur and Raghavendra, 2005). This has been supported recently by findings that a plasma membrane dicarboxylate channel SLAC1 localised in guard cells (Negi et al., 2008) and an ABC malate importer AtABCB14 (Lee et al., 2008) are essential for the CO_2 response of stomata.

A strong involvement of ABA-signalling in the stomatal CO_2 response has been shown. Impaired CO_2 responses have been measured in the ABA-insensitive mutants *abi-1* and *abi-2* (Webb and Hetherington, 1997) and *gca2* (Young et al., 2006), but not in some others (Mustilli et al., 2002). Stomatal CO_2 and ABA signalling pathways thus seem to converge and to share some components. Links between ABA and the malate flux have also been identified. ABA inhibits the phosphorylation of PEPC and malate accumulation in guard cells (Du et al., 1997). Mutants lacking the malate export channel SLAC1 were also impaired in stomatal closing in response to ABA (Vahisalu et al., 2008) and

were CO_2-insensitive (Negi et al., 2008), suggesting that the effects of ABA and/or CO_2 signalling may be mediated by malate transport downstream. Impaired CO_2 responses of stomata have been described in loss of function mutants of a nitrate transporter (Guo et al., 2003), a calcium-independent protein kinase specific to guard cells (Hashimoto et al., 2006) and, in a C_4 species, the photosynthetic isoform of PEPC (Cousins et al., 2007).

Stomatal opening and closing are dynamic and relatively rapid processes. The metabolic conversions required during stomatal movements necessitate rapid filling and draining of large pools of metabolites. This requires large fluxes and their tight dynamic regulation to produce the output of the system – changes in stomatal conductance. The guard cells are thus are good model not only for the study of cellular signalling, but are also a unique system for the study of metabolic regulation.

4.1.5. Possible role of trehalose and/or Tre-6-P

As trehalose is a known stress protectant, there have been many attempts to increase trehalose production in plants with the aim of achieving stress tolerance. These studies have expressed bacterial, yeast as well as plant genes encoding TPS and TPP proteins under the control of constitutive, tissue specific and stress-inducible promoters as well as intra-cellular targeting approaches. Tolerance to drought stress could be achieved in several species (Holmstrom et al., 1996; Pilon-Smits et al., 1998; Jang et al., 2003; Almeida et al., 2007; Karim et al., 2007), however the phenotypes could not always be attributed to trehalose as it rarely accumulated to substantial degrees due to the presence of trehalase, which degrades trehalose to glucose (Goddijn et al., 1997; Frison et al., 2007). This implicated its precursor trehalose-6-phosphate as the cause of the stress tolerance.

Alterations in stomatal function have been proposed as one of the mechanisms of drought tolerance in these lines (Gaff, 1996). An involvement of Tre-6-P in stomatal function may be hypothesised as Tre-6-P is involved in sensing sucrose and regulating starch metabolism while starch and sucrose are key players in the specialised metabolism and the function of guard cells. Transcripts encoding the catalytically active TPS1 and non-catalytic class II TPS's (*or* non-catalytic TPS-like proteins) have been detected in guard cells (Leonhardt et al., 2004). The TPS1 protein has been detected in guard cell protoplasts in a proteomic study (Zhao et al., 2008). Unpublished evidence indicates active expression of TPP's as well as trehalase in *Arabidopsis* stomata (Lopez, 2011). Plants homozygous for the mutant allele of Tps1 have also been shown to have defective ABA responsiveness of stomata (Gómez et al., 2010).

The evidence for an involvement of stomata in the drought-tolerant phenotypes of trehalose-producing plants comes from water-loss experiments. Transgenic potato plants expressing a yeast TPS were shown to retain water for longer during drought in the whole plant and in detached leaves during desiccation (Stiller et al., 2008), with similar results reported in tobacco (Gaff, 1996; Holmstrom et al., 1996). Such an effect was not evident in all studies however (Romero et al., 1997; Almeida et al., 2005; Almeida et al., 2007). A direct involvement of stomata is also not always evident as, for example, water was retained even though stomata stay open (Stiller et al., 2008) and drought tolerance (protection of photosynthetic function) was observed even though stomata stayed open (Almeida et al., 2007). The interpretation of the results from these plants is also complicated due to the often-severe developmental phenotypes observed in plants over-expressing TPS enzymes (Goddijn et al., 1997; Romero et al., 1997; Schluepmann et al., 2003). These have been shown to affect stomatal densities ((Stiller et al., 2008), see also Chapter 3). The situation is further confounded by the presence of severe metabolic alterations in such plants (Pellny et al., 2004) making it difficult to separate the effects of trehalose on stomatal function from the pleiotropic effects as there is known cross-talk between leaf metabolism and stomatal function.

4.1.6. Aims of the chapter.

These previous studies strongly suggest that trehalose metabolism plays an important, but so far poorly characterised, role in stomatal function. To shed more light on this, stomatal function was investigated using *Arabidopsis* plants engineered to overexpress the *E. coli* TPS (*OtsA*) and TPP (*OtsB*) enzymes under the control of either the constitutive 35S promoter or the stomatal-specific MYB60 promoter. This chapter documents the isolation and characterisation of MYB60:OtsA and MYB60:OtsB transgenic lines. The Gus reporter gene was used to investigate the specificity of MYB60 promoter expression. The patterns of starch accumulation in guard cells were examined microscopically and stomatal behaviour in response to light and CO_2 are assessed using dynamic gas exchange measurements. The contribution of stomata to plant water use efficiency is then assessed by measurements of carbon isotope fractionation. Finally, the performance of the plants under controlled water-limiting conditions was assessed to investigate whether alterations in stomatal function lead to improved plant performance.

4.2. Results.

4.2.1 Screening of lines.

T_1 MYB60:OtsA transformants presented a severe growth and developmental phenotype. 18 out of 20 retained plants were severely stunted, with very small, dark-green leaves with an abnormal shape (Fig. 4.1). All plants flowered and produced seed, although seed yields were low. MYB60:OtsB transformants were superficially indistinguishable from the MYB60:Gus control transformants. In subsequent generations the severe phenotype seen in the MYB60:OtsA lines was no longer apparent and the plants closely resembled wild types.

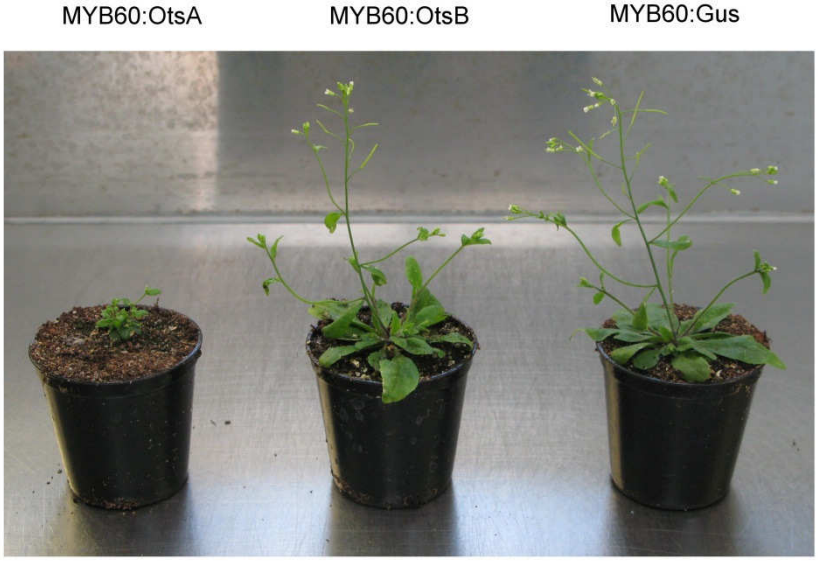

Fig. 4.1 Phenotypes of first generation stomatal-specific transformant plants.
First-generation primary transformants of *Arabidopsis thaliana* Col-0 harbouring constructs expressing bacterial OtsA, OtsB and β-glucuronidase under the control of the MYB60 stomatal-specific promoter from *Arabidopsis thaliana*.

Expression of trans-genes was detected in the lines by RT-PCR analysis of leaf RNA with 25 cycles of amplification. *OtsA* and *OtsB* transcripts could be detected in leaves of the respective homozygous lines. Fig. 4.2 shows the detection of the transcripts in the transgenic MYB60 lines and 35S positive controls by electrophoresis on agarose gels. All three *OtsA* lines contained the *OtsA* transcript, with one line (#14) showing stronger expression than the others. Both OtsB lines contained detectable *OtsB* transcript. RNA was treated with DNase prior to reverse-transcription to remove contaminating genomic DNA. Control PCRs were carried out with equivalent amounts of RNA that had not been reverse transcribed, and gave no detectable product, indicating the absence of residual genomic DNA.

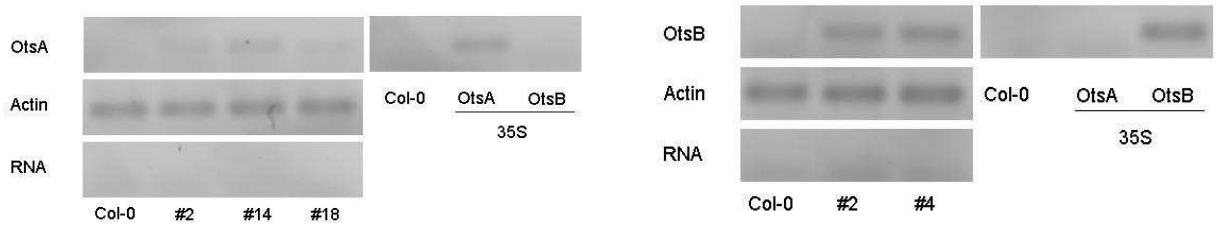

Fig. 4.2 Detection of trans-gene expression in stomatal-specific transgenic lines using RT-PCR. Leaves of MYB60 stomatal promoter-driven transformants harbouring the OtsA and OtsB genes were analysed by RT-PCR with *OtsA* and *OtsB* gene-specific primers. Actin10 is used as an amplification and loading control, in lanes labelled RNA, non-reverse transcribed RNA at equivalent dilution was loaded as a control for genomic DNA contamination. 35S:OtsA and 35S:OtsB lines were used as positive controls. PCR was run for 25 cycles. Electrophoresis was conducted on 1% agarose gel in TAE buffer. Gels were stained with GelRed for visualisation.

4.2.2. MYB60:Gus expression.

Strong Gus-staining could be detected in MYB60:Gus lines after as little as three hours of incubation with reaction mixture (Fig. 4.3). Gus staining was strongly localised in stomatal guard cells. Expression of the promoter seemed to be activated only in mature guard cells. In younger developing leaves, Gus staining appeared in the distal regions of the leaves, corresponding to the oldest and most mature sections of the leaf. Weak staining was observed in leaf veins.

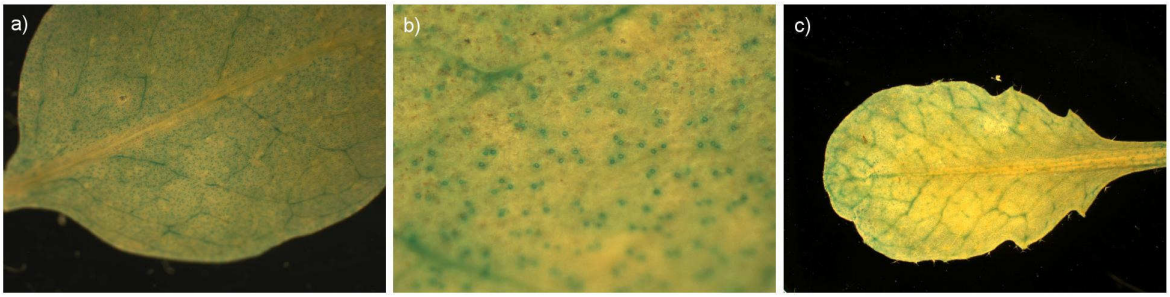

Fig. 4.3 Cell-specificity of MYB60 promoter expression in Arabidopsis leaves. Detection of Gus-reporter gene expression driven by the MYB60 stomatal-specific promoter from *Arabidopsis thaliana* by histochemical staining with X-gluc. A) – mature leaf showing staining in stomata and background staining in leaf veins, b) close-up of mature leaf, showing staining in stomata, c) young expanding leaf showing staining in stomata on distal portions of the leaf and in veins.

4.2.3. Guard cell starch.

Starch was visible in guard cells of epidermal strips fixed in ethanol:acetic acid or hot 80% ethanol and stained with Lugol iodine solution (Fig. 4.4). Boiling in hot ethanol appeared to improve the visibility of starch compared to ethanol:acetic acid fixation at room temperature. Guard cells of wild type plants contained substantial starch when sampled 5 hours into the light period. Almost no starch was visible in guard cells of 35S:OtsA as well as MYB60:OtsA plants. The 35S:OtsB and MYB60:OtsB plants appeared to have similar amounts of starch to the wild type, however their starch grains appeared to be larger and more densely staining.

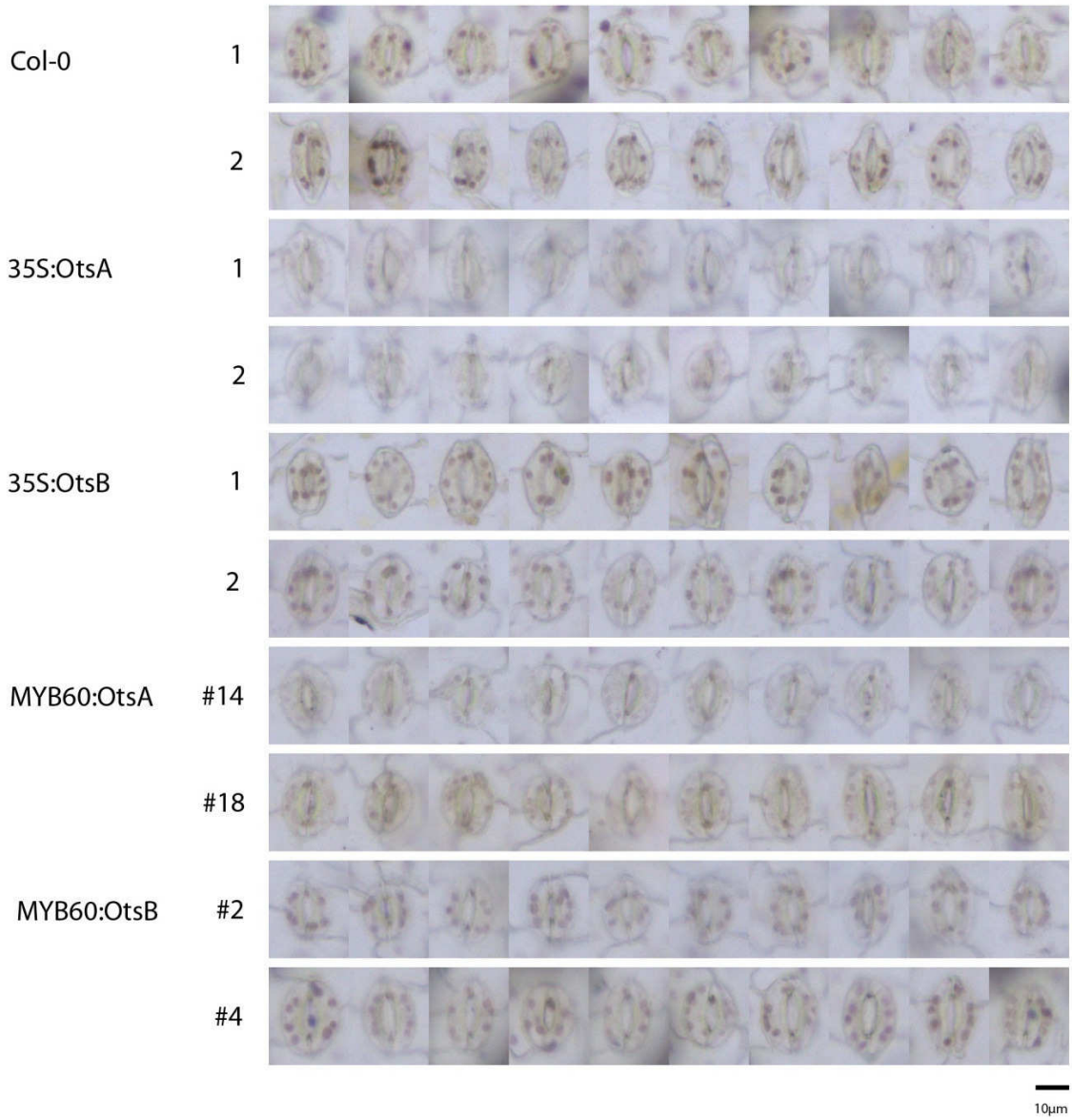

Fig. 4.4 Guard cell starch accumulation in transgenic lines.
Stomata stained with Lugol-iodine in fixed abaxial epidermal strips obtained from mature leaves of transgenic lines harbouring constructs which express bacterial OtsA and OtsB genes from constitutive 35S and stomatal-specific MYB60 promoters in *Arabidopsis*, grown in parallel in 8h days and sampled 5 hours into the light period at 35 days after germination. Starch is visible as a dark-blue coloration. For wild type Col-0 and 35S transgenics stomata from two separate plants of each genotype are displayed (labelled 1 and 2). For MYB60 transgenics stomata from single plants from two separate insertional lines are displayed. Stomata were chosen at random.

4.2.4. Stomatal function.

4.2.4.1. Stomatal opening in saturating light.

The function of stomata in the transgenic lines was assessed using sensitive measurements of CO_2 and water vapour exchange on intact leaves in various conditions. Impairments in metabolic capacity in guard cells may be expected to limit the speed of maximal stomatal opening. In order to assess the ability of stomata to open rapidly from a closed state plants were kept in the dark until the time of measurement and a saturating irradiance of 1000 µE m^{-2} s^{-1} was applied to elicit a strong opening response and stomatal conductance was recorded every 60 seconds for 50 minutes. Fig. 4.5 shows the traces of stomatal conductance in the dark and during stomatal opening.

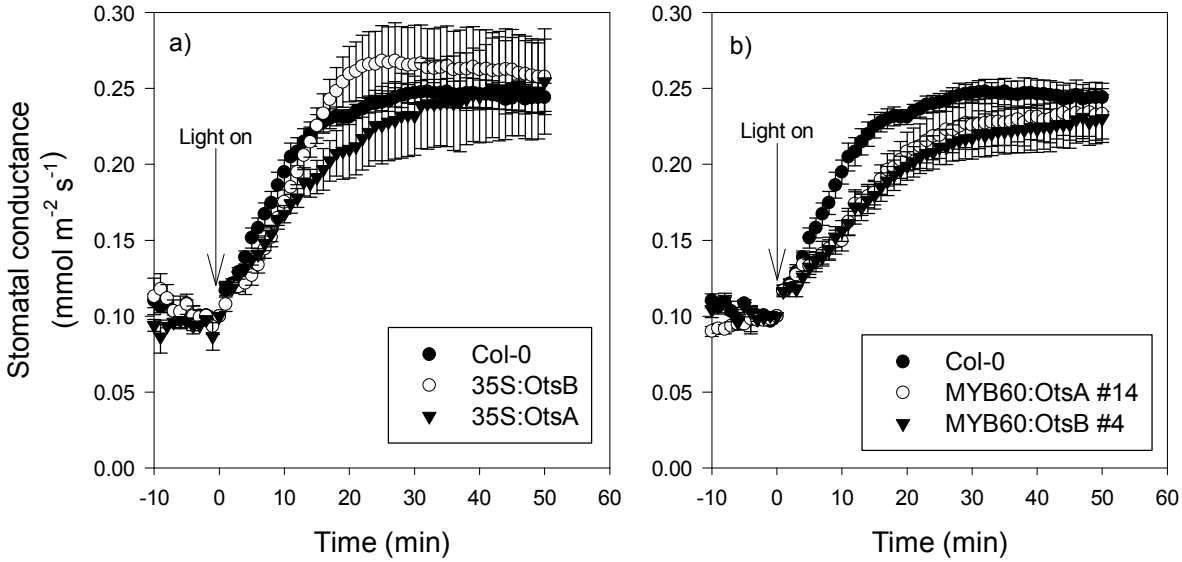

Fig. 4.5 Stomatal opening in response to saturating light in constitutive 35S (a) and stomatal-specific MYB60 (b) transgenics.
Plants were dark-adapted overnight. Stomatal conductance was measured at 60-second intervals. Light at 1000 µE m^{-2} s^{-1} irradiance was switched on at the time point indicated by arrow. Each point is a mean of 6 measurements on different plants with the exception of 35S:OtsA, where four plants were measured. Bars are standard error. Standard error was used in this graph (as an exception) for clarity purposes. Statistical analysis in text reveals whether differences are significant.

Stomatal conductance in the dark averaged 0.07 mmol m^{-2} s^{-1} and there were no differences between genotypes. All traces in Fig. 4.5 were normalised to start at 0.1 mmol m^{-2} s^{-1} for comparison. Saturating light of 1000 µE m^{-2} s^{-1} elicited a strong stomatal opening response during which stomatal conductance almost tripled in the wild type. Stomatal conductance became stable at the new steady state after 15-20 minutes.

35S and MYB60 genotypes of both OtsA and OtsB genes had significantly lower rates of stomatal opening than wild type (Fig. 4.6a). MYB60:OtsA exhibited the lowest opening rate which was 56% lower than the wild type while in MYB60:OtsB it was 48% lower than wild type. The 35S lines exhibited smaller reductions in stomatal opening, with 35S:OtsA more severely affected. Consequently, all genotypes took longer to reach their final stomatal conductance, however the differences in the half time of stomatal opening were not significant (not shown).

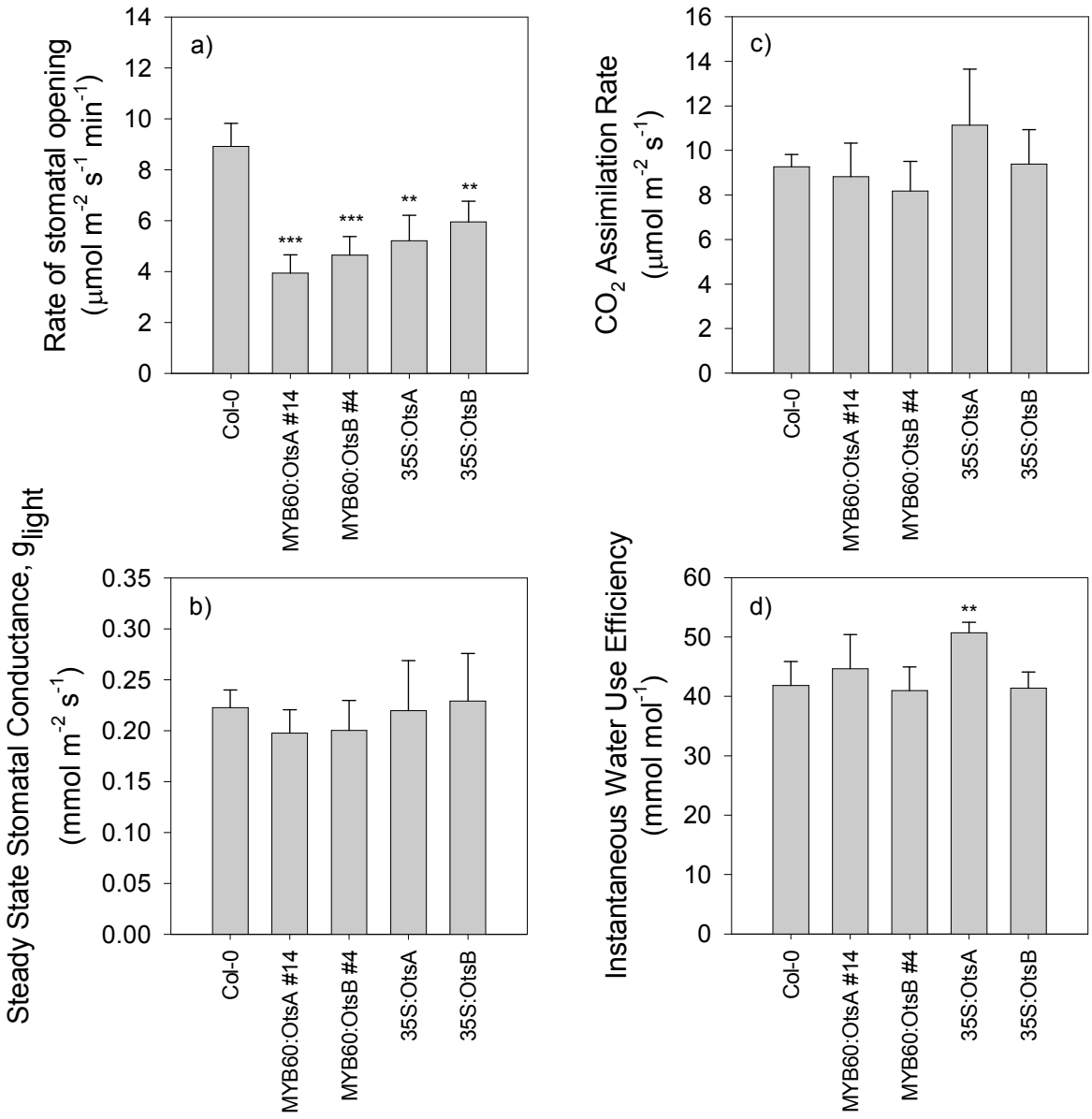

Fig. 4.6. Rate of stomatal opening (a), stomatal conductance at steady state in saturating light (b), rate of CO_2 assimilation (c) and instantaneous water use efficiency of photosynthesis (d) in constitutive 35S (a) and stomatal-specific MYB60 (b) transgenics.
Significant differences (t-test with Holm-Sidak correction) from the wild type are shown as * $P < 0.05$, ** $P < 0.01$, *** $P < 0.001$. N=6. Bars are standard deviations.

While the transgenic genotypes had lower rates of stomatal opening, they did not differ from wild type in the extent of opening in response to high light and reached similar final operating stomatal conductance at steady state (g_{light}) in saturating light (Fig. 4.6b). There were no significant differences in the rate of photosynthesis at steady state in saturating light in any genotype relative to wild type Col-0 however the statistical power of the test was low due to high variance (Fig. 4.6c). Instantaneous water use efficiency of photosynthesis, defined as the ratio of photosynthetic rate to stomatal conductance (A/g, Fig. 4.6d) did not differ significantly from wild type in any genotype with the exception of the 35S:OtsA line, which had a 21% higher water use efficiency than the wild type. There was a small increase in the MYB60:OtsA line, but this was not significant.

4.2.4.2. Response to low CO_2.

Stomatal opening in response to low CO_2 was also investigated. After the plants reached a steady state operating stomatal conductance in saturating light the CO_2 concentration in the sample chamber was changed from 400 to 50ppm and stomatal conductance tracked for a further 40 minutes. Fig. 4.7 shows the traces of stomatal opening following the application of low CO_2 in high light.

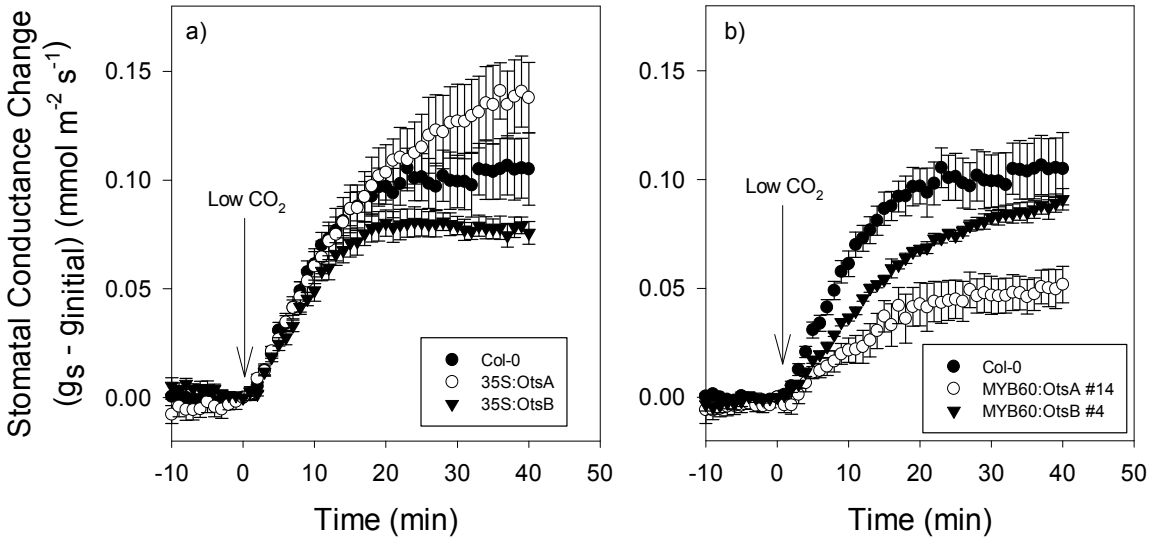

Fig. 3.7. Stomatal opening in response to low ambient CO_2 concentration in constitutive 35S (a) and stomatal-specific MYB60 (b) transgenics. Leaves at steady state under an irradiance of 1000 µE m^{-2} s^{-1} were exposed to air with 50 µmol mol^{-1} CO_2 concentration and stomatal conductance tracked at 60 second intervals. Each point is a mean of 6 different plants. Bars are standard error. Standard error was used in this graph (as an exception) for clarity purposes. Statistical analysis in text reveals whether differences are significant.

When the CO_2 concentration was lowered to near-compensation point in high light, stomata responded by opening further. Stomatal conductance reached a new steady state after 18-20 minutes in the wild type. This increase in stomatal conductance was approximately half of that elicited by high light treatment (Fig. 4.5) The stomatal response of 35S lines could not be distinguished from the wild type with statistical significance (Fig. 4.7a). The increase in stomatal conductance was attenuated in MYB60:OtsA plants and was less than half that of wild type plants ($P<0.001$, Fig. 4.7b). Stomata of MYB60:OtsB plants opened slower than wild type but reached equivalent stomatal conductance at the end of the 40 minute measuring period.

4.2.5. Dry Matter Carbon Isotope Fractionation.

Two stable isotopes of carbon exist in nature – ^{12}C and ^{13}C. Isotope fractionation consists of a number of physical processes which cause the abundance of ^{13}C in particular materials to deviate from its natural abundance of 1.109% of total carbon. Rubisco fractionates against $^{13}CO_2$ during its catalysis (Roeske and O'Leary, 1984). CO_2 containing the heavier ^{13}C isotope also diffuses slower than the lighter $^{12}CO_2$, which causes some fractionation to occur during CO_2 diffusion into the leaf through the gas and liquid phases in the leaf (O'Leary, 1981). The isotopic composition of carbon fixed through photosynthesis is an indication of the CO_2-conditions prevailing around Rubisco during carbon fixation. This is strongly influenced by stomatal conductance and in turn directly influences the water use efficiency of photosynthesis (Farquhar et al., 1982; Farquhar and Richards, 1984). The abundance

of ^{13}C in plant matter is a robust indicator of stomatal function integrated over the growth period of the plant and is thus an important tool in the study of stomata and water use.

In order to assess the long-term function of stomata in the transgenic lines, plants were grown in a greenhouse away from any artificial sources of CO_2 and mature leaf material collected and dried for analysis by isotope-ratio mass-spectrometry (IR-MS). In this technique dry plant material is incinerated at high temperature and the isotopic composition of the evolved CO_2 is measured. The starchless *pgm* mutant was also included for comparison as it has been demonstrated previously to have impaired stomatal function (Lasceve et al., 1997), but no isotope fractionation data has been published previously for this mutant.

Fig. 4.8 shows the $\delta^{13}C$ values of the wild type and the transgenic plants, along with the starchless *pgm* mutant. The units of $\delta^{13}C$ are per mil (‰) which is equivalent to parts per thousand and are expressed relative to the isotope composition of a universal standard, the fossil rock Pee Dee Belemnite. Lower (more negative) values indicate depletion in ^{13}C, which occurs when the kinetic fractionation during carboxylation by Rubisco dominates the isotopic fractionation of the leaf because the diffusional limitation by stomata is low. Higher (less negative) values indicate relative enrichment in ^{13}C and occur when CO_2 supply is restricted by low stomatal conductance, causing more ^{13}C to accumulate in inorganic carbon pools in the leaf and to be fixed into biomass.

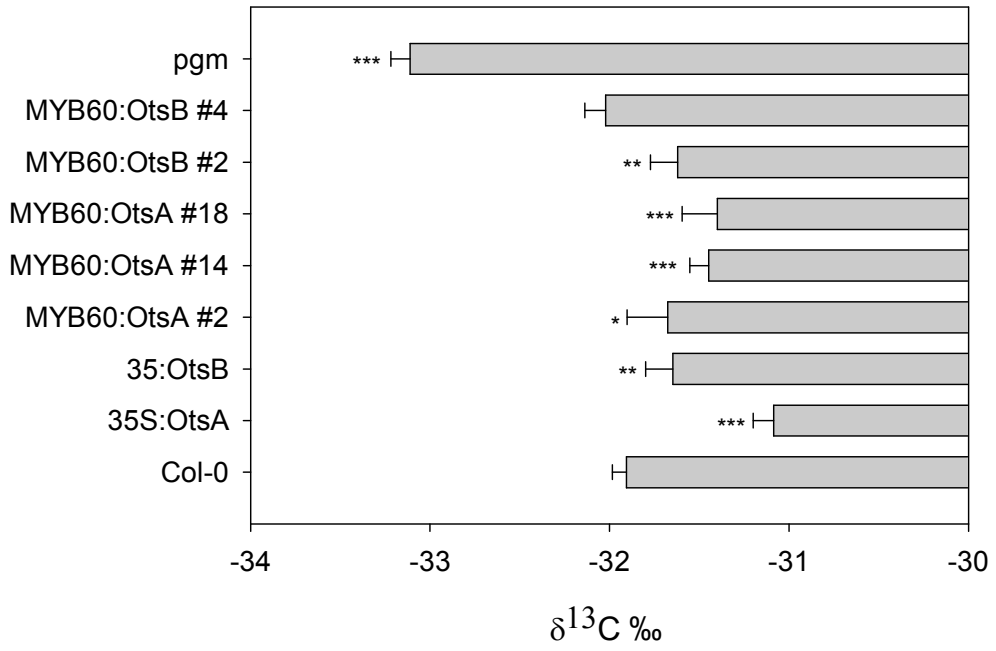

Fig. 4.8 Carbon isotopic signature of dry matter ($\delta^{13}C$) in constitutive 35S and stomatal-specific MYB60 transgenics.
Transgenic lines harbouring constructs which express bacterial OtsA and OtsB genes from constitutive 35S and stomatal-specific MYB60 promoters in *Arabidopsis thaliana* were grown in well-watered conditions in a greenhouse in 12-hour days. Significant differences (t-test with Holm-Sidak correction) from the wild type are shown as * $P < 0.05$, ** $P < 0.01$, *** $P < 0.001$. N=6. Bars are standard deviations.

The dry matter of wild type plants was strongly depleted in ^{13}C, with average $\delta^{13}C$ values of -31.9‰. Small but highly statistically significant differences could be observed in several of the transgenic lines. 35S:OtsA lines were enriched in ^{13}C relative to wild type (-31.1‰, $P<0.001$). 35S:OtsB plants were also slightly ^{13}C-enriched relative to wild type (-31.6‰, $P=0.004$). The three lines harbouring the

MYB60:OtsA construct were also enriched in ^{13}C. The strongest effect was observed in the stronger-expressing lines #14 and #18 (-31.4‰, P<0.001) while the weaker expressing line #2 showed a more modest effect (-31.7‰, P=0.01). Among the lines containing the MYB60:OtsB construct, line #2 was significantly enriched in ^{13}C (-31.6‰, P=0.003) while line #4 was not significantly different from the wild type (-32.0‰, P=0.197). The starchless *pgm* mutant had an isotopic signature which was significantly more depleted in ^{13}C than the wild type (-33.1‰, P<0.001).

Using the robust mathematical background of $^{12}C/^{13}C$ fractionation associated with leaf photosynthesis (Farquhar et al., 1982), the average operating ratio of intercellular/ambient CO_2 concentration (C_i/C_a ratio) could be derived from the $\delta^{13}C$ values (Table. 4.1). The C_i/C_a ratio is an indication of the diffusional limitation exerted by stomata. In the absence of any stomatal resistance there would be no CO_2 concentration gradient across stomata and the ratio would be 1. Resistance to diffusion imposed by stomata causes a concentration gradient to form in the presence of a flux (photosynthesis), as the CO_2 inside the leaf is depleted. The lower the ratio, the higher the CO_2 concentration gradient and the higher the diffusional limitation. The C_i/C_a ratio is inversely proportional to the water use efficiency of photosynthesis.

There were mild but significant reductions in derived C_i/C_a ratio in all transgenic genotypes relative to the wild type value of 0.77. The lowest value was in 35S:OtsA, where it was 0.738 (P<0.001). All MYB60:OtsA lines and one MYB60:OtsB line (#2) exhibited intermediate values while MYB60:OtsB line #4 was not altered. The *pgm* mutant had a significantly higher operating C_i/C_a ratio of 0.81 (P<0.001).

	$\delta^{13}C$ ‰		C_i/C_a ratio	
	Mean	SD	Mean	SD
Col-0	-31,905	0,079	0,770	0,003
35S:OtsA	-31,086***	0,113	0,738***	0,004
35S:OtsB	-31,646**	0,153	0,760**	0,006
MYB60:OtsA #2	-31,675*	0,227	0,761*	0,009
MYB60:OtsA #14	-31,446***	0,106	0,752***	0,004
MYB60:OtsA #18	-31,399***	0,196	0,750***	0,008
MYB60:OtsB #2	-31,620**	0,152	0,759**	0,006
MYB60:OtsB #4	-32,022	0,115	0,774	0,005
pgm	-33,110***	0,108	0,817***	0,004

Table. 4.1 Carbon isotopic signature in dry matter ($\delta^{13}C$) and inferred C_i/C_a ratio in constitutive 35S and stomatal-specific MYB60 transgenics.
Lines harbouring constructs which express bacterial *OtsA* and *OtsB* genes from constitutive 35S and stomatal-specific MYB60 promoters in *Arabidopsis thaliana,* grown in well watered conditions in a greenhouse in 12-hour days. C_i/C_a ratio was calculated using the relation derived in Farquhar et al. (1982), Eq. 12 using the fractionation parameters: isotopic composition of the atmosphere -7.8‰ (Ciais et al., 1995), fractionation during diffusion through air -4.4‰, fractionation during carboxylation at Rubisco -30‰ (Roeske and O'Leary, 1984). Significant differences (t-test with Holm-Sidak correction) from the wild type are shown as * P < 0.05, ** P < 0.01, *** P < 0.001.

4.2.6. Gene expression.

Trans-gene expression was confirmed in each leaf of the MYB60 lines used for gas exchange measurements. Leaf disks were taken from the portion of the leaf which was in the measurement cuvette during gas exchange measurements and RNA was extracted for qRT-PCR using *OtsA* and *OtsB* gene-specific primers. Actin10 was used as a normalisation control. C_t values and apparent "fold-change" over the background are displayed in Table. 4.2. All measured plants expressed the

OtsA and *OtsB* trans-genes well over background at the transcript level. The expressed genes are of bacterial origin and plants do not express them normally. Therefore, calculation of relative expression levels does not have a straightforward meaning. The absolute C_t values obtained by qRT-PCR are presented and the apparent fold-change is expressed relative to the background signal in the wild type. Actin10 was used as a reference gene and all relative expression changes are normalised to the expression of this gene (as shown in the Materials and Methods).

	OtsA	*OtsB*	*Actin10*	"Fold-change" vs Col-0
Col-0	33.26	30.41	18.82	
MYB60:OtsA #14	27.85	30.32	19.10	28.20
MYB60:OtsB #4	32.44	25.70	19.20	20.00

Table. 4.2 qRT-PCR analysis of stomatal-specific transgenic plants used for gas-exchange analysis.
C_t values of OtsA and OtsB transcripts in MYB60 transgenics and apparent "fold-change" over the background in leaf disks obtained from plants used for gas exchange analysis. Values are means of six samples. Fold-change is calculated assuming a PCR efficiency of 1.8 in the REST normalisation tool, normalised to the expression of Actin.

As Tre-6-P has been implicated in stomatal ABA signalling (Gómez et al., 2010), it is possible that the stomatal phenotypes in the transgenic lines are caused by secondary effects of the trans-genes and/or Tre-6-P on ABA signalling in guard cells. To investigate this possibility, expression levels of a series of ABA-responsive and signalling genes were measured in the leaf disks of transgenic plants using qRT-PCR. Two experiments were carried out. In one experiment whole-rosette material from 35S:OtsA and 35S:OtsB lines grown in a separate experiment was analysed. In the second experiment, leaf disks from the MYB60 transgenic lines taken from the plants directly following gas exchange analysis were analysed.

Fig. 4.9 shows the relative abundance of transcripts of a series of ABA-responsive genes in the 35S lines (a) and in the MYB60 lines (b) relative to wild type. There were some very minor alterations in the expression levels, some of which were significant. In general, *35S:OtsA* lines had slightly elevated levels of transcript of most of the analysed genes and these were statistically significant for *ABF4* and *ABI1*, which were upregulated by factors of 2.2 and 1.4 respectively, while *Rab18* was very mildly downregulated (1.3-fold). No statistically significant differences were observed in *35S:OtsB* plants.

MYB60 lines differed from their 35S counterparts in the pattern of expression of ABA-related genes. The *OtsA* and *OtsB* lines largely responded in a similar manner to each other. *Rab18* and *OST1* were induced compared to the wild type in both lines, although very mildly (1.5-fold at the most). In addition, *ABF4* and *ABI4* were significantly induced in MYB60:OtsB plants.

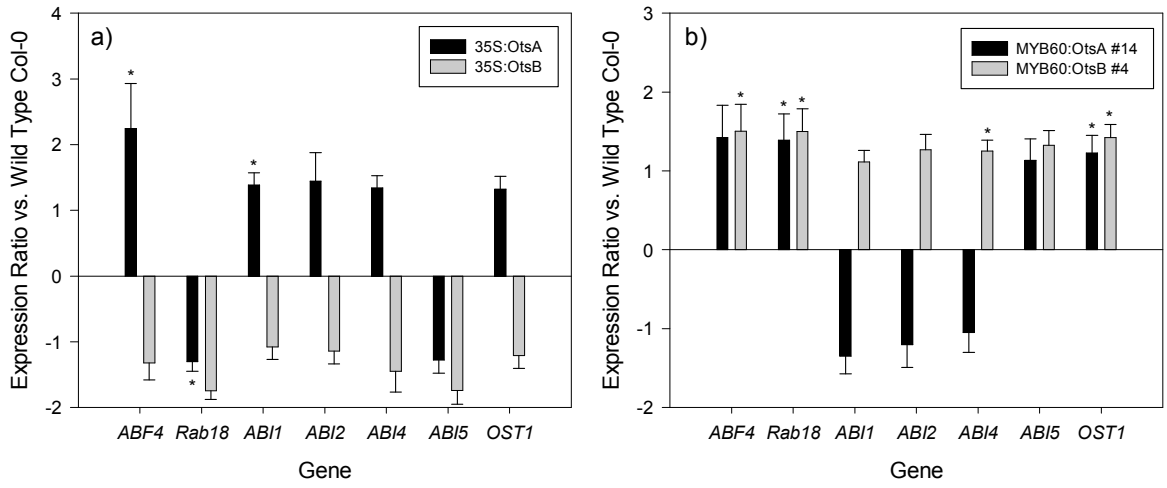

Fig. 4.9. Expression levels relative to wild type Col-0 of some ABA-responsive and ABA-signalling genes in constitutive 35S (a) and stomatal-specific MYB60 (b) transgenics.
qRT-PCR data were analysed using the REST normalisation tool (Pfaffl et al., 2002). Actin10 was used as a reference gene for normalisation. Expression ratios were calculated assuming PCR efficiency of 1.8. Differences were statistically tested using the Pairwise Fixed Reallocation Randomisation Test, significant differences from wild type at α=0.05 (from a ratio of 1 or -1) are indicated by stars. 35S samples were pools of six 21-day old rosettes grown in 12-hour days, N=3, MYB60 samples were leaf disks taken from leaves analysed for by gas exchange, grown in 8-hour days, N=6.

4.2.7. Drought Tolerance.

Altered function of stomata would be expected to have an effect on plant performance in conditions where growth and photosynthesis are limited by the availability of water. A controlled water-deficit experiment was set up in order to assess whether the transgenic lines perform differently when growing under mild water stress. Plants were initially grown in controlled environment chambers under well watered conditions. The pots in the drought treatment group were then allowed to dehydrate to 30% of field capacity of the soil, after which this soil water level was maintained by daily gravimetric watering of pots on a balance. The data from the drought experiment were analysed using analysis of variance, the results of which are presented in Table. 4.3. Pairwise comparisons between groups were performed using the Holm-Sidak step-down method.

Trait	Factor:	Genotype df=7	Treatment df=1	Genotype x Treatment df=7
Rosette fresh weight (g)	F	27.8	160.2	2.6
	p value	**<0.001**	**<0.001**	**0.015**
Rosette fresh weight relative to well-watered control	F	0.6	158.1	0.6
	p value	0.718	**<0.001**	0.718
Rosette fresh weight relative to WT (within treatment)	F	28.2	4.0	0.4
	p value	**<0.001**	**0.047**	0.876

Table. 4.3 Analysis of variance of drought experiment data.
Two-way analysis of variance table for the effects of genotype, drought treatment and their interaction on the biomass growth of transgenic lines harbouring constructs which express bacterial OtsA and OtsB genes from constitutive 35S and stomatal-specific MYB60 promoters. Statistically significant effects at α=0.05 are highlighted in bold-face.

Fig. 4.10a shows the growth of the transgenic genotypes in well-watered control conditions and under controlled mild drought. Drought treatment had a significant effect on plant biomass ($P<0.001$). Biomass was significantly reduced in all genotypes with the exception of 35S:OtsA (Fig 3.10a). 35S:OtsA plants were smaller than wild type in both treatments ($P<0.001$), however drought did not affect their biomass significantly ($P=0.419$). The different behaviour of the 35S:OtsA line drove a significant genotype:treatment interaction ($P=0.02$).

When expressed as a percentage of the well-watered control treatment (Fig. 4.10b) there was no longer a significant effect of genotype on growth ($P=0.718$) and most of the variance was driven by treatment ($P<0.001$). The biomass of wild type plants was reduced by 43% compared to well watered control plants ($P<0.001$, Fig. 4.10b). All transgenic lines responded similarly and there were no significant differences from the wild type in the other lines.

When expressed as a percentage of the wild type value within treatments (Fig. 4.10c), genotype was the main source of variation ($P<0.001$) while drought treatment also had a significant effect ($P=0.047$). In both control and drought treatments, 35S:OtsA plants were severely stunted compared to the wild type, with biomass of 28% and 37% of the wild type in the control and drought treatment respectively ($P<0.001$ in both cases). The other genotypes did not respond differently to the wild type and there were no significant differences from wild type in either treatment.

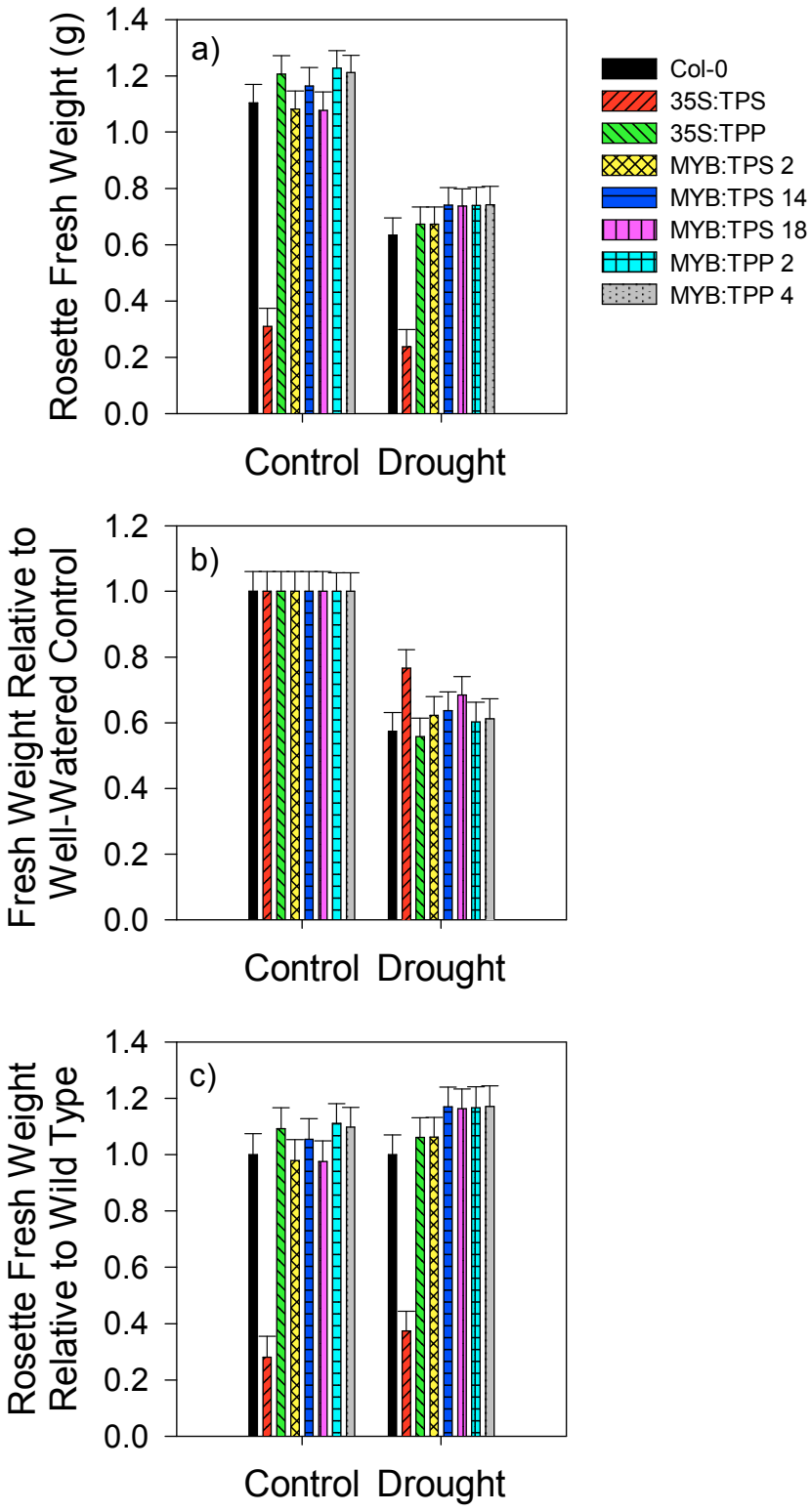

Fig. 4.10 Growth of constitutive 35S and stomatal-specific MYB60 transgenics under controlled water limitation.

Transgenic lines harbouring constructs which express bacterial OtsA and OtsB genes from constitutive 35S and stomatal-specific MYB60 promoters were grown in well-watered and controlled mild drought conditions (30% of field capacity of the soil) expressed as rosette fresh weight at harvest (a), rosette fresh weight relative to the well watered control of the same genotype (b), and rosette fresh weight relative to the wild type in the same treatment (c). Bars are standard deviations, N=8 plants. df=degrees of freedom.

4.3. Discussion.

The relationship between trehalose metabolism and stomatal function was explored using both constitutive and targeted expression of enzymes involved in trehalose metabolism. This is the first study to undertake a detailed investigation of trehalose metabolism in the context of stomatal function using a targeted mis-expression approach and one of the first to use a stomatal-specific promoter for targeted expression of any gene.

4.3.1. Stomatal starch.

Starch could be observed in guard cells following staining of fixed epidermal strips with iodine however its reliable quantification is problematic for several reasons, which will be briefly outlined.

Epidermal peels from *Arabidopsis* leaves are invariably highly contaminated with adhering mesophyll cells, which contain much starch, making even slight contamination a significant problem. Epidermal preparations from *Arabidopsis* can be obtained by mechanical blending and filtration and are relatively free of mesophyll contamination (Smart et al., 1999). The direct measurement of starch in such preparations is possible but is confounded by the presence of starch-containing plastids in the surrounding epidermal cells, which may be at least as abundant as the starch in the guard cells themselves (from visual inspection of epidermal strips in this study). Methods exist for the reliable isolation of guard cell protoplasts which are relatively free of mesophyll contamination (Zeiger and Hepler, 1976; Shimazaki and Zeiger, 1985; Pandey et al., 2002). This method has been used for transcriptomic (Leonhardt et al., 2004) and proteomic (Zhao et al., 2008) studies on guard cells. The use of protoplasts is however not suitable for the study metabolite pools, particularly transient ones like malate, but also starch. The preparation of guard cell protoplasts is a long process of sequential cell-wall digestion and washing steps taking place in highly artificial conditions at room temperature for many hours. As most metabolite pools have turnover times on the order of seconds to minutes (Arrivault et al., 2009), the metabolite contents of guard cell protoplasts do not reflect the situation in the intact leaf and are thus difficult to interpret, although they are occasionally published (Negi et al., 2008; Araújo et al., 2011). In addition, given the many links between the metabolism of the mesophyll and the function of stomata (see introduction), the analysis of guard cells separated from the rest of the leaf is also of questionable validity, a criticism which can also be applied to studies of stomatal movements in isolated epidermal peels.

The founding work on guard cell starch, malate and sugars used stomata micro-dissected from whole freeze-dried leaves of *Vicia faba* and amplification by enzyme cycling assays to achieve sensitivity (Outlaw and Lowry, 1977; Outlaw and Manchester, 1979). The small size of stomata in *Arabidopsis* in comparison with *Vicia faba* precludes the possibility of this approach for *Arabidopsis*. In fact, the few studies which report guard cell starch in *Arabidopsis* have only used image-based methods to assess starch amounts - transmission electron micrographs in two cases (Lasceve et al., 1997; Gómez et al., 2010) and light microscopy with iodine staining in another (Valerio et al., 2011). It is proposed as a future direction to confirm the starch accumulation phenotype of the lines presented here using transmission electron micrographs.

Tre-6-P was not measure in the MYB60 transgenic plants. Stomata are a very minor proportion of the whole leaf by volume and it is unlikely that changes in metabolite levels occurring in stomata will be reflected in whole-leaf measurements. Thus, it is not known how much Tre-6-P is present in stomata and to what extent it is altered in the transgenic lines. It can only be presumed that lines expressing *OtsA* have higher Tre-6-P contents in their stomata and lines expressing *OtsB* have lower levels.

The decreased starch accumulation in stomata of plants expressing *OtsA* (and thus presumably having high Tre-6-P) contrasts with the findings from whole-rosette starch measurements in 35S-over-expressors of this protein. Plants with artificially elevated levels of Tre-6-P have consistently been reported to have high starch levels in their leaves ((Kolbe et al., 2005), Martins, 2011, see also Chapter 2) while their stomata seem to be nearly starch-free. These findings suggest that Tre-6-P may have widely different effects on starch metabolism in different cell types. A parallel can be drawn between this observation and the fact that guard cells have a reversed diurnal cycle of starch accumulation relative to that in the leaf (Outlaw and Manchester, 1979). The observation of this phenotype in both 35S and guard-cell-specific transgenics suggests that the effect is mediated by the guard cell itself and not by modified metabolism elsewhere in the leaf. Plants expressing OtsB (which degrades Tre-6-P) showed the opposite effect, with more starch apparent in guard cells. This indicates that Tre-6-P, and not trehalose, is the causal factor behind the observed starch accumulation phenotype.

While the diurnal patterns of starch accumulation in the leaf and in the guard cell are opposite, a common factor between them is that the key regulatory events in both systems are exerted by redox regulation. On the one hand, redox regulation plays a key role in the activation of starch synthesis in leaves during the day (Hendriks et al., 2003). On the other hand, redox regulation activates the breakdown of starch by the guard-cell specific β-amylase 1 (BAM1) in guard cells during the day (Sparla et al., 2006; Valerio et al., 2011). Trehalose-6-phosphate has been shown to stimulate the redox activation of ADP-glucose pyrophosphorylase in leaves (Kolbe et al., 2005). It would be interesting to investigate whether Tre-6-P is also involved in modulating the redox regulation of guard cell enzymes, and BAM1 as a known redox-regulated enzyme and possible target.

4.3.2. Stomatal function.

A detailed investigation of stomatal function was performed on the transgenic lines using gas exchange analysis to analyse the dynamic behaviour of stomata in response to different stimuli. The use of gas exchange on intact leaves ensures that *in vivo* functions of stomata are being measured and get around the limitations of using isolated stomata or epidermal peels, which is artificial and non-physiological, as discussed previously.

Stomata can open using imported sugars as osmolytes just as well as using K^+ ions balanced by malate and in fact seem to preferentially use sugars when these are available (Outlaw et al., 2002). The use of dark-adapted plants after a 16-hour night simplifies the interpretation of the analysis, as sugar levels in the leaf would be low and the immediate opening response would be expected to be driven by cations and malate derived from starch degradation.

During the stomatal opening protocol, dark adapted leaves were exposed to saturating light. The application of strong light stimulates a rapid stomatal opening response which would require the breakdown of starch and its conversion to malate through glycolysis and PEPC. Under these conditions metabolic impairments in this pathway would be expected to affect the maximum speed of stomatal opening. Previous applications of this protocol have demonstrated the effects of metabolic restrictions in the starch-malate pathway on stomatal function. Light-induced stomatal opening has been shown to be slower in plants deficient in PEPC (Gehlen et al., 1996; Cousins et al., 2007), in the starchless *pgm* mutant (Lasceve et al., 1997) and in plants over-expressing a malate-consuming enzyme (Laporte et al., 2002) while severe photosynthetic impairment did not cause any effects (von Caemmerer et al., 2004; Baroli et al., 2008), demonstrating the importance of the starch-sugar-malate pathway rather than photosynthesis as the key metabolic flux necessary for stomatal opening in response to light.

Slower light-induced stomatal opening in MYB60 transgenics points to a possible limitation of stomatal opening by the starch-sugar-malate pathway in guard cells. The observation of altered starch content in guard cells of these lines suggests that starch supply may be limiting stomatal opening as starch content has previously been related to stomatal aperture (Outlaw and Manchester, 1979). It is not yet clear whether the reduced starch content observed in OtsA transgenics is the result of its faster degradation in the light or if the guard cells are generally accumulating less starch. Future work should aim to clarify this by examining the diurnal patterns of starch accumulation in guard cells of these plants.

The similar stomatal opening phenotype observed in both MYB60:OtsA and MYB60:OtsB lines is puzzling. Both these enzymes are involved in trehalose synthesis in plants. The observation of a similar effect of both proteins on stomatal function suggests that this phenotype may not be caused by Tre-6-P or starch but by trehalose itself. The testing of this possiblity would require the measurement of trehalose in the guard cells of these plants.

In an alternative model, which is purely speculative, it may be imagined that OtsA plants may be limited in stomatal opening by a lack of starch accumulation while OtsB plants are limited by a decreased ability to degrade starch. This can be explained if Tre-6-P is envisaged as an activator of starch degradation in guard cells (for example through regulation of BAM1). Thus in OtsA plants starch may not be able to accumulate because it is constitutively degraded due to the ubiquitous presence of super-physiological amounts of Tre-6-P. In OtsB plants starch degradation may be constitutively down-regulated because Tre-6-P is constantly at low levels due to its degradation by the over-expressed bacterial TPP enzyme (OtsB).

Such a model would conflict heavily with the current understanding of Tre-6-P action in leaves. The proposed role of Tre-6-P in plants is as a signal of sucrose availability (Lunn et al., 2006; Yadav, 2009), which feeds back to activate starch synthesis during the day (Kolbe et al., 2005; Stitt et al., 2007)) and to inhibit starch degradation at night (Martins, 2011) in times when sucrose supply exceeds demand. The degradation of starch to form malate in guard cells is also suppressed when sucrose is available to support stomatal opening as well as when inorganic anions such as chloride are available instead (Outlaw et al., 2002). However, Tre-6-P as a signal of sucrose availability in stomata would be difficult to reconcile with the findings that starch accumulation in guard cells was suppressed in MYB60:OtsA plants. This suggests that the regulation of Tre-6-P levels in stomata may not be linked to sugar status or that its function there is also largely different from that in mesophyll cells.

The stomatal opening protocol was conducted using high intensity light containing both red and blue wavelengths. While the MYB60 transgenic lines exhibited slower stomatal opening there was no effect on stomatal conductance at steady state. Starch and malate may limit the rate of stomatal opening during initial light exposure following a long night, however photosynthetic sucrose production may compensate and allow the stomata to open to normal levels. As discussed in the introduction, blue-light at low intensities specifically stimulates stomatal opening through the starch-malate mechanism without activating photosynthesis to a significant degree. The starchless *pgm* mutant has been shown to be impaired in stomatal opening in response to low-intensity blue light but functioned normally in high-intensity red light and during the diurnal cycle in white light (Lasceve et al., 1997). Its response to blue light could be restored by supplying chloride in epidermal strips, bypassing the requirement for malate. This again suggests that the starch-malate mechanism is very specific to particular subsets of conditions and is somewhat redundant. This may explain why the trehalose transgenics were affected in initial stomatal opening in response to light but not in steady state function.

While the MYB60 transgenics exhibited stomatal phenotypes, there were no effects in the corresponding 35S over-expressors. The interpretation of the phenotypes of the 35S plants is complicated by their severe metabolic phenotypes in the plants, as observed at the whole rosette level (See chapter 2). For example 35S:OtsB plants accumulated large amounts of sucrose while 35S:OtsA had low sucrose and accumulated very large amounts of malate, both key regulators of stomatal function and proposed links between mesophyll metabolism and stomata. It is thus impossible to separate the effect of trehalose metabolism in the guard cells themselves from the substantially perturbed metabolism in the rest of the leaf. The MYB60 transgenics, in contrast, are primarily affected in stomatal metabolism and thus allow stomatal-specific effects to be distinguished.

The stomatal response to low CO_2 was somewhat attenuated in MYB60:OtsA transgenics and was also slower in MYB60:OtsB plants. As discussed in the introduction, the stomatal CO_2 response seems to involve malate metabolism and/or transport and also involves a large part of the ABA-signalling network. As Tre-6-P has been implicated in stomatal ABA signalling (Gómez et al., 2010), it is possible that the stomatal phenotypes in the transgenic lines are caused by secondary effects of the trans-genes and/or Tre-6-P on ABA signalling in guard cells. Expression analysis of ABA-responsive and ABA-signalling genes was performed to investigate this possibility. While some expression changes were detected with statistical significance, the differences with respect to wild type plants were small (<2-fold). These differences are far smaller than those typically observed for these genes upon ABA application and drought treatment, which are typically more than 10-fold (Zimmermann et al., 2004; Hruz et al., 2008). There is a possibility that much greater changes in expression occurred in specific cell types, but the response was attenuated when measured in whole-leaf extracts, due to dilution effects from unresponsive cell types. This might be a particularly significant factor in the MYB60 lines. However, in leaves most of the ABA-responsive and signalling genes are expressed almost exclusively in guard cells only, e.g. *ABI1*, *ABI2*, *ABF4*, *OST1* and *Rab18* (Leonhardt et al., 2004). Therefore any changes observed on a whole leaf basis should reflect the changes in the guard cells and it may be concluded that there do not appear to be strong alterations in ABA signalling in the transgenic lines. Thus the altered CO_2 response in the transgenics again points to alterations in starch and malate metabolism as a possible causal factor, which seems to be more severe in MYB60:OtsA plants.

4.3.3. Carbon Isotope Fractionation.

The fractionation of stable isotopes of carbon in dry matter is a robust integrative measure of water use efficiency during carbon fixation (Farquhar et al., 1982; Evans et al., 1986). The isotopic signal can be measured very precisely using mass spectrometry and has the advantage of integrating the water use efficiency over the lifetime of the plant. This integrative property makes it a very reliable and robust indicator of water use efficiency and stomatal function (Farquhar and Richards, 1984; Wright et al., 1988; Hubick and Farquhar, 1989) and it has been successfully applied in functional genetic approaches to investigate the genetic basis of water use efficiency (Hausmann et al., 2005; Masle et al., 2005) and in plant breeding for water use efficiency traits (Hall et al., 2010).

Dry matter $\delta^{13}C$ measured in the 35S and MYB60 transgenic lines suggests some impairment in stomatal function, as shown by the tendency toward lower C_i/C_a ratios. This indicates a stronger stomatal limitation of photosynthesis and corresponds to higher water use efficiency. Again, both OtsA and OtsB showed the same effect, similar to what was seen in gas exchange analysis, with a stronger effect in OtsA. $\delta^{13}C$ measurements are a much more sensitive indicator of water use efficiency than gas exchange analysis and this allowed very small differences to be picked up reliably and with statistical significance. The derived C_i/C_a ratios indicate very minor changes from the wild type. The biggest change was in 35S:OtsA plants and was only 4.2% relative to the wild type, which

would be expected to improve water use efficiency by a similar magnitude. This is a very small effect compared to other studies (Masle et al., 2005; Araújo et al., 2011). It may, nevertheless, be meaningful as small differences in water use, if they are robust, build up to substantial water savings over time in crop situations, where water use is measured in mega-litres/ha. Due to the integrative nature of $\delta^{13}C$ values the small effects may not reflect steady state conductance but effects which occur only a small percentage of the time, such as during initial stomatal opening in the morning, as seen in gas exchange analysis.

35S:OtsA plants exhibited a small increase in water use efficiency in both gas exchange and $\delta^{13}C$ measurements. This is consistent with the reported drought tolerance of TPS over-expressing lines of various species (Holmstrom et al., 1996; Jang et al., 2003; Avonce et al., 2004) and suggests that stomatal control of water use efficiency may be a component of the drought tolerance in these lines, although it does not seem to be very strong. The observation of increased water use efficiency is also surprising in light of very high stomatal densities in this genotype (see Chapter 2) as most of the genes that have so far been shown to influence water use efficiency have actually been stomatal density determinants (Yoo et al., 2009). This suggests that stomatal aperture may determine the observed improvement in water use efficiency in the 35S:OtsA plants and points to impairments in the function of individual stomata. Changes in photosynthesis, the other major determinant of water use efficiency, can be excluded as a contributing factor, because photosynthetic rates in the transgenic lines were not significantly different from wild type plants.

The observed enrichment in ^{13}C observed in 35S:OtsA plants may also be treated with caution because these plants were seen to accumulate very large amounts of malate and fumarate (see Chapter 2). Leaf malate and fumarate pools have been shown to be strongly ^{13}C-enriched relative to other metabolites and total organic matter (Tcherkez et al., 2011). one out of their four carbon atoms originating from carboxylation by PEPC (Melzer and O'Leary, 1987; Schmidt, 2003). In contrast to Rubisco, PEPC has a near-zero discrimination against ^{13}C (O'Leary, 1981).

The more-negative $\delta^{13}C$ value of the starchless *pgm* mutant compared to wild type implies lower water use efficiency. This is also surprising, given that this mutant has been shown to exhibit impairments in stomatal opening (Lasceve et al., 1997), although this was only evident under certain conditions (weak blue light) while stomatal function was not altered during normal diurnal operation. The lower water use efficiency may also be caused by the photosynthetic impairment that this mutant displays (see next chapter). The possibility of altered fractionation due to the extensive metabolic alterations in this mutant also cannot be excluded. For example, this mutant exhibits somewhat de-regulated respiration during the day (Rasse and Tocquin, 2006) although this cannot explain the observed depletion as respiration also fractionates slightly against ^{13}C (Tcherkez et al., 2011), which should cause more ^{13}C to remain in biomass.

4.3.4. Drought Tolerance.

The stomatal function alterations observed in the transgenics failed to produce a significant improvement in growth under water-limited conditions. This is consistent with the very small reductions in lifetime water use efficiency ($\delta^{13}C$) that the lines exhibited. The controlled drought treatment, however, only reduced plant fresh weight by less than 50%, which would translate to a very mild reduction in the rate of growth of only 2-3% d^{-1} over the time period of the experiment and might not have allowed small differences to be resolved. A longer growth period or more severe water limitation may need to be applied to resolve a difference in growth given the weak effect of the trans-genes.

The expression of the MYB60 promoter has also been found to be inhibited in response to desiccation, as well as in response to the drought-related hormone ABA (Cominelli et al., 2005). This factor might have contributed to the lack of effect in the MYB60 transgenics, although the expression of the transgenes was not tested in the drought experiment. This would make this promoter somewhat less useful as a biotechnological tool to improve drought tolerance through stomatal function. It is also not known how stable the expressed proteins are in the cell. OtsA protein was found to persist for at least 4 days in leaves following induction in an inducible OtsA line (data not shown).

4.4. Chapter Summary.

In summary, an investigation of trehalose metabolism in the context of stomatal function was performed using a transgenic approach to perturb trehalose metabolism in leaves and specifically in stomata. Alterations in guard cell starch contents consistent with a role of Tre-6-P as a regulator starch degradation were observed, however the effect was opposite from that seen in mesophyll cells. Tre-6-P seemed to inhibit the accumulation of starch in guard cells. Stomatal-specific expression of both TPS and TPP enzymes gave gas exchange phenotypes and the plants were somewhat impaired in rapid stomatal opening in response to light as well as stomatal opening in response to low CO_2 concentration. Analysis of carbon isotope abundance in dry matter revealed small positive effects on lifetime water use efficiency. No effect on plant performance under water-limited conditions could be observed.

Chapter 5. The role of endogenous sugar levels in developmental light acclimation

5.1 Introduction.

5.1.1. Developmental light acclimation.

As outlined in the introductory chapter, sugar delivery from mature to developing leaves has been implicated as the systemic signal which drives the morphological acclimation of leaves to irradiance. This chapter aims to test the hypothesis that endogenous sugar levels drive the development of "sun" and "shade" leaves in *Arabidopsis thaliana*.

The leaves of most dicotyledonous plants acclimate to the light environment they are growing in by modifying chloroplast biochemistry as well as adjusting the developmental program of the leaves (Evans and Poorter, 2001; Terashima et al., 2001; Evans, 2004). The topic of "sun and shade" leaves is an enduring theme in plant developmental science. Leaves developed in high light tend to be thicker, have low SLA and high dry matter content (Lichtenthaler et al., 1981). Stomatal numbers increase and in hypostomatous leaves stomata may appear on the upper side of the leaf (Mott and Michaelson, 1991; Casson et al., 2009). The thick leaves also develop larger supportive structures and become more rigid, with thicker veins and more xylem vessels to support increased transpiration. The thicker leaf lamina is generated chiefly by elongation of palisade mesophyll cells perpendicular to the plane of the leaf (along the abaxial/adaxial leaf axis) and periclinal cell division may also generate more layers of mesophyll.

The thick leaves and increased cellular proliferation in "sun" leaves allows them to develop a higher capacity for gas exchange at a given light level by increasing the area of mesophyll exposed to the gas phase in the leaf (Terashima et al., 2001; Oguchi et al., 2003). This is only favourable from an economic perspective when light is sufficiently concentrated to energise the metabolic requirements of high rates of CO_2 uptake. Thus the plant can make use of the high light intensities through increased photosynthetic capacity per unit leaf area. (Roderick et al., 1999; Evans and Poorter, 2001).

While the existence of sun/shade acclimation was described as early as 1880 (Stahl, 1880), the mechanisms of how the light is sensed and how the signal is transduced to generate a thicker leafremained largely a matter of speculation for more than a century. However, within the last decade several mechanisms have been proposed and tested to various degrees. It has also become apparent that the process might be regulated by multiple signals.

5.1.2. Photoreceptors.

A number of photoreceptors control a variety of processes in plants, including the phenomena of light-stimulation of seed germination, hypocotyl growth, clock entrainment and photoperiodism of flowering (Chen et al., 2004). Some amount of blue light is required to generate a full "sun" leaf morphology in Arabidopsis. However complete knockout mutants of the blue-light photoreceptors cryptochrome and phototropin acclimate to irradiance in a normal manner and produce typical "sun" leaves in high light (Weston et al., 2000; Lopez-Juez et al., 2007). While cryptochrome and phototropin can be ruled out as likely photoreceptors for signalling sun-shade leaf development, there is some evidence to support the involvement of phytochrome, particularly phytochrome B (PhyB).

Phytochrome B mutants (*phyB*) have thinner leaves with lower photosynthetic activity than wild type plants (López-Juez et al., 1998; Boccalandro et al., 2009), while overexpression of Arabidopsis PhyB in potato gave rise to thicker leaves and mesophyll layers and enhanced photosynthesis, which was described by the authors as a "light-exaggerated phenotype" (Thiele et al., 1999). In addition, PhyB is essential for the increase in stomatal density and stomatal index in high light (Boccalandro et al., 2009; Casson et al., 2009). It is, however, unclear, to what extent high-light-induced leaf thickening ("sun-leaf" formation) can occur in *phyB* mutants as all published data come from plants grown in a single environmental condition. Without more comprehensive testing under a wider range of conditions, we cannot be certain that the response is completely abolished in the *phyB* mutants. Therefore, the possibility remains that PhyB is not an exclusive signal. There are some indications that developmental acclimation to light does occur in this mutant (Kim et al., 2005). Future work should aim to verify these observations.

If phytochrome is indeed involved, this involvement cannot be related to its traditionally-accepted function of sensing light quality through the red:far red ratio, as gross changes in irradiance still cause strong morphological acclimation without changes in light quality. An irradiance-sensing function has been proposed for phytochrome B (Casson et al., 2009; Poorter et al., 2009). It has also been suggested that both irradiance and red:far-red ratios affect leaf thickness in a complementary manner (McLaren and Smith, 1978). Red:far-red ratios do not, however, alter leaf mass per area (a proxy to leaf thickness) which responds much more strongly to changes in irradiance (Heraut-Bron et al., 1999; Poorter et al., 2009).

The use of changes in red:far-red ratios as an experimental manipulation is not without drawbacks, as the effects are confounded by simultaneous changes in the excitation balance between photosystem I and photosystem II. This, in turn, affects plastid redox states (Pfannschmidt et al., 1999), which are also known to have light signalling functions (see next section). This property makes it notoriously difficult to separate the effects of plastid redox signalling from phytochrome signalling when applying the well-established "PSI and PSII light" methodology, which essentially constitutes varying the red:far-red ratio.

5.1.3. Plastid signals.

Energised components of the light reactions of photosynthesis also have light signalling functions. Several mechanisms are known and a number are proposed (Baier and Dietz, 2005; Woodson and Chory, 2008). One well-studied signal originates at the acceptor side of photosystem II and constitutes the basis of the "excitation pressure" hypothesis (Huner et al., 1998). In this model, excitation pressure is the reduction state of the mobile thylakoid redox carrier plastoquinone (PQ). PQ is reduced by electrons from water splitting at PSII, diffuses in the thylakoid membrane and donates its electrons to the cytochrome b_6f complex, from where they are further channelled to PSI. Its redox state thus reflects the balance between the excitation rate of PSII upstream and the use of electrons downstream by PSI and ultimately by metabolism or by alternative pathways such as the Mehler ascorbate-peroxidase reaction (Badger et al., 2000). PQ redox state is quantitatively responsive to light quantity, light quality (excitation imbalance between PSI and PSII), electron utilisation as well as temperature.

It has been shown experimentally that PQ redox state is the origin of signals for "state transitions" of light harvesting complexes in the plastid (Allen et al., 1981) as well as retrograde signals regulating the gene-transcription of nuclear-encoded plastid proteins (Escoubas et al., 1995; Maxwell et al., 1995; Pfannschmidt et al., 1999; Fey et al., 2005). Furthermore, there is evidence that acclimatory changes in chloroplast composition in response to high light are signalled by redox at PQ (Savitch et al., 1996; Gray et al., 1997; Terashima et al., 2005).

The second well-known plastid-derived light signal lies downstream of PSI and involves thioredoxins. The signal begins in the plastid stroma when electrons are donated from reduced ferredoxin to thioredoxin, via ferredoxin-thioredoxin reductase. Thioredoxins are known to be involved in the regulation of many stromal enzymes through reduction of disulfide bonds (Porter et al., 1988; Scheibe, 1990; Buchanan et al., 1994; Jacquot et al., 1997; Zhang et al., 2002; Hendriks et al., 2003) as well as regulation of plastid translation (Irihimovitch and Shapira, 2000; Kim and Mayfield, 2002) and control of nuclear gene expression (Oswald et al., 2001).

Several other plastid redox carriers and factors that influence plastid redox status have been proposed as having a signalling function, including reduced glutathione (Montané et al., 1998; Mullineaux and Rausch, 2005) the redox state of the cytochrome b_6f complex (Pearson et al., 1993), the trans-thylakoid proton gradient (Chen et al., 2004), the redox state of $NADP^+$/NADPH (Baier et al., 2004), reactive oxygen species (Bouvier et al., 1998; Pfannschmidt, 2003) and carotenoids (Corona et al., 1996). The porphyrin precursors of chlorophyll have also been implicated in retrograde signalling between chloroplast and nucleus (Oster et al., 1996).

The evidence for a connection of plastid signals to leaf development is based upon the investigation of various variegated mutants with incomplete plastid biogenesis or defective plastids. Many variegated mutants display aberrant morphological phenotypes in their white leaf sectors (Rodermel, 2001) suggesting that plastids are required for normal leaf development. Most of the identified phenotypes involve alterations in cell expansion and growth and do not resemble light-acclimation phenotypes. The variegated Arabidopsis mutant *chm1-3* lacks plastids and is unable to increase its leaf thickness and number of mesophyll layers in white leaf sectors in response to high light (Tan et al., 2008). These observations demonstrate that the presence of functional plastids is also required for morphological acclimation to light. There have been suggestions that plastoquinone redox state may be involved in the developmental aspect of light acclimation (Huner et al., 1998; Kim et al., 2005; Terashima et al., 2005; Lopez-Juez et al., 2007) however experimental evidence for this is lacking. There is also no documented evidence for the involvement of other redox signals.

5.1.4. Systemic signals.

It is possible that light itself might not be a direct signal for the morphological aspect of “sun” and “shade” leaf development. A series of studies in three different species have shown that various aspects of leaf morphology that are normally associated with high light, including palisade tissue morphology and stomatal characters, respond to the light environment prevailing around the developed, mature leaves (Yano and Terashima, 2001; Thomas et al., 2004; Coupe et al., 2006). There was also a similar response to changes in CO_2 levels (Lake et al., 2001). Together these results strongly imply a spatial separation of light sensing and the perception of the signal in developing leaves, for which a systemic signalling process is required. In contrast, the acclimation of chloroplast composition and properties to light was driven by the local light environment at the developing leaves, indicating a separation between the two acclimation processes (Yano and Terashima, 2001).

5.1.5. Assimilates as a possible systemic signal.

The underlying mechanism of systemic signalling is unknown. Several authors have proposed the products of photosynthesis (sugars) and their translocation to the growing sinks (ie. developing leaves) as a plausible mechanism. It has been suggested as early as 1903, that light may drive leaf morphogenesis at the early stages of development indirectly through bud nutrition rather than directly (Nordhausen, 1903) and later authors suggested that assimilate supply to developing leaves may constitute a signal (Friend et al., 1962). This is supported by various other observations, among them:

1) High CO_2 makes leaves thicker in a similar manner to high light (Koerner and Diemer, 1987; Vu et al., 1989; Radoglou and Jarvis, 1990)
2) Plants grown at low temperatures accumulate large amounts of sugars, in part due to slow growth, and also have very thick leaves (Stitt and Hurry, 2002; Gorsuch et al., 2010)
3) Plants compromised in photosynthesis (e.g. Rubisco anti-sense) have been observed to have leaves with a low leaf mass per area (Stitt and Schulze, 1994)
4) Mutants of plastid sugar transporters *gpt1* and *tpt* have been shown to be impaired in dynamic light acclimation of photosynthesis (Walters et al., 2003; Athanasiou et al., 2010), although no characterisation of leaf morphology in these lines has been published

More recently, sugars have been proposed in several publications to act as morphogenetic signals for light acclimation (Kim et al., 2005; Coupe et al., 2006; Terashima et al., 2006). Evidence in support of this proposal is scarce due to the difficulty of manipulating *in planta* sugar levels without confounding effects. As yet no evidence, correlative or otherwise, has been presented for a role for sugar levels as morphogenetic signals for leaf anatomical traits.

5.1.6. Advantages of sugar signals.

Using sugars to sense the light environment presents several conceptual advantages. Sugars are the direct and immediate output of photosynthesis. Photosynthetic rates depend almost linearly on light irradiance over a certain range and the flux of sugar is thus an indirect quantitative indicator of light irradiance through its effect on photosynthetic activity. Since photosynthesis is the eventual main function of the developing leaf, a quantitative indication of photosynthetic activity in already existing leaves can be a functionally informative cue for a leaf primordium, which may not receive light directly during its early growth before emergence. Thus, if existing mature leaves are limited by light, this will be reflected in photosynthetic activity and sugar output, allowing a developing leaf to adjust pre-emptively and optimise its morphology and photosynthetic capacity for the prevailing light environment.

Sugar delivery to developing leaves (i.e. sinks) can also be an integrative signal which reflects the prevailing light conditions integrated over the general vicinity, allowing the plant to average the signal from several locations (i.e. the source leaves). This is an obvious advantage in plant canopies, where the light environment is complex and highly heterogeneous in both space and time, with irradiance varying up to 100-fold between a shaded leaf and a sun-fleck over a distance of sometimes only centimetres and a time-scale of seconds to minutes (Chazdon and Pearcy, 1991). Thus sensing light in only one location (e.g. one developing leaf) can give very misleading estimates of actual light availability. Finally, the integrative property of sugars as morphogenetic signals is evident from the fact that sugar flux originating from photosynthesis can simultaneously integrate light quantity, CO_2 concentration and temperature, all of which have been shown to affect leaf morphology in a manner analogous to light irradiance.

There is a general scarcity of experimental data on leaf thickness and mesophyll morphology in the literature on leaf development and photomorphogenesis, particularly in Arabidopsis. Leaf thickness is not often measured in developmental and eco-physiological studies. This may be due to the relative difficulty in measuring this parameter. Preference is usually given to other characters that are easier to measure such as petiole lengths and hypocotyl growth or to indirect indicators of leaf thickness such as specific leaf area, leaf density or dry matter contents, which are easier to measure.

In order for sugar concentrations to drive developmental changes in response to light, the sugar levels themselves would have to respond to light in quantitative manner. While this may be expected due to increased photosynthesis, it is not necessarily obvious as, for example, growth rates may increase with

increasing irradiance and consume the extra photosynthate, keeping the sugar pool constant. Furthermore, testing the hypothesis that sugars regulate leaf development indirectly in response to light presents obvious difficulties which may have contributed to the lack of published investigations on the subject. The first issue is the difficulty in separating the light input and its potential signalling role from effects of sugar levels and sugar-related signals in their own right. Any change in light quantity would be expected to alter sugar levels downstream and it is impossible to deconvolute these two responses by manipulating light conditions.

Manipulating sugar levels independently of light brings a second complication: how to manipulate sugar levels in the plant in a meaningful and exclusive manner. A popular and simple experimental system for the study of sugar-related phenomena is supplying sugars exogenously in sterile culture media. This method has been employed in the context of photomorphogenesis and shade avoidance (Kozuka et al., 2005), however an examination of leaf thickness and mesophyll morphology in such a system is yet to appear in the literature.

The results of such experiments must be treated with caution due to the non-physiological nature of the treatments. Experiments have often included high sugar concentrations that would have osmotic side effects, and sometimes sugars that are not usually translocated by the plant (e.g. glucose) have been used. Even if low or moderate concentrations of a translocated sugar (e.g. sucrose) have been applied, the movement of sugars from root to shoot is in the opposite direction to normal, which has the potential to cause complex and abnormal responses due to perturbation of systemic signalling (including hormone signalling) via the phloem. Exogenous sugar treatments do not always alter the actual levels of sugars *in planta*, (Stitt et al., 2007). In addition, they affect the function of the circadian clock (McWatters and Devlin, 2011; Flis, unpublished work), affect signalling processes involved in the determination of flowering time (Ohto et al., 2001) and affect photoreceptor signalling pathways (Dijkwel et al., 1997). Although exogenous sugar supplementation in sterile media is experimentally simple, the results of such experiments are difficult to interpret, for the reasons outlined above, and so this approach is not really appropriate for studies attempting to differentiate between direct light signals and indirect light signals mediated by sugars.

An obvious and simple way to alter sugar levels without altering light and without exogenous application is by manipulating CO_2 levels, to alter the rate of photosynthesis. While this uncouples sugar production from light, it introduces a further complication as light and CO_2 act synergistically on some traits related to light acclimation e.g. SLA and leaf thickness, and in opposing ways on other traits e.g. stomatal densities (Woodward, 1987; Lake et al., 2001). The recent elucidation of CO_2 sensing and signalling pathways in stomatal guard cells clearly showed that CO2 can affect leaf function independently of its effects on photosynthesis and sugars (Young et al., 2006; Hu et al., 2010).

A number of *Arabidopsis* mutants with defects in primary metabolism could be useful as a system for the study of sugar signals and resolving these from light signals. Mutants in plastidial phosphoglucomutase (*pgm*) and ADP-glucose pyrophosphorylase (*adg1*) lack the ability to synthesise starch and undergo large fluctuations in sugar levels during the diurnal cycle and accumulate high concentrations of soluble sugars during the day (Caspar et al., 1985; Sun et al., 2002; Gibon et al., 2004) but experience carbon-starvation at the end of the night. The severity of the metabolic and growth phenotypes of these mutants is known to be daylength-dependent, which gives them added flexibility as an experimental tool to vary sugar levels.

Mutants with defects in sugar metabolism or its regulation can also have altered sugar levels. Plants with decreased levels of the regulatory metabolite fructose 2,6-bisphosphate (e.g. *f2kp* mutants) have

altered partitioning of carbon in favour of sucrose and elevated sugar levels (Stitt, 1990; Draborg et al., 2001; Lee et al., 2006)

A recently published double mutant of two cytosolic invertase proteins in *Arabidopsis* (*cinv1cinv2*) is partially impaired in sucrose utilisation for growth and also accumulates sugars (Barratt et al., 2009). Interestingly, a mutant of an invertase homologue in *Lotus japonicus* was shown to exhibit a phenotype with very thick leaves and greatly increased proliferation of mesophyll cell layers, which is very reminiscent of high-light-adaptated leaves (Welham et al., 2009).

5.1.7. Aims of the chapter.

The aim of the work described in this chapter was to test the hypothesis that *in planta* sugar levels determine leaf morphological traits independently of light irradiance. This was done by comparison of wild type and mutant plants with altered sugar levels grown under different environmental conditions. Morphological traits were assessed using both direct microscopic observations as well as well as analysis of leaf composition. A possible interaction of metabolic phenotype with plastid redox function was also investigated.

5.2 Results

5.2.1 Leaf development in different light environments in *Arabidopsis thaliana* Heynh. Col-0

5.2.1.1. Leaf morphology.

Strong morphological acclimation was observed when *Arabidopsis thaliana* Col-0 was grown at four different irradiances (75-420 µE m^{-2} s^{-1}) with a fixed 12-h daylength (Fig. 5.1).

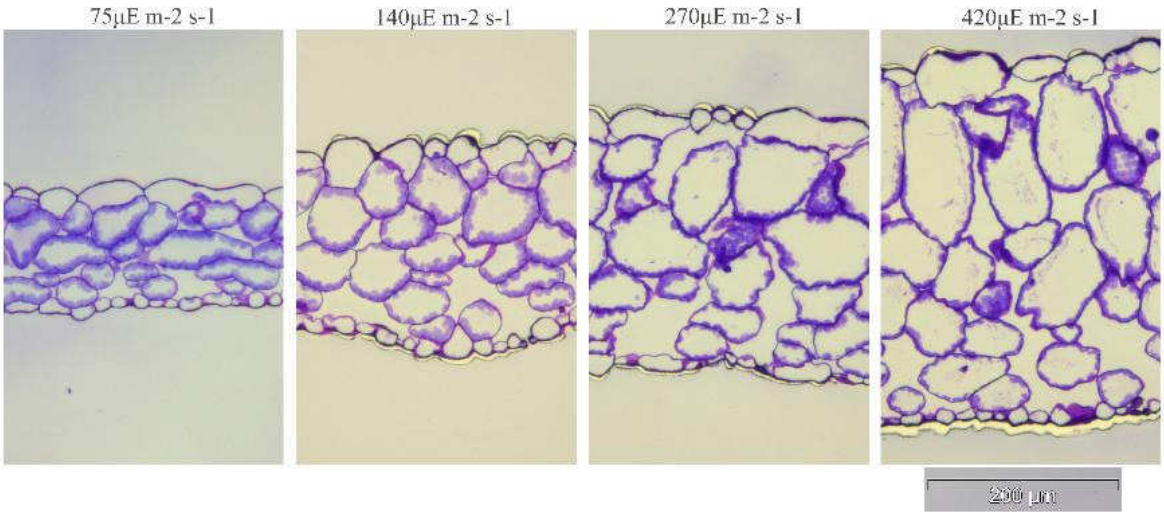

Fig. 5.1 Developmental light acclimation in *Arabidopsis thaliana* Col-0.
Transverse sections of *Arabidopsis thaliana* Heynh. Col-0 mature sixth leaf grown in light environments indicated above in 12 hour daylength and a 20°C/20°C day/night temperature regime. Magnification 200X, Toluidine-Blue staining.

Leaf thickness increased more than 2-fold in a linear manner with growth irradiance (Fig. 5.2a). The indirect leaf thickness estimation method, described by Vile et al., (2005) predicted actual leaf thickness (measured by microscopy) very accurately ($r^2 = 0.99$ between values obtained by both methods). The increase in leaf thickness was driven by a linear increase in the number of cell layers in the leaf (Fig. 5.2b) as well as longitudinal elongation of cells along the abaxial/adaxial axis, leading to a higher average thickness per cell layer (Fig. 5.2c).

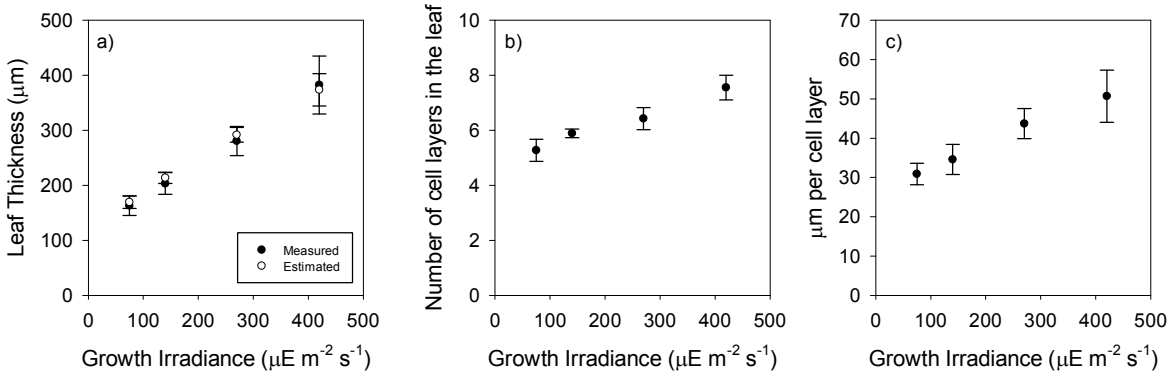

Fig. 5.2. Morphological phenotype of Arabidopsis wild-type Col-0 grown in different light environments.
Leaf thickness (a), number of cell layers (b) and the average thickness of one cell layer (c) in mature sixth leaves of *Arabidopsis thaliana* Heynh. Col-0 grown in four light environments in 12 hour daylength and a 20°C/20°C day/night temperature regime. N=160 measurements on 32 sections from eight leaves. Using the indirect method (Vile et al., 2005), mature leaves of the same eight plants were analysed. Bars are stadard deviation.

Specific leaf area (SLA) decreased from 86 $m^2\ kg^{-1}$ at 75 μE $m^{-2}\ s^{-1}$ to 32 $m^2\ kg^{-1}$ at 420 μE $m^{-2}\ s^{-1}$ growth irradiance (Fig. 5.3a) while leaf dry matter content was constant except in the highest light treatment, where it was 25% higher (Fig. 5.3b).

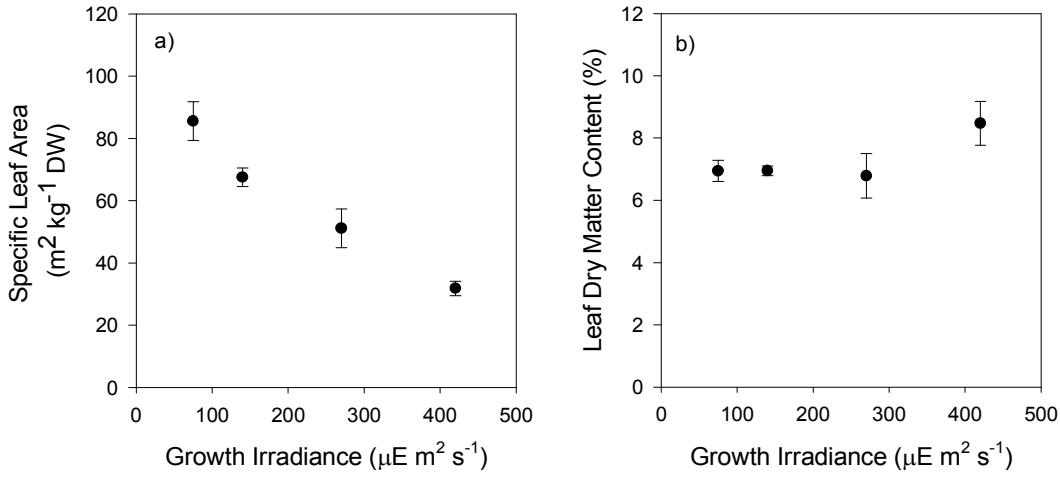

Fig. 5.3. Morphological phenotype of Arabidopsis wild-type Col-0 grown in different light environments.
Specific leaf area (a) and leaf dry matter content (b) in mature leaves of *Arabidopsis thaliana* Col-0 grown in four light environments in 12 hour daylength and a 20°C/20°C day/night temperature regime. N = 8. Bars are standard deviation.

5.2.1.2. Soluble sugars.

The plants grown in four light levels in a 12-hour photoperiod were harvested at the end of the day and the end of the night for metabolite analysis. A two-way nested ANOVA design was used to analyse metabolite data for effects of light irradiance and timepoint. Pairwise differences between groups were tested for significance using the Holm-Sidak step-down method. T-test probabilities are shown where they are significant.

There were significant effects of light irradiance treatment (P=0.018) and time of day (<0.001) on the levels of glucose (Fig. 5.4a) in rosettes. Levels of glucose at the end of the day did not increase with light irradiance, with the exception of the highest light treatment, where levels of glucose were almost double the levels in the other three conditions, and this difference was significant (P<0.001). The pattern of glucose accumulation measured at the end of the night period was different and there was a significant treatment:timepoint interaction (P=0.015). Glucose levels at the end of the night decreased with increasing growth irradiance up to 270 µE m^{-2} s^{-1}, however no significant difference was found in pairwise comparisons.

Levels of fructose (Fig. 5.4b) were very low and sometimes close to the limit of detection, particularly in the two low-light treatments. There was no significant trend in fructose levels with different light environments and the concentrations did not vary significantly between the day and night.

Levels of sucrose (Fig. 5.4c) varied with both irradiance and time of day with a high degree of significance (P=<0.001) and there was a significant treatment:timepoint interaction (P<0.001) Levels of sucrose at the end of the day increased in a near-linear manner with light irradiance and were almost three-fold higher in high light than the lowest light treatment (all pairwise comparisons significant, Holm-Sidak Test). End of night levels were 2-3-fold lower than end of day in all light treatments (P<0.001) while also increasing with growth light irradiance, although by a smaller factor.

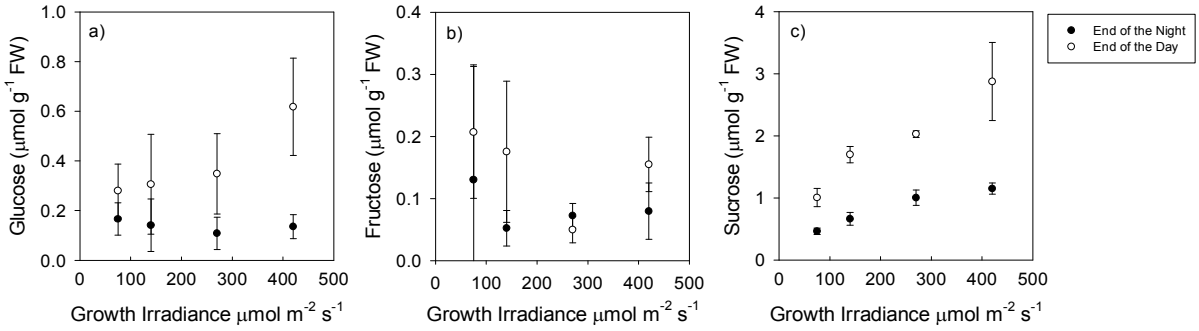

Fig. 5.4. Sugar accumulation at the end of the day and end of the night in Arabidopsis wild-type Col-0 grown in different light environments.
Soluble sugar content in whole rosettes of *Arabidopsis thaliana*. Col-0 grown in four light environments in 12 hour daylength and a 20°C/20°C day/night temperature regime and harvested at the end of the day and end of the night. N=5 samples containing 5 plants pooled. Bars are standard deviation.

5.2.1.3. Relationship of leaf morphology with sugar levels.

There was a strong linear relationship between sucrose levels at the end of the day and both leaf thickness and number of cell layers in the leaf (Fig. 5.5). Glucose showed a weaker relationship with the morphological traits, but fructose was not correlated at all (not shown).

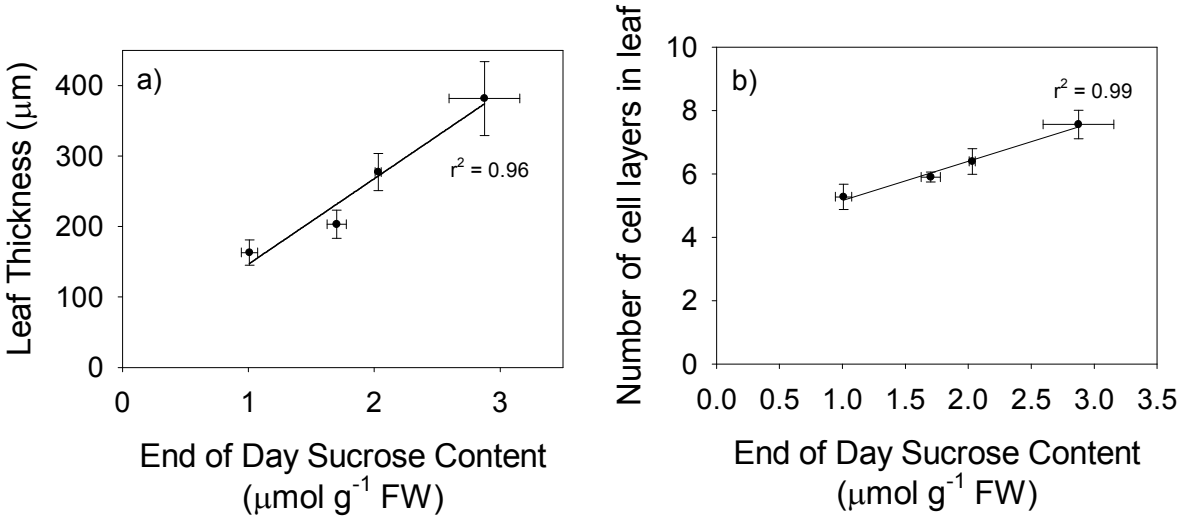

Fig. 5.5. Relationship between levels of sucrose at the end of the day and leaf thickness and number of cell layers in the leaf in *Arabidopsis thaliana*. Col-0 grown in four light environments Plants were grown in four light environments in 12 hour daylength and a 20°C/20°C day/night temperature regime. The lines show the linear regression between the traits. Bars are standard deviation.

5.2.2. Leaf morphology in metabolic mutants of *Arabidopsis thaliana* with altered levels of sugars.

5.2.2.1. Leaf morphology

In order to differentiate direct light signalling from indirect light signalling by sugars, the patterns of sugar accumulation and leaf morphology were examined in a set of Arabidopsis mutants – *pgm*, *f2kp* (two independent T-DNA lines in the same gene, named here: *f2kp-1* and *f2kp-2*), and the *cinv1cinv2* double mutant – which all have altered levels of sugars in the rosettes. Two control genotypes were included in the experiment, wild type Col-0 and a wild type line segregant from a SALK T-DNA insertional mutant (SALK WT). The aim of the experiment was to test the hypothesis that endogenous sugar levels influence the developmental program of the leaf, generating 'sun' or 'shade'-like morphological traits.

The starchless *pgm* and the *cinv1cinv2* double mutants both exhibited severe growth and developmental phenotypes when grown with a 12-h photoperiod and an irradiance of 160 µE m^{-2} s^{-1}. Relative growth rates were the same in both mutants and amounted to 0.22 d^{-1}, which was 30% lower than the wild type ($P<0.001$) and resulted in an 8-fold reduction in biomass at the time of harvest. The two wild type genotypes did not differ significantly from each other in relative growth rate.

Fig. 5.6 shows the leaf thickness and the number of cell layers in the leaf determined by microscopic examination of transverse thin sections of leaves in the six examined genotypes. Both wild type genotypes had a similar leaf thickness of 219 and 231µm in the Col-0 and SALK WT respectively

(Fig. 5.6a). The pgm mutant had very thick leaves (359μm) which was 64% higher than wild type and a highly significant difference ($p<0.001$). None of the other mutants were significantly different from wild type.

Both wild type genotypes had the same number of cell layers in the leaf (Fig. 5.6b), averaging 5.9. The *pgm* mutant had more cell layers in the leaf, with a mean of 6.9 ($P<0.001$). The *f2kp-2* mutant showed a small but significant increase in the number of cell layers compared to both wild types with 6.3 layers on average ($P=0.008$). The *cinv1cinv2* double mutant showed a marginal increase in cell layers to 6.2. This difference had a marginally significant t-test probability in a test against Col-0 ($P=0.04$) and SALK wild type ($P=0.05$), however using the Holm-Sidak correction for Type I error in multiple comparisons, this was judged as a false discovery.

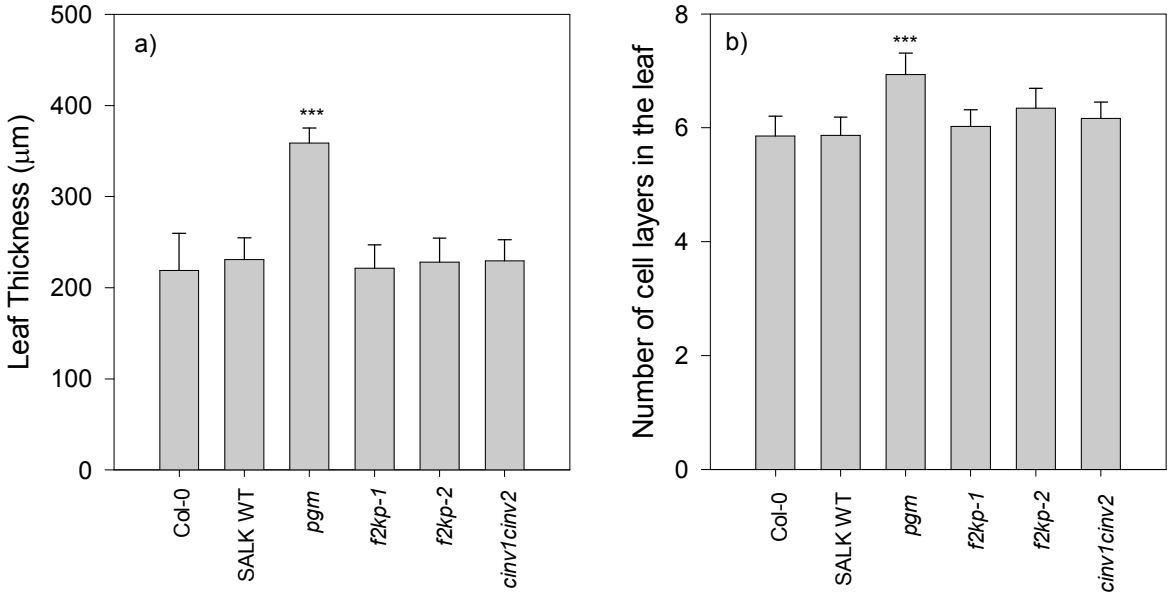

Fig. 5.6. Leaf morphology in metabolic mutants of Arabidopsis grown in one light environment. Leaf thickness (a) and the number of cell layers in leaf 6 (b) in metabolic mutants of *Arabidopsis thaliana* growing in 12h days at an irradiance of 160 μE m^{-2} s^{-1}. Significant differences (t-test with Holm-Sidak correction) from the relevant wild type are shown as * $P < 0.05$, ** $P < 0.01$, *** $P < 0.001$. N=8. Bars are standard deviation. Values are means of measurements on 8 leaves, with 20 measurements from four separate sections per leaf.

Both leaf thickness and the number of cell layers were subject to significant effects of the plant's position within the growth cabinet (ANOVA $P=0.002$ for thickness and $P=0.038$ for cell layers), presumably due to light and temperature gradients within the cabinet. Higher values of both traits were observed in plants from the centre of the cabinet, which received more light and experienced slightly higher temperatures. The genotype means are assembled from a balanced selection containing eight samples, each from a different part of the growth cabinet, to minimise bias from position effects.

The changes in leaf thickness and cell layers were accompanied by changes in leaf composition (Fig. 5.7). Leaf dry matter content was significantly elevated in the *cinv1cinv2* double mutant ($P<0.001$) while the *pgm* mutant had less dry matter in the leaf ($P<0.001$), corresponding to a higher water content (Fig. 5.7a). Compared to both wild types, SLA (Fig. 5.7b) was significantly lower in both *cinv1cinv2* and *pgm* mutants ($P=0.008$ and $P<0.001$ respectively vs. Col-0). The wild type genotypes were not significantly different from one another.

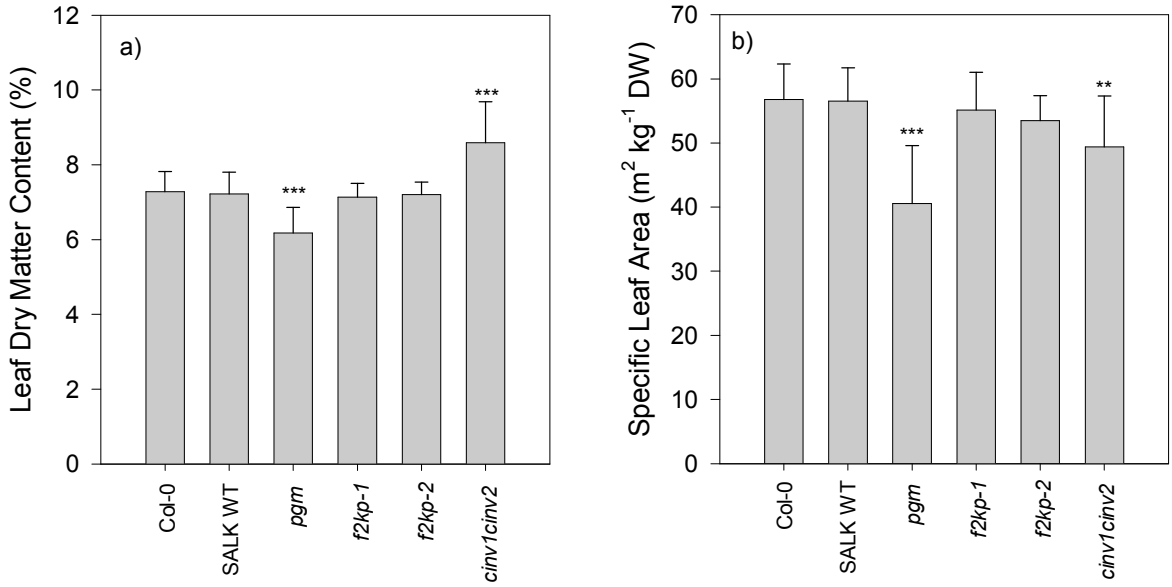

Fig. 5.7. Leaf dry matter content (a) and specific leaf area (b) in metabolic mutants of *Arabidopsis thaliana*
Plants were grown in 12h days at an irradiance of 160 µE m^{-2} s^{-1}. Significant differences (t-test with Holm-Sidak correction) from the relevant wild type are shown as * $P < 0.05$, ** $P < 0.01$, *** $P < 0.001$. N=8. Bars are standard deviations.

5.2.2.2. Sugar levels.

Plants were harvested at the end of the day and end of the night for metabolite measurements. Metabolite levels were analysed for effects of genotype and timepoint in a two-way nested ANOVA design. Pairwise differences between ANOVA groups were tested for significance using the Holm-Sidak step-down method.

Fig. 5.8 shows the soluble sugar contents of the six genotypes samples at the end of the day and end of the night.

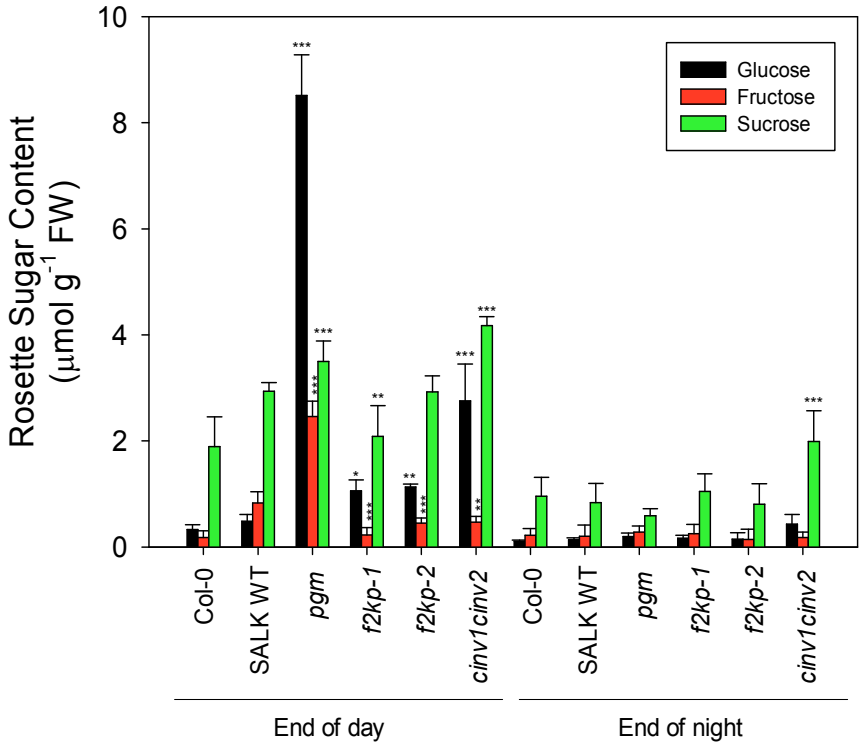

Fig. 5.8. Soluble sugar levels in metabolic mutants of Arabidopsis.
Soluble sugar content at the end of the day (ED) and the end of the night (EN) in metabolic mutants of *Arabidopsis thaliana* grown in 12h days at an irradiance of 160 µE m^{-2} s^{-1}. Significant differences (t-test with Holm-Sidak correction) from the relevant wild type within timepoints are shown with probabilities * P < 0.05, ** P < 0.01, *** P < 0.001. N=5 rosettes. Bars are standard deviations.

Glucose varied significantly between genotypes (P<0.001) and time of day (P<0.001) and there was a significant genotype:timepoint interaction (P<0.001). Differences in glucose content between the two wild type genotypes were not significant at either timepoint. All of the mutants tested had significantly elevated levels of glucose at the end of the day compared to both wild types. This was particularly pronounced in the *pgm* mutant, where glucose levels were 25-fold higher than in Col-0. The *cinv1cinv2* double mutant accumulated 5.6-fold higher glucose levels than the SALK wild type, a highly significant difference (P<0.001). The *f2kp* mutants were not significantly different from one another and both had double the glucose levels found in the SALK wild type, which was significant (P=0.004 and 0.015 for the two *f2kp* lines). End of night levels were not significantly different between genotypes.

Fructose levels were also significantly affected by genotype (P<0.001) and time of day (P<0.001). The *pgm* mutant had 14-fold higher fructose concentrations than the Col-0 wild type at the end of the day (P<0.001). The *cinv1cinv2* and *f2kp* mutants had lower daytime fructose levels than the SALK wild type (P=0.001). There was also a significant difference between the two wild type genotypes, with more fructose in the SALK wild type (P<0.001). End of night levels did not differ significantly between genotypes.

Levels of sucrose varied significantly between genotypes (P<0.001) and timepoints (p<0.001). Sucrose was the most abundant and the least variable sugar between genotypes. In contrast to glucose and fructose, the levels of sucrose in the *pgm* mutant were elevated only 87% at the end of the day compared to Col-0 (P<0.001). At the end of the night the *pgm* mutant had lower levels of sucrose,

however this was not significant. The *cinv1cinv2* mutant had significantly elevated levels of sucrose both at the end of the day and end of the night, with 41% higher levels than the SALK wild type at the end of the day. The two *f2kp* mutants differed significantly between each other. The *f2kp-1* mutant line had lower levels of sucrose than the SALK wild type at the end of the day while *f2kp-2* was not significantly different. End of night sucrose levels were not significantly different between genotypes except in the *cinv1cinv2* double mutant, where they were elevated to more than double the wild type values (P=0.001).

5.2.3. Leaf morphology and sugar levels in the starch-deficient *adg1* and *pgm* mutants.

5.2.3.1. Leaf morphology.

A second starch-deficient mutant was used to test whether the increased leaf thickness and cell layer phenotype observed in the *pgm* is specific to this mutant or if it is a general feature of starchless mutants. The *adg1* mutant lacks the small subunit of plastidial ADP-glucose pyrophosphorylase which is part of the biosynthetic pathway of starch, converting glucose-1-phosphate to ADP-glucose, the substrate of starch synthase.

Fig. 5.9 shows the leaf thickness and the number of cell layers in the *adg1* mutant grown in 16h days along with the *pgm* mutant for comparison and the Col-0 wild type. Cross sections of leaves from Col-0 and the *adg1* mutant, stained with iodine to show the absence of starch in the latter, can be seen in Fig 4.9.

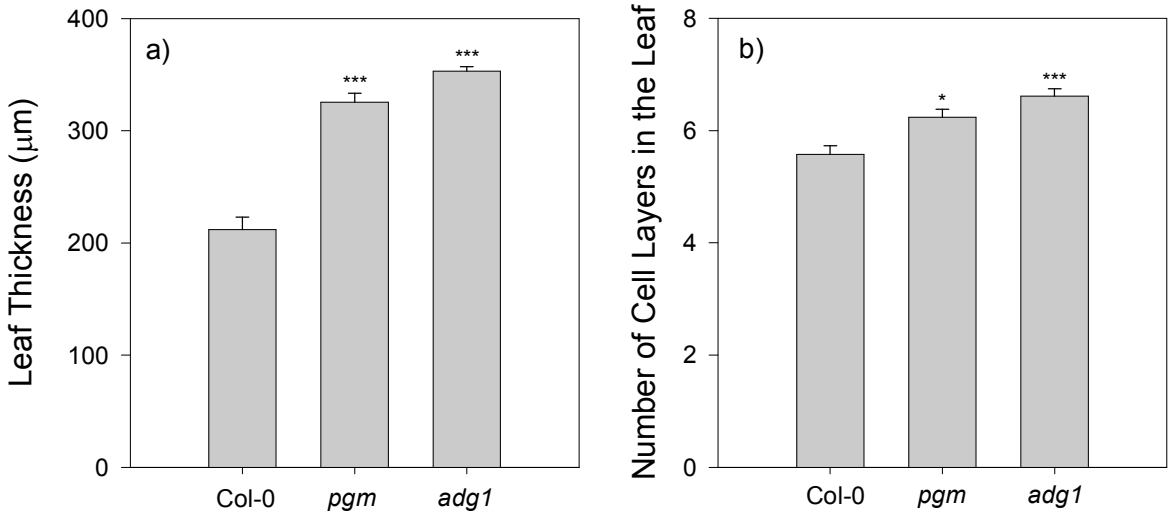

Fig. 5.9. Leaf morphology in two starch-deficient mutants of Arabidopsis.
Leaf thickness (a) and number of cell layers in leaf 6 of starchless mutants in *Arabidopsis thaliana* grown in 16h days at an irradiance of 160 µE m^{-2} s^{-1}. Significant differences (t-test with Holm-Sidak correction) from wild type are shown as * $P < 0.05$, ** $P < 0.01$, *** $P < 0.001$. N=5 leaves. Bars are standard error of the mean.

The *adg1* mutant had a similar phenotype to the *pgm*, with leaf thickness significantly elevated by 67% compared to the wild type (P<0.001). This was accompanied by a significant increase in the number of cell layers in the leaf (P<0.001). The phenotype was more pronounced in the *adg1* mutant than the *pgm*, however the differences between them were not significant.

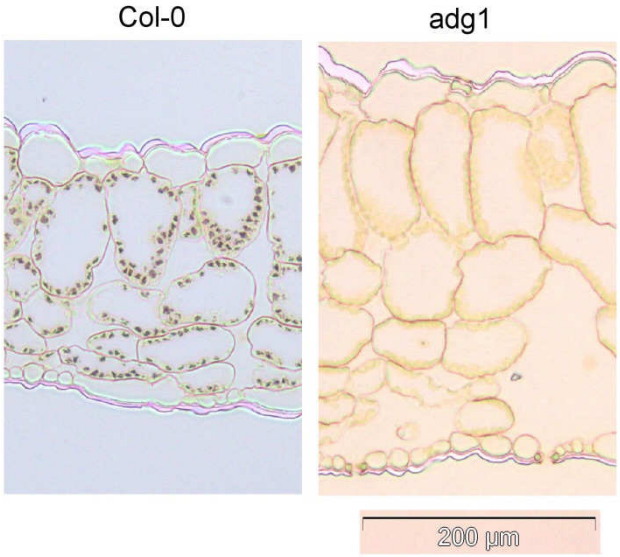

Fig. 5.10. Leaf cross-section of starch-deficient *adg1* mutant of Arabidopsis.
Transverse sections of *Arabidopsis thaliana* Col-0 wild type and starchless *adg1* mutant grown in 16h days at an irradiance of 160 µE m^{-2} s^{-1}. Lugol-iodine staining makes starch visible as dark blue granules.

5.2.3.2. Sugar levels.

Sugar levels at the end of the day were similarly elevated in the *adg1* mutant as in the *pgm* (Fig. 5.11). Like pgm, the *adg1* mutant had significantly elevated levels of glucose (P=0.009) and sucrose (P<0.001) compared to wild-type Col-0 however it also accumulated significantly more sucrose than *pgm* (P<0.001). Starch contents in both mutants were negligible at the end of the day and were <1% of the wild type values (not shown). The lack of starch is also evident in Fig. 5.10, where starch is visible as a dark-blue coloration due to iodine staining.

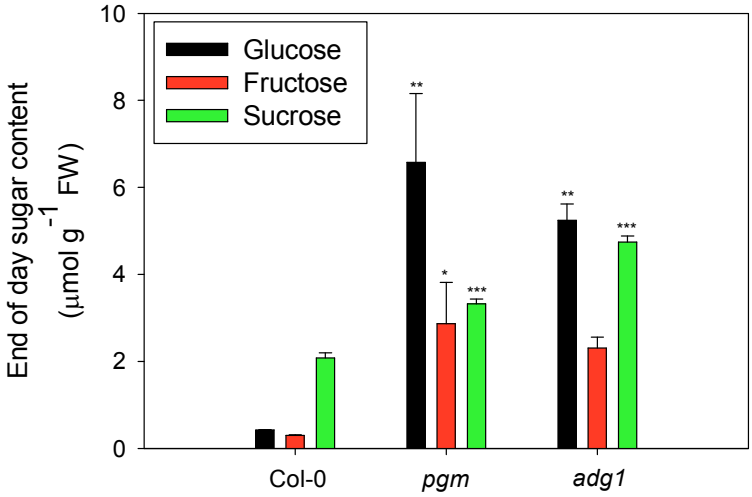

Fig. 5.11 Sugar accumulation in two starch-deficient mutants of Arabidopsis.
Soluble sugar content at the end of the day in *Arabidopsis thaliana* Col-0 wild type and starchless *pgm* and *adg1* mutants grown in 16h days at a light irradiance of 160 µE m^{-2} s^{-1}. Bars are standard deviations. N=5. Significant differences (t-test with Holm-Sidak correction) from wild type are shown as * P < 0.05, ** P < 0.01, *** P < 0.001.

5.2.4. Effect of daylength on leaf morphology in the *pgm* mutant.

5.2.4.1. Sugar levels.

The metabolic and growth phenotypes of the *pgm* mutant are known to vary with daylength, offering a further opportunity to manipulate sugar levels in the plant. The effects of sugars on leaf development were studied in further detail by growing wild type Col-0 and the *pgm* plants in three daylengths – medium (12 h), long (16 h) and very long (22 h) – at the same irradiance (160 µE m^{-2} s^{-1}). Sugars were measured in rosettes sampled at the end of the day.

There were significant effects of daylength on the levels of glucose ($P<0.001$), fructose ($P=0.029$) and sucrose ($P<0.001$) as well as highly significant effects of genotype ($P<0.001$). The two genotypes differed in their response to daylength and there were significant genotype:daylength interactions for the levels of all three sugars ($P<0.001$). There was an upward trend in the levels of all three sugars with increasing daylength in the wild type (Fig. 5.12). Levels of glucose increased almost three-fold between 12-h and 16-h days ($P=0.012$) but did not increase further in 22-h days. Fructose levels increased 5.5-fold between 12 and 22 hours ($P=0.002$) while sucrose rose 81% ($P<0.001$).

The *pgm* mutant exhibited a contrasting phenotype. No significant differences from wild type could be distinguished in any of the sugars in 22-hour days. A progressively more pronounced sugar accumulation phenotype became evident with a shortening in the length of the day period. Levels of glucose in the *pgm* were more than 5-fold higher in 12-h days compared to 22 hours, reaching 26-fold higher levels than the wild type in the same conditions. Fructose levels rose similarly in shorter days, being almost 3-fold higher than in 22-h days and 14-fold higher than wild type levels. Sucrose behaved slightly differently with a drop between 22 and 16 hours ($P=0.007$) and rising again in shorter days to reach 84% higher levels than wild type ($P<0.001$).

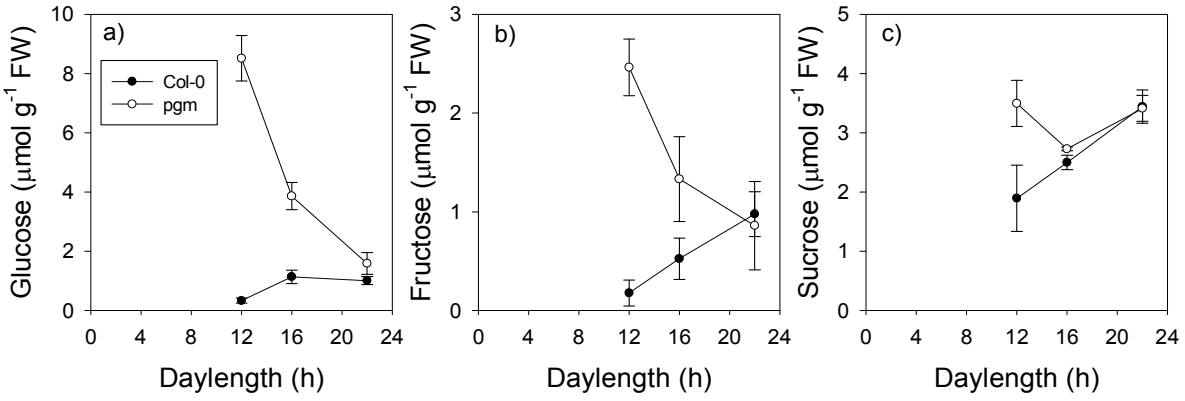

Fig. 5.12 Daylength-dependence of sugar accumulation in the starch-deficient *pgm* mutant of Arabidopsis.
Levels of glucose (a), fructose (b) and sucrose (c) in *Arabidopsis thaliana* Col-0 wild type and starchless *pgm* mutant rosettes grown in three different daylengths at an equivalent irradiance of 160 µE m^{-2} s^{-1} and sampled at the end of the day. Bars are standard deviations. N=5.

5.2.4.2. Leaf morphology.

Leaf morphology followed a similar pattern to the metabolic phenotype and largely tracked changes in the content of sucrose (Fig. 5.13). In the wild type, leaf thickness increased between 12 and 16-h days, followed by a sharper increase in 22-h days. The number of cell layer did not change between 12 and 16 hours but increased sharply in 22-h days.

The phenotype of the *pgm* mutant grown in 22-h days was not significantly different from wild type in leaf thickness and number of cell layers. In 16-h days leaf thickness and number of cell layers were slightly elevated relative to wild type but these differences were not significant while in 12-h days the *pgm* mutant had significantly thicker leaves relative to wild type ($P<0.001$), with significantly more cell layers in the leaf ($P<0.001$). Overall in the *pgm* mutant leaf thickness decreased in 16-h days relative to 22 hours, sharply rising again in 12-h days compared to 16 hours.

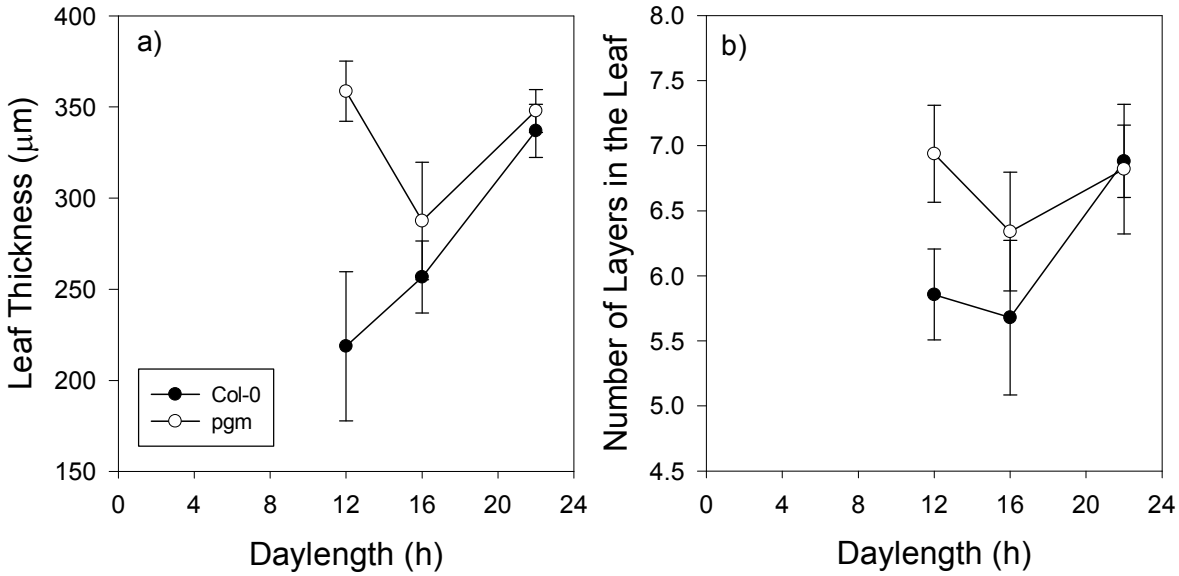

Fig. 5.13. Daylength-dependence of leaf morphology in the starch-deficient *pgm* mutant of Arabidopsis.
Leaf thickness (a) and the number of cell layers in leaf 6 (b) in *Arabidopsis thaliana* Col-0 wild type and starchless *pgm* mutant grown in three different daylengths at an equivalent irradiance of 160 µE m^{-2} s^{-1}. Bars are standard deviations. N=5-8 leaves.

5.2.5. Photosynthetic properties of the *pgm* mutant.

As pointed out in the introduction, plastid function has been implicated in leaf development and light acclimation. The restriction in carbohydrate utilisation and the consequent high sugar accumulation may exert a feedback effect onto the plastid. Both these metabolic restrictions may result in altered or inhibited carbon metabolism in the chloroplast and this may in turn feed back onto the light reactions which energise it. Plastid redox components involved in the light reactions are well known sources of several light signalling processes (see introduction). Furthermore, excitation pressure, a plastid redox phenomenon, has been implicated in morphological light acclimation. The use of the starchless *pgm* mutant allowed these possibilities to be tested. For this a combination of gas exchange and sensitive measurements of chlorophyll fluorescence were employed.

5.2.5.1. Photosynthesis

Fig 5.14 shows the net rates of CO_2 assimilation in the *pgm* mutant in comparison with the wild type in response to different irradiance levels of white light. The *pgm* mutant was compromised in photosynthesis on a mass basis measured on a whole rosette level throughout the range of light irradiances and the differences were significant above 50 µE m^{-2} s^{-1}.

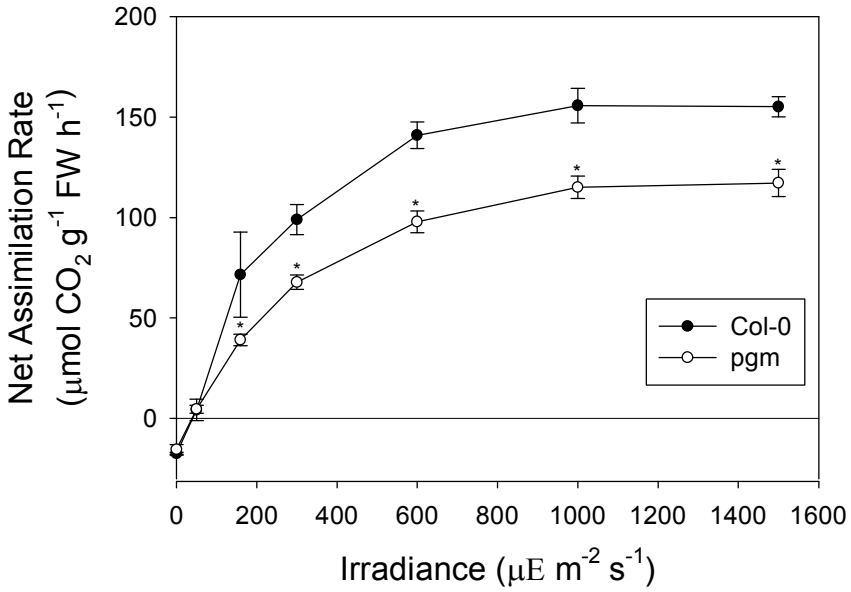

Fig. 5.14. Light-response of photosynthetic rate in the starch-deficient *pgm* mutant of Arabidopsis compared to wild type.
Net rates of CO_2 fixation measured on whole rosettes of *Arabidopsis thaliana* wild type Col-0 and *pgm* mutant grown in 16 hour days at an irradiance of 160 µE m^{-2} s^{-1}. Bars are standard deviation, significant differences from the wild type are marked with stars (Holm-Sidak).

5.2.5.2. Hexose phosphates.

Table. 5.1 shows the content of some of the hexose phosphate sugars in rosettes of wild type and *pgm* mutant sampled at the end of the day. The *adg1* mutant is analysed for comparison.

	G1P	G6P	F6P	FBP	Total
Col-0	32±5	270±25	173±25	66±10	542±59
pgm	34±3	**411±23**	**275±18**	**120±10**	**834±20**
adg-1	**54±3**	**478±86**	**239±109**	**119±6.0**	**966±35**

Table. 5.1 Hexose-phosphate content (nmol g^{-1} FW) of leaves from wild type *Arabidopsis thaliana* Col-0 and the starchless *pgm* and *adg1* mutants.
Data are mean ± SD. Plants were grown in 16-h days at an irradiance of 160 µE m^{-2} s^{-1} and harvested at the end of the day. Glucose-1-phosphate (G1P), glucose-6-phosphate (G6P), fructose-6-phosphate (F6P), and fructose-1,6-bisphosphate (FBP) and total hexose-phosphates were measured by LC-MS/MS. Significant differences from wild type ($P<0.05$) are highlighted in boldface (Holm-Sidak). N=5.

5.2.5.3. Chlorophyll fluorescence.

Analysis of chlorophyll fluorescence is a non-invasive method with which the fate of absorbed light energy in the chloroplast can be assessed in a living leaf. Pulse-amplitude modulated fluorescence (PAM) measurements were used to assess the fate of excitation energy at photosystem II. Fig. 5.15 shows: (a) the quantum efficiency of electron transport at PSII (φPSII), (b) the fraction of absorbed light quanta dissipated by regulated thermal dissipation (φNPQ) and (c) the fraction of PSII reaction centres which are closed, which is also known as excitation pressure (1-qL). This latter parameter corresponds to the reduction state of the primary quinone acceptor at PSII (Q_A), which is a proxy to the redox state of plastoquinone just downstream. All three measures occur on scales from 0 to 1. The measurements were carried out in plants grown in 12-hour days, where the *pgm* mutant has a very severe metabolic and developmental phenotype (the measurements were carried out on the same plants used for morphology and metabolite measurements, shown previously).

At very low light irradiance almost all PSII reaction centres were in the open state, regulated thermal dissipation was not induced, with values close to 0 and PSII was operating close to its maximum quantum efficiency of around 0.8, which is observed in a dark adapted state (F_v/F_m). With increasing irradiance, excitation pressure increased sharply as more reaction centres were excited and reduced the quinone acceptor, becoming closed. φNPQ showed a threshold response, becoming induced and rising sharply with light irradiance above 200 μE m^{-2} s^{-1} while φPSII steadily decreased with increasing light.

The *pgm* mutant did not differ significantly from the wild type at low light irradiances. With increasing irradiance PSII in the *pgm* mutant became progressively less efficient than in the wild type at providing electrons (φPSII), the differences becoming significant above 310 μE m^{-2} s^{-1} while a significantly higher proportion of absorbed light quanta was dissipated as heat compared to the wild type (φNPQ). Excitation pressure did not differ significantly from wild type at any light irradiance.

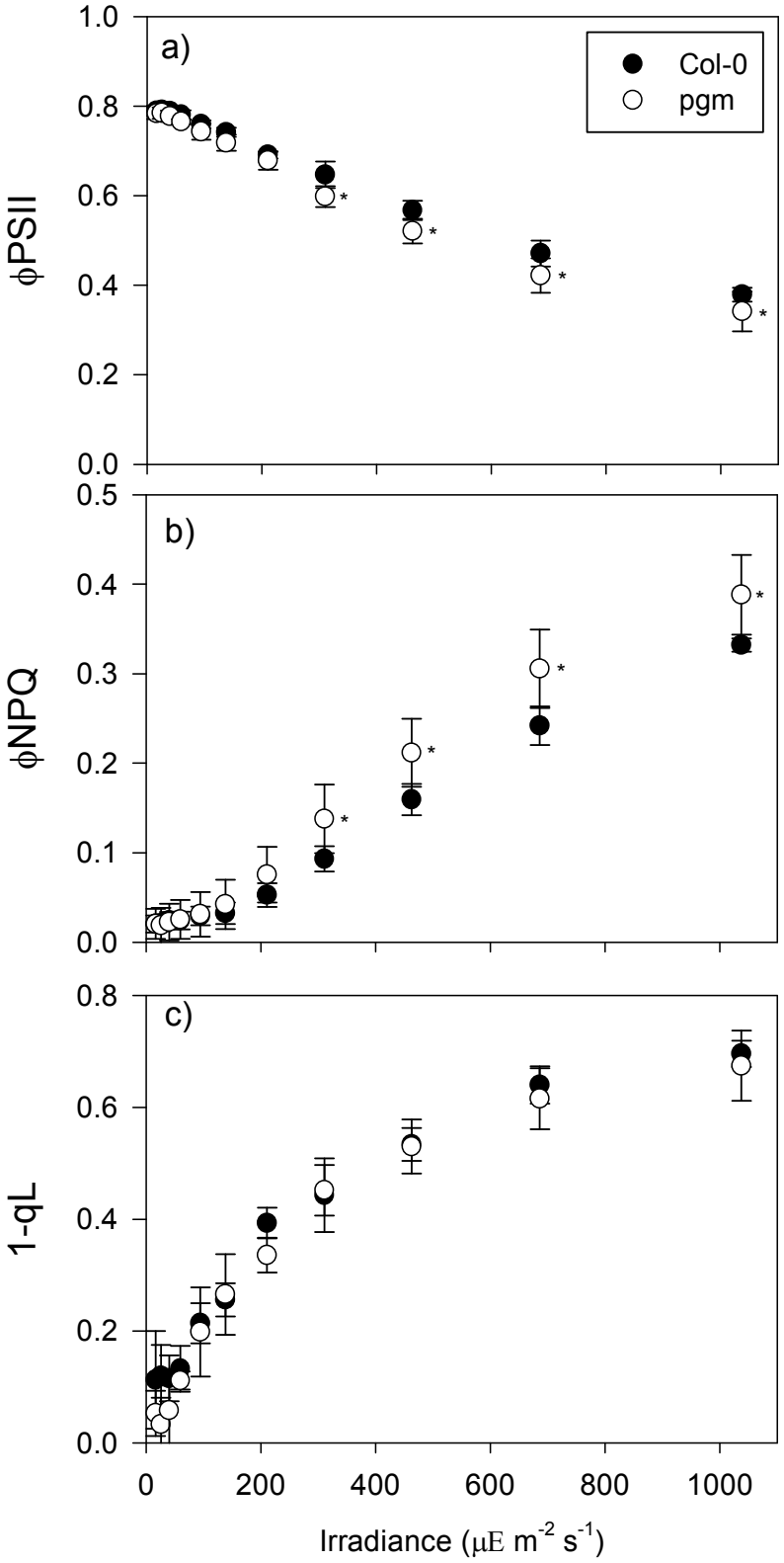

Fig. 5.15. Excitation energy conversion by photosystem II in Arabidopsis wild type and the starch-deficient *pgm* mutant.

Quantum yield of electron transport at PSII (a), fraction of absorbed excitation energy dissipated by regulated non-photochemical quenching, φNPQ (b), and excitation pressure (1-qL, c) measured by chlorophyll fluorescence at different irradiances of red light in *Arabidopsis thaliana* wild type Col-0 and starchless *pgm* mutant grown in 12-hour days at a light irradiance of 160 μE m^{-2} s^{-1}. Bars are standard deviation. N=6 plants. Significant differences from wild type ($P<0.05$) are indicated by stars (Holm-Sidak).

5.3. Discussion.

5.3.1. Irradiance, sugars and leaf morphology in Arabdiopsis wild type Col-0.

Arabidopsis thaliana wild type Col-0 plants exhibited a strong acclimatory response to light irradiance, with leaf morphology showing marked changes. This illustrates the value of Arabidopsis as a model organism for the study of developmental light acclimation. It also contrasts with previous suggestions that *Arabidopsis* and Col-0 in particular cannot acclimate to light (Athanasiou et al., 2010).

The levels of soluble sugars varied strongly between light treatments which is consistent with the idea that sugar concentration could act as a signal. The observed increase in sugars in response to light refutes the possibility that growth matches the supply flux of sugars, resulting in a constant pool size across the range. The observed close covariance between sucrose levels and morphology further supports the possibility of a signalling connection between the two.

Even though sugar contents were measured in whole rosettes, there is little doubt that sugars are translocated to the growing tissues and this is also supported by evidence from systemic signalling experiments, where sugar levels were found to be elevated in developing leaves when mature leaves were exposed to high light or high CO_2 (Coupe et al., 2006). The sugar content of whole plants is thus a reflection of plant sugar status. In a plant such as *Arabidopsis* the whole-rosette sugar content should directly reflect the sugar status of the growing tissues as there is only one growing meristem in the shoot, which receives nutrition from all the leaves on the plant.

5.3.2. Metabolism and leaf morphology in mutants with altered sugar levels.

The use of metabolic mutants allowed manipulations of plant sugar levels to take place without changing light, CO_2 or temperature, providing the opportunity to study interactions between metabolism and development with no complications from changing environmental conditions. This study is one of the first to characterise developmental phenotypes in well-known metabolic mutants. The identification of strong developmental phenotypes linked to metabolism in the starch-deficient mutants highlights the potential of this approach for finding possible metabolic inputs into the regulation of plant development.

The *pgm* mutant appeared to have a leaf phenotype similar to that of high-light grown plants. This is consistent with a proposed role for sugars as indirect signals of light levels. The increased leaf thickness was associated with the leaves having more cell layers, which indicates that cell development changes are required, rather than the increased leaf thickness being caused simply by turgor-driven cell expansion. Although the *pgm* mutant had a lower dry matter content, this can probably be ascribed to the lack of starch, as the samples were collected during the light period. The lower SLA in the *cinv1cinv2* mutant can be ascribed to higher leaf dry matter content rather than an increase in leaf thickness. These results in the Arabidopsis *cinv1cinv2* mutant contrast with the findings of a mutant in an invertase homologue in *Lotus japonicus*, where leaves were much thicker than wild type and had more cell layers in the leaf (Welham et al., 2009). Although some of the observed developmental phenotypes appeared to be linked to sugar levels, comparison of the starch-deficient mutants against the other mutants suggests that sugars are not the causal factor for the developmental differences. Like the starch-deficient *adg1* and *pgm* mutants, the *cinv1 cin2* double mutant had high soluble sugar levels, but its leaf phenotype was essentially indistinguishable from wild type, or from the *f2kp* mutants which had only slightly elevated sugar levels. In addition to their

high-sugar phenotype, the two starch-deficient mutants are likely to share other metabolic differences with each other that set them apart from the *cinv1cinv2* mutants, despite this also having high sugar levels. For example, neither *adg1* nor *pgm* is likely to contain much maltose, the main product of starch degradation at night, and the *cinv1cinv2* had notably high sucrose levels at night (Fig. 4.7). Such metabolic differences are likely to have a broader impact on patterns of gene expression and growth, which might account for the contrasting leaf phenotypes of the starch-deficient mutants compared with other high-sugar mutants and wild type plants.

Although developmental phenotypes were observed which appear to be linked to sugar levels, the sugar concentrations seem not to be causal as the same phenotypes were not observed in the *cinv1cinv2* mutant in spite of severe sugar accumulation and in the *f2kp* mutants which have a mild metabolic phenotype. The identification of the same phenotype in two different starch-deficient mutants suggests that this phenomenon is restricted to this group only and is not caused directly by sugars or at least not by the sugars measured here. The generality of this effect in two starchless mutants suggests that lack of starch synthesis as a whole, and not specific metabolic steps or metabolites, is responsible for the observed effects.

The effect of daylength on the leaf phenotype of *pgm* was investigated in detail. The experiments revealed a dramatic increase in sugar accumulation at shorter daylengths, which at first sight seems paradoxical. Caspar et al. (1985), who first described the *pgm* mutant, concluded that: "because it is unable to store net photosynthate in starch, it accumulates relatively large quantities of sucrose and hexose in both leaf and stem tissue". The implication from this interpretation of the phenotype is that when *pgm* is grown under short-day conditions, it should have less time to produce photosynthate and thus accumulate less sugar, not more, than when grown under long-day conditions. Caspar et al. (1985) also noted in their study that the growth phenotype of *pgm* became more severe in short days but disappeared in long days.

It was later shown by other groups that the *pgm* mutant exhibits numerous transcriptional changes at night which are similar to those seen in wild type plants after an extension of the night This treatment causes the plants to exhaust their reserve carbohydrate supply and enter a period of starvation, during which growth and carbohydrate utilisation are repressed to conserve energy (Gibon et al., 2004). Thus the sugars in *pgm* leaves, although initially high at the beginning of the night, are rapidly consumed, and the absence of reserve starch means that they cannot be replenished. Therefore, *pgm* plants enter C-starvation prematurely during the night. This causes a cessation of growth which carries on to the following day period, when the decreased use of newly-synthesised carbohydrates causes them to accumulate to high levels again. The inhibition of night growth has since been confirmed in the *pgm* mutant using high-resolution growth analysis of leaves (Wiese et al., 2007) and roots (Yazdanbakhsh and Fisahn, 2011). This pattern of night-time C-starvation and suppression of growth during the early part of the day is repeated on a daily basis. This also explains why the growth and metabolic phenotypes of *pgm* become less evident with increasing daylength, and when grown under very long day conditions (22-h photoperiod) they are essentially indistinguishable from wild type (Fig. 4.12). Under such conditions, carbon starvation is avoided because the soluble sugar stores are sufficient to last the short (2-h) night. In shorter daylengths, the period of night-time carbon starvation becomes longer and more severe, causing a proportionally stronger sugar accumulation the next day.

Given the described mechanism, two causal scenarios are possible for the morphological phenotype observed in the *pgm* mutant in different daylengths. First, the morphological phenotype may be dependent on the severity of carbon starvation at night and not on the daytime sugar accumulation. This would explain the apparent link between sugar accumulation and the morphological phenotype, as both would have the same cause, i.e. carbon starvation at night. It may also explain the lack of observed phenotypes in the other mutants; *cinv1cinv2* maintains high sugar levels at night and has

starch, *f2kp* mutants had essentially wild type starch levels (not shown) and showed no signs of carbon-starvation at night as sugar levels at the end of the night were very similar to wild type (Fig. 4.7). However, if the morphological phenotype of the starch-deficient mutants does depend on night-time starvation, it would be difficult to compare this to actual light acclimation as high-light grown wild type plants did not starve at night and, instead, had higher sugar levels.

The second possible explanation for the different leaf phenotypes of the mutants could involve some other factor that is not directly related to metabolism but is affected by the differences in metabolism between the mutants. The possibility that a plastid signal might be such a factor is discussed in the following section.

5.3.3. Plastid function in the starch-deficient *pgm* mutant.

The *pgm* mutant was compromised in photosynthesis. It has previously been reported otherwise when photosynthetic rates were measured on a leaf area basis (Gibon et al., 2004) The *pgm* mutant has thicker leaves than wild type plants. Therefore, if both have the same rates of photosynthesis on an area basis, the *pgm* will have lower rates when these are expressed on a mass basis, as was seen in the current study. The mutant may have compensated for its metabolic restriction by increasing leaf thickness to maintain equivalent photosynthesis per area. This is further supported by the observation of lower photosynthetic rates in starchless mutants when expressed on a chlorophyll basis in Arabidopsis (Caspar et al., 1985; Sun et al., 1999) and in other species (Krickerberg et al., 1989). Some other studies have shown reductions on an area basis as well (Hanson, 1990; Peterson and Hanson, 1991; Eichelmann and Laisk, 1994; Lytovchenko et al., 2002) thus confirming the results of this study.

Elevated levels of phosphorylated sugars in the *pgm* mutant suggest that plastid metabolism may be disturbed in these plants, although the metabolites presented are also present in other compartments in the cell, which may also be affected. Similar results have been presented previously in starchless mutants of Arabidopsis (Kofler et al., 2000), tobacco (Eichelmann and Laisk, 1994) and potato (Lytovchenko et al., 2002), where high levels of hexose phosphates were found to accumulate. A possible mechanism of photosynthetic limitation in the starchless mutants may be a limitation by inorganic phosphate as the free phosphate pool in the plastid stroma is locked up in phospho-ester bonds with carbohydrates. The release of inorganic phosphate from organic compounds can limit the maximum rate of photosynthesis in some conditions (Sage, 1990), particularly in high light, high CO_2 and low O_2 conditions, where the maximum possible photosynthetic rates are observed (Sharkey et al., 1986). Phosphate is released from phosphorylated intermediates during starch synthesis in the plastid as well as during sucrose synthesis in the cytosol, after which it is recycled back to the plastid through stoichiometric exchange with triose phosphate through the chloroplast triose phosphate translocator (Häusler et al., 2000). Starchless mutants are unable to release inorganic phosphate inside the plastid and must rely exclusively on phosphate release in the cytosol through sucrose synthesis and its transport back into the plastid (Sun et al., 1999). It has been suggested previously that photosynthesis may be limited in the starchless mutants by the capacity for cytosolic phosphate release and recycling back to the chloroplast (Peterson and Hanson, 1991; Eichelmann and Laisk, 1994; Lytovchenko et al., 2002). This is supported by several observations of oxygen-insensitive photosynthesis at saturating light and CO_2 levels in starchless mutants (Eichelmann and Laisk, 1994; Sun et al., 1999). The ability of inorganic phosphate to limit photosynthesis has been confirmed by mannose or glycerol-feeding experiments, which depletes the free phosphate pools in the cytosol and stroma and causes feedback limitation of photosynthesis and oxygen insensitivity (Sharkey and Vanderveer, 1989; Morcuende et al., 1997; Takizawa et al., 2008). Manipulations of free phosphate pools by phosphate deprivation and phosphate feeding have also been shown to be able to cause or alleviate phosphate limitation and

oxygen insensitivity of photosynthesis (Leegood and Furbank, 1986; Sivak and Walker, 1986; Takizawa et al., 2008). Phosphate feeding was not, however, able to rescue photosynthetic rates in a starchless tobacco (Eichelmann and Laisk, 1994).

CO_2 fixation via the Calvin-Benson cycle is the major sink for reductant produced by chloroplast electron transport. Therefore, as photosynthetic CO_2 fixation is compromised in the *pgm* mutant, the capacity of this sink to consume reducing equivalents is decreased. Electrons would thus be expected to accumulate in plastid electron carriers and cause them to become over-reduced. This may have implications for signalling as plastid redox states are the sources of various light signals (see introduction). It is conceivable that metabolic restriction in starchless mutants feeds back to affect the redox state of plastoquinone, a known light signal. However, chlorophyll fluorescence analysis of the *pgm* mutant does not support this hypothesis. Linear electron transport was indeed decreased, as expected, but a higher amount of regulated thermal dissipation (NPQ) served to decrease the excitation rate of PSII reaction centres. This effectively compensated for the decreased electron demand, keeping the redox state of plastoquinone unchanged.

The increase in regulated non-photochemical energy dissipation observed in the *pgm* mutant points to an increase in the trans-thylakoid pH gradient. NPQ is mediated by the enzymatic conversion of thylakoid carotenoids into active excitation-quenching species by violaxanthin de-epoxidase (VDE) in the xanthophyll cycle (Bassi and Caffarri, 2000; Ma et al., 2003) and also by another mechanism involving the PsbS protein, which is not yet understood (Hieber et al., 2004). Both mechanisms are directly induced by thylakoid lumen acidification as VDE requires low lumen pH to become active (Yamamoto, 1979) and specific amino acid residues within PsbS become protonated at at low lumen pH, which is necessary for the induction of non-photochemical quenching (Li et al., 2004). NPQ has a photoprotective function and quenches excess light energy in high light conditions, preventing PSII from becoming photoinhibited (Li et al., 2002).

The increased induction of NPQ in the *pgm* mutant may be caused by the phosphate limitation discussed above. It has been shown that the proton conductivity of plastid ATP synthase can drop if the concentration of free phosphate in the stroma is decreased below its K_m by mannose feeding, trapping more protons in the thylakoid lumen (Takizawa et al., 2008). This was shown to result in greater acidification of the thylakoid lumen and an up-regulation of non-photochemical quenching, similar to that observed in this study. An increase in NPQ has been observed previously in a starchless mutant of tobacco (Peterson and Hanson, 1991). The redox state of plastoquinone thus seems to be buffered against downstream restrictions in electron consumption and severe phosphate limitation through decreases in the excitation rate of PSII, which may be adaptive because it should prevent catastrophic PSII damage in such cases.

It is concluded that plastoquinone redox state (excitation pressure) cannot be the signal causing the leaves of the *pgm* mutant to develop the characteristics of a “sun” leaf, as the plastoquinone pool was not over-reduced. However its role in light acclimation cannot be ruled out. It may still be part of a complex of signals regulating developmental adaptation. Plastoquinone redox state was not affected in spite of decreased electron utilisation due to compensatory photoprotective mechanisms which decreased the excitation rate of PSII. Other redox components, for example those downstream of photosystem I, also cannot be ruled out. Although some components of NPQ may also be involved in regulating the excitation of PSI, for example some xanthophyll carotenoids (Thayer and Björkman, 1992), PSI largely possesses different photoprotective mechanisms (Munekage et al., 2002). These may or may not be able to compensate fully for an increased electron pressure at the acceptor side. An over-reduction of the PSI acceptor side has been inferred from measurements of light absorption at 830nm in leaves of a starchless tobacco mutant (Eichelmann and Laisk, 1994). Future work should aim to clarify this issue by examining in more detail the function of PSI in the starchless mutants.

5.4. Chapter summary.

In summary, the work presented in this chapter aimed to investigate the acclimation of leaf morphology to irradiance in Arabidopsis with special reference to the hypothesis that the amounts of sugars arriving from mature leaves to developing leaves may act to indirectly signal the light environment and adjust the development of leaves. Leaves of wild type Arabidopsis became thicker and developed more cell layers in the leaf in high irradiance and sugar levels were correlated with these morphological traits. A series of knockout mutants with perturbed primary metabolism were then grown in one light environment and their leaves investigated. The mutants contained a range of sugar levels which were higher than wild type. Very thick leaves were observed in the starchless *pgm* mutant, which was reminiscent of high-light-adapted leaves, while no alterations to leaf thickness could be observed in other mutants in spite of high sugar levels. A similar phenotype was observed in *adg1*, a different starchless mutant. The *pgm* mutant was grown in three different daylengths and compared to the wild type. Both the metabolic and developmental phenotypes became progressively more pronounced in shorter daylengths, with very high sugar content and very thick leaves in a short daylength. It was then investigated whether the metabolic alterations observed in the *pgm* affect plastid function and alter the redox state of plastoquinone, a known light-signalling component of chloroplasts. The *pgm* mutant had lower rates of CO_2 uptake and this was accompanied by lower rates of electron transport in the chloroplast. However, a higher proportion of light energy was dissipated as heat and this compensated for decreased electron demand. As a result, plastoquinone redox state was unaltered. It is concluded that sugar levels do not signal the developmental changes which occur in leaves in response to light. A morphological phenotype resembling high-light-adaptation seems to be restricted to starchless mutants, where it correlates with the severity of their metabolic alterations in different daylengths. Alterations in plastoquinone redox state are not responsible for this phenotype as they did not occur.

Chapter 6. Natural variation in leaf morphology, its relationship to growth, leaf function and plant performance.

6.1. Introduction.

6.1.1. Leaf morphology traits.

As discussed in the introduction, plant growth is measured relative to existing biomass and expressed as RGR, which is often decomposed into three components: NAR, SLA and LMR (Hunt, 1982) Decomposing RGR into its components has been very useful in partitioning variation in growth in a simple mechanistic framework which has greatly aided our understanding of plant growth and its regulation (Poorter and van der Werf, 1998; Poorter and Nagel, 2000; Wright and Westoby, 2000). However, there is scope for deeper exploration by examining leaf morphology and leaf function in more detail.

Leaf morphology can be thought of as an integrative or emergent phenotype that is generated by interactions between a complex of traits. Not all leaves in nature are the same and both leaf morphology and the underlying traits are variable. It is obvious that some trait combinations will be subject to tradeoffs. Probably most or all of the traits vary within certain upper and lower limits due, for example, to developmental or structural constants. Some of the varying traits can be dependent on each other or can co-vary with other traits. It is also probable that some trait combinations will be subject to tradeoffs. Evolution may select for certain sets of traits and trait covariances which confer fitness advantages in certain environments or all environments (e.g., (Shipley et al., 2006)), with implications that different environments may be expected to produce different trait relationships due to changes in associated tradeoffs. There is limited information on the relationships between leaf morphological traits themselves, and especially their relationships to whole plant processes and growth.

6.1.2. Cell division.

Leaf size has often been decomposed into cell number and average cell size, which provides information about the relative contributions of cell division and cell and tissue expansion to variation in leaf size. The expansion of cells is well coordinated with cell division and shows similar responses to diverse environmental conditions (Granier et al., 2000). Strong correlations between leaf area and cell number are usually identified while the contributions of cell size to leaf area variation have been low (Cookson et al., 2005; Gonzalez et al., 2010). Such studies have shown that cell number chiefly drives variation in leaf area in response to light irradiance (Cookson and Granier, 2006), daylength (Cookson et al., 2007) and temperature (Granier and Tardieu, 1998). These observations are consistent with a cell theory of organ size control. The cell theory states that the cell is the basic morphogenetic unit which determines the shapes and sizes of organs (Fleming, 2007). The cell theory has been challenged by observations of uncouping between cell division and cell expansion in some cell division mutants (De Veylder et al., 2001; Horiguchi et al., 2006) which, within some limits, results in compensation for altered cell number by reciprocal changes in cell size. Responses consistent with the compensation mechanism also occur under some natural conditions e.g. during shade acclimation (Cookson and Granier, 2006) and mild water limitation (Aguirrezabal et al., 2006). Further analysis of leaf size control using chimeric plants has implicated non-cell-autonomous compensation mechanisms and interactions between cells in leaf size control (Kawade et al., 2010; Marcotrigiano, 2010). These observations imply that there are organ and even organism-level controls on leaf size (Tsukaya, 2003)

and support the broader organismal theory of organ size control (Kaplan and Hagemann, 1991; Day and Lawrence, 2000; Fleming, 2002; Fleming, 2006).

6.1.3. Cell expansion.

The expansion of cells and biomass is a component of leaf morphology and function. The determination of SLA is related to the expansion of biomass during leaf growth (Tardieu et al., 1999). As SLA is a major functional parameter associated with growth, variations in cell size driven by biomass expansion have the potential to influence whole plant function and growth rates. This is due to the compound return on investment that extra leaf area brings, which should drive more growth. The state of biomass expansion may also be reflected in the dry matter content of leaves. This is particularly interesting, since recent studies on Arabidopsis accessions have identified robust negative associations between plant growth and rosette protein content on a fresh weight basis (Sulpice et al., 2010). Protein is a significant component of plant dry matter and is relatively expensive to produce and maintain (Poorter, 1994; Piques et al., 2009). Further work has shown that high protein content in small accessions is associated with increased copy numbers of ribosomes and the loading of these ribosomes on active polysomes, indicating higher rates of protein synthesis and, possibly, turnover (Ishihara, unpublished data). These seemingly counter-intuitive observations suggest that the biomass of small accessions has a higher synthesis and maintenance cost and this may constitute an inefficient use of carbon and may therefore preclude higher growth rates. It is unclear how leaf morphology is involved in this trend. For example, less cell expansion in smaller accessions may cause more dry weight biomass to be concentrated in leaves, driving a trend for a high content of dry matter and its components in smaller accessions, which may explain the observed trend in protein. Biomass expansion should be reflected in SLA, dry matter content and perhaps cell size, but it also carries with it a hidden component which is related to the abovementioned benefits of creating more leaf area from biomass and therefore intercepting more light. This component may be seen as part of the efficiency of carbon use which is driven by returns on biomass investment and may thus also be one of the components of NAR.

6.1.4. Leaf thickness.

The vast majority of previous studies treat leaves as flat two-dimensional objects while the third dimension of the leaf (leaf thickness) is not explored. As seen in chapter 4, leaf thickness variation can be brought about by elongation of mesophyll cells and/or extra cell divisions to generate more cell layers. It thus potentially involves cell division as well as cell and biomass expansion, but in a different plane to that which drives leaf area generation. Leaf thickness correlates with the capacity for gas exchange per unit leaf area. This is because a thicker leaf allows a larger internal cellular surface area per unit leaf area, and thus aids CO_2 uptake within the leaf (Syvertsen et al., 1995; Terashima et al., 2001). At a given biomass input, leaf thickness trades-off with leaf area, which can be seen as the capacity for light interception (Roderick et al., 1999; Terashima et al., 2001). Leaf thickness also has a role in light interception along with leaf area. As leaf thickness is decreased below a critical value, which will depend on the irradiance regime, an increasing proportion of the incident light will pass through the leaf rather than being absorbed. On the other hand, if a leaf is too thick, not enough light will reach the lower layers of the leaf and drive photosynthesis, which would leave un-used capacity and decrease the efficiency of resource use (Evans et al., 1993). Therefore, leaf thickness is a major component of developmental acclimation to high light, where a high capacity for gas exchange is required.

It has been proposed that leaf thickness is regulated at the organ level. During light acclimation in *Chenopodium album* leaves, cell divisions are partitioned to extra mesophyll cell layers while keeping a constant total cell number in the leaf (Yano and Terashima, 2004). Vile et al., (2005) demonstrated that leaf thickness can be accurately predicted from SLA and leaf dry matter content. Little is known about leaf thickness and its relationship to leaf growth and other traits in Arabidopsis. Due to the inherent trade-offs that leaf thickness is associated with, it may be expected to be related to leaf size. Furthermore, as leaf thickness is strongly involved in light acclimation, its genotypic variation in plants grown in one light environment is not expected to be large and to potentially drive some variation in growth.

6.1.5. Leaf number.

Analysis of leaf growth is almost always carried out in the context of a single leaf (Cookson et al., 2005; Gonzalez et al., 2010). A good example is the large EU-financed integrated project AGRON-OMICS, which focuses on a detailed molecular and metabolic analysis of the development of the sixth leaf of Arabidopsis (Micol, 2009). On the other hand, in whole plant growth analysis, terms like SLA and NAR are sometimes applied to data that is obtained by analysis of a single representative leaf, or to an average value obtained by analysis of the whole shoot or rosette. However, a shoot or rosette usually consists of many leaves. It can be anticipated that there will be interdependencies between the growth rates of different leaves. In principle, a given leaf area could be generated by having a small number of large leaves, or a large number of small leaves. It can also be anticipated that the growth of individual leaves or all leaves will be affected by the overall rate of plant growth.

The number of leaves puts leaf size and leaf morphology in a whole plant context and offers an opportunity to investigate organism-level controls on leaf development i.e. interactions between leaves. Positive correlations between the rate of leaf initiation and the rate of cell division during early leaf growth indicate that early organ growth and organ production may be co-regulated (Cookson et al., 2005). This implies that more plant growth results in larger organs as well as more of them being produced. However, different leaf primordia can also be viewed as a set of sinks competing for limited photosynthate. This viewpoint indicates there may be a trade-off between an increased rate of leaf initiation, and leaf area growth. Resources are limited and a set amount of growth (or a set number of cells) may be partitioned between more or fewer leaves. Seen from this viewpoint, variation in leaf initiation rate should have a direct inverse effect on the size of leaves. However this inverse relationship may only be evident if growth were held constant, and would otherwise be masked. If there is an increase in the growth rate, the plant would be able to accommodate more leaves and make leaves bigger. Nevertheless, the question still arises, if there is variation in the relation between the rate of leaf initiation and the rate of leaf growth and the consequent traits, leaf number and leaf size. A trade-off between leaf number and leaf size may (and in some ways must) be a part of organism-level control of leaf size and, perhaps, morphology.

The preceding discussion prompts the question: what is the optimal rate of leaf initiation? Should a growing plant make many small leaves or a few large ones from a set amount of biomass? Which strategy leads to better outcomes (growth, fitness etc?). How does this affect the morphogenesis of leaves? What regulates the number and size of leaves at the genetic, molecular, cellular, organ and organism level, and how do regulatory mechanisms at these different levels interact? In reality, plant growth, leaf production and leaf size vary simultaneously and the relationships between them are not obvious and not well explored. The three components must thus be studied together in a whole plant context. There is evidence for such a trade-off on leaf number from studies of trees, where leaf number has been shown to trade-off isometrically with leaf size when normalised on current year growth of a

single module (Kleiman and Aarssen, 2007; Yang et al., 2008), however its relationship with whole-plant growth is unclear.

An understanding of morphological trait variation and trait relationships may shed light on the fundamental ways leaves are constructed and the inherent trade-offs which shape their form. Such an examination in natural, genetically diverged populations should give information on the factors and pressures shaping the evolution of individual traits and of leaf form as a phenotype. Since the populations are geno typically-differentiated, the manifest traits in such a system are genetically determined (rather than being environmentally-influenced); the genetic bases for them should be accessible to quantitative genetic methods.

6.1.6. Aims of the chapter.

In this chapter, leaf and rosette morphology and function were characterised in 20 wild accessions of *Arabidopsis thaliana* with the aim of establishing relationships between leaf morphology components in the context of leaf and whole plant function and performance and to build a model of Arabidopsis growth incorporating leaf morphological variables, leaf function indicators and whole plant growth. Leaf morphology is probed on multiple facets and includes cellular traits such as cell size and cell number data, composition traits, the third dimension of the leaf in the form of leaf thickness and combined with the number of leaves to put morphology in a whole rosette context. Photosynthesis and respiration rate measurements are used as indicators of leaf function and their relationship with leaf morphology and plant growth is explored. Such a comprehensive analysis on Arabidopsis accessions has not been published previously.

The aims of the chapter are:

1. Identify key axes of variation in leaf morphology traits and their relationships in natural accessions of *Arabidopsis thaliana*

2. Construct a model and identify the relative importance of variation in different variables to whole plant growth, leaf size, cell size and leaf thickness

3. Identify and explore tradeoffs between traits

4. Assess the contribution of leaf morphology to leaf function

5. Assess the contribution of leaf function to plant performance (growth)

6.2 Results.

6.2.1. Leaf morphological trait variation in Arabidopsis accessions.

Twenty wild accessions differing in growth rate and morphology were grown for 38 days in a short day (8h), low light (160 μE m-2s^{-1}) environment and a number of morphological traits measured at harvest. Accession means and their cross-genotypic variability (coefficients of variation, CV) are displayed in Table. 6.1, together with the abbreviations and units for each measured and calculated trait. Accessions means were normally-distributed in all traits (Shapiro-Wilk Test) with the exception of abaxial stomatal density, where the distribution was strongly skewed to the right by two strong outliers (data not shown).

Leaf initiation was measured by counting leaves emerging from the apical region at four times during growth (14, 19, 24 and 29 days after sowing) and taking the average rate in the three time periods leaves d^{-1}. The rate of leaf initiation (RLI) varied between accessions somewhat more than the growth rate. Total leaf area, cell number per leaf and cell density were determined in leaf 6, as a representative for mature leaves. The area of leaf 6 varied substantially, as did the number of cells in the leaf. Cell size, determined as the inverse of mesophyll density was less variable. Traits relating to leaf morphology and composition - specific leaf area (SLA), the amount of leaf area displayed per unit leaf biomass, leaf dry matter content (LDMC) and leaf thickness showed very low variance between accessions. Stomata were present on both sides of the leaf, with a higher density on the abaxial side. Two accessions (Ler-1 and Van-0) were very strong outliers with respect to stomatal density on the abaxial side, with very high densities found there.

Rosette fresh weight at harvest exhibited a large genotypic variability (Table. 6.1) and ranged more than three-fold between the smallest and largest accessions, with a CV of 29.5%. This was the largest variance for any of the traits studied. However, as discussed in the introduction, fresh weight is a product of incremental growth over a period of time, which allows small differences in growth rate to accumulate over time and thus greatly over-represents the actual variance in growth.

The actual rate of growth is given by the relative growth rate (RGR). RGR was estimated by taking the difference between the log-transformed biomass values at two points in time and dividing it by the length of the time interval. The differences in the estimated RGR were quite modest between accessions. The CV for RGR (5.1%) was actually the smallest found of all traits that were measured or calculated in this study. Other traits with relatively small CVs included leaf dry matter content (LDMC, 6.2%), leaf thickness (LT, 6.4%) and specific leaf area (SLA, 7.1%), while intermediate CVs were found for the rate of leaf initiation and leaf number (RIL, LN, both 13%) and mesophyll cell density (CellDens; 15.9%) stomatal density (13%) and stomatal density (16.7 and 25.7% for adaxial and abaxial, respectively) and cell number per leaf (CellNo, 22.6%).

Analysis of variance was used to test whether accessions differed in growth and morphology, as well as for position effects. The results of the ANOVA are listed in Table 6.2. There were strong and highly significant effects of genotype (accession) on all morphological parameters and genotype was the largest source of variation in the dataset for most traits. Most traits (with the exception of stomatal characters) were also subject to weak but significant position effects within the growth chamber (tray). The pattern of variation between trays was consistent with gradients of irradiance and/or heating received. Variance between trays accounted for up to 26% of total variance in traits, with the strongest effects on fresh weight and leaf thickness (both were higher in trays in the middle of the chamber, which received more light, data not shown). The accessions were randomised through the growth space using a random number generator and accession means are an average from many trays

Parameter	Rosette Fresh Weight	Relative Growth Rate	Leaf 6 area	Mesophyll cell density	Cell number per leaf	Specific Leaf Area	Leaf Dry Matter Content	Leaf Thickness	Stomatal Density (Adaxial)	Stomatal Density (Abaxial)	Rate of Leaf Initiation	Leaf Number	Leafing Intensity
Abbreviation	FW	RGR	LA	MD	CellNo	SLA	LDMC	LT	StAd	StAb	RLI	LN	LI
Units	g	$g\ g^{-1}\ d^{-1}$	mm^2	cells mm^{-2}	cells x 10^3	$m^2\ kg^{-1}$ DW	g DW g^{-1} FW	µm	Stomata mm^{-2}	Stomata mm^{-2}	leaves d^{-1}	leaves	leaves g^{-1} FW
Ang-0	0.399	0.212	161.4	313.4	49.9	83.9	0.078	153.2	53.8	102.5	0.553	16.3	40.9
Bla11	0.668	0.236	282.0	275.6	77.1	93.4	0.071	151.7	52.7	96.7	0.585	17.2	25.8
Bsch2	1.273	0.259	351.2	256.9	90.1	88.4	0.070	164.5	62.4	98.5	0.757	22.1	17.4
Bu-2	0.551	0.216	191.0	313.1	57.9	80.0	0.081	157.6	58.3	99.4	0.611	18.1	32.9
C24	0.640	0.231	164.6	392.6	64.4	82.4	0.070	175.0	56.7	97.3	0.662	19.6	30.7
Col-0	0.660	0.232	234.4	275.4	63.5	79.8	0.071	181.4	60.1	87.2	0.625	18.8	28.5
Cvi	0.506	0.221	306.7	297.4	86.7	87.4	0.070	164.0	63.6	97.7	0.449	12.9	25.4
Da-0	0.727	0.240	291.9	295.2	85.6	77.3	0.074	177.1	64.2	105.7	0.590	17.6	24.2
Ei-2	0.617	0.232	220.4	331.4	74.4	87.6	0.070	163.7	63.6	109.8	0.652	19.0	30.7
Hl-3	0.898	0.244	274.7	267.1	73.5	86.3	0.068	171.9	61.2	100.7	0.724	21.2	23.7
Kl-0	0.736	0.236	282.9	288.4	80.9	86.6	0.070	168.9	69.2	144.1	0.561	16.8	22.9
Kn-0	1.019	0.249	283.4	270.3	76.6	86.0	0.073	161.9	53.3	89.4	0.819	23.8	23.4
Ler-1	0.648	0.233	256.4	229.5	58.1	73.1	0.067	198.3	85.5	145.1	0.555	16.7	25.7
Lip0	1.007	0.248	258.7	220.2	57.3	86.0	0.072	162.4	40.7	104.5	0.702	21.2	21.0
Mh1	0.758	0.237	211.7	260.0	55.9	89.0	0.067	171.7	48.2	79.3	0.693	20.4	26.9
Old1	0.938	0.246	355.6	251.6	90.0	86.2	0.069	170.6	56.4	85.7	0.631	19.0	20.3
Peter	0.624	0.228	216.7	235.9	50.8	95.5	0.067	160.8	63.2	94.7	0.608	18.0	28.8
RRS7	0.653	0.234	217.1	254.9	54.9	79.8	0.078	160.9	59.0	94.1	0.660	19.4	29.7
Van-0	0.463	0.221	158.9	235.8	36.9	88.0	0.072	160.5	76.5	196.7	0.575	16.8	36.2
Wei1	0.963	0.246	290.7	202.1	58.3	99.1	0.061	173.8	47.6	84.8	0.617	18.1	18.8
Mean	0.737	0.235	250.5	273.3	67.1	85.8	0.071	167.5	59.8	105.7	0.631	18.6	26.7
SD	0.217	0.012	57.9	43.5	15.2	6.1	0.004	10.7	10.0	27.2	0.082	2.4	5.8
CV%	29.5	5.1	23.1	15.9	22.6	7.1	6.2	6.4	16.7	25.7	13.0	13.0	21.9

Table. 6.1 Morphological variation in 20 wild accessions of Arabidopsis.
Plants were grown in 8-hour days at an irradiance of 160µE m^{-2} s^{-1} in a 20°C/20°C diurnal temperature regime. Parameter estimates (LS Means) of morphological variables determined in 20 wild accessions of *Arabidopsis thaliana* grown in 8-hour days at an irradiance of 160µE m^{-2} s^{-1} in a 20°C/20°C diurnal temperature regime. Values are means of 8 plants.

(although not every tray was always represented in each accession sample), thus compensating for this variance due to position effects. All but one accession:tray interactions were not significant, indicating that tray position affected accessions in the same way. The exception was cell number per leaf, where the interaction was significant. No generalisation could be made about this interaction.

Trait	Factor:	Accession	Tray	Accession x Tray	Error
		df=19	df=7	df=109	df=24
FW (g)	F	10.9	15.2	0.71	
	p value	**<0.0001**	**<0.0001**	0.87	
	Variance %	51	26	18	5
RLI (leaves d^{-1})	F	24.5	9.9	0.96	
	p value	**<0.0001**	**<0.0001**	0.585	
	Variance %	60	9	14	18
LA (mm^2)	F	15.5	10.1	0.7	
	p value	**<0.0001**	**<0.0001**	0.89	
	Variance %	63	15	16	5
MD (cells mm^{-2})	F	8.9	2.6	0.99	
	p value	**<0.0001**	**0.036**	0.54	
	Variance %	53	6	33	7
Cell No (cells)	F	24.1	11.7	2.5	
	p value	**<0.0001**	**<0.0001**	**0.005**	
	Variance %	54	10	33	3
SLA (m^2 kg^{-1})	F	5.5	2.6	1.4	
	p value	**<0.0001**	**0.038**	0.156	
	Variance %	35	6	52	8
LDMC (g DW g^{-1} FW)	F	3.4	5.7	0.9	
	p value	**0.003**	**0.001**	0.649	
	Variance %	29	18	43	11
LT (μm)	F	9.5	19.4	1.6	
	p value	**<0.0001**	**<0.0001**	0.089	
	Variance %	35	26	34	4
StAd (stomata mm^{-2})	F	6.2	1.1	0.7	
	p value	**<0.0001**	0.403	0.881	
	Variance %	52	3	34	11
StAb (stomata mm^{-2})	F	29.3	1.7	1.3	
	p value	**<0.0001**	0.152	0.226	
	Variance %	76	2	19	3

Table. 6.2. Analysis of variance of morphological variation in 20 wild accessions of Arabidopsis. Two-way fixed effects analysis of variance (Model I) of the effects of accession, tray position and their interaction on morphological parameters measured on 20 wild accessions of *Arabidopsis thaliana* grown in 8-hour days at an irradiance of 160 μE m^{-2} s^{-1} in a 20°C/20°C diurnal temperature regime. F (variance ratio) is the ratio of the mean squares between groups to the error mean square (within group error). P values were calculated by testing the F statistic against the F-distribution with the listed degrees of freedom (df). Significant effects at $P < 0.05$ are highlighted in boldface. Variance components are the sum of squares of each factor and the error variance as a proportion of the total sum of squares. All parameters were measured on 8 replicates per accession, randomly distributed across 8 trays. For rate of leaf initiation the number of replicates was 14 per accession in 8 trays, making the corresponding degrees of freedom 19 (accession), 7 (tray), 111 (interaction) and 141 (error). A model I design was chosen to allow an exact variance partitioning between the factors and to have an exact estimate of the error variance as a percentage of the total.

6.2.2. Principal Components Analysis.

Table 6.3 shows the Pearson correlations between all variables. Fresh weight and RGR were significantly and positively correlated with leaf area (LA), ($r = 0.71$ and 0.72 respectively, $p < 0.001$), the rate of leaf initiation (RLI) ($r = 0.72$ and 0.68 respectively, $p<0.001$) and leaf number at harvest (LN) ($r = 0.73$ and 0.69 respectively, $p<0.001$) and positively but less strongly correlated with cell number per leaf (CellNo) ($r = 0.47$ and 0.50, $p = 0.04$ and 0.02 respectively). RGR was significantly correlated with leaf dry matter content (LDMC, $r = 0.46$, $p = 0.04$). Leaf area (LA) was strongly and positively correlated with cell number per leaf (CellNo, $r = 0.82$, $p<0.001$). Specific leaf area (leaf area per unit dry weight) was negatively correlated with leaf dry matter content (LDMC, $r = -0.51$, $p = 0.02$) and with leaf thickness (LT, $r = -0.47$, $p = 0.04$). The density of stomata on the adaxial and abaxial surface was correlated strongly with each other ($r = 0.72$, $p < 0.001$) but not with any other traits.

Principal components analysis (PCA) was used as an exploratory tool to identify key axes of variation in the multivariate dataset and to look for patterns in the data. To do this, the data were first normalised as standard deviates, normalising it to give every trait a mean of 0 and a standard deviation of 1. PCA was then carried out on the correlation matrix. The results were visualised using a biplot (Fig. 6.1). The multivariate dataset had a high total variance, requiring a large number of principal axes to summarise it. The first two principal axes of variation accounted for only 54% of the total variance in the dataset while the 3rd and 4th explained a further 29%. The first four components were retained as informative as they captured the majority of the variation (82%) and were the components with eigenvalues greater than 1. Rescaled principal component coefficients of each variable (also referred to as factor loadings) are presented in Table. 6.4.

The first principal component axis separated large accessions from small ones based on rosette fresh weight. Variables relating to leaf size and leaf number as well as CellNo per leaf and SLA were strongly loaded on the first PC along with FW, while MD and LDMC had opposing laodings.

The second principal component was dominated chiefly by variance in leaf morphology variables. A dichotomy between LT and stomatal densities on one hand and cell size (inverse of MD) and high LDMC on the other, dominated the axis. MD was strongly associated with LDMC on the second principal component while LT was negatively related to these variables. MD was equally loaded on the first and second axis, identifying it as a contributor to both growth and morphology. Interestingly, neither total biomass (FW), nor SLA was not a component of the second axis.

On the third principal axis leaves with high SLA are contrasted with leaves with high LDMC and small cells (high MD). CellNo was also a strong contributor to the third axis.

The fourth principal component was dominated by a trade-off between high RLI and high numbers of cells per leaf (CellNo).

	FW	RGR	LA	CellDens	CellNo	SLA	LDMC	LT	StAd	StAb	RLI	LN	LI
	g	g g^{-1} d^{-1}	mm^2	cells mm^{-2}	cells x 10^3	m^2 kg^{-1} DW	g DW g^{-1} FW	µm	Stomata mm^{-2}	Stomata mm^{-2}	leaves d^{-1}	Leaves	Leaves g^{-1} FW
FW	1.00	0.96***	0.71***	-0.40	0.47*	0.24	-0.38	0.13	-0.35	-0.34	0.72***	0.73***	-0.86***
RGR		1.00	0.72***	-0.40	0.50*	0.21	-0.46*	0.23	-0.28	-0.29	0.68***	0.69***	-0.88***
LA			1.00	-0.36	0.82***	0.18	-0.38	0.18	-0.06	-0.29	0.14	0.14	-0.88***
MD				1.00	0.23	-0.31	0.41	-0.13	0.01	-0.12	-0.10	-0.11	0.44
CellNo					1.00	-0.01	-0.13	0.08	-0.02	-0.33	0.10	0.09	-0.63**
SLA						1.00	-0.51*	-0.47*	-0.42	-0.19	0.08	0.04	-0.25
LDMC							1.00	-0.50*	-0.05	0.04	-0.04	-0.03	0.57**
LT								1.00	0.43	0.09	-0.06	-0.02	-0.31
StAd									1.00	0.72***	-0.41	-0.41	0.20
StAb										1.00	-0.34	-0.34	0.31
RLI											1.00	0.99***	-0.35
LN												1.00	-0.36
LI													1.00

Table. 6.3. Pearson correlations between morphological variables determined in 20 wild accessions of *Arabidopsis thaliana.*
Plants were grown in 8-hour days at an irradiance of 160µE m^{-2} s^{-1} in a 20°C/20°C diurnal temperature regime. Correlations were calculated on the means of accession values. Variable abbreviations are same as in Table 6.1. Significant correlations are displayed with stars, with * ($p<0.05$), ** ($P<0.01$), *** ($P<0.001$).

Axis:	PC1	PC2	PC3	PC4
Variance Explained, %	33	21	18	12
Rosette Fresh Weight (FW, g)	**0.50**	0.03	-0.12	0.32
Rate of Leaf Initiation (RLI, leaves d^{-1})	0.29	-0.19	-0.09	**0.66**
Leaf 6 Area (LA, mm^2)	**0.45**	0.17	-0.24	-0.24
Mesophyll cell density (MD, cells mm^{-2})	-0.23	**-0.32**	**-0.36**	-0.27
Cell Number in Leaf 6 (CellNo, cells x 10^3)	0.33	0.00	**-0.48**	**-0.40**
SLA (m^2 kg^{-1} DW)	0.25	-0.03	**0.58**	-0.29
LDMC (g DW g^{-1} FW)	-0.32	**-0.31**	**-0.36**	0.20
Leaf Thickness (LT, µm)	0.08	**0.51**	-0.22	0.12
Adaxial Stomatal Density (StAd, stomata mm^{-2})	-0.23	**0.54**	-0.19	-0.03
Abaxial Stomatal Density (StAd, stomata mm^{-2})	-0.28	**0.42**	0.07	0.18

Table. 6.4. Rescaled coefficients of the first four principal component axes derived from a dataset of morphological variables collected from 20 wild accessions of *Arabidopsis thaliana*.

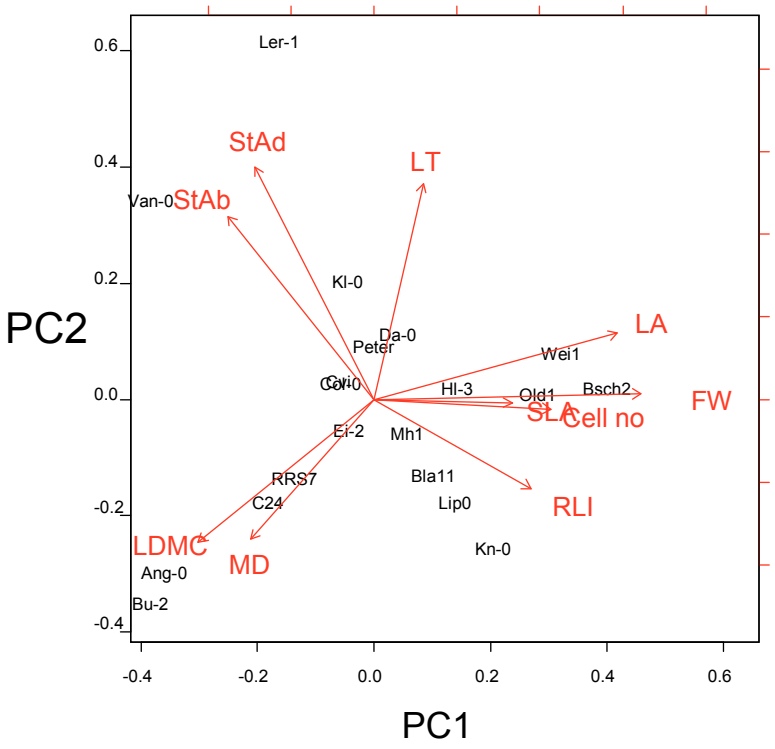

Fig. 6.1 Principal components analysis of leaf morphological variation in 20 wild accessions of Arabidopsis thaliana.
Biplot of the first two principal components of a dataset of morphological parameters in 20 wild accessions of *Arabidopsis thaliana* growing in short day conditions. Variable abbreviations are: FW – rosette fresh weight at harvest (g), LA – leaf 6 area (mm^2), MD – mesophyll cell density (cells mm^{-2}), Cell no – cell number per leaf (cells), SLA – specific leaf area (m^2 kg^{-1} DW), LDMC – leaf dry matter content (g DW g^{-1} FW), LT – leaf thickness (µm), StAd – stomatal density on the adaxial side (stomata mm^{-2}), StAb – stomatal density on the abaxial side (stomata mm^{-2}), RLI – rate of leaf initiation (leaves d^{-1}).

6.2.3. Factor analysis.

While principal component analysis summarised the principal axes of variation in the multivariate data, further insight can be gained by trying to explain the variation by means of a small number of derived common factors which explain as much variance as possible in multiple variables. The principal component axes can be rotated orthogonally in such a way as to maximise the loadings of multiple variables on them. In this way, the multivariate dataset can be simplified for interpretation. The isolation of a small number of important factors also allows a model to be postulated for the data, something which is not possible with principal components alone. Rotation of principal components is one of the methodologies of exploratory factor analysis.

Principal components were rotated using Varimax rotation (Kaiser, 1958). This method finds optimal rotation parameters in order to achieve a few large loadings and many near-zero loadings on each axis. Four rotated axes (factors) were retained. The factors each explained approximately the same proportion of total variance (18-23%). Table. 6.5 shows the rotated loadings of the variables on the factors. The four factors achieved a high degree of communality (the proportion of variance in each variable explained by the factors).

	Factor 1	Factor 2	Factor 3	Factor 4	Communality
Rosette Fresh Weight (FW, g)	**0.52**	-0.04	-0.3	**0.77**	0.95
Rate of Leaf Initiation (RLI, leaves d^{-1})	0.05	-0.19	0.04	**0.92**	0.88
Leaf 6 Area (LA, mm^2)	**0.86**	0.08	-0.31	0.23	0.90
Mesophyll cell density (MD, cells mm^{-2})	0.11	-0.27	**0.71**	-0.34	0.70
Cell Number in Leaf 6 (CellNo, cells x 10^3)	**0.96**	-0.05	0.11	0.03	0.95
SLA (m^2 kg^{-1} DW)	-0.01	**-0.42**	**-0.85**	-0.11	0.90
LDMC (g DW g^{-1} FW)	-0.25	-0.11	**0.87**	-0.02	0.82
Leaf Thickness (LT, µm)	0.27	**0.76**	-0.12	0.14	0.67
Adaxial Stomatal Density (StAd, stomata mm^{-2})	-0.03	**0.87**	0.09	-0.3	0.86
Abaxial Stomatal Density (StAd, stomata mm^{-2})	**-0.41**	**0.68**	-0.02	-0.18	0.67

Table. 6.5. Factor analysis of leaf morphological variation in 20 wild accessions of Arabidopsis thaliana.
Loadings of morphological variables on four factors derived from principal components by Varimax rotation.

Each factor represents an unobserved or *latent* variable which can be linked to a growth process or a strategy, with associated trade-offs.

Factor 1 can be interpreted as a leaf growth factor and was strongly related to leaf size and cell number in leaves, as well as fresh weight.

Factor 2 was a leaf thickness factor which was also associated with high stomatal densities as well as low SLA.

Factor 3 was a cell expansion factor not related to leaf thickness (cell expansion in the plane of the leaf). In this factor, small cells (high MD) were associated with high LDMC and low SLA. There was a discernable effect on leaf area but it was largely independent of leaf thickness (cell expansion in the plane of the leaf).

Factor 4 was a leaf number factor which was strongly related to both rate of leaf initiation and fresh weight.

6.2.4. Morphology and rosette size – a modelling approach

In order to further investigate trait relationships and their integration in the context of plant growth and development a series of models derived from the generalised linear model were constructed. The fresh weight of an Arabidopsis plant is divided between a number of leaves of a certain size. In this experiment leaf 6 was chosen as a representative leaf and its area was measured. The area of the leaf can be factorised into a number of cells of a certain size. The density of palisade mesophyll cells, i.e. how many cells there are per unit leaf area, was measured. Their size is the inverse of cell density and is the cross-sectional area in the paradermal plane. It should be noted that the density estimation includes all the area of the leaf, including the intercellular air spaces. Therefore no area is left unaccounted for and cell number and cell size are directly multiplicative to give leaf area. Finally, leaf area can be related to leaf fresh weight through an appropriate conversion factor. Specific leaf area (SLA) expresses the amount of leaf area displayed per unit biomass invested in the leaf. Since SLA is expressed on a dry weight basis, the content of leaf dry matter in a unit of leaf fresh weight biomass (leaf dry matter content, LDMC, g DW g^{-1} FW) completes the conversion. It can thus be shown that rosette fresh weight is related to the above components by the relation:

$$FW = \frac{CellNo * CellArea * LN}{SLA * LDMC} \tag{6.1}$$

SLA and LDMC are inversely related to leaf thickness (Vile et al., 2005) by the relation

$$LT = \frac{1}{SLA * LDMC} \tag{6.2}$$

It can be shown that leaf thickness is the conversion factor relating leaf area to leaf fresh weight, assuming a specific gravity of 1g cm^{-3}. This assumption has been shown to be true across a range of species (Vile et al., 2005). Equation 6.1 essentially captures multiple levels of variation in leaf and rosette morphology, and encompasses the four factors derived from factor analysis.

Equation 6.1 can be converted to a linear form by log-transformation of all variables.

$$\ln(FW) = \beta_1 \ln(CellArea) + \beta_2 \ln(CellNo) - \beta_3 \ln(SLA) - \beta_4 \ln(LDMC) + \beta_5 \ln(LN) + C \tag{6.3}$$

where β_i are coefficients and C is a constant intercept term. This relationship can now be subjected to multiple linear regression modelling and the contribution of each trait to the variation in fresh weight assessed by computing the coefficients of each variable using least squares regression.

Table 6.6 shows the multiple linear regression model for rosette fresh weight based on Eq. 6.3. The same data was treated in two different ways and two models are presented. The first model was computed using log-transformed data and the table lists the partial regression coefficients. For the second model the log-transformed traits were transformed a second time into standard deviates (subtracting the mean and dividing by standard deviation) and the table lists the standardised partial regression coefficients. For both models, confidence intervals of coefficient estimates were obtained by non-parametric re-sampling 1000 times. To control for over-fitting and to test the performance of the model on an independent dataset, 5-fold cross validation was performed on the multiple regression model, yielding low RMSE values of 0.09 and 0.31 for the ordinary and standardised models respectively.

Model:	$\ln(FW) = \beta_0 + \beta_1\ln(CellArea) + \beta_2\ln(CellNo) + \beta_3\ln(SLA) + \beta_4\ln(LDMC) + \beta_5\ln(LeafNo)$
Multiple R^2 (adjusted)	0.939
F Ratio	59.2
df	5, 14
p value	6.39×10^{-9}

Coefficient	Variable	Estimate	Standard Error of Estimate	t Statistic	p value	Bootstrap Bias	Bootstrap 95% CI Lower	Bootstrap 95% CI Upper
β_0	Constant	-7.36	3.26	-2.3	0.041	0.63	-12.20	2.28
β_1	Cell Area	0.79	0.14	5.8	<0.001	0.08	0.43	1.36
β_2	Cell No	0.69	0.08	8.7	<0.001	0.02	0.46	0.87
β_3	SLA	-0.21	0.31	-0.7	0.497	0.00	-1.26	0.28
β_4	LDMC	-0.82	0.34	-2.4	0.031	0.12	-1.98	0.07
β_5	LeafNo	1.37	0.13	10.4	<0.001	-0.03	1.18	1.97

Standardised Model: $\ln(FW) = \beta'_0 + \beta'_1\ln(CellArea) + \beta'_2\ln(CellNo) + \beta'_3\ln(SLA) + \beta'_4\ln(LDMC) + \beta'_5\ln(LeafNo)$

Standardised Coefficient	Variable	Estimate	Standard Error of Estimate	t Statistic	p value	Bootstrap Bias	Bootstrap 95% CI Lower	Bootstrap 95% CI Upper
β'_0	Constant	0.00	0.06	0.0	1.000	-0.01	-0.09	0.19
β'_1	Cell Area	0.41	0.07	5.8	<0.001	0.05	0.22	0.69
β'_2	Cell No	0.54	0.06	8.7	<0.001	0.02	0.34	0.68
β'_3	SLA	-0.05	0.07	-0.7	0.497	0.00	-0.39	0.07
β'_4	LDMC	-0.20	0.08	-2.4	0.031	0.03	-0.61	0.00
β'_5	LeafNo	0.60	0.06	10.4	<0.001	-0.01	0.52	0.90

Table. 6.6. Multiple linear regression model predicting rosette fresh weight from five morphological parameters.
Parameter estimates, significance tests and non-parametric bootstrap validation of multiple linear regression model predicting rosette biomass at harvest from 20 *Arabidopsis thaliana* accessions using mesophyll cell area, number of cells in the leaf, specific leaf area, dry matter content and leaf number. Model fitting was by ordinary least squares, bootstrap validation was conducted with 1000 non-parametric re-sampling steps and 95% confidence intervals are shown.

The partial regression coefficients in the first model in Table 6.6 represent the unique effect of each trait on rosette fresh weight when all other variables are kept fixed. In essence they state how much change in fresh weight is to be expected (or predicted) for a one unit change in each trait. However, each trait is expressed in its own arbitrary units and the coefficients cannot be directly compared. The standardised partial regression coefficients of the second model allow direct comparisons to be made because they express the unique effects of each trait in standard deviation units of fresh weight per one standard deviation change in each variable.

Fig. 6.2 plots the regression model and its five log-transformed components individually against log-rosette biomass. Least squares regression is susceptible to being strongly influenced by outliers and robust regression based on M-estimation (Huber, 1964) in the MASS package for R (Venables and Ripley, 2002) was used to correct for this. The lines of both regression methods are presented. Robust regression made little difference to the regressions.

The regression model explained 94% of the variance in fresh weight, which was highly significant. The signs of the partial regression coefficients agree with the postulated model in equation 5.3. Cell area, cell number, dry matter content and leaf number all contributed to predicting fresh weight while the effect of SLA was not significantly different from 0. Leaf number exhibited the greatest unique effect (coefficient $\beta = 1.37$), while the effects of cell area and cell number (together giving the area of leaf 6) were also large and positive and were, when summed, approximately equal to the effect of leaf number ($0.79+0.69 = 1.48$). Dry matter content had a smaller negative effect ($\beta = -0.82$).

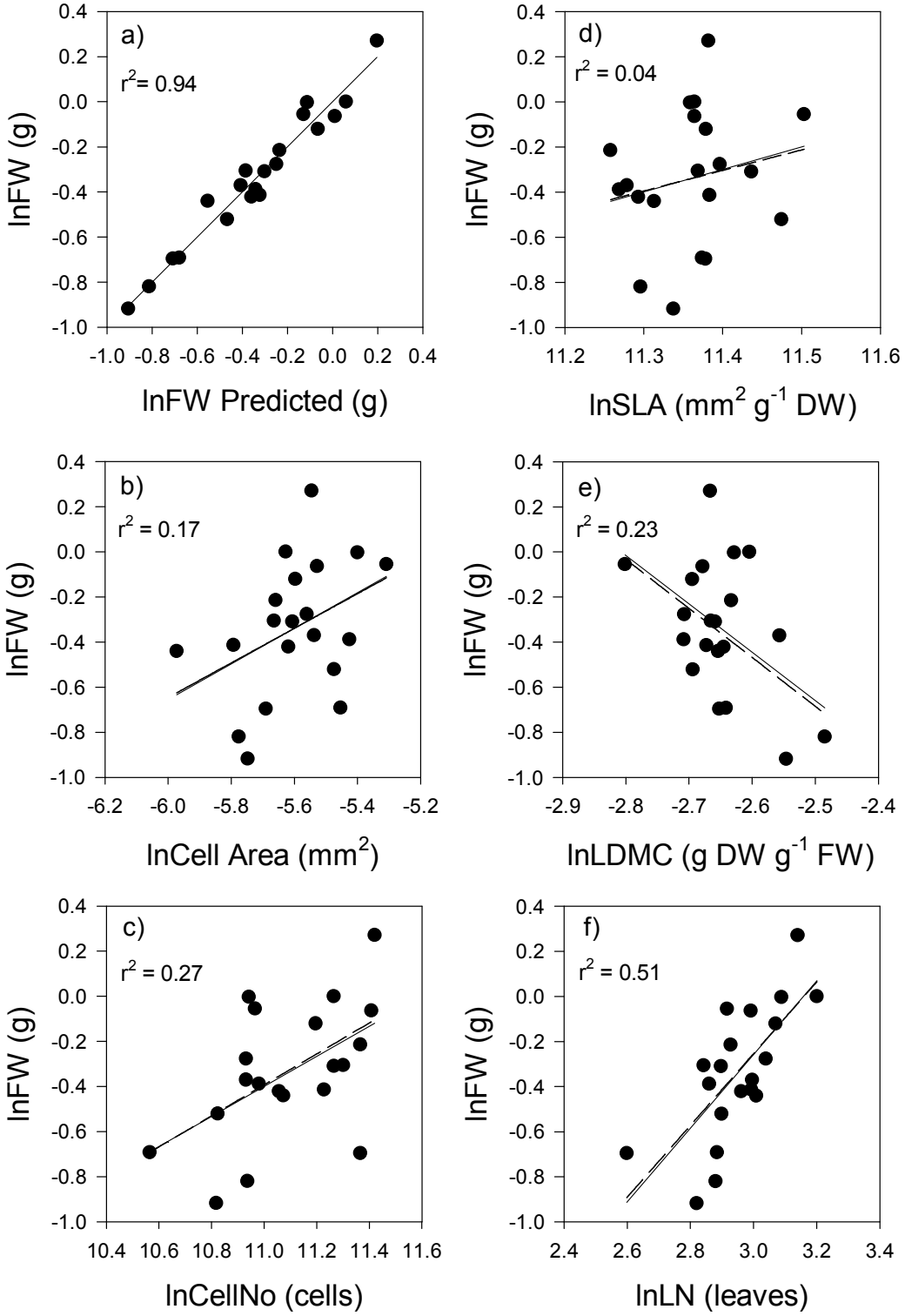

Fig. 6.2. Variation in morphology parameters in 20 wild accessions of *Arabidopsis thaliana* and their relationship to rosette fresh weight at harvest.
Complete linear model predicting fresh weight as a function of all five components (a) and partial models of the bivariate relationships of fresh weight with mesophyll cell area (b), cell number in leaf 6 (c), specific leaf area (d), leaf dry matter content (e) and leaf number (f). Model parameters are listed in Table 6.6. Solid lines are linear regressions, dotted lines are robust regressions performed using the rlm() function the MASS package in R.

The amount that variation in a trait actually contributes to the observed variation in fresh weight is distinct from the unique effect and requires further calculation. A trait can have a large unique effect within its range of variation but contribute little to fresh weight because it does not vary very much (i.e. it explains only a small part of the variation in fresh weight). An example of this is LDMC. This parameter had a large negative unique effect. This is expected, because if LDMC were doubled, fresh weight biomass would be halved given the same dry weight input. However, its total variance was quite low (Table. 6.1) and its actual contribution would thus be expected to be smaller.

A trait's apparent contribution can also be decreased if its variation is counteracted by variation in another variable which compensates for the change in the first, i.e. when there are negative covariances between predictors. An example of this is SLA. This parameter would also be expected to have a large positive unique effect. A doubling in SLA should double leaf area, doubling light interception per unit biomass, which should have large implications for growth. However, SLA was seen to co-vary strongly and negatively with LDMC, as a high LDMC means dry weight biomass is more concentrated and not spread over a large area by expansion. Thus the effect of SLA might be masked by its negative co-variance with LDMC.

The assessment of the real effect of a predictor calls for statistical methods to calculate relative importance. The existence of several methods and a lack of a clear consensus on which method is best make this field somewhat controversial. Four metrics were calculated here, ranging from simple bivariate correlation (marginal effect) to the computationally-intensive lmg statistic based on analysis of variance. The results are shown in Table. 6.7.

Marginal effect, represented by r^2 values of bivariate association, identified leaf number as the main contributor to variation in biomass, followed by cell number in the leaf while LDMC had a moderate effect and SLA was not associated with rosette size. The sum of the explained variances exceeded the total variance in fresh weight by 19%, indicating some co-incident variation. Marginal effects are, by definition, not a measure of relative importance.

The variance decomposition method (Importance) takes into account negative covariances between variables and calculates importance values by decomposing the variance in biomass into individual variance and covariance components of the predictors (Rees et al., 2010). This method instead identified variation in cell number per leaf and cell area as the stronger sources of variation determining fresh weight while leaf number was less important.

The ANOVA effect size η^2 (Eta square) partitions the total sum of squares of the model in Table 6.6 (the multiple r^2 of the model) between the different model components. This statistic again identified cell number per leaf as the strongest determinant of fresh weight, ascribing 42% of total variance to cell number. It identified leaf number as another important contributor (35% of the total variance in FW). The effect sizes sum up to 95.4%, the variance explained by the multiple linear model.

Explained variances are dependent on the order in which the components are added to the model, the model being of a Type I design. The η^2 statistic shows the effect sizes of the single model with the order of components as shown in Table. 6.6. The hierarchical partitioning technique (Chevan and Sutherland, 1991), presented here as the lmg statistic (Groemping, 2006), permutes all possible models with different parameter ordering and calculates an average effect size between all possible models. The lmg metric is here considered the most robust due to its exhaustive methodology. When the lmg method was used, variation in leaf number explained the most variance in fresh weight (43%), with cell number, cell area and LDMC the next strongest, in that order. The summed importance of cell number and cell size was again approximately equal to that of leaf number.

	Marginal effect r^2	Importance	ANOVA Effect Size η^2	Lmg
Cell area (μm^2)	16.7	26.6	16.7	14.1
Cell no. (cells)	27.1	42.1	42.7	26.9
SLA (m^2 kg^{-1} DW)	4.1	7.4	0.3	1.6
LDMC (g DW g^{-1} FW)	19.0	9.7	1.0	9.9
Leaf no. (leaves)	51.0	14.2	34.8	43.0
Sum	118.5	100.0	95.4	95.4

Table. 6.7. Relative importance of modelled leaf morphological traits to rosette fresh weight. Effect sizes, relative importance and variance decompositions, in percentage terms, of five morphological parameters predicting rosette fresh weight in a dataset collected from 20 Arabidopsis accessions. Marginal effect is the coefficient of determination (r^2) of each variable's bivariate relationship with fresh weight, Importance was calculated by decomposing the variance in fresh weight into variance and covariance components of the component variables, as in Rees *et al*. (2010), η^2 is the r^2 decomposition of the linear model (ANOVA effect size) of each component of the multiple linear model (each predictor's explained percentage of the total sum of squares), lmg is an extension of η^2, showing the average effect size from all possible permutations of predictor variable combinations, computed by hierarchical partitioning (Chevan and Sutherland, 1991). The variance explained by the multiple linear model was 95.4%.

While the methods differed in their assessment of which variable was the most important (cell number or leaf number), they clearly identified that SLA had a negligible effect on fresh weight growth while LDMC had a small negative effect, similar to the effect of cell size, with which it was also correlated. Combining all four models and taking into consideration their robustness, it appears likely that leaf number is one important determinant of total biomass (explaining 35-50% of the total variance), and that leaf area makes a similar contribution (40-50%), the latter being driven by cell number (27-43%) and, to a lesser extent, by cell area (14-17%). It might be noted that leaf number (which is probably strongly dependent on proliferation in the shoot meristem) and the cell number per leaf are both strongly dependent on the rate of cell division at different times during the establishment of the leaf.

6.2.5 Leaf size – more cells or bigger cells?

The above analysis shows that leaf cell number has more impact on rosette FW than leaf cell area. The next section investigates the impact of the various leaf morphology and composition variables in the context of a single leaf. Leaf 6 area can be factorised as:

$$\ln Leaf\,6\,Area = \ln CellNo + \ln CellArea + C \qquad (6.4)$$

Since cell number was calculated from area per cell (including air spaces) and leaf size, the above relation is true by definition and regression modelling would always yield a perfect fit with coefficients of 1 and an intercept (C) of 0, conveying little information. In such cases, the slope of a log-log regression represents the variation explained by each variable (Renton and Poorter, 2011). The log-log slopes in such datasets sum to 1 between all predictors and explain all the variation. This

method is superior to coefficients of determination (r^2) as they do not necessarily add up to the total variance when summed. It has been shown by Renton and Poorter (2011) that lo-log slope analysis is equivalent to decomposing the variance in a dependent variable into the variance and covariance components of the independent variables (this is similar to the Importance measure in Table 6.7).

Fig. 6.3 shows log-log correlation plots of cell area (a) and cell number (b) in leaf 6 with least squares regression slopes. Coefficients of determination (r^2) are listed for comparison. Leaf area was determined chiefly by variation in the number of cells in the leaf, which explained 76% of the variation while the remaining 24% was explained by cell area.

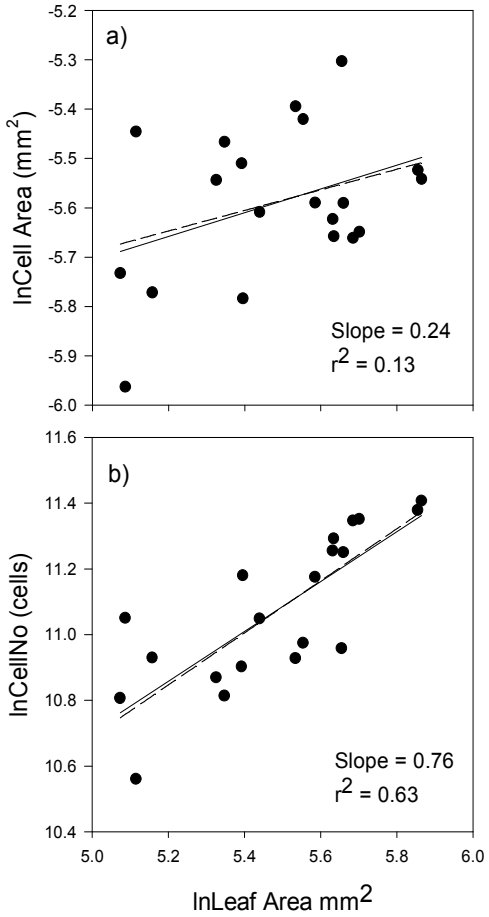

Fig. 6.3. The contributions of variation in cell area (a) and number of cells per leaf (b) to leaf 6 area.
The log-log scaling slope shows the proportion of variance explained by mesophyll cell area (a) and the number of mesophyll cells in the leaf (b) in 20 wild accessions of *Arabidopsis thaliana*. Ordinary least squares slopes are shown. Solid lines are linear regressions, dotted lines are robust regressions performed using the rlm() function the MASS package in R.

Cell area can in turn be factorised into cell biomass and the degree of expansion of that biomass. A "fresh weight per cell" was calculated from cell area, SLA and LDMC. log-log slopes were then used to analyse their relative contributions. Fig. 6.4 shows the log-log plots and the corresponding slopes. Cell area was basically determined by cell fresh weight (slope = 1.10) and there was a positive effect of SLA on cell area, while LDMC counteracted this variation. Leaves with larger cells tended to have higher SLA (explaining 13% of variation) and lower LDMC (23% of variation) corresponding to a high water content. Thus, in accessions with larger leaves, cell expansion by addition of water, effectively diluting the biomass invested and at the same time increasing SLA, played a part in the

variation in cell size, accounting for 36% of its variation. Both strategies effectively increased the area available for light interception per unit biomass invested.

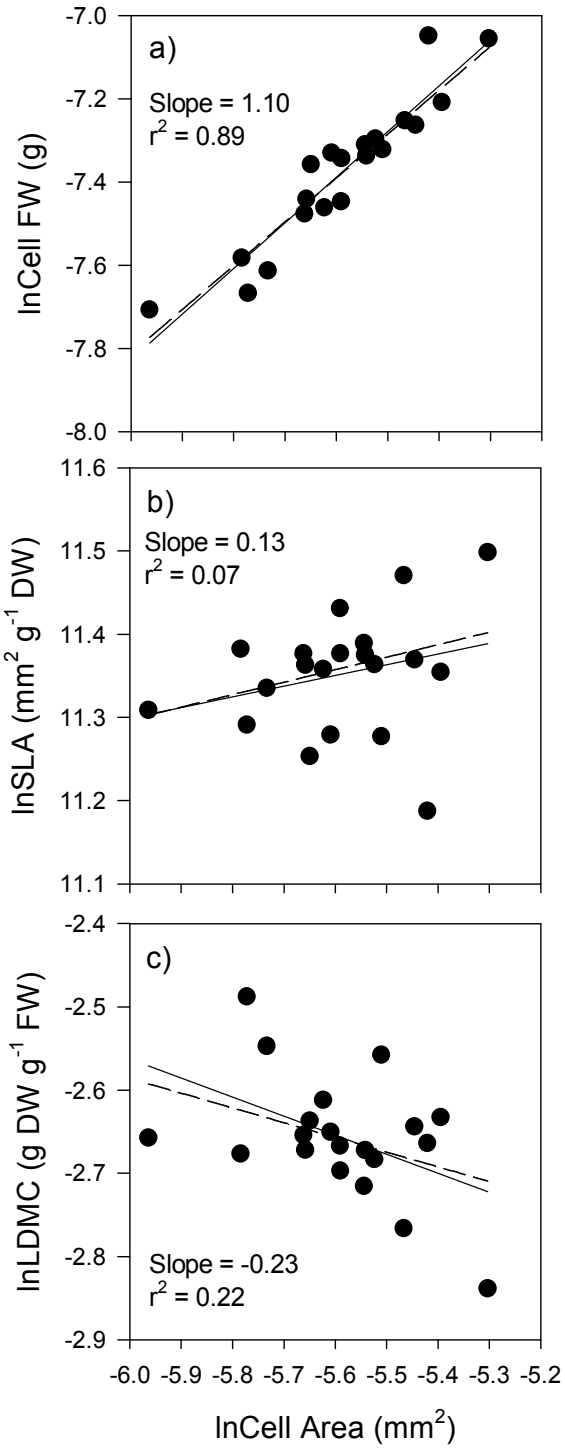

Fig. 6.4. The contributions of variation in cell fresh weight (a) specific leaf area (b) and leaf dry matter content (c) to leaf 6 area.
The log-log scaling slope shows the proportion of variance in cell area explained by cell fresh mass (a), specific leaf area (b) and leaf dry matter content (c) in 20 wild accessions of *Arabidopsis thaliana*. Ordinary least squares slopes are listed. Solid lines are linear regressions, dotted lines are robust regressions performed using the rlm() function the MASS package in R.

6.2.6 Leaf thickness

While SLA made an apparently minimal contribution to growth and leaf size, it was an important determinant of leaf thickness, accounting for a little under half the variation, and LDMC explaining the remainder. Log-log slopes against leaf thickness were -0.47 for SLA and -0.53 for LDMC. Fig 6.5 shows the log-log correlation plots and corresponding slopes.

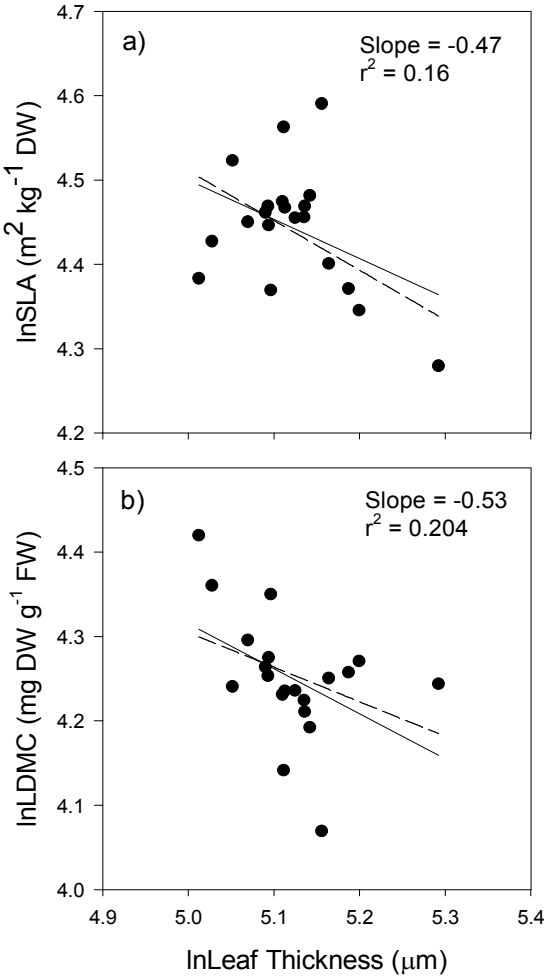

Fig. 6.5. The contributions of variation in specific leaf area (SLA, a) and leaf dry matter content (LDMC, b) to leaf thickness.
The log-log scaling slope shows the proportion of variance in leaf thickness explained by specific leaf area (SLA, a) and leaf dry matter content (LDMC, b) in 20 wild accessions of *Arabidopsis thaliana*. Ordinary least squares slopes are listed. Solid lines are linear regressions, dotted lines are robust regressions performed using the rlm() function the MASS package in R.

6.2.7. Leaf Fresh Mass.

Leaf fresh mass is the product of leaf area and leaf thickness, assuming a specific gravity of 1 (equivalent to an equal volume of water, as shown by Vile et al. (2005)). In Fig. 6.6 log-log slope analysis was used to assess the contribution of these two components to variation in leaf fresh mass. Variation in leaf fresh mass was chiefly determined by leaf area, which explained 89% of the variation while the remaining 11% was explained by leaf thickness.

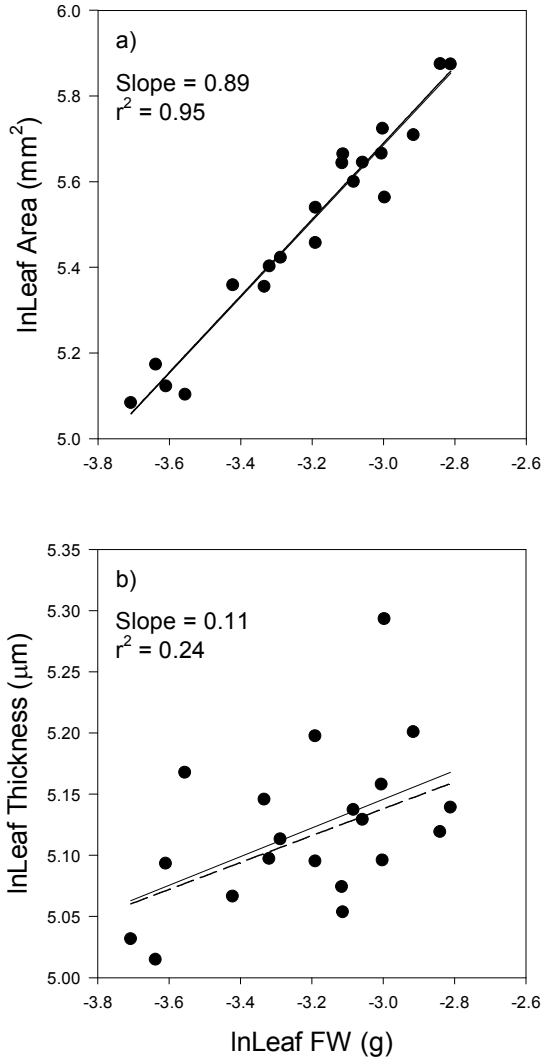

Fig. 6.6. The contributions of variation in leaf area (a) and leaf thickness (b) to leaf fresh weight. The log-log scaling slope shows the proportion of variance in leaf fresh weight (LeafFW) explained by leaf area (a) and leaf thickness (b) in 20 wild accessions of *Arabidopsis thaliana*. Ordinary least squares slopes are listed. Solid lines are linear regressions, dotted lines are robust regressions performed using the rlm() function the MASS package in R.

6.2.8. Rosette Fresh Weight

Finally, the contribution of leaf fresh weight and leaf number to rosette fresh weight was assessed. Fig. 6.7 shows the log-log slope analysis. Rosette fresh weight was chiefly determined by leaf mass, which explained 71% of the variation, while leaf number explained 28%

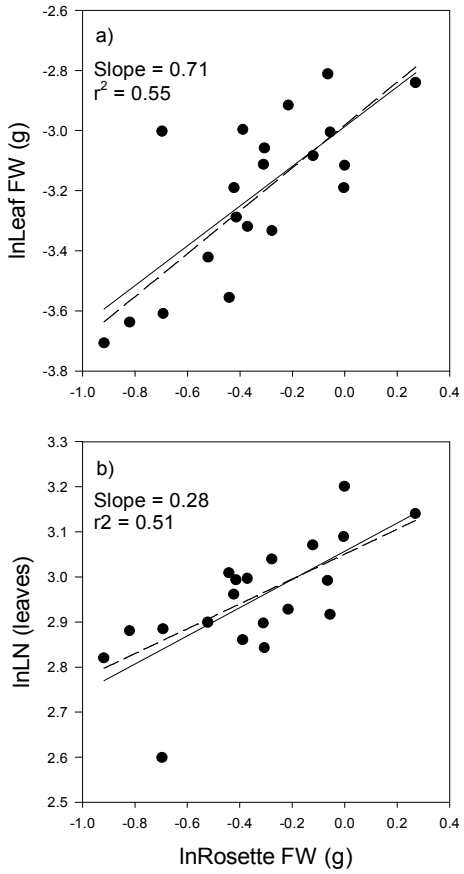

Fig. 6.7. The contributions of variation in leaf fresh weight (a) and leaf number (b) to leaf fresh weight.
The log-log scaling slope shows the proportion of variance in rosette fresh weight explained by leaf fresh weight (a) and leaf number (b) in 20 wild accessions of *Arabidopsis thaliana*. Ordinary least squares slopes are listed. Solid lines are linear regressions, dotted lines are robust regressions performed using the rlm() function the MASS package in R.

Fig 6.8 shows a summary of the relationships between the traits, as identified by log-log scaling slope analysis above.

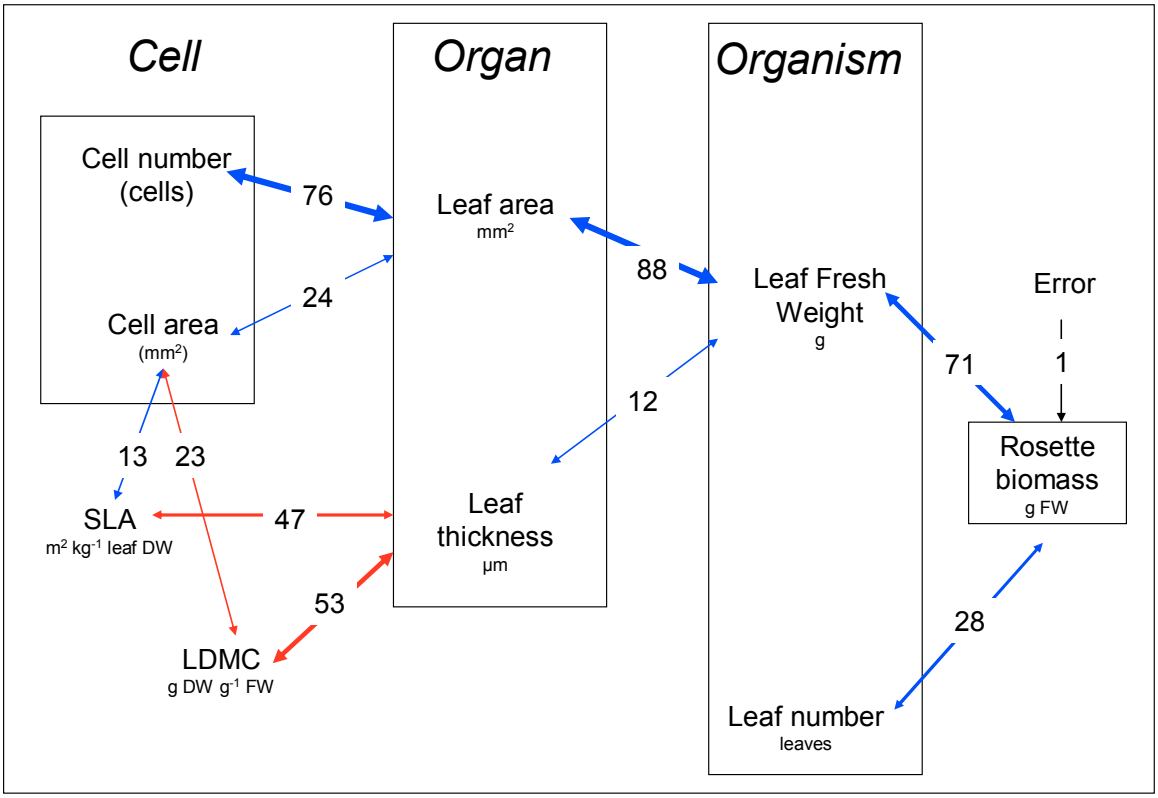

Fig. 6.8. Summary of trait relationships at the cellular, organ and organism levels in 20 wild accessions of Arabidopsis.
Arrows and show variance explained in percentage terms, determined by log-log scaling slope analysis.

6.2.9. Leaf Size vs. Leaf number

High plant biomass was simultaneously associated with high leaf initiation rates and larger leaves (Fig. 6.9). Leaf initiation rates and leaf size, here shown as leaf area, were not correlated (r^2=0.03). Nevertheless, the largest accessions were clearly making more leaves (r^2=0.52) and those leaves were larger at the same time (r^2=0.53). Thus, superficially, there does not seem to be a trade-off between leaf number and leaf size.

However, the analysis performed so far does not take into account that a different amount of total growth had occurred in each accession. The positive correlations between rosette biomass and both leaf number and leaf size might therefore still mask a more complex relationship. The key question is: how does each genotype partition a set amount of biomass between leaves. To investigate the trade-off between leaf size and leaf number in a whole plant context, the number of leaves was normalised on plant biomass. The resulting parameter is analogous to the "leafing intensity" found in studies of the numbers of leaves on tree branches (Kleiman and Aarssen, 2007). However, for the Arabidopsis data set, the analysis was done for the whole rosette, and the units are leaves per gram rosette fresh weight).

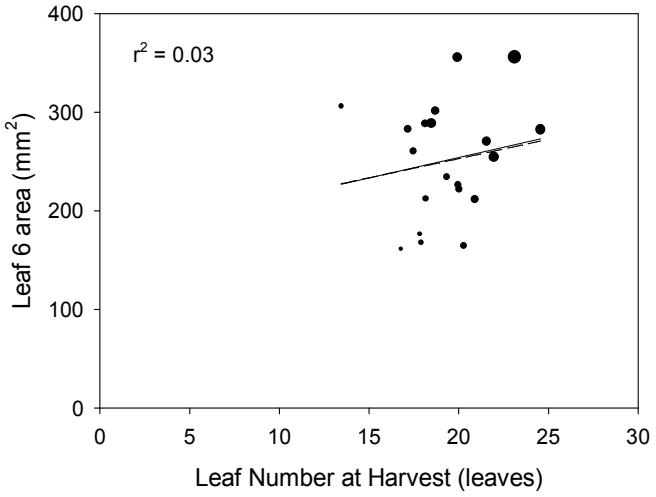

Fig. 6.9. Relationship between leaf 6 area at full expansion and the rate of leaf initiation in 20 *Arabidopsis* accessions.
Plants were grown in 8h days. Size of points indicates fresh weight at harvest. Line is linear regression r^2=0.03

Leafing intensity showed a strong negative relationship to whole plant growth (r^2=0.73, p<0.001, Fig. 6.10). The contribution of leaf number to variation in leafing intensity was not significant (r^2=0.15, p=0.09, not shown). Log-normalised leafing intensity scaled linearly and negatively against log-leaf fresh weight (r^2=0.81, p<0.001, Fig. 6.11a) and log-leaf area (r^2=0.80, p<0.001, Fig. 6.11b) with a slope not significantly different from -1, indicating an isometric trade-off. Per unit biomass, the larger accessions had fewer leaves, which were consequently larger while small accessions had more leaves and their leaves were smaller. Both decreased cell division and decreased cell expansion were behind the decreased leaf size in accessions with high leafing intensities. High leafing intensity was associated with fewer cells per leaf (r^2=0.39, p=0.003) as well as with smaller cells (cell density r^2=0.22, p=0.04) and a low degree of biomass expansion LDMC (r^2=0.42, p=0.002). The relationship with leaf thickness was not significant (r^2=0.17, p=0.07), indicating that cell expansion and not leaf thickness was responsible for the effect of LDMC.

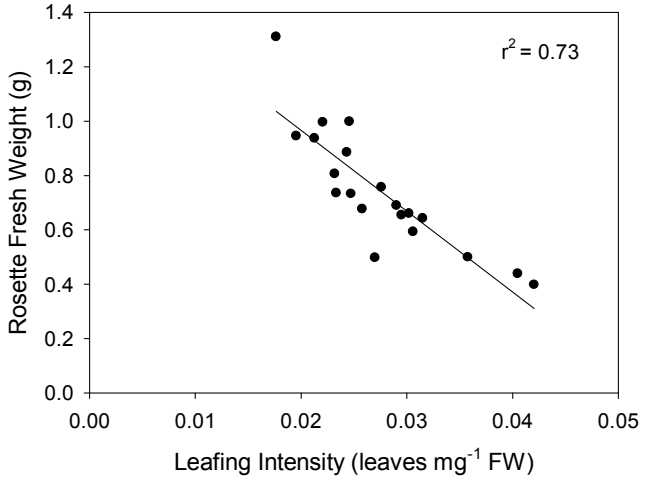

Fig. 6.10. The relationship between rosette fresh weight at harvest and leafing intensity (in leaves g^{-1} rosette fresh weight at harvest).
Line is linear regression.

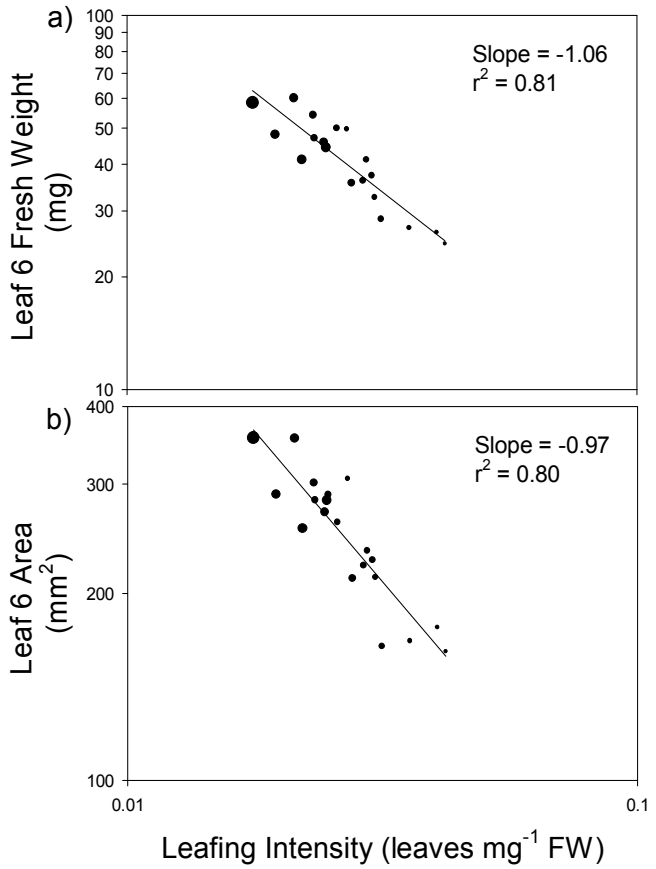

Fig. 6.11. Leafing intensity and its relationship to leaf size, expressed as leaf fresh weight (a) and leaf area (b).
Rosette fresh weight at harvest is displayed as dot size. Axes are log-scale. Lines are linear regressions of log-transformed data.

The interactions of leafing intensity with rosette fresh weight, leaf number and leaf size are summarised in Fig 6.12.

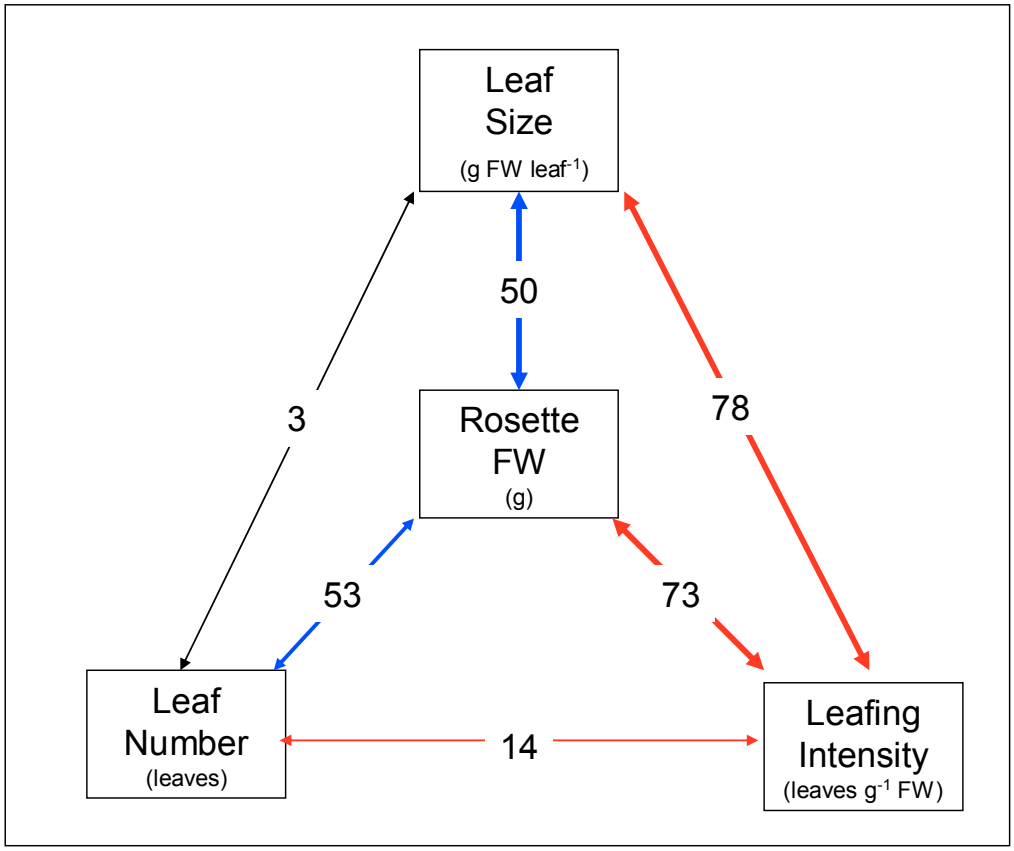

Fig 6.12. The relationships between rosette fresh weight, leaf size, leaf number and leafing intensity.
Arrows and numbers represent coefficients of determination (r^2) in percentage terms.

6.2.10. Photosynthesis and dark respiration.

A subset of 10 accessions with variation in growth rates were grown in a separate experiment in the same above-ground conditions to perform measurements of CO_2 exchange on whole rosettes. There were differences in the below-ground conditions, because the plants were grown in different pots, which allowed gas exchange measurements to be conducted. Relative growth rates were nevertheless highly reproducible between the two experiments (r^2=0.90).

Rates of photosynthesis at growth irradiance measured on whole rosettes varied little between accessions (Table. 6.8). A large proportion of the genotypic variation was driven by a single outlier, C24, which had much lower rates than all the other accessions on both mass and area basis (see Table 6.8).

Interpretation of measurements of CO_2 exchange conducted on whole rosettes is complicated by the fact that rosette leaves overlap and shade each other to some extent. This causes complications when normalising gas exchange rates on a rosette area basis, as not all leaf area is accounted for, resulting in over-estimated rates on an area basis. Mass-based rates are unaffected as all rosette mass is accounted for when the plant is weighed. An estimate for the amount of leaf overlap was obtained by comparing the mass per area of leaves (LMA) with the mass per projected area of whole rosettes (RMA). Leaf

Accession	Leaf Area Basis				Fresh Weight Basis					
	A_{max}	A	R	Net Daily	A_{max}	A	R	Net Daily	Area Overlap	RGR
		µmol CO_2 m^{-2} s^{-1}		µmol CO_2 m^{-2} d^{-1}		µmol CO_2 g^{-1} FW h^{-1}		µmol CO_2 g^{-1} FW d^{-1}	%	g g^{-1} d^{-1}
Bsch	11.93	6.27	0.776	37.8	188.8	99.4	12.3	597.8	37.9	0.224
Bu-2	10.30	5.74	0.730	34.2	191.1	106.7	13.6	635.7	29.3	0.194
C24	8.98	5.54	0.960	28.9	119.0	73.4	12.7	383.6	56.0	0.196
Col-0	10.67	5.75	0.823	32.8	166.5	89.8	12.9	511.8	30.2	0.196
Cvi	10.94	5.71	0.850	32.1	182.5	95.4	14.3	534.5	33.0	0.181
Kn-0	12.45	6.53	0.759	40.1	185.7	97.8	11.4	599.7	52.4	0.215
Ler1	12.55	6.06	0.971	32.9	167.6	80.8	13.1	437.0	35.4	0.196
Lip-0	11.42	6.57	0.845	39.1	170.5	98.1	12.7	581.8	48.6	0.220
Peter	10.16	5.47	0.756	31.6	172.6	92.9	12.8	537.5	36.9	0.191
Van0	11.07	5.70	0.698	34.4	193.3	99.6	12.2	602.3	27.4	0.191

Table. 6.8 CO_2 exchange, leaf overlap percentage and relative growth rates in 10 wild accessions of *Arabidopsis thaliana*. A_{max} – net assimilation rate at saturating irradiance (1000µmol m^{-2} s^{-1}). A – net assimilation rate at growth irradiance (160µmol m^{-2} s^{-1}), R – dark respiration rate. Net daily – daily CO_2 gain calculated assuming constant photosynthesis for 8h and constant respiration for 16h per 24h cycle. RGR – relative growth rate.

overlap percentage, derived from the ratio of RMA to LMA, ranged between 27 and 56% and was somewhat positively related to growth (r^2=0.30, not shown), meaning that faster-growing plants overlapped more. This may of course be a consequence of their larger biomass at harvest, rather than a cause of the faster growth.

Leaf and rosette morphology had some impact on gas exchange rates. Table 6.9 lists Pearson correlation coefficients between gas exchange variables expressed on a FW and leaf area basis and leaf morphological parameters. There were few significant associations of gas exchange and morphological traits. Leaf thickness was significantly negatively correlated with photosynthetic rate (p=0.003) and net daily CO_2 gain on a FW basis (p=0.003). The density of mesophyll cells was negatively related to photosynthetic rates on an area basis measured at saturating (p=0.02) and growth irradiance (p=0.03) as well as to net daily CO_2 gain (0.05), however this was driven chiefly by one outlier (C24) which also had the highest overlap percentage. Overlap percentage did not significantly affect photosynthetic rates. Respiration on an area basis was significantly correlated with leaf thickness, but this relation disappeared when respiration was expressed on a FW basis.

			SLA	LDMC	Thickness	Cell Density	Overlap	RGR
	Parameter	Units	m^2 kg^{-1} DW	g DW g^{-1} FW	µm	cells mm^{-2}	%	g g^{-1} d^{-1}
FW Basis	Amax	µmol CO^2 g^{-1} FW h^{-1}	0.25	0.28	-0.48	-0.58	-0.60	0.10
	A		0.38	0.46	-0.79**	-0.36	-0.42	0.21
	R		-0.17	0.15	0.07	0.22	-0.46	-0.63
	Net Daily	µmol CO^2 g^{-1} FW d^{-1}	0.40	0.43	-0.79**	-0.39	-0.34	0.31
Area Basis	Amax	µmol CO_2 m^{-2} s^{-1}	-0.23	0.08	0.17	-0.72*	-0.62	0.08
	A		-0.20	0.31	-0.09	-0.68*	-0.60	0.27
	R		-0.67*	-0.16	0.82**	0.04	-0.23	-0.40
	Net Daily	µmol CO_2 m^{-2} d^{-1}	0.07	0.35	-0.39	-0.64*	-0.47	0.40

Table. 6.9. Correlations between morphological traits and gas exchange rates in 10 Arabidopsis accessions.
Pearson correlations (r) between CO_2 exchange variables on a FW and area basis and morphological variables determined in 10 wild accessions of Arabidopsis thaliana grown in 8-hour days at an irradiance of 160 µE m-2 s-1 in a 20°C/20°C diurnal temperature regime. Correlations were calculated on the means of accession values. Area-based rates were corrected for leaf overlap. Amax – net assimilation rate at saturating irradiance (1000 µE m-2s-1). A – net assimilation rate at growth irradiance (160 µE m^{-2} s^{-1}), R – dark respiration rate. Net daily – daily CO2 gain calculated assuming constant photosynthesis for 8h and constant respiration for 16h per 24h cycle. RGR – relative growth rate. Significant correlations are displayed with stars, with * (p<0.05), ** (P<0.01), *** (P<0.001).

Gas exchange rates expressed on a projected rosette area basis were corrected using the estimates of leaf overlap percentage (column Overlap % in Table. 6.8) to express them on a total leaf area basis. The corrected area-based rates of photosynthesis were not correlated with RGR (r^2=0.07, Fig. 6.13a) and there was a very weak negative correlation of respiration rate and RGR, which was not significant (r^2=0.16, Fig. 6.13b). The rate of dark respiration on an area and FW basis was more strongly negatively correlated with biomass (r^2 = 0.39). The net daily carbon gain per unit area, calculated by assuming constant photosynthesis for 8 hours of daylight and constant respiration for the 16-hour night, was similarly not associated with RGR (r^2=0.00, Fig. 6.13c). The rates of photosynthesis and respiration were not correlated with each other (r^2=0.00, not shown).

Expressed on a rosette fresh weight basis, photosynthetic rates were also not correlated with RGR (r^2=0.04, Fig. 6.13d) while respiration rates were negatively related, which was marginally significant

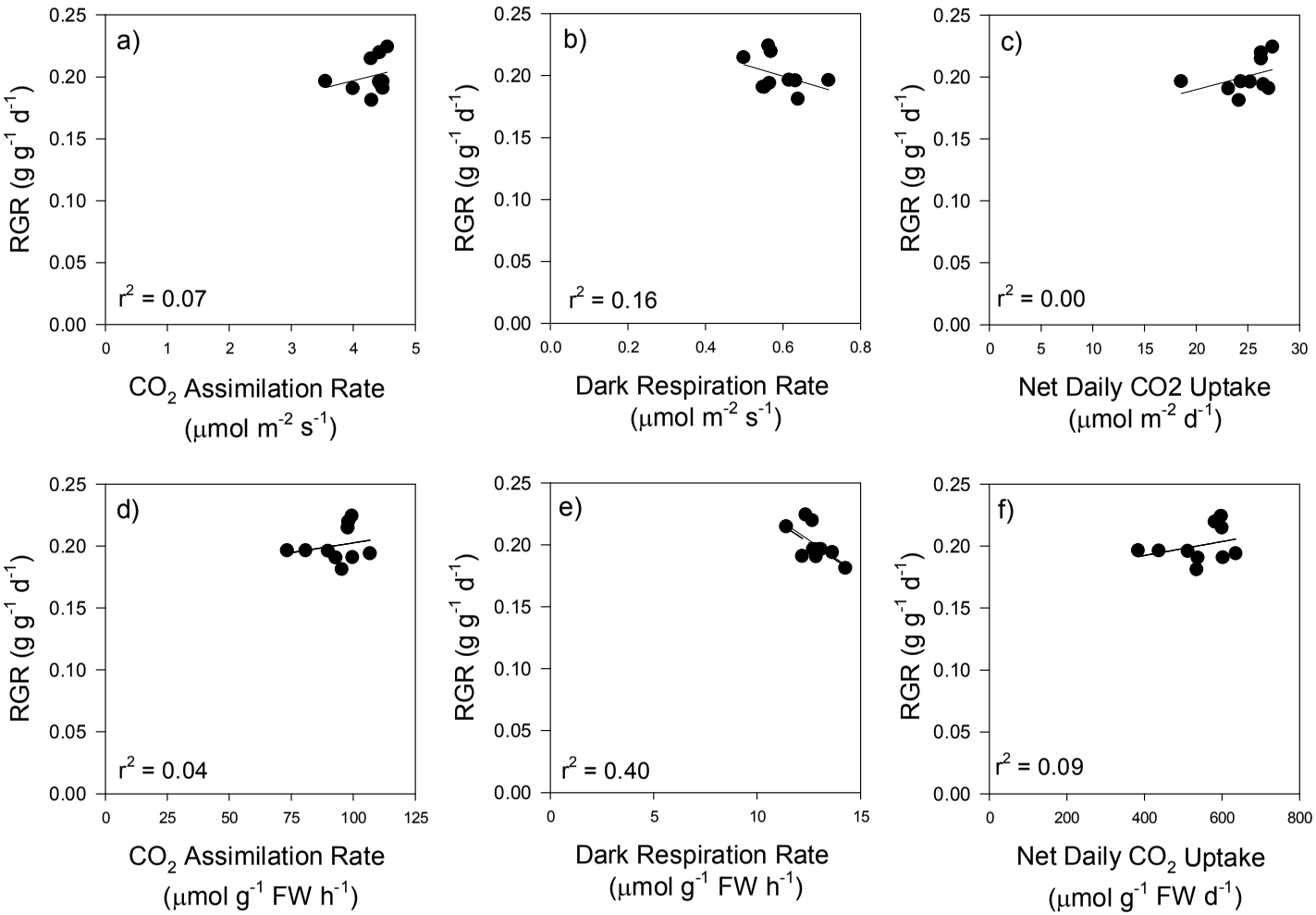

Fig. 6.13. Relationships between rates of CO_2 exchange measured on whole rosettes and relative growth rate in 10 *Arabidopsis thaliana* accessions.

a) Net assimilation rate at growth irradiance on a total leaf area basis (corrected for leaf overlap, a), dark respiration rate on a total leaf area basis (b), net daily CO_2 gain calculated assuming constant photosynthesis for 8h and constant respiration rates for 16h. (d), (e) and (f) – the same rates on a rosette fresh weight basis. Lines are ordinary least squares linear regressions.

(r^2=0.40, p=0.05, Fig. 6.13e). Net daily carbon gain did not correlate with RGR (r^2=0.09, Fig. 6.13f). The percentage of daily photosynthesis respired at night averaged 28% and was weakly negatively related to RGR (r^2=0.21, not shown). This parameter was, however, itself driven chiefly by photosynthesis, with higher percentage respired when photosynthesis was low, as respiration rates did not vary much.

The main findings of these gas exchange measurements are that there is a weak negative relation between R and RGR, irrespective of whether R is expressed on a rosette area or a FW basis. This is interesting because it implies either (i) the costs of growth are lower in the large accessions or (b) the large accessions grow less at night than do smaller accessions or (c) the maintenance costs of the large accessions are lower. These possibilities are not mutually exclusive. The interpretation of the photosynthesis data are complicated by leaf overlap. It appears that there is only a very weak and non-significant, or even no relation between, RGR and either the ambient or the maximum rate of photosynthesis. There is also only a weak and non-significant positive relation between RGR and net carbon gain per day. Another interesting finding is that R on an area basis is strongly related with leaf thickness.

6.3 Discussion.

A series of simple techniques were assembled and optimised to allow a comprehensive array of morphological variables to be measured on a single leaf with sufficient throughput to enable an analysis of 20 accessions with reasonable replication. This study is the most comprehensive study of leaf morphology and function conducted in Arabidopsis accessions. Further application of this set of methods should expedite efforts to understand and integrate morphological variation in Arabidopsis.

In performing such studies, choices needed to be made about which variables to select as "representative". Leaf 6 was chosen as it is a standard leaf often analysed in literature. It is initiated relatively early in the development of the plant and completes its expansion before flowering or the beginning of leaf senescence in other leaves. In contrast to the majority of literature, however, palisade mesophyll cells were chosen as an indicator of cell size instead of epidermal pavement cells, which have traditionally been the model of choice. Only a very few studies have addressed the size of mesophyll cells as a morphological parameter (Terashima et al., 2001; Miyazawa et al., 2003). Mesophyll cells were chosen in this study chiefly because they are the main photosynthetic tissue of the leaf and the study aimed to link morphological properties with photosynthetic function. It is intuitively difficult to link leaf photosynthesis with epidermal cells as an indicator, while mesophyll cells are conceptually easier to link to function. Mesophyll cells are also much easier to quantify as they are approximately uniform in shape and size and can be easily counted while epidermal cells have irregular shapes, cannot be easily counted and have a very broad size distribution, requiring very many measurements to have reasonable confidence in the mean values obtained. Another advantage of mesophyll cells as part of a comprehensive set of traits is that differences in leaf thickness are driven by the cells elongating and/or dividing perpendicular to the plane of the leaf, while the cells dividing an expanding the plane contributes to leaf expansion. This makes it possible to compare the different expansion modes of the same cells and cell size and thickness as manifestations of these expansion modes. In contrast, epidermal cells hardly contribute to thickness variation as they expand chiefly in two dimensions only. This study is one of a very few to address mesophyll cell size as a morphological and functional parameter in any species.

Wild Arabidopsis accessions proved a good system for the study of leaf morphology. All the measured traits varied between accessions with a high degree of significance, although not all traits were highly variable. It is ironic that the trait which seems superficially to be the most variable between the

genotypes, namely plant size in the form of fresh weight, was actually the result of very small differences in relative growth rate, which turned out to be the least variable trait in the set. This is also related to the fact that many morphological variables, such as leaf thickness or cell size, are not superficially obvious which, together with inherent difficulties in measuring some of them, may be the reason they are often ignored in routine studies.

Key axes of variation were identified using exploratory statistical techniques. A simple model can be proposed based on the results of factor analysis where leaf cell division, cell expansion, leaf thickness and leaf number are the main drivers of variation in rosette size. This analysis could be extended to include these four factors as latent variables in a structural equation model and explore causal relationships between the factors and the observed variables, similar to what was done by Tisné et al., (2008) however the current dataset lacks sufficient size to attempt such a model.

The multivariate dataset had a high degree of total variance. Since principal components are, by definition, not correlated with each other, the large number of them explaining substantial portions of variation indicates that there is much independent, uncorrelated variation. This contrasts with the results of the similar analysis in Chapter 3, where most traits were correlated to high degrees with each other. A high degree of scatter reduces the statistical power and makes it difficult to resolve potentially important relationships which have a low effect size i.e. explain only a small percentage of the variation in the target trait. An example of this are negative associations of leaf protein content with rosette biomass in Arabidopsis accessions, which explained approximately 10% of the variation in biomass but are only robustly resolved in large datasets of 100 accessions or more (Sulpice et al., 2009). In this dataset, LDMC and cell area had similar low effect sizes on rosette growth. Their bivariate correlations with fresh weight were, in fact, not significant, however when included in a linear model integrating several morphological components, both parameters came out as significant predictive components of the model. This highlights the utility of integrating the variation of different traits rather than considering them separately. The effect of SLA on growth was not resolved as significant by any approach, suggesting that if it does have an effect, it is likely to be low. Statistical power was also a major issue in the analysis of gas exchange, where only 10 accessions were measured, increasing the likelihood that any trends, or lack of them, may be driven by single points or outliers. Thus caution must be taken when interpreting this data, as contributions from traits with a low variance may have been missed, even if they have quite a large impact on the target trait.

6.3.1 Sources of variation in rosette size.

The model presented in Table. 6.5 is a model predicting rosette weight from, essentially, leaf number, leaf area and leaf thickness, the last of which is divided into the biomass allocation strategy to leaf area (SLA) and the state of hydration of the biomass (LDMC). The multiple linear model presented in Table. 6.6 explained 95% of the variation in fresh weight (94% adjusted). The prediction is not perfect even though Equation 6.3 should be true by definition. The residual variance can probably be explained by the use of only leaf 6 as a representative leaf, as well as various error components, including measurement error. This leaf was chosen because it occurs relatively early in the development of the plant and completes its expansion before flowering or the beginning of leaf senescence. The best but not very practical approach would be to quantify each leaf of the rosette and compute and average leaf size, which should give a perfect model fit. However, assuming variation in the size of leaf 6 is correlated with the variation in all the other leaves (i.e. that leaf 6 is truly representative of leaf size), it should be sufficient for modelling purposes and should give approximately the same result because it is not the absolute sizes of the leaves but the extent of variation in leaf size between genotypes that are of interest. The discrepancy between the model and a

perfect prediction is quite narrow, suggesting that measuring leaf 6 alone is sufficient to capture the variation in leaf size.

While the methods in Table. 6.7 differed in their assessment of which variable was the most important for rosette growth, they all identified leaf number and cell number per leaf as having a large positive effect on total rosette biomass, cell size having a moderate positive effect and LDMC a small negative effect, while SLA had a negligible effect on fresh weight growth. The strong effects of leaf number and cell number per leaf on growth broadly indicate, that cell division activity in meristems and in growing leaves largely underlies the variation in growth between genotypes while the contribution of cell size was relatively small. Similar results have been presented previously in Arabidopsis leaves (Cookson et al., 2005; Tisné et al., 2008; Gonzalez et al., 2010). SLA and LDMC were associated with both cell expansion and leaf morphology. However, as the contribution of cell expansion to growth was low, so was the contribution of SLA and LDMC. These two parameters were much stronger contributors to morphological variation, being strongly related to leaf thickness. There was some leaf morphological variation, however it was a largely independent axis of variation from that of growth.

6.3.2. Specific leaf area.

In light of the overwhelming amount of literature evidence for SLA being strongly related to growth, as discussed in the introduction, one would expect it to have a dominant role in determining RGR among Arabidopsis accessions, however this was not the case. The few published studies where growth and SLA data is available in Arabidopsis all found near-zero effects of SLA on growth or fitness, with some studies even finding negative effects, which is a puzzling result. In a study of forty Arabidopsis accessions where a complete growth analysis was conducted both LAR and SLA were negatively related to growth while LMR was weakly positive and the contribution of NAR was strong (Li et al., 1998). A study of Arabidopsis recombinant inbred lines growing in two CO_2 environments also found a negative covariance between SLA and growth (Lau et al., 2007), as did a study of a set of forty accessions growing in two light environments (Pigliucci and Kolodynska, 2002).

Did SLA simply not vary enough between Arabidopsis accessions to cause a noticeable effect on growth? Indeed, both the variation in SLA and its contribution to RGR were very small. This constrasts with cross-species studeisn, where the ranges of variation in both SLA and RGR are very large, especially if different functional groups are included. However in a study of genotypes of a single grass species Poorter et al. (2005) found SLA variation to be quite low and of a similar range to this experiment, however SLA was still the strongest predictor of growth (Poorter et al., 2005). While SLA did not co-vary with growth in this experiment, it did strongly affect other traits, in particular mass-based photosynthetic rates, cell size and leaf thickness. Thus the argument that variation in SLA is irrelevant to growth because it did not occur is not adequate. These results suggest that other factors may counter-act the supposed benefits of high SLA. Since SLA cannot explain a significant proportion of growth, attention must be turned to the other components of RGR: NAR and LMR.

6.3.3Net Assimilation Rate and Leaf overlap.

Li et al. (1998) concluded that NAR was responsible for the majority of growth variation between 40 Arabidopsis accessions. Since a complete growth analysis was not conducted in this study (root biomass was not measured), the values of NAR are not available. Photosynthesis and respiration are significant components of NAR (Poorter and van der Werf, 1998). However, photosynthesis was unrelated or only very weakly and non-significantly related to RGR in the study presented here, while R showed a slightly stronger negative relation but coulds at the best only exlain a small part of the

varaiton in RGR and (by implication, as SLA does not affect RGR) NAR. The interpretation of this relationship of these gas exchange traits is again complicated by leaf overlap. Gas exchange was measured at the time of harvest when significant leaf overlap had developed while much of the growth had occurred before leaves began to overlap. Thus, leaf overlap not only decreases the rates of photosynthesis but may also decrease the apparent contribution of photosynthesis to growth, if growth is measured by classical growth analysis. Whole-plant gas exchange measurements may instead reflect instantaneous growth rates (for example on the day of measurement) while comparing them with mean RGR over the life of the plant may not be very informative due to the confounding effects of leaf overlap.

Since the measurable components of NAR (photosynthesis and respiration) as well as SLA explained, at best, only a negligible portion of the variation in growth, other (non-apparent) components of NAR may be responsible. In addition to photosynthesis, both carbon content and the efficiency of carbon use have been shown to be components of NAR (Poorter and van der Werf, 1998; Loveys et al., 2002). The efficiency of carbon use has been interpreted as the amount of growth per unit fixed carbon. One of its components is the amount of fixed carbon which is lost through respiration (Loveys et al., 2002). However the rate of respiration was only weakly associated with growth and explained a small portion of the variance. As discussed in the introduction, NAR is a complex variable which may include components other than photosynthesis and respiration. Another component of NAR may be the efficient investment of biomass in the capacity for light interception i.e. leaf area, for which biomass expansion is required.

6.3.4. Leaf mass ratio.

It is also possible that LMR, the third component of RGR, may be responsible for some of the variance in growth. In an Arabidopsis rosette there is a minute stem fraction and the whole rosette may be considered to consist of leaves, making LMR essentially equivalent to shoot:root ratio. Thus, under these conditions, genetically encoded differences in biomass allocation to roots may explain both the lack of effect of SLA on growth and the lack of association of mass-based photosynthesis and RGR, however this requires experimental verification. Unfortunately, root biomass could not be reliably measured in my study, which used soil-grown plants. Arabidopsis roots are very fine and it is practically impossible to quantitatively extract them from the soil. This mean that any contribution of LMR can only be imputed. Variation in shoot:root ratio has been observed in Arabidopsis accessions although they do not seem to be large (Narang et al., 2000; Reymond et al., 2006). Further, the shoot.root ratio in nutrient-replete conditions, like those used in my study, is usually > 3, so that it is unlikely that differences in the shoot:root ratio could have a large impact o RGR.

The relative biomass allocation to shoots, of which leaves are a part, responds to the prevailing conditions in a manner consistent with the "functional equilibrium" hypothesis, which states that plants increase their investment in structures involved in the acquisition of a limiting resource (Brouwer, 1962, 1963). Thus allocation to leaves increases in low light environments while allocation to roots increases on low-nutrient soils (Poorter and Nagel, 2000). Consequently, the contribution of LMR to growth rate variation becomes stronger in studies where plants from growing on nutrient gradients are compared (Wright and Westoby, 1999) and where nutrient manipulations drive changes in growth rates (Poorter et al., 1995). This trend has been shown to influence selection and species adapted to low nutrient soils tend to have low SLA and LMR and higher root mass fractions and, consequently, low RGR (Wright and Westoby, 1999). Biomass allocation fractions have also been found to be heritable traits within a single grass species growing on high and low productivity sites with similar rainfall (Elberse et al., 2004; Poorter et al., 2005), suggesting that soil and nutrient factors may drive genotypic differentiation of within-species populations through selection.

The collection of Arabidopsis accessions in general and the set used in this experiment are mainly derived from a relatively narrow geographic range in northern Europe, dominated by sites in Germany. The range of habitats lies in broadly similar climatic zones with respect to rainfall and temperature (temperate-humid continental to humid oceanic). Arabidopsis accessions show some phenotypic differentiation on the basis of latitude, in which temperature and photoperiod may be the main factors (Li et al., 1998), however the latitudinal range of the accessions used here is also quite narrow.

In the narrow range of climatic environments and latitudes, variation in soil properties, particularly nutrient contents, may be the biggest source of variation among populations because soils are extremely heterogeneous, being strongly affected by numerous factors over small distance scales, among them: mineralogy of the bedrock, position along topographic clines, run-on and run-off effects on nutrient and water availability, soil age, composition and state of weathering of clay minerals (which affects nutrient holding capacity), soil structure, erosion, sediment deposition and biotic factors affecting mineralisation of nutrients. Thus variation in shoot:root ratios, which are related to soil nutrient acquisition, may be expected to be important factors in the phenotypic differentiation between wild Arabidopsis populations as nutrient availability may be the biggest source of variation the species encounters in its natural range.

6.3.5 Cell Number and Cell Size.

The dominant role of cell number in determining leaf size is in broad agreement with previous studies on Arabidopsis (Cookson et al., 2005; Tisné et al., 2008; Gonzalez et al., 2010) and is superficially consistent with the cell theory of leaf size control, however the relatively smaller role of cell size must not be ignored, as it may be functionally important.

Increasing leaf size through cell expansion has advantages and disadvantages. Building a leaf from bigger cells may be a “cheaper” strategy to increase light interception by a given biomass investment i.e. increasing SLA and the amount of light capture per unit leaf biomass. This can occur through addition of water to increase the volume of the vacuole and expand cells, requiring no additional biomass investment and thus lowering LDMC. The expansion of cells and biomass was clearly beneficial for growth as larger accessions had lower LDMC (corresponding to a higher water content in fresh weight biomass), which was also associated with larger cells, suggesting that differential cell expansion may drive this trend. This differential cell and biomass expansion may also explain previously-observed negative associations between growth and leaf protein content (Sulpice et al., 2009), ribosome abundance (Ishihara, unpublished) and leaf nitrogen content (Wright and Westoby, 2001) which all had similar effect sizes (around 10%) to that of LDMC in this study.

The increase in cell size can occur in three dimensions and may increase leaf size, leaf thickness or both. When cells expand in the plane of the leaf by increasing their water content (and lowering LDMC) leaf size increases and dry weight biomass is spread across a larger area, increasing SLA at the same time. Thus, if this mode of leaf expansion is important in leaf size variation, LDMC and SLA must be intrinsically linked. Indeed, LDMC and SLA were negatively related. Furthermore, in the model in Table. 6.6 the contribution of SLA to both rosette and leaf area growth, which was apparently minimal, may in fact be masked by the negative covariance between these two predictors and the fact that they are closely related in this way. In contrast to the other methods in Table. 6.7, the “Importance” variance decomposition measure (Rees et al., 2010) takes negative covariances into account by taking absolute values, and here the apparent contributions of SLA and LDMC are approximately equal, although not large.

When rationalising cell size variation between accessions, it must be considered that, at 50-60µm in diameter the mesophyll cells in Arabidopsis are very large relative to other plants (Terashima et al., 2001) with variation between accessions occurring on this high background value. Arabidopsis is a fast growing herbaceous pioneer species. Such species are characterised by high SLA, high photosynthetic rates on a mass basis, fast growth and low longevity (Reich et al., 1997). The SLA values found in Arabidopsis are relatively high compared to many species (Reich et al., 1997). Large cells with high water content may be a strategy for achieving high SLA without making leaves unduly thin. It is also obvious that at a set rate of growth and a given rate of cell division, a larger final cell size allows a much faster growth rate, which has been demonstrated experimentally in Arabidopsis roots (Beemster et al., 2002). This allows for faster leaf expansion rates and maturation of photosynthetic function (Miyazawa et al., 2003), which is consistent with the strategy of rapid growth. The largest accessions indeed had the largest leaves and the largest cells, however the overall effect size of cell size on total rosette growth was not large, indicating that this strategy did not contribute strongly.

On the other hand, large cells have a low surface area:volume ratio and an increased resistance to CO_2 diffusion. In order to maintain high photosynthetic rates and decrease wasteful photorespiratory losses the CO_2 concentration in solution at Rubisco must be maximised (Caemmerer and Farquhar, 1981). This requires a high chloroplast surface area in contact with the intercellular airspaces in the leaf, which decreases the resistance to CO_2 diffusion (Terashima et al., 2005; Tholen et al., 2008; Evans et al., 2009). Large cells have longer diffusion paths as well as decreased surface area available for chloroplasts to occupy, which causes a high resistance to CO_2 diffusion (Terashima et al., 2001) and this may limit photosynthesis, particularly in high light (Niinemets et al., 2009, 2009). Consistent with this theory, Arabidopsis has a low internal conductance relative to many species (Flexas et al., 2007; Flexas et al., 2008) although the role of cell size in this remains to be established, as other factors also play a role in internal conductance.

The data presented here showed no trend towards lower photosynthetic rates (on mass and area bases) in accessions with smaller cells. In fact a distinct effect of cell size on photosynthesis could not be discerned. The results suggest that the benefits of large cells, i.e. high SLA and light interception per biomass, may outweigh the purported negative effects. The downsides of large cells may also be compensated for. One mechanism of compensation could be an increase in leaf thickness when cells become large, which allows for a maintenance of exposed chloroplast surface on a leaf area basis (Terashima et al., 2001). This was however also not evident, with no correlation between cell size and leaf thickness. This also suggests that expansion of mesophyll cells in the plane of the leaf is independent from the expansion which occurs to increase leaf and mesophyll thickness.

When cells expand perpendicular to the plane of the leaf, changes in leaf thickness are the result. Here, again, both SLA and LDMC are involved. If cells expand purely by water addition to make the leaf thicker the amount of biomass per area stays the same and SLA is unchanged. If cells expand purely by biomass addition, LDMC should not change and SLA would determine thickness exclusively. Changes in thickness may also be driven by more cell layers being generated, in which case extra cross walls and other cell components need to be built, decreasing SLA. In fact, both LDMC and SLA contributed almost equally to leaf thickness variation, indicating that thickness differences are driven partly by both: extra biomass input as well as some degree of expansion by addition of water. Furthermore, this again constrains SLA and LDMC to co-vary negatively. This constraint has been predicted theoretically (Roderick et al., 1999). Empirical evidence also exists (Stewart et al., 1990).

It is clear that the large accessions were using light more efficiently for growth (since they were all grown in the same light environment). Given the low-light growth environment used in this experiment, photosynthesis would be expected to be limited by electron transport (and thus light

capture) rather than Rubisco carboxylation rate (Ögren and Evans, 1993). Since light capture is directly proportional to leaf area, the benefits of large cells with high water content and the consequent high SLA are obvious. Together these results suggest that in this growth environment large leaves with large cells and high SLA are clearly beneficial for growth and the benefits outweigh possible disadvantages of large cell size. Consistent with these results are observations that mesophyll cells become larger in low light in *Chenopodium album* (Yano and Terashima, 2004). Arabidopsis leaf epidermal cells are also larger in shade (Cookson and Granier, 2006). The variation in cell size observed between accessions may thus be part of a differential adaptive response to low light.

6.3.6. Leaf number

The number of leaves in the rosette was a major component of variation in fresh weight growth. Information on the number of leaves allows leaf size and morphology to be treated in a whole-plant context and allows possible whole-organism regulatory processes to be investigated. While both leaf number and leaf size correlated strongly with rosette growth, there appeared to be variation in the balance between them (leafing intensity). The observed trade-off between leaf size and leaf number, when expressed per unit biomass, supports the findings of previous studies. Similar results have been found when studying single modules of deciduous trees (Kleiman and Aarssen, 2007; Yang et al., 2008) and this approach has also been scaled up to stand level in a forest model (Ogawa, 2008). These studies used a different method and leafing intensity was expressed on the basis of the growth in a season of a single module, a twig or stem, not including the leaves. Since Arabidopsis does not have a stem and all the growth occurred in a single "season", the whole shoot biomass was used, i.e. the rosette. The trade-off of leafing intensity with leaf size is partly self-evident. Leafing intensity in leaves per mg fresh weight is the inverse of mg fresh weight per leaf i.e. the average size of a leaf in the rosette at harvest. Thus leaf size should scale with leafing intensity as the hyperbolic function $\frac{1}{x}$ which, after logarithmic transformation, becomes the straight line -1 log(x), hence the slope of -1. However, this holds only for a comparison of plants with the same growth rate. In my experiments, there were differences in RGR. Accessions with a higher RGR tended to have, per unit plant weight, a smaller number of larger leaves. This finding poses several questions. First, what are the molecular are cellular mechanisms that underlie these differences in leaf intensity. Second, how is resource allocated to maintain appropriate rates of cell division and cell growth in the meristem and primordia, and in growing leaves? Third, do changes in leafing intensity and leaf size have any functional significance? The observation that leafing intensity correlates negatively with rosette biomass and RGR indicates that a growth strategy that is biased to producing a smaller number of larger leaves either increases growth efficiency or increases leaf performance.

A high leafing intensity implies that more leaf primordia are initiated at the apex relative to the plant biomass which supplies resources to the apex. Leaf primordia and young growing leaves are strong sinks until they reach a certain threshold and become self-sufficient. This threshold is known as the sink-source transition and occurs when the leaf is 30%-60% of its final length (Guedes Corrêa, 2009). High leafing intensity may thus be associated with a higher competition between individual sinks (primordia) for resources. Since the rates of photosynthesis did not vary very much between accessions, this may mean less assimilate supply to individual primordia at the early stages of their development. This may constitute a metabolic organism-level input at the early developmental phases of leaf growth.

The rates of cell division and relative leaf expansion at the early stages of leaf growth have been shown to correlate with final leaf size and cell number (Cookson et al., 2005), indicating that this is a

crucial phase when leaf size is determined and when regulatory inputs should be acting strongly. This early stage of leaf development has also been implicated in determining the events of the later stages, where the duration of leaf expansion provides some plasticity in leaf growth through control of cell size. This last phase has been implicated as the factor responsible for the compensation phenomenon (Tsukaya, 2003; Cookson et al., 2005). No compensation-like behaviour was observed in response to variations in leafing intensity as high leafing intensity was associated with both fewer and smaller cells. This suggests that variations in sink demand caused by leafing intensity may exert effects on both the early and late processes in leaf size control and it may thus be a true organism-level influence. Based on these results, it is proposed that in plants with a high leafing intensity high sink demand from the many growing leaves may prompt growing leaves to stop expanding sooner. This may prevent a full cell and biomass expansion, resulting in smaller cells with a high LDMC, which has further negative effects on growth due to the importance of biomass expansion for generation of leaf area and its payback effects. This may be one of the factors in the missing variance in growth, which could not be accounted for by SLA and photosynthesis.

Alternatively, if a larger number of leaf primordia are initiated per unit plant growth, the plant may have a higher proportion of sink tissue at any given time, and consequently a smaller proportion of source tissue to supply it, which may reduce growth. This may explain the strong negative association of leafing intensity with rosette fresh weight.

A relatively larger number of leaf primordia in small accessions may also explain the observation of high abundances of biosynthetic machinery (ribosomes) in the rosette biomass of small accessions compared to large ones (Ishihara, unpublished data). These puzzling observations suggest that the efficiency of ribosome use may drive the variation in growth between accessions. Ribosomes are a substantial part of the total protein pool (Warner, 1999). Young leaf primordia contain high concentrations of ribosomes, which decline as the leaf expands (Ishihara, unpublished data). Smaller accessions may have more ribosomes per unit biomass because they have more growing leaf primordia. The creation of a leaf primordium requires not only active synthesis of new cell components (proteins etc), but also the production of the biosynthetic machinery required to synthesise them (ribosomes). As leaf primordia and growing leaves are strong sinks before acquiring photosynthetic competence after emergence, they are heterotrophic and rely on imported carbon.

Continuing this arguments, the expansion of an existing leaf may be cheaper than the creation of a new one because 1) the leaf already contains biosynthetic machinery, which can be re-used, increasing the efficiency of its use and 2) emerged leaves become photosynthetic and can grow from their own fixed carbon rather than growing heterotrophically from imported carbon, which is more expensive. The latter point may also be related to the fact that protein synthesis is less expensive in energy terms in the light, as reducing equivalents and ATP are available from chloroplast electron transport and photophosphorylation respectively, while they must be provided by respiration in heterotrophic conditions. In the light, this considerably decreases the cost of nitrate reduction and protein synthesis, which are major sinks for reducing power and ATP in plant cells (De Vries, 1975). There is both theoretical and experimental evidence that protein synthesis in plants is cheaper in the light (Sajitz-Hermstein and Nikoloski, 2010). This may explain why low leafing intensity is associated with higher growth – by making fewer heterotrophic leaf primordia and expanding existing leaves the plants can grow more efficiently by re-using existing ribosomes for growth, as well as allocating more growth to autotrophic tissues, where biosynthesis is cheaper in the light. This may also explain the lack of correlation between growth and photosynthesis and SLA as the biomass of slower-growing accessions may be more expensive to produce, requiring more photosynthate per unit carbon fixed. As this is clearly part of carbon-use-efficiency, this may be a hidden component of NAR.

Leafing intensity may thus link together variation in leaf number, leaf size and whole plant growth as a whole-organism process. Investigations on the source-sink relationships associated with leafing intensity, as well as how it may contribute to protein and ribosome contents in the context of growth, should prove very interesting and may unravel the causes and effects of this phenomenon.

The existence of variation in leafing intensity leads to the presumption that it may be adaptive. If low leafing intensity is beneficial for growth, why should it be high in some accessions? It has been suggested that high leafing intensity may have fitness benefits in trees because it creates a larger number of axillary meristems, which are needed for profuse flowering, as well as to regenerate from herbivore damage (Kleiman and Aarssen, 2007). It remains to be tested whether this is also true in Arabidopsis. It is also clear that not all plants have evolved to simply grow very fast or very large, indicating that something other than growth rates constrains the evolution of plant form. There is evidence from a number of species that the fitness benefits of fast growth are compromised when plants experience disturbance, and in such conditions slow growth leads to higher fitness in an ecological setting (Rose et al., 2009).

6.4. Chapter Summary.

In summary, this chapter documents exploratory work to attempt to integrate leaf morphology in the context of whole plant growth and function using natural accessions of *Arabdopsis thaliana* as a source of variation and exploring variation in the traits at the cellular, organ and organismal levels of variation. There were four key axes of variation in rosette and leaf morphology – leaf area growth and cell division, leaf thickness, cell expansion and leaf number. These four processes were integrated in the context of whole plant growth by models that employed a multiple linear regression approach. This identified variation in leaf number and cell number per leaf as the main positive drivers of variation in plant growth rate and rosette biomass, with a relatively smaller effect of cell size and a smaller impact of leaf dry matter content. The relationships between the parameters were then explored further by using log-log scaling slope analysis to partition the variance in leaf size, cell size, leaf thickness and plant size between their components to identify further relationships between traits. The variance in plant growth could not be explained by variation in SLA or photosynthetic rates on a mass or area basis and only to a small degree by variation in rates of dark respiration, implicating LMR or a hidden component of NAR as a major causal factor underlying the differences in growth rates. The relationship of leaf number to whole plant growth and leaf size was further investigated by normalising leaf number on rosette fresh weight to estimate a parameter termed leafing intensity. Leafing intensity integrates leaf number, leaf size and whole rosette growth in a series of trade-off interactions, which seem to result in a growth benefit when plants make fewer but larger leaves per unit biomass. This may be related to the strong sink-capacity of leaf primordia or to intrinsic differences in the matter and energy costs of making new leaf primordia compared to expanding existing leaves. These factors are implicated as a causal driver of variation in leaf and whole plant growth and may account for the hidden variance in growth, which could not be accounted for by other components. The relationship of leaf number to leaf and whole plant growth is addressed in more detail in the next chapter.

Chapter 7. Relationship between leaf production and growth

7.1. Introduction.

As seen in the previous chapter, the initiation of new leaves is a major component of plant growth and contributes substantially to variation in growth rates between wild genotypes. However, the rate of leaf production as a component of plant growth has not received a quantitative treatment in a mathematical framework. This chapter aims to gain a quantitative understanding of the rate of leaf production in the context of whole plant growth.

Biomass growth and leaf initiation are conceptually separate from one another. Initiations of leaf primordia at the apical meristem are discrete physical events which determine the beginning of a continuous process – the subsequent growth of the leaf. The growth of the primordium and later the leaf contributes biomass to the plant while initiation events can be seen simply as a pattern-forming process. Seen from this perspective, primordium initiation per se involves almost no biomass formation, which makes it difficult to link leaf production with growth directly. In addition, leaf number is a discrete variable and occurs on an integer scale while biomass growth is clearly a continuous process. Each discrete event leading to leaf initiation creates a large demand for biomass formation in the future. Putting this another way, growth is often viewed by physiologists as an issue of resource gain and allocation that is studied independently of the fact that the resources are allocated to a discrete number of individual organs (leaves). On the other hand, leaf initiation is often viewed by developmental biologists as a localised developmental switch in part of the meristem and is studied without reference to the fact that this switch creates a sink that will require considerable resources for its future growth. Further, leaf initiation is often taken as an internal chronometer (plastochron index) with which to measure the chronological age of a plant (Lamoreaux et al., 1978). Some of the environmental variation in the rates of leaf production can be accounted for by thermal time as an indicator of physiological age (Granier et al., 2002). However this approach might be called into question if there is also genotypic variation in the leafing index in plants grown in the same conditions.

Physiologists have studied the number of leaves in the context of the conductive tissue architecture needed to supply and support them – the stems, branches and twigs. It has generally been observed within and between species that total and individual leaf area is proportional to the amount of conductive tissue supporting it (Corner, 1949; Westoby and Wright, 2003; Whitman and Aarssen, 2010). This may mean a stem, branch or twig in woody species or all above-ground non-leaf biomass in herbaceous plants. Leaf number constrained to twig size, the so called leafing intensity, is seen to trade-off isometrically with leaf size in a variety of species (Kleiman and Aarssen, 2007; Yang et al., 2008; Whitman and Aarssen, 2010) however direct tradeoffs of leaf number and leaf size have rarely been observed. The topic is extensively reviewed in (Westoby et al., 2002).

Arabidopsis and other rosette plants are a special case within herbaceous species because they have a negligible stem during vegetative growth and leaves can be thought, simplistically, to constitute the whole above-ground portion of the plant. The production of leaves, its trade-off with leaf size and its relation to growth must thus be examined on a whole plant basis. The relationship of appendage sizes and proportions to whole body size is a special branch of biomathematics – the study of allometry (Huxley, 1932; Niklas, 1994, 2004). It can be seen throughout nature that the sizes of constituents (organs, appendages etc) scale with the size of the organism as power laws. Two scaling scenarios are possible:

1) In isometric scaling (or isometric growth), size increases in such a way that proportions are maintained – all parts grow at the same rate as the whole. The roots, stems and leaves of plants (as fractions of total biomass) grow isometrically and maintain constant (but species and environment-specific) ratios of shoot:root and root:leaf throughout growth (Poorter and Nagel, 2000; Niklas, 2004).

2) Any deviation (positive or negative) from isometry results in allometric scaling – parts increase at different rates from the whole, leading to a change in proportion with increasing size. Allometric scaling laws apply on broad scales spanning many orders of magnitude of size variation throughout nature and extend beyond size and shape to also include physiological processes and growth (West et al., 1999; Enquist et al., 2007). They can also be extended beyond the individual organism to encompass whole community properties in ecology (Niklas, 2004; Ogawa, 2008). They have thus been interpreted as "universal laws" guiding the evolution of plant form and function (Enquist, 2002).

An examination of leaf number in an allometric context may yield insights into the relationship between leaf production and growth. It may, in particular, provide a conceptual framework to analyse partitioning of growth between leaf number and size. Arabidopsis and other rosette plants are a good choice of species for such an approach due their simple growth form. During early growth the above-ground portion of the plant consists of a single growing module, which grows in biomass by producing leaves This makes Arabidopsis an attractive experimental system to search for relations between leafing intensity, leaf size and biomass production. This is a simpler system than in plants where complications are introduced by stems and branching. The life cycle of Arabidopsis also bypasses the limitation of using single season growth of single modules (twigs), encountered in larger plants such as trees.

A whole plant approach to leaf number and its relation to plant size has only been conducted theoretically in the past. Based on fractal-like hierarchical properties of living organisms, a series of universal allometric scaling laws have been predicted for various attributes by (West et al., 1999). This model was applied to plant vascular systems with several constraints to predict scaling laws for different plant parts in trees (Enquist, 2002). Using this approach, leaf number was predicted to scale with plant size as a ¾ power law. Surprisingly, this prediction has not been empirically tested before or since the publication of that notable theoretical study.

Total shoot biomass increases exponentially, at least during the early stages of plant growth (see e.g. Tschoep et al., 2009 for a recent study in Arabidopsis). The temporal kinetic of leaf production during growth in Arabidopsis (or in other plants) is not clear. A prediction of allometric scaling implies a pattern of leaf initiation which is also exponential in time. Many Arabidopsis studies ignore leaf number while some simply present leaf number data at a given point in time, ignoring temporal patterns as well as whole plant growth. Where temporal data is available, some literature suggests leaf production at constant rates, giving a linear increase in leaf number over time (Cookson and Granier, 2006; Cookson et al., 2007) while other studies present curves with clearly accelerating rates which bear resemblance to exponential growth, particularly during the early growth of the plant (Wang et al., 2008; Méndez-Vigo et al., 2010). At least three distinct developmental phases have been distinguished in the vegetative growth of Arabidopsis, differentiated by cell and leaf morphology (Wu and Poethig, 2006; Poethig, 2009; Wu et al., 2009) and, incidentally, leaf initiation rates (Wang et al., 2008; Méndez-Vigo et al., 2010).

As pointed out in the introductory chapter, leaf initiation rates also respond to environmental factors and metabolic status. However these factors are also known to affect whole plant growth and the sizes

of leaves. An investigation of leaf initiation in a whole plant context is needed in order to assess how leaf number is integrated in variation in plant and organ growth.

7.1.1. Aims of the chapter

In this chapter the production of leaves in Arabidopsis will be quantitatively analysed in a whole plant context with the following aims:

1. Examine the temporal pattern of leaf initiation during early growth of Arabidopsis and describe it mathematically
2. Examine the relationship between the temporal pattern of leaf initiation and the exponential growth in biomass in an allometric context – test for the existence of a scaling law with plant biomass during growth and examine its properties
3. Examine how the allometry of leaf production relates to leaf size during growth and in plants where it is altered
4. Examine responses of leaf number and leaf number allometry when growth rates are altered by changing the light regime.

7.2. Results.

7.2.1. Leaf initiation is allometric with respect to biomass growth.

Leaf number growth may be predicted to be allometric to plant biomass growth if the profile of leaf size throughout the life of the Arabidopsis plant is examined. Each leaf of Arabidopsis at full size is larger than the leaf preceding it (Fig 7.1). Similar changes have been seen in innumerable studies. This is clearly a change in proportion with increasing plant size, and would therefore not be expected if leaf production had the same rate of increase as biomass (i.e. if it was isometric with growth). It suggests, instead, that biomass growth is relatively faster than leaf initiation, necessitating an increase in leaf size which must, itself, also be allometric. This may, among other things, reflect the fact that with time the sink tissues at the apex of Arabidopsis plant are being supplied with carbon from an increasing number of leaves, which will drive increasingly rapid growth. The same conclusion can be reached from the fact that young Arabidopsis plants grow exponentially (Tschoep et al., 2009). This simple observation implies that the shoot apex produces an increasing amount of leaf material per unit time. However, this earlier study did not resolve the extent to which the increase in rate of production of leaf material was due to an increase in the rate of leaf initiation or leaf growth.

Fig. 7.1. Consecutive fully expanded leaves of an *Arabidopsis thaliana* rosette.

Data was collected during the experiment on metabolic mutants in Arabidopsis presented in Chapter 5 and analysed to provide quantitative information about the temporal kinetics of leaf initiation and the increase in total shoot biomass. Fig. 7.2 shows the growth in rosette biomass and the number of emerged leaves over time during the growth of wild type *Arabidopsis thaliana* Col-0 and two metabolic mutants in starch biosynthesis (*pgm*) and sucrose breakdown (*cinv1cinv2*). In Fig. 7.2a biomass growth was modelled assuming exponential growth between the two harvests. Wild type plants grew at a rate of 0.303 g g^{-1} d^{-1} while the *pgm* and *cinv1cinv2* mutants had lower and almost identical growth rates of 0.225 and 0.223 g g^{-1} d^{-1} respectively.

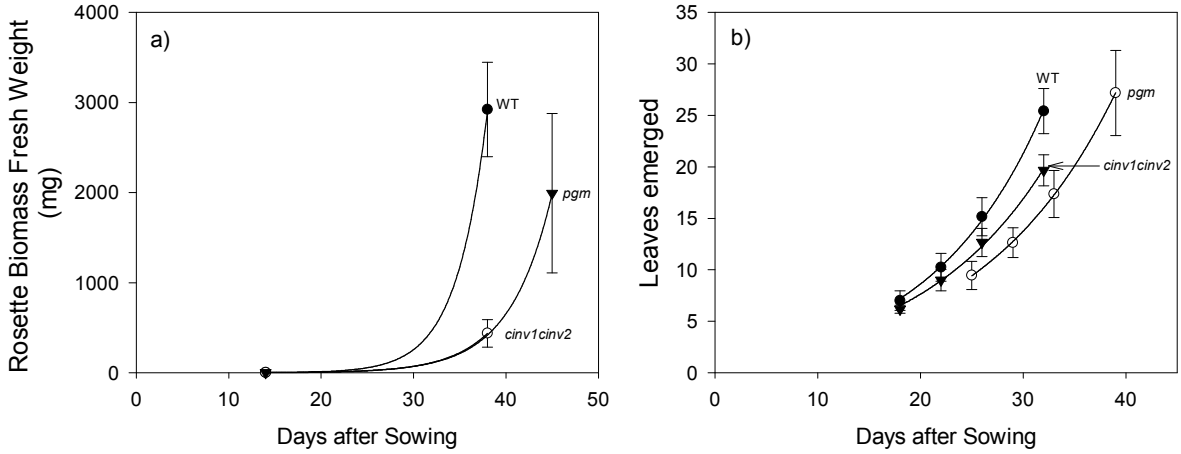

Fig. 7.2. Biomass and leaf number growth in Arabidopsis wild type and two metabolic mutants. Biomass growth (a) and leaf emergence (b) of *Arabidopsis thaliana* wild type Col-0 and two metabolic mutants. Bars are standard deviations, N=8 (biomass), N=12 (leaf number). Curves are exponential functions fitted to the data. Biomass growth was modelled from initial (14 days after sowing) and final harvest biomass with constant relative growth rates. The plants were grown in a 12-hour photoperiod, with 160 μE m^{-2} s^{-1} light irradiance and a 20°/20° day/night temperature regime.

The number of emerged leaves was scored by visual inspection at 4 time points. Leaf emergence accelerated with time and the fitted curves were mildly exponential (Fig. 7.2b). An observation that was made during these investigations is that leaf production is close-to linear with time when plants are grown in small pots (6cm diameter and 5cm high, 140cm^3) but is clearly exponential when each plant was grown in one large pot. The plants in Fig 6.2 were growing in large pots (9.5cm diameter, 7cm high, 500cm^3), with one plant in each pot. This suggests that pot space and/or nutrient constraints may influence the growth and developmental program of Arabidopsis and this should be taken into account in developmental studies. The exponential curves regressed onto the leaf number data yielded almost perfect fits ($r^2 > 0.99$). The *pgm* and *cinv1cinv2* mutants formed leaves slower than the wild type Col-0 and had fewer leaves at any given point in time however the *cinv1cinv2* double mutant formed leaves faster than *pgm* even though both increased in biomass at the same rate. Leaf emergence rates reflected by the exponents of the curves were 0.09 d^{-1} for wild type, 0.076 d^{-1} in *pgm* and 0.079 d^{-1} in *cinv1cinv2*. The exponents have the same interpretation as that of relative growth rate, expressed as leaves $leaf^{-1}$ d^{-1} and will be termed "relative leaf emergence rate".

To investigate the relationship between leaf number and growth, growth trajectories of leaf number and biomass were modelled using the parameters determined above and leaf number was plotted against biomass (Fig. 7.3a and b). Relative growth rate (of biomass) was predicted to exceed relative leaf emergence rate, which results in a non-linear trajectory during growth. The trajectories become linear on a log-log plot (Fig. 7.3b). This is the defining feature of a power law or scaling law.

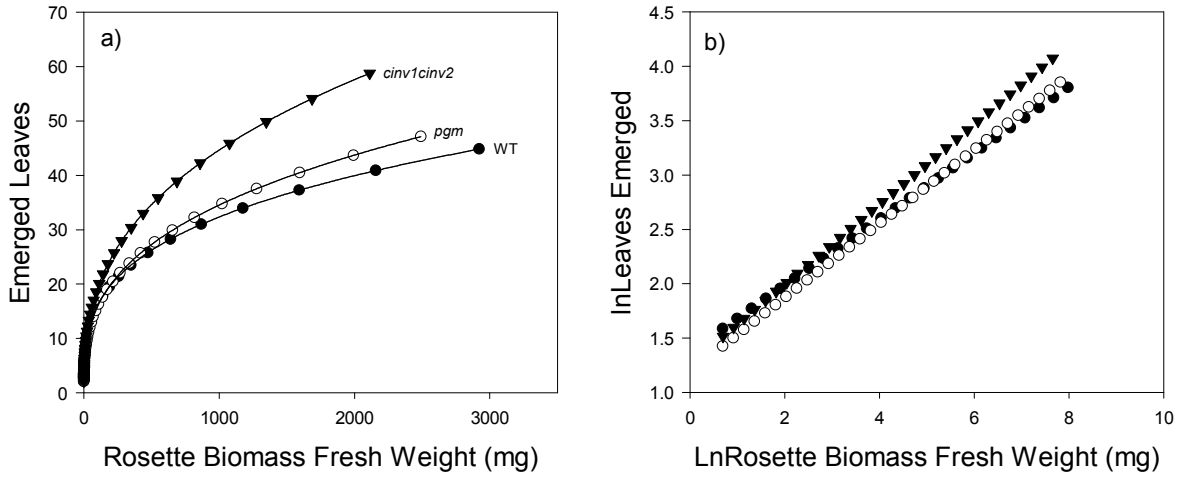

Fig. 7.3. Leaf production as a function of biomass during growth in Arabidopsis wild type Col-0 and two metabolic mutants.
Modelled growth trajectories of leaf production against plant biomass in *Arabidopsis thaliana* Col-0 wild type and two metabolic mutants modelled from values for RGR and the relative leaf emergence rate that were estimated form the data and parameters presented in Fig. 7.2 and in the text. Each point is the modelled cumulative response during one further day of growth.

Since biomass growth was relatively faster than leaf production, mean leaf size is predicted to increase as the plant grows. In Fig. 7.4 the mean biomass per leaf is modelled a plant grows in size. This is the inverse of the leafing intensity parameter described in Chapter 6.

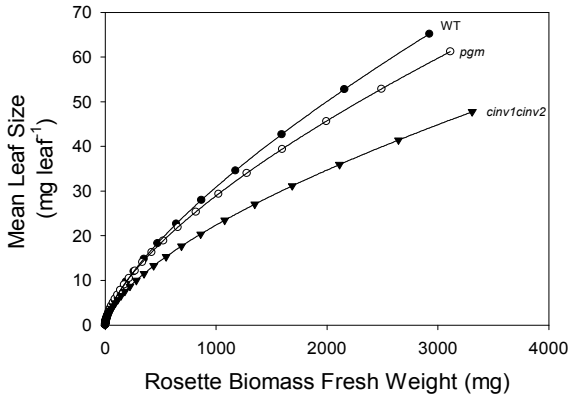

Fig. 7.4. Mean biomass per leaf as a function of whole plant biomass during growth of Arabidopsis wild type Col-0 and two metabolic mutants.
Each point is the modelled cumulative response during one further day of growth.

The log-log trajectory of leaf number as a function of biomass (Fig. 7.3b) can be described by the linear function:

$$\ln LeafNo = \ln b + k \ln FW \qquad (7.1)$$

The reader may recognise Eq. 7.1 as an application of the allometric growth equation (Huxley, 1932). The slope k can be interpreted as an unchanging ratio between the relative rates of increase in leaf number and biomass during growth (White and Gould, 1965) and is otherwise known as an allometric coefficient. Table 7.1 lists the model parameters obtained. Two coefficients can be obtained. One is the allometric coefficient of leaf number, which is derived from Fig. 7.3. The second is the allometric coefficient of mean leaf size, which is derived from Fig. 7.4.

The slopes (allometric coefficients) for the relation log LeafNo = logb +k logFW were different from 1, indicating that leaf production is allometric with respect to biomass growth (rather than isometric). The allometric coefficient for leaf number in wild type Col-0 was 0.304. This means that the relative rate of increase in leaf number is 0.304 of the rate of biomass growth. Both metabolic mutants had higher allometric coefficients of leaf number, indicating that leaf production relative to biomass growth was faster compared to wild type. Both mutants thus had more leaves than wild type Col-0 at an equivalent plant size. They had fewer leaves than wild type Col-0 at any point in time but this is because they grew more slowly.

Mean leaf mass also increased allometrically with respect to biomass, with a coefficient of 0.696 in the wild type. The metabolic mutants had their biomass distributed over more leaves at a given plant size and average leaf mass was lower at a given total biomass. Consequently, their allometric coefficients of mean leaf size were also lower.

Mean leaf size is the residual component of whole plant growth and is reciprocal to leafing intensity. Consequently, the allometric coefficients of leaf production and of mean leaf size sum up to 1 in each genotype, a consequence of the additive nature of leaf number and leaf size to give total growth. Mean leaf size is a complex parameter which includes all the leaves on the plant, some of which are growing and some of which are mature. While mean leaf size increased with increasing biomass, the slope of this increase was high at the start, when all the leaves are growing, but decreased with time, probably reflecting an increasing proportion of leaves which have stopped growing. It thus does not have a straightforward interpretation, however it is probable that mean leaf size also reflects the final size of leaves. It is also probable, that with data on the momentary sizes of leaves throughout growth as well as their final sizes, a mathematical formulation can be devised to decompose mean leaf size into (i) the final size of each leaf and (ii) how much of the final size has been obtained by each leaf at a given time.

log LeafNo = logb +k logFW		
Genotype	b	k
Wild Type Col-0	3.962	0.304
pgm	3.291	0.340
cinv1cinv2	3.531	0.367

log LeafFW = logb +k logFW		
Genotype	b	k
Wild Type Col-0	0.252	0.696
pgm	0.304	0.660
cinv1cinv2	0.283	0.633

Table. 7.1. Allometric equation parameters of the relationship between leaf number and mean leaf mass with plant mass during growth in *Arabidopsis thaliana* wild type Col-0 and two metabolic mutants.
The numbers were derived by extracting the slopes and intercepts of the modelled lines in Fig. 7.3 and 7.4.

As already pointed out, the mean leaf mass is a complex trait. To obtain better insights into the consequences for the mature leaf, the measured area, fresh mass and thickness of leaf 6 at harvest in the three genotypes is plotted in Fig. 7.5. Both mutants had smaller leaves than the wild type. The sixth leaf of the *pgm* mutant weighed 85% as much as a wild type leaf (Fig. 7.5a) but was only 52%

the area (Fig. 7.5b). In the *cinv1cinv2* mutant the sixth leaf was 38% of the mass and 37% the area compared to wild type. Thus the area of *pgm* mutant leaves was decreased much more than leaf mass compared to the wild type. This can be explained by leaf thickness. It was 70% higher in the mutant (Fig. 7.5c), which results in more fresh mass per area. Thus, at a given biomass investment in a leaf, higher leaf thickness results in a smaller leaf area. The smaller size of leaves in the mutants can be understood to be a consequence of more leaves being produced compared to biomass, which results in less biomass per leaf and, in the case of *pgm*, increased leaf thickness causing a further decrease in area per mass invested in the leaf.

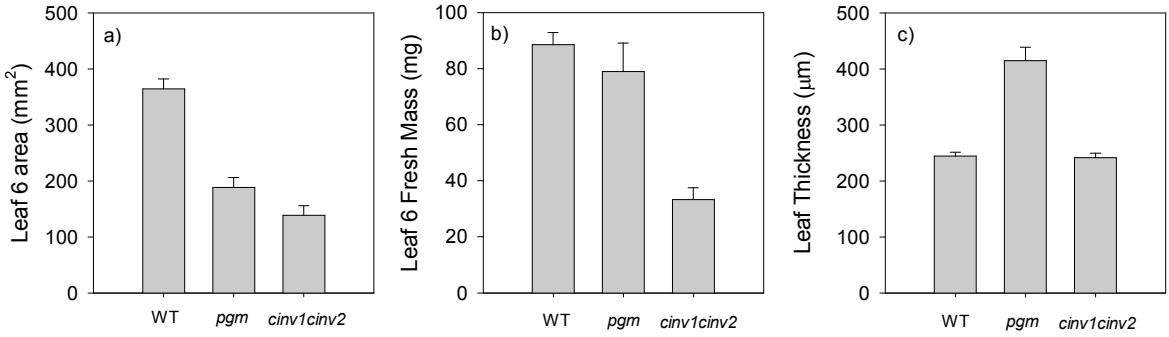

Fig. 7.5. Measured area of leaf 6 and leaf fresh mass and leaf thickness measured at full expansion in *Arabidopsis thaliana* Col-0 wild type and two metabolic mutants.

7.2.2. Leaf size is a balance between whole-plant growth rate and leaf production.

In Fig. 7.6 mean leaf mass at 35 days after germination is modelled as a function of the allometric coefficient of leaf production at three arbitrary growth rates (Fig. 7.6a) and as a function of growth rate at two arbitrary allometric ratios (Fig. 7.6b). At a constant growth rate, high allometric ratios led to an exponential decline in mean leaf size. At constant allometric ratios, higher growth rates led to exponentially larger leaves. A very large mean leaf size was possible only with a combination of high biomass growth rates and low allometric ratios. It should be noted that this simple model does not make any predictions about the momentary size or the final size of individual leaves. It is likely that a decrease in average leaf size will usually be accompanied by a decrease in all final leaf sizes, rather than a large variation in final leaf size, with some being large and the others small. This is supported by visual inspection of the rosettes of wild-type Col0, *pgm* and *cinv1cinv2*. However, a larger data set would be needed to quantify this tentative conclusion, and to learn whether it can be generalised.

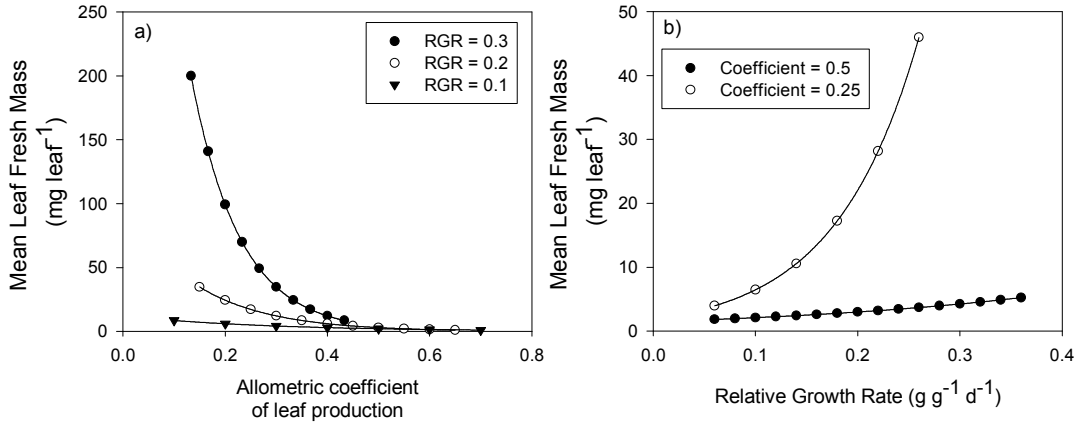

Fig. 7.6. Modelled mean leaf size at different rates of biomass growth and different allometric coefficients.
Modelled mean fresh mass per leaf after 35 days of growth at three growth rates and varying allometric ratios of leaf production (a) and two allometric coefficients and varying growth rate (b). Lines are exponential regressions fitted to modelled data.

7.2.3. Leaf production rates vary in concert with the rate of growth in different environments.

To further investigate the relationship between leaf production and growth, *Arabidopsis thaliana* Col-0 wild type was grown in a series of light environments. The data was collected during the irradiance experiment presented in Chapter 5, where plants were grown in a daylength of 12h and four light irradiance levels ranging from 75 to 420 µE m^{-2} s^{-1}, and a separate experiment where plants were grown in a constant irradiance of 200 µE m^{-2} s^{-1} and daylengths ranging from 4 to 18 hours light. In the irradiance experiment, all seedlings were first grown at an intermediate irradiance (160 µE m^{-2} s^{-1} and were transferred to the different light environments 14 days after germination. The plants were grown in the large pots discussed above (500cm^3) and the number of leaves was counted on two occasions between 17 and 20 days after germination. In the daylength experiment all seedlings were first grown in an intermediate daylength (8h) and were transferred to different daylengths after 21 days. The plants were grown in smaller long pots which are used for gas exchange analysis on whole rosettes (115cm^3) and the number of leaves was counted between 22 and 31 days, which was extended to a third count at 42 days in the shorter daylengths. The experiments were thus conducted in different conditions and had different sampling strategies. Data is therefore comparable within the experiments but may not be exactly comparable between them.

When RGR is plotted against the daily quantum input, RGR increased with increasing quantum input and then saturated (Fig. 7.7a). Quite similar maximum rates were obtained in both experiments (0.31 g g^{-1} d^{-1} in the daylength experiment and 0.34 g g^{-1} d^{-1} in the irradiance experiment) indicating that the slight differences in the growth protocol may not greatly affect maximum growth rates. At limiting daily quantum inputs, there was a linear relation between quantum input and RGR over the range 2.8 – 8.8 mol m-2 (equivalent to 4-12 hours light) for the photoperiod data set. At these limiting daily quantum inputs a higher RGR was obtained in the experiment where plants were grown in a 12 h and irradiance was decreased.

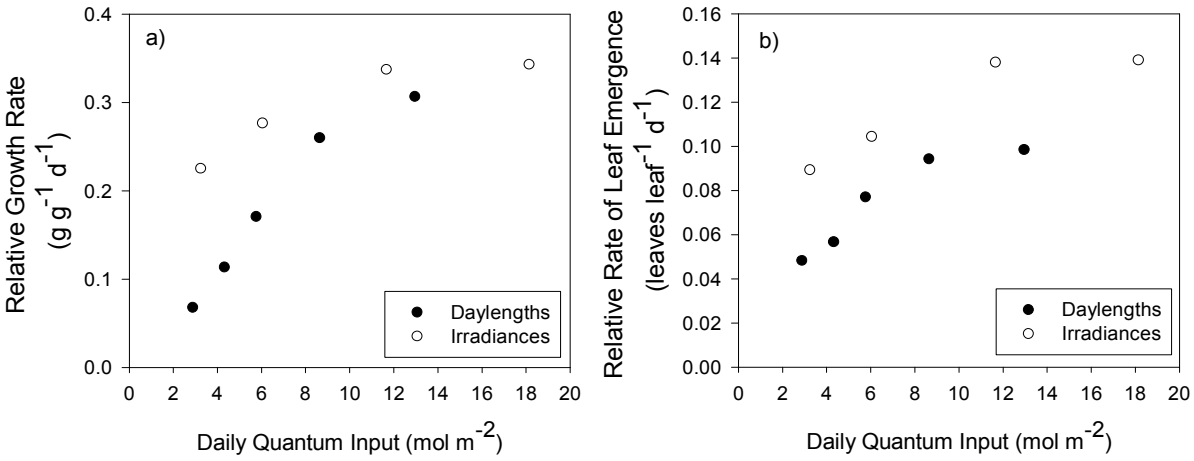

Fig. 7.7. Biomass growth and leaf production in different light environments.
Relative growth rate (a) and relative rate of leaf emergence in *Arabidopsis thaliana* Col-0 wild type grown in constant light irradiance and different daylengths (black dots) and constant daylength and different irradiances (white dots). Light inputs are shown as daily input of light quanta for comparison between experiments.

Leaf emergence rates increased in a pattern similar to that of growth rate before saturating at high light and long daylengths (Fig. 7.7b). Plants grown in longer daylengths or higher irradiances formed leaves faster and had more leaves at a common age. Relative rates of leaf emergence at equivalent daily photon input were higher in the irradiance experiment than the daylength experiment at all levels of light input. This may be related to the size of the pots in this experiment, as the plants were grown in small pots to enable analysis of gas exchange on whole rosettes.

In both experiments, leaf emergence was linearly related to the rate of growth (Fig. 7.8). Leaf emergence increased with a higher slope in the experiment where irradiance was varied than in the experiment where daylength was varied.

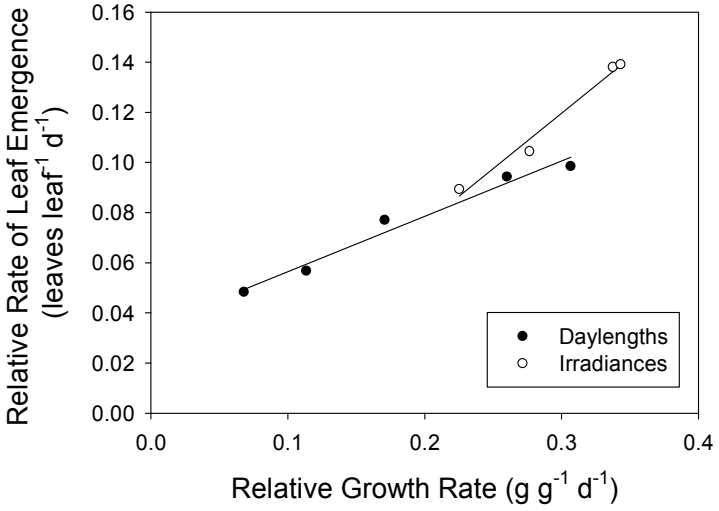

Fig. 7.8. Relative rate of leaf emergence as a function of relative growth rate in biomass in Arabidopsis wild type Col-0 grown in different light environments.
Arabidopsis thaliana Col-0 wild type were grown in constant irradiance and different daylengths (black dots) and constant daylength and different irradiances (white dots). Lines are linear regressions.

7.2.4. The allometry of leaf production varies with the rate of growth in different light environments.

Acclimation to variation in daylength was associated with changes in the allometric ratio of leaf production (Fig. 7.9a). The allometric coefficient of leaf production was high in very short daylengths, indicating that plants produced a larger number of leaves relative to their biomass. The coefficient decreased with increasing daylength and became almost stable at the top of the range. In contrast, variation in light irradiance at constant daylength did not lead to a change in the allometric coefficient of leaf production. However, as seen above, low irradiances did not lower RGR to very low levels, leading to different rates of growth at the same daily quantum input in the two experiments. When the allometric ratio is plotted against the rate of biomass growth (Fig. 7.9b) the responses to daylength and irradiance converged, with similar values at high growth rates, and a high value at low growth rates. Thus variation in growth rate, not light input, seems to drive responses in the allometric coefficient of leaf production, with the most notable feature being an increase n the allometric coefficient at low growth rates.

The values obtained in these experiments in Col-0 in a wide range of light environments lay between 0.49 and 0.30, with higher values in short day conditions, but rather stable values in neutral and long days, which were independent of irradiance. The latter values agree well with those obtained in an independent experiment on Col-0 wild type, presented in Table. 7.1.

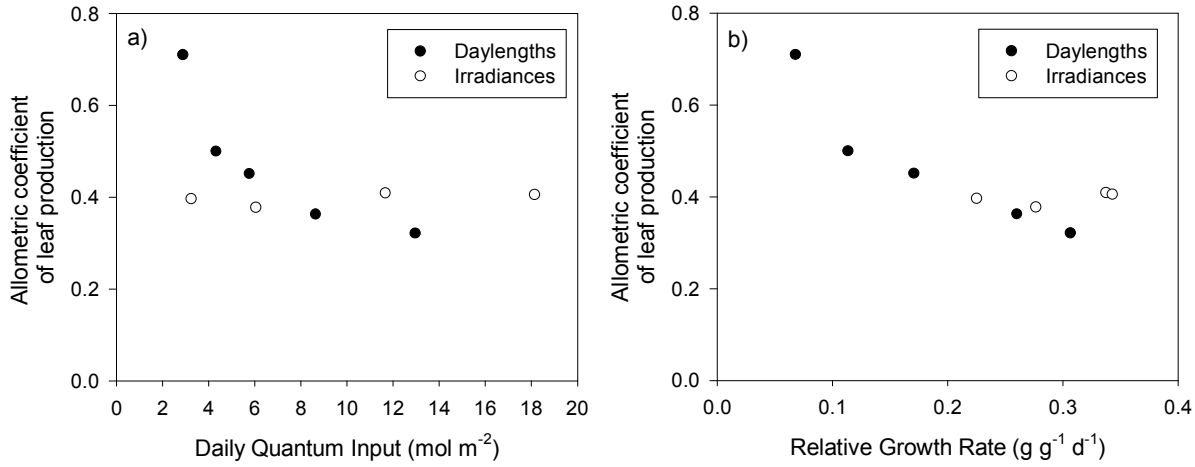

Fig. 7.9. The dependence of the allometric coefficient of leaf production on the light environment and on relative growth rate in biomass.
Allometric coefficient of leaf production as a function of daily light input (a) and relative growth rate (b) in *Arabidopsis thaliana* Col-0 wild type grown in constant light irradiance and different daylengths (black dots) and constant daylength and different irradiances (white dots).

Leaf growth will require a much larger energy input than leaf initiation; it is therefore possible that in conditions where growth is strongly resource limited, more leaves are initiated than can be supplied during subsequent growth. However, this is a tentative conclusion, that requires testing by experiments at lower light intensities, and also in other where growth is limited by other resources. Further, the observed variation must, be interpreted with caution due to issues with the growing conditions. The plants were initially grown in the same conditions and were later moved to higher or lower light conditions (irradiance or daylength). Subsequent to the transfer, leaf initiation may adjust to the new conditions, however a pool of pre-formed and yet un-emerged primordia is present, which emerges at a later date. In high light conditions this emergence may under-estimate the real new rate of leaf initiation in high light because fewer leaf primordia were formed in the initial conditions. In low light

conditions the number of emerging primordia may be higher than the real new rate as they were formed in higher-light conditions, where they are formed faster. This issue may be particularly pronounced at the extremes of the range, in very low and very high light conditions, as they are the farthest removed from the initial conditions. Thus this data should be treated with caution and should be verified in plants germinated and grown in a constant environment from the start. The allometric coefficient in Col0 may therefore be more stable between conditions than is indicated by the initial analysis presented here.

7.2.5. The allometry of leaf production varies with the rate of growth in different accessions.

In Chapter 6 it was found that leafing intensity was negatively related to plant growth in twenty Arabidopsis accessions. Leafing intensity is the ratio of the number of leaves to plant biomass at a given timepoint and varies with time as the plant grows while the allometric coefficient is the slope of this variation and is therefore the constant determining factor behind leafing intensity. Allometric coefficients of leaf production were estimated for the accession data presented in Chapter 6 by comparing leaf initiation rates with biomass growth. The accessions were grown in 8-h days at 160 µE m^{-2} s^{-1}. The allometric coefficients lay in a relatively narrow range between 0.32 and 0.40, in close agreement with the values obtained in the experiments presented in this chapter. The allometric coefficient was negatively related to rosette biomass growth in the accessions (r^2=0.74, $p<0.001$, Fig 6.10). The relationship of plant biomass and RGR have also been calculated for a number of other morphological and dry matter content in Chapter 6, as well as total protein, starch and over 60 low-molecular-weight metabolites (Sulpice et al., 2009), over 20 enzymes (Sulpice et al., 2010) and ribosome numbers and polysome loading (Ishihara, unpublished). The relation between the allometric coefficient of leaf production and RGR is the strongest correlation uncovered to date.

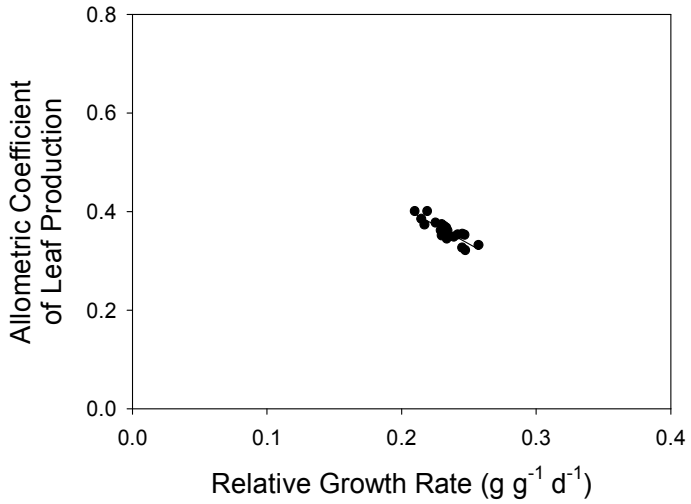

Fig. 7.10. Genetic variation in the allometric coefficient of leaf production in Arabidopsis accessions and its relationship with relative growth rate.
Allometric coefficient of leaf production as a function of relative growth rate is 20 wild accessions of *Arabidopis thaliana* grown in 8-hour days at an irradiance of 160 µE m^{-2} s^{-1}. Line is linear regression, r^2=0.74.

7.3. Discussion.

7.3.1. Development of a model and estimation of the allometric coefficient for leaf initiation in Arabidopsis

A simple growth model is presented, placing the production of leaves in the context of whole plant growth. It has frequently been observed in Arabidopsis that sequential leaves increase in size. The theoretical analysis presented in this Chapter analyses this phenomenon in an allometric context. The results clearly indicate that leaf production is allometric with respect to biomass growth, yielding new insights into plant and leaf growth. By applying this analysis to empirical data, this chapter also provides parameterised values for the allometric constant and provides some initial information about how it may vary between different genotypes and environments.

The allometric properties presented here are estimates. The deficiencies of the method are as follows. Biomass growth was modelled with constant RGR, ignoring temporal variation in growth, which is known to occur. Growth rates decline with plant size, in fact RGR itself has been predicted to scale with biomass with an allometry of -¼ (Enquist et al., 1999). In addition, biomass measurements included only the above-ground portion of the plant, ignoring the roots. Since roots grow isometrically with the shoot and with the whole plant (Niklas, 2004), this should not affect the RGR estimate as it is the same in all plant parts. It would affect the estimates of allometric scaling however, as leaf number should be compared against total plant biomass, which includes the roots. Furthermore, even though leaf number was quantified at several timepoints during growth, only emerged leaves were recorded. A large number of young growing primordia can be present at the shoot apex before emerging. For example Arabidopsis leaf 6 spends the first seven days of its life concealed there before emerging (Cookson and Granier, 2006).

The model presented identifies leaf size as the result of a trade-off interaction between plant growth rate and the rate of leaf production. The allometry of leaf production was seen to have a complementary relationship to that of leaf size, the two coefficients summing to 1, reflecting the additive nature of leaf number and leaf size to give total rosette size. It is possible that the trade-off between faster leaf initiation and slower leaf growth has the consequence that at high allometries of leaf production a larger proportion of the leaves will still be growing. This would lead to a decrease in mean leaf size (independent of any effect on the final leaf size) and, as a mathematical consequence, an increase in the allometric coefficient of leaf production. Alternatively, a high allometry of leaf production may mean that leaves stop expanding sooner and the number of growing leaves is the same. This may also explain the lower mean leaf size in these situations. Analysis of Arabidopsis accessions in Chapter 6 indicates that high leafing intensity (and therefore the allometric coefficient of leaf production) is in fact related negatively to final leaf size (of leaf 6), suggesting that mean leaf size is also an indicator of final leaf size, although perhaps not an absolute one.

A treatment of leaf primordia as sinks competing for a limited resource can explain the trade-off, with more primordia the available biomass (i.e. growth) is split between more sinks, and each sink grows less. This property illustrates how leaf number has a direct inverse effect on leaf size at a given growth rate – the leaf number vs. size trade-off is an inevitable part of plant growth. This highlights the importance of considering leaf number and whole plant growth when thinking about variation in leaf size. This is largely missing from studies on leaf and organ size in Arabidopsis, for example Gonzalez et al. (2010). In that study it was attempted to alter the size of leaves by modifying the expression of single genes belonging to different functional classes. The results were varying depending on environment and leaf position, with some genes only affecting the sizes of growing leaves and others

affecting mature leaves. However it was not taken into account that the size of leaves involves trade-offs with leaf number, with growth and with sizes of other leaves on the plant. It can be seen from this chapter that plant growth rate alone can determine the size of leaves, without changes in leaf production or its allometry. In practice, leaf production, growth rates and the relationship between them (allometry) were seen to vary between genotypes and environmental conditions.

Clear effects on leaf size consistent with allometric scaling are evident in a study where leaf initiation rates were manipulated by manipulating the expression of miR156, which targets SPL genes and regulates developmental stage progression (Wang et al., 2008) and leaves became bigger when there were fewer of them and smaller when more were initiated while plant biomass growth seemed to be equal (judging from presented images).

In my experiments, several observations are also consistent with a primary role for the allometry of leaf production. First, despite an acceleration of leaf initiation, final leaf size also increases in successive leaves in Arabidopsis Col-0 (see Fig. 7.1). This implies leaf initiation is being accelerated more slowly than the resource generation which supports biomass growth. Second, the starch metabolism mutant *pgm* and the sucrose breakdown mutant *cinv1cinv2*, which had lower growth rates, both showed an increased allometric coefficient, resulting in a larger number of smaller leaves at a given total shoot biomass than in wild type Col-0. Third, accessions with lower rates of growth had a higher allometric coefficient, again resulting in a larger number of smaller leaves at a given total shoot biomass. In this case, the slow-growing accessions actually tend to have higher levels of starch, sugars, amino acids and other low weight metabolites (Sulpice et al., 2009; 2010; Sulpice and Keurentjes, unpubl.), indicating that the high allometric coefficient for leaf production in slow-growing accessions is not a secondary consequence of low resources leading to slow growth. Fourth, there was a trend to a higher allometric coefficient when Col-0 was grown with a decreased daily quantum input (although see the results section for possible sources of error in this experiment). However, it should be stressed that changes in the rate of leaf initiation may not always be the main driver that determines the relation between leaf number and leaf size. It is also possible that in some cases, feedback mechanisms that are triggered by resource availability or other physiological states in growing leaves may regulate the rate of leaf initiation. It has been proposed that (Caspar et al., 1985; Fleming, 2006) that the meristem activity determining leaf production is flexible and accommodates regulatory inputs from metabolism, particularly from carbon status.

In the studies in my preliminary analysis, the response of leaf production to the environment seems to be disproportionate to variation in biomass growth and biomass is allocated disproportionally to fewer, larger leaves at higher growth rates. Analysis of natural accessions growing in one environment yielded an essentially equivalent trend. The existence of genotypic variation for this trait suggests that there may be an adaptive advantage of having fewer leaves and making them bigger. This is possible if a lower allometric coefficient allows a more efficient investment of resources, which leads to higher growth in a particular environment.

The allometric coefficient of leaf production found in this study (0.303) is very different to the theoretically-predicted ¾ allometric scaling law for trees (Enquist, 2002) meaning that fewer leaves were produced than would be predicted. Some drawbacks of the approach in the present study were discussed above. If the missing root biomass is included in the calculation, it would decrease the allometric slope, not increase it, thus this factor cannot account for the discrepancy. Un-emerged primordia are also unlikely to explain the difference, since the number of them would have to be very large to allow for a ¾ slope. Thus, there may be other reasons for a lower than expected allometric coefficient of leaf production. The ¾ scaling law prediction for trees in Enquist (2002) was made with a number of key assumptions, among them a constant size of leaves and petioles. This assumption may well be true in leaves of trees on branches but clearly does not hold in the case of Arabidopsis (see Fig

6.1). The model of Enquist (2002) also includes a biomechanical component which constrains the lengths of branches to scale with their radius, which is important in trees for resistance to buckling. Since the Arabidopsis rosette does not have stems or branches and is not prone to experiencing the dynamic loads which cause buckling in trees (i.e. wind gusts), the above assumption may well be irrelevant to Arabidopsis.

A scenario deviating from the prediction may be possible if the creation of extra biomass is included. This can occur if leaves grow from their own fixed carbon after becoming net sources. Having fewer primordia in total may allow them to emerge earlier and expand faster, which might allow an earlier sink-source transition with the result that the leaves become self-sufficient sooner. This may improve growth due to the possible efficiency benefits of growth in the light, compared to heterotrophic import-driven growth, as discussed in Chapter 6. On the other hand, if leaves expand preferentially using their own fixed carbon they may be able to export less, which may affect leaf initiation downstream and therefore further lower the allometry. This may also be a reason for the deviation from the predicted ¾ slope since fewer leaves were initiated than predicted.

The optimal allometric coefficient may depend on the environment. The findings presented here suggest that it may vary between environments, although this requires verification due to issues with experimental design. There may be an adaptive advantage of high allometry at very low growth rates. As seen in Chapter 5, increasing light interception by increasing leaf area should be an advantage in light-limited environments. However, as also pointed out there and in literature (Westoby et al., 2002) large leaves overlap more, which decreases carbon fixation and is therefore an inefficient use of biomass. At very low growth rates large leaves are not possible, even at very low allometry of leaf production. Decreasing self shading in a rosette with a few small leaves, such as that which occurs in very low light, can be achieved using two strategies – lengthening the petiole (increasing the distance between leaves) or making relatively more smaller leaves. Lengthening the petiole requires extra biomass, which will decrease the amount of leaf lamina that can be produced for the same biomass investment. In contrast, altering the allometry to make more, smaller leaves requires only a re-partitioning of the same amount of biomass between leaves. The nature of phyllotaxy in Arabidopsis is such that new leaves grow into the gaps between pre-existing leaves, thus avoiding self-shading and optimising the use of available space. A rosette with a few small leaves does not use space efficiently and leaves unused spaces between leaves. In this way, making many small leaves may be a strategy to cover more ground area and increase light interception without investing in additional structural components in the petiole. On the other hand, it can also be argued that the increase in the allometric coefficient in plants that are growing slowly is due to a resource-restriction of leaf growth. Viewed from the perspective of rosette function, this would lead to the same result.

Smaller leaves also have fewer structural support requirements in the form of vascular architecture within the leaf. Large leaves require thicker (and probably longer, see previous paragraph) petioles and thicker veins for mechanical support and the hydrodynamic requirements of transpiration, a factor contributing to a lower SLA in large leaves both within and between species (Milla and Reich, 2007; Niinemets et al., 2007). Fibres and tracheary elements, the load-bearing components of plant vascular systems, contain a high percentage of lignin, a phenolic polymer which is among the most costly substances that plants produce, (Poorter, 1994) and is present in substantial amounts to constitute a significant synthesis cost to the plant (lignin is the second most abundant biological substance on Earth). Minimising the production of costly biomass components may be advantageous in carbon and energy-limited environments and may favour the production of small leaves where this is advantageous – in rosettes with low growth rates, few leaves and limited carbon.

7.3.2. Possible functional consequences of allometric scaling of leaf size

One consequence of the proposed allometric scaling of leaf size is the slope of the increase in final leaf size with leaf number in Arabidopsis (as in Fig. 7.1). A low coefficient of leaf number allometry (and as a formal consequence, a high one for leaf size) would cause a steeper increase in mean leaf size (Fig. 7.3), which may be accompanied by steeper increases in the sizes of consecutive leaves at full expansion. If leaf growth were to be modelled with strictly isometric scaling with plant biomass (with a coefficient of leaf number allometry of 1), all of the leaves on the rosette would have the same final size. In such a scenario, for a set increase in biomass (e.g. a doubling) there is an increase in leaf number of the same magnitude (also a doubling), leaving no scope for variation in mean leaf size and, possibly, final leaf size. For very high allometry of leaf number, as occurred in 4-h days, the model predicts a rosette made of many small leaves and a more uniform final leaf size distribution (with an allometric slope of leaf size of only 0.31 compared to 0.69 in the wild type example above). Final leaf size data and size distributions are not available for the daylength data, however this may be an interesting future line of research.

Further experiments should aim to clarify whether the observed changes in allometry in different environments are real within a genotype. Analysis of the phenotypic plasticity of this trait in different genotypes should help to establish to what extent it is genotypically determined. Its relationship to growth performance and to other traits in different genotypes grown in different environments may shed light on the adaptive significance of the allometry of leaf production. For example an analysis of petiole size in different light environments and its relationship with allometry may clarify to what extent high allometry is adaptive for avoiding inefficient self-shading through leaf overlap.

7.4. Chapter Summary.

In summary, a simple allometric model was presented linking leaf number, leaf size and plant growth rate together in a whole plant context in *Arabidopsis thaliana*. The present model may be instructive in understanding plant growth and its components. The consideration of leaf number in an allometric context is a new approach and some of the first empirical evidence is presented for allometric scaling of leaf number with plant size in a plant species. The model illustrates the inter-relatedness of leaf number, leaf size and whole plant growth rate and highlights the importance of considering all three parameters in morphological and developmental studies. The allometric coefficients of leaf production in wild type plants were much lower than the theoretical prediction for tree leaves, made by Enquist (2002). The rates of leaf production and the allometric relationship were found to vary between genotypes differing in growth rates due to metabolic restrictions, between light regimes which drove changes in growth rate and between natural accessions differing in growth rate and grown in the same environment. Leaf number allometry was seen to be strongly negatively related to the rate of growth in each experiment. As a consequence, high plant growth rates were associated with fewer leaf initiations per unit biomass growth and a smaller number of larger leaves. The possible adaptive significance and the functional consequences of this phenomenon may be prevention of leaf-overlap in low light environments, and a more efficient investment of resources in biomass at high growth rates. The genetic and molecular regulation of the allometry of leaf formation is a topic for future research, and should deliver important insights into how meristem activity is coordinated with the growth of many discrete organs, and how resource availability modulates these processes.

Chapter 8. General Discussion.

The general aim of the work presented in this thesis was to investigate how leaf morphology is regulated in *Arabidopsis thaliana* with particular reference to possible regulatory influences of carbon and sugar status. Three approaches were taken to investigate this question.

In one approach it was asked whether specifically altering the levels of trehalose-6-phosphate, a putative signal of sucrose availability, through genetic means has effects on leaf growth and morphology. The success of this specific genetic approach depends on whether the initial hypotheses are true, namely that 1) Tre-6-P is indeed a signal of sugar status and 2) that sugar status does indeed regulate leaf morphology. Robust correlative evidence has been presented previously supporting a role for Tre-6-P as a specific sucrose signal (Lunn et al., 2006; Yadav, 2009). The metabolic analysis presented in Chapter 3 confirmed the previous results. It also uncovered a new potential involvement of Tre-6-P in the regulation of sucrose metabolism, which builds on and extends previous work to support the role of Tre-6-P as a regulator of primary carbon metabolism (Kolbe et al., 2005; Lunn et al., 2006). However, given the data presented here, it is difficult to establish a role for Tre-6-P as a specific regulator of leaf morphology. The effects of its constitutive modulation in plants were inconsistent with what are thought to be the effects of carbon status on growth and development, namely that more carbon results in more growth. In addition, the complex metabolic phenotypes of the plants as well as concerns about pleiotropic effects and a dependence of some of the morphological phenotypes on the presence or absence of starch make these phenotypes somewhat difficult to interpret.

The use of metabolic mutants allowed the broader hypothesis, that sugar status affects leaf morphology, to be tested. This approach goes above the level of known sugar sensing pathways and asks the general and simple question of whether leaf morphology is affected when central metabolism is perturbed and sugar levels are altered. The genetic approach which was taken was successful at producing a range of perturbed sugar levels in plants and leaf thickness alterations could be observed in some mutants, but not in all and not in all conditions. The mutants chosen are affected in various aspects of central carbon metabolism. They have complex and in some cases very severe metabolic alterations which also affect their growth, and this also makes them similar to the plants with perturbed Tre-6-P levels. For example the lack of starch in the *pgm* mutant causes extensive depletion of carbon pools at night and this leads to coordinated transcriptional responses of more than 4000 genes and upregulation of starvation responses, while during the day the opposite response occurs (Bläsing et al., 2005; Stitt et al., 2007). The *cinv1cinv2* double mutant is likely to be even more severely perturbed as it has been suggested that cytosolic invertase may be the main route through which carbon from sucrose is broken down in non-photosynthetic cells, i.e. the sink tissues where growth and development occur (Barratt et al., 2009). Amid such complexity it would be naïve, using either targeted or broader approaches, to attribute any morphological alterations to changes in the levels of single metabolites such as sugars or even Tre-6-P. The same can probably be said about attempts to manipulate complex processes such as development through the modification of single genes, which invariably also lead to diverse and complex phenotypes (Gonzalez et al., 2010). An exception may be approaches to modulate metabolism specifically in particular cell types, as seen in Chapter 4, where this strategy was employed to investigate the involvement of guard cell metabolism in stomatal function. In fact, in a similar approach it was also attempted to modulate Tre-6-P in specific zones of developing leaf primordia, however the results were difficult to interpret due to questions about the spatial specificity of the metabolic modulation and were not presented here.

It may well be impossible to manipulate metabolites in an exclusive manner, particularly if they also have known regulatory functions on metabolism, as in the case of Tre-6-P, or if altering them necessitates broad perturbations of metabolism, as is the case of sugars or starch. Attempts to find links between metabolism and developmental processes may be aided by broader characterisation of metabolism in many different mutants perturbed at various points in metabolism and looking for similarities. Such approaches should be possible given the combination of modern 'omics technologies and the excellent genetic resources of the Arabidopsis model. The approach is exemplified on a small scale by the results presented in Chapter 5, where a developmental phenotype was narrowed down to a particular group of mutants which lack starch. This offers promise that with a denser coverage of metabolic mutants other metabolic inputs into the regulation of leaf development may become evident and it may be possible to identify specific segments of metabolism which may be involved in regulating them.

Altering metabolism, even in particular cell types, also has systemic implications for the entire plant as the metabolism of different plant parts is essentially linked by the systemic process of sucrose transport and the relations between source activity and sink demand. Thus, any consideration of metabolic signalling on growth and development cannot be restricted simply to the study of single organs and must be considered from a whole plant perspective, considering also the number of leaves and the rate of plant growth. In general, relationships between the morphological properties of single leaves and these whole plant processes are not clear. This led to the general approach which was presented in Chapter 6 and the theoretical approach in Chapter 7. This was successful at identifying which morphological components are related to leaf function and plant growth and which are not as well as finding some interesting relationships between traits. The organ and organismal levels of organisation seem to be linked by a balance between leaf formation and plant growth, which can be measured at specific timepoints in the form of leafing intensity and arises from underlying variation in the allometry of leaf production, which was observed to vary between wild genotypes, metabolic mutants and environmental treatments.

The putative metabolic and sugar signals identified to date have all attracted attention primarily due to their effects on whole-plant growth. Their involvement in leaf morphogenesis was speculated from their effects on leaf size. Little was known about how they may affect other morphological traits. As seen in chapter 6, leaf size is itself a component of plant growth while the model presented in chapter 7 exemplifies how changes in the rate of growth alone can affect the size of leaves. Many mutants with decreased leaf size have been found, however these have usually also been smaller plants (Devvitte et al., 2007). A question arising from this is: can mutants be found where leaf size is uncoupled from whole plant growth? As an extreme theoretical example it may be asked, can a mutant be found which consists of one very large leaf, and weighs as much as a wild type plant of the same age? This is of course unlikely, as leaves are determinate organs and must stop growing at some stage, requiring more leaves to be produced to maintain further growth. However it must be noted that this is by no means impossible and a whole family of one-leaf plants exists in Angiosperms in the genus *Monophyllaea* (Tsukaya, 1997). While this is obviously a very extreme example, the observed genotypic variation in leafing intensity and its underlying component, the allometric coefficient of leaf production, in Arabidopsis accessions suggests that there may be genetic factors regulating this particular aspect. As an example, the Cvi accession seems to be one such case – it had the lowest rate of leaf initiation of all accessions in the set and had some of the largest leaves. As leafing intensity is very easy to assess, it would be an exciting future direction to examine this trait genetically.

The preceding discussion and the extreme example of the one-leaf plant prompt another question regarding the balance in resource allocation between sinks. The shoot apical meristem is a very minor portion of the volume of the plant, however it is one of the most vital as it initiates all the growth of the above-ground plant body. The meristem itself probably has a very low carbon and energy

requirement as a proportion of the whole plant, however it is in intense competition for resources with a much larger population of sinks, namely the growing heterotrophic leaf primordia that it has initiated and the growing leaves which are not yet self sufficient, which have a large resource requirement for their growth. Moreover, the growing sinks are located basal to the meristem and in closer proximity to the phloem which supplies them. There must thus be tight regulation ensuring that the meristem is not out-competed for resources by its own leaf primordia. Incidentally, the one-leaf growth habit in *Monophyllaea*, as described above, arises because one cotyledon outcompetes the other and the shoot apical meristem for resources in a phenomenon which was termed "competitive organogenesis" by the author (Tsukaya, 1997), showing that this is in fact possible. This is, again, an extreme example. However the previous discussion implies that, while being a very small part of the plant, the meristem must also be an extremely strong sink which must draw enough resources in the face of strong internal competition in order to survive and maintain growth and organogenesis.

It may be supposed that mutants impaired in this regulation may turn out embryo-lethal if their meristem is starved by the rest of the plant. Indeed, impaired delivery of sucrose has been implicated in the phenotype of an embryo-lethal meristem-organisation mutant as the phenotype could be rescued by sucrose (Wu et al., 2005; Fleming, 2006). A number of metabolic enzymes show specific localisation patterns at the meristem (Pien et al., 2001) and some of them have been implicated in determining sink strength (Fleming, 2006). Leafing intensity, again, is very interesting in this context as it may potentially reflect the number of growing sinks relative to the photosynthetic biomass which supplies them and may thus be a reflection of the level of resource competition within the plant. Leafing intensity may thus also be interesting for the study of source-sink relations and the determinants of the sink strength of leaf primordia and, possibly, the meristem.

There must also be regulation which balances the allocation of resources between growing leaves as Arabidopsis does not exhibit obvious imbalances in the growth of different leaves, e.g. one very large leaf and many very small ones. It may be supposed that this may be ensured by the symmetrical properties inherent in plant growth and organogenesis, however the observation of flowers with obvious asymmetry in the shapes as well as sizes of appendages in such plants as *Antirrhinum* (Da et al., 1999) and, for example, the Orchidacea suggests that there is no requisite requirement for strict symmetry in plants and the growth of organs can be unbalanced. Recent genetic work has shown that both the symmetry and phyllotaxy of leaf formation can be unbalanced by inducing leaf primordia in locations where they would not normally form by targeted manipulation of expansin gene expression (Pien et al., 2001). Remarkably, the leaves that resulted from this manipulation were largely comparable to the other leaves on the plant in size and shape, suggesting that there are intrinsic mechanisms that balance the allocation of resources between leaves and these must be independent of symmetry.

This previous genetic work also prompts the question of whether there are compensatory effects on the sizes of the other leaves when leaf initiation rate is altered in this manner. This indeed appears to be the case in a study where leaf initiation rates were manipulated by altering the expression of miR156 (Wang et al., 2008) and leaves became bigger when there were fewer of them and smaller when more were initiated while plant growth was equal. Essentially the same relationship was also observed in the study of 20 Arabidopsis presented in this thesis when variation in plant growth was taken into account. This is a fascinating finding from which a parallel can be drawn to the compensation phenomenon in leaf morphogenesis, where cell size compensates for altered cell number in the leaf (Tsukaya, 2003). Just like compensation is an organ-level regulatory influence in the development of single leaves, the control of leafing intensity may be an organism-level process serving to maximise leaf area.

Bibliography.

Extensive use of the following printed books was made for reference:

Sokal RR, Rolf FJ (1998) Biometry. Third Edition. W. H. Freeman & Co. New York

Everitt BS, Dunn G (2001) Applied Multivariate Data Analysis. Second Edition. Arnold. London

Peer-reviewed Publications:

Ache P, Bauer H, Kollist H, Al-Rasheid KAS, Lautner S, Hartung W, Hedrich R (2010) Stomatal action directly feeds back on leaf turgor: new insights into the regulation of the plant water status from non-invasive pressure probe measurements. The Plant Journal **62:** 1072-1082

Adler I, Barabe D, Jean RV (1997) A History of the Study of Phyllotaxis. Annals of Botany **80:** 231-244

Aguirrezabal L, Bouchier-Combaud S, Radziejwoski A, Dauzat M, Cookson SJ, Granier C (2006) Plasticity to soil water deficit in Arabidopsis thaliana: dissection of leaf development into underlying growth dynamic and cellular variables reveals invisible phenotypes. Plant, Cell & Environment **29:** 2216-2227

Allaway W (1981) Anions in stomatal operation. *In* P Jarvis, T Mansfield, eds, Stomatal physiology. Cambridge, pp 71-87

Allaway WG (1973) Accumulation of malate in guard cells of <i>Vicia faba</i> during stomatal opening. Planta **110:** 63-70

Allen JF, Bennett J, Steinback KE, Arntzen CJ (1981) Chloroplast protein phosphorylation couples plastoquinone redox state to distribution of excitation energy between photosystems. Nature **291:** 25-29

Almeida A, Cardoso L, Santos D, Torné J, Fevereiro P (2007) Trehalose and its applications in plant biotechnology. In Vitro Cellular & Developmental Biology - Plant **43:** 167-177

Almeida A, Villalobos E, Araújo S, Leyman B, Van Dijck P, Alfaro-Cardoso L, Fevereiro P, Torné J, Santos D (2005) Transformation of tobacco with an *Arabidopsis thaliana* gene involved in trehalose biosynthesis increases tolerance to several abiotic stresses. Euphytica **146:** 165-176

Almeida AM, Silva AB, Araujo SS, Cardoso LA, Santos DM, Torne JM, Silva JM, Paul MJ, Fevereiro PS (2007) Responses to water withdrawal of tobacco plants genetically engineered with the AtTPS1 gene: a special reference to photosynthetic parameters. Euphytica **154:** 113-126

Araújo WL, Nunes-Nesi A, Osorio S, Usadel B, Fuentes D, Nagy R, Balbo I, Lehmann M, Studart-Witkowski C, Tohge T, Martinoia E, Jordana X, DaMatta FM, Fernie AR (2011) Antisense Inhibition of the Iron-Sulphur Subunit of Succinate Dehydrogenase Enhances Photosynthesis and Growth in Tomato via an Organic Acid–Mediated Effect on Stomatal Aperture. The Plant Cell Online **23:** 600-627

Arrivault S, Guenther M, Ivakov A, Feil R, Vosloh D, van Dongen JT, Sulpice R, Stitt M (2009) Use of reverse-phase liquid chromatography, linked to tandem mass spectrometry, to profile the Calvin cycle and other metabolic intermediates in Arabidopsis rosettes at different carbon dioxide concentrations. Plant Journal **59:** 824-839

Assmann S, Zeiger E (1987) Guard cell bioenergetics. *In* E Zeiger, G Faquhar, I Cowan, eds, Stomatal function, Stanford, pp 163-193

Assmann SM (1999) The cellular basis of guard cell sensing of rising CO2. Plant Cell and Environment **22:** 629-637

Assmann SM (2010) Hope for Humpty Dumpty: Systems Biology of Cellular Signaling. Plant Physiology **152:** 470-479

Athanasiou K, Dyson BC, Webster RE, Johnson GN (2010) Dynamic Acclimation of Photosynthesis Increases Plant Fitness in Changing Environments. Plant Physiology **152:** 366-373

Avonce N, Leyman B, Mascorro-Gallardo JO, Van Dijck P, Thevelein JM, Iturriaga G (2004) The Arabidopsis Trehalose-6-P Synthase AtTPS1 Gene Is a Regulator of Glucose, Abscisic Acid, and Stress Signaling. Plant Physiology **136:** 3649-3659

Azpiroz R, Wu Y, LoCascio JC, Feldmann KA (1998) An Arabidopsis Brassinosteroid-Dependent Mutant Is Blocked in Cell Elongation. The Plant Cell Online **10:** 219-230

Badger MR, von Caemmerer S, Ruuska S, Nakano H (2000) Electron flow to oxygen in higher plants and algae: rates and control of direct photoreduction (Mehler reaction) and rubisco oxygenase. Philosophical Transactions of the Royal Society of London. Series B: Biological Sciences **355:** 1433-1446

Bae H, Sicher R, Natarajan S, Bailey B (2009) In situ expression of trehalose synthesizing genes, *TPS1* and *TPPB* in *Arabidopsis thaliana* using the GUS reporter gene. Plant Cell, Tissue and Organ Culture **98:** 311-319

Baier M, Dietz K-J (2005) Chloroplasts as source and target of cellular redox regulation: a discussion on chloroplast redox signals in the context of plant physiology. Journal of Experimental Botany **56:** 1449-1462

Baier M, Ströher E, Dietz K-J (2004) The Acceptor Availability at Photosystem I and ABA Control Nuclear Expression of 2-Cys Peroxiredoxin-A in Arabidopsis thaliana. Plant and Cell Physiology **45:** 997-1006

Baroli I, Price GD, Badger MR, von Caemmerer S (2008) The Contribution of Photosynthesis to the Red Light Response of Stomatal Conductance. Plant Physiology **146:** 737-747

Barratt DHP, Derbyshire P, Findlay K, Pike M, Wellner N, Lunn J, Feil R, Simpson C, Maule AJ, Smith AM (2009) Normal growth of Arabidopsis requires cytosolic invertase but not sucrose synthase. Proceedings of the National Academy of Sciences **106:** 13124-13129

Bassi R, Caffarri S (2000) Lhc proteins and the regulation of photosynthetic light harvesting function by xanthophylls. Photosynthesis Research **64:** 243-256

Beemster GTS, De Veylder L, Vercruysse S, West G, Rombaut D, Van Hummelen P, Galichet A, Gruissem W, Inzé D, Vuylsteke M (2005) Genome-Wide Analysis of Gene Expression Profiles Associated with Cell Cycle Transitions in Growing Organs of Arabidopsis. Plant Physiology **138:** 734-743

Beemster GTS, De Vusser K, De Tavernier E, De Bock K, Inzé D (2002) Variation in Growth Rate between Arabidopsis Ecotypes Is Correlated with Cell Division and A-Type Cyclin-Dependent Kinase Activity. Plant Physiology **129:** 854-864

Beerling DJ (2005) Leaf Evolution: Gases, Genes and Geochemistry. Annals of Botany **96:** 345-352

Bell W, Sun W, Hohmann S, Wera S, Reinders A, De Virgilio C, Wiemken A, Thevelein JM (1998) Composition and Functional Analysis of the Saccharomyces cerevisiae Trehalose Synthase Complex. Journal of Biological Chemistry **273:** 33311-33319

Bergmann DC, Sack FD (2007) Stomatal Development. Annual Review of Plant Biology **58:** 163-181

Bläsing OE, Gibon Y, Günther M, Höhne M, Morcuende R, Osuna D, Thimm O, Usadel B, Scheible W-R, Stitt M (2005) Sugars and Circadian Regulation Make Major Contributions to the Global Regulation of Diurnal Gene Expression in Arabidopsis. The Plant Cell Online **17:** 3257-3281

Blazquez MA, Lagunas R, Gancedo C, Gancedo JM (1993) Trehalose-6-Phosphate, a New Regulator of Yeast Glycolysis That Inhibits Hexokinases. Febs Letters **329:** 51-54

Blázquez MA, Santos E, Flores C-l, Martínez-Zapater JM, Salinas J, Gancedo C (1998) Isolation and molecular characterization of the Arabidopsis TPS1 gene, encoding trehalose-6-phosphate synthase. The Plant Journal **13:** 685-689

Boccalandro HE, Rugnone ML, Moreno JE, Ploschuk EL, Serna L, Yanovsky MJ, Casal JJ (2009) Phytochrome B Enhances Photosynthesis at the Expense of Water-Use Efficiency in Arabidopsis. Plant Physiology **150:** 1083-1092

Bouvier F, Backhaus RA, Camara B (1998) Induction and Control of Chromoplast-specific Carotenoid Genes by Oxidative Stress. Journal of Biological Chemistry **273:** 30651-30659

Brouwer R (1962) Nutritive influences on the distribution of dry matter in the plant. Netherlands Journal of Agricultural Sciences **10:** 361-376

Brouwer R (1963) Some aspects of the equilibrium between overground and underground plant parts. Jaarboek van het Instituut voor Biologisch en Scheikundig onderzoek aan Landbouwgewassen **1963**

Buchanan BB, Schürmann P, Jacquot J-P (1994) Thioredoxin and metabolic regulation. Seminars in Cell Biology **5:** 285-293

Byrne ME (2009) A role for the ribosome in development. Trends in Plant Science **14:** 512-519

Caemmerer S, Farquhar GD (1981) Some relationships between the biochemistry of photosynthesis and the gas exchange of leaves. Planta **153:** 376-387

Caspar T, Huber SC, Somerville C (1985) Alterations in Growth, Photosynthesis, and Respiration in a Starchless Mutant of Arabidopsis thaliana (L.) Deficient in Chloroplast Phosphoglucomutase Activity. Plant Physiology **79:** 11-17

Casson SA, Franklin KA, Gray JE, Grierson CS, Whitelam GC, Hetherington AM (2009) phytochrome B and PIF4 Regulate Stomatal Development in Response to Light Quantity. Current Biology **19:** 229-234

Chary SN, Hicks GR, Choi YG, Carter D, Raikhel NV (2008) Trehalose-6-Phosphate Synthase/Phosphatase Regulates Cell Shape and Plant Architecture in Arabidopsis. Plant Physiology **146:** 97-107

Chazdon RL, Pearcy RW (1991) The Importance of Sunflecks For Forest Understory Plants : Photosynthetic Machinery Appears Adapted to Brief, Unpredictable Periods of Radiation, Vol 41. American Institute of Biological Sciences, Washington, DC, ETATS-UNIS

Chen M, Chory J, Fankhauser C (2004) Light signal transduction in higher plants. Annual review of genetics **38:** 87-117

Chen Y-B, Durnford DG, Koblizek M, Falkowski PG (2004) Plastid Regulation of Lhcb1 Transcription in the Chlorophyte Alga Dunaliella tertiolecta. Plant Physiology **136:** 3737-3750

Chevan A, Sutherland M (1991) Hierarchical partitioning, Vol 45. American Statistical Association, Alexandria, VA, ETATS-UNIS

Chia DW, Yoder TJ, Reiter W-D, Gibson SI (2000) Fumaric acid: an overlooked form of fixed carbon in <i>Arabidopsis</i> and other plant species. Planta **211:** 743-751

Cho Y-H, Yoo S-D, Sheen J (2006) Regulatory Functions of Nuclear Hexokinase1 Complex in Glucose Signaling. Cell **127:** 579-589

Ciais P, Tans PP, Trolier M, White JWC, Francey RJ (1995) A Large Northern Hemisphere Terrestrial CO2 Sink Indicated by the 13C/12C Ratio of Atmospheric CO2. Science **269:** 1098-1102

Clerget B, Dingkuhn M, Gozé E, Rattunde HFW, Ney B (2008) Variability of Phyllochron, Plastochron and Rate of Increase in Height in Photoperiod-sensitive Sorghum Varieties. Annals of Botany **101:** 579-594

Cockcroft CE, den Boer BGW, Healy JMS, Murray JAH (2000) Cyclin D control of growth rate in plants. Nature **405:** 575-579

Cominelli E, Galbiati M, Vavasseur A, Conti L, Sala T, Vuylsteke M, Leonhardt N, Dellaporta SL, Tonelli C (2005) A guard-cell-specific MYB transcription factor regulates stomatal movements and plant drought tolerance. Current Biology **15:** 1196-1200

Cookson SJ, Chenu K, Granier C (2007) Day Length Affects the Dynamics of Leaf Expansion and Cellular Development in Arabidopsis thaliana Partially through Floral Transition Timing. Annals of Botany **99:** 703-711

Cookson SJ, Granier C (2006) A Dynamic Analysis of the Shade-induced Plasticity in Arabidopsis thaliana Rosette Leaf Development Reveals New Components of the Shade-adaptative Response. Annals of Botany **97:** 443-452

Cookson SJ, Van Lijsebettens M, Granier C (2005) Correlation between leaf growth variables suggest intrinsic and early controls of leaf size in Arabidopsis thaliana. Plant, Cell & Environment **28:** 1355-1366

Corner EJH (1949) The Durian Theory or the Origin of the Modern Tree. Annals of Botany **13:** 367-414

Corona V, Aracri B, Kosturkova G, Bartley GE, Pitto L, Giorgetti L, Scolnik PA, Giuliano G (1996) Regulation of a carotenoid biosynthesis gene promoter during plant development. The Plant Journal **9:** 505-512

Cortina C, Culiáñez-Macià FA (2005) Tomato abiotic stress enhanced tolerance by trehalose biosynthesis. Plant Science **169:** 75-82

Coupe SA, Palmer BG, Lake JA, Overy SA, Oxborough K, Woodward FI, Gray JE, Quick WP (2006) Systemic signalling of environmental cues in Arabidopsis leaves. Journal of Experimental Botany **57:** 329-341

Cousins AB, Baroli I, Badger MR, Ivakov A, Lea PJ, Leegood RC, von Caemmerer S (2007) The Role of Phosphoenolpyruvate Carboxylase during C4 Photosynthetic Isotope Exchange and Stomatal Conductance. Plant Physiology **145:** 1006-1017

Cross JM, von Korff M, Altmann T, Bartzetko L, Sulpice R, Gibon Y, Palacios N, Stitt M (2006) Variation of Enzyme Activities and Metabolite Levels in 24 Arabidopsis Accessions Growing in Carbon-Limited Conditions. Plant Physiology **142:** 1574-1588

Da L, Carpenter R, Copsey L, Vincent C, Clark J, Coen E (1999) Control of Organ Asymmetry in Flowers of Antirrhinum. Cell **99:** 367-376

Day SJ, Lawrence PA (2000) Measuring dimensions: the regulation of size and shape. Development **127:** 2977-2987

De Veylder L, Beeckman T, Beemster GTS, Krols L, Terras F, Landrieu I, Van Der Schueren E, Maes S, Naudts M, Inzé D (2001) Functional Analysis of Cyclin-Dependent Kinase Inhibitors of Arabidopsis. The Plant Cell Online **13:** 1653-1668

De Vries FWTP (1975) The Cost of Maintenance Processes in Plant Cells. Annals of Botany **39:** 77-92

Deprost D, Yao L, Sormani R, Moreau M, Leterreux G, Nicolai M, Bedu M, Robaglia C, Meyer C (2007) The Arabidopsis TOR kinase links plant growth, yield, stress resistance and mRNA translation. EMBO Rep **8:** 864-870

Devvitte W, Scofield S, Alcasabas AA, Maughan SC, Menges M, Braun N, Collins C, Nieuwland J, Prinsen E, Sundaresan V, Murray JAH (2007) Arabidopsis CYCD3 D-type cyclins link cell proliferation and endocycles and are rate-limiting for cytokinin responses. Proceedings of the National Academy of Sciences of the United States of America **104:** 14537-14542

Dijkwel PP, Huijser C, Weisbeek PJ, Chua NH, Smeekens S (1997) Sucrose Control of Phytochrome A Signaling in Arabidopsis. The Plant Cell Online **9:** 583-595

Dittrich P, Raschke K (1977) Malate metabolism in isolated epidermis of *Commelina communis* L. in relation to stomatal functioning. Planta **134:** 77-81

Donnelly PM, Bonetta D, Tsukaya H, Dengler RE, Dengler NG (1999) Cell Cycling and Cell Enlargement in Developing Leaves of Arabidopsis. Developmental Biology **215:** 407-419

Douady S, Couder Y (1992) Phyllotaxis as a physical self-organized growth process. Physical Review Letters **68:** 2098

Draborg H, Villadsen D, Nielsen TH (2001) Transgenic Arabidopsis Plants with Decreased Activity of Fructose-6-Phosphate,2-Kinase/Fructose-2,6-Bisphosphatase Have Altered Carbon Partitioning. Plant Physiology **126:** 750-758

Du Z, Aghoram K, Outlaw WH (1997) RESEARCH REPORT: In VivoPhosphorylation of Phosphoenolpyruvate Carboxylase in Guard Cells ofVicia fabaL. Is Enhanced by Fusicoccin and Suppressed by Abscisic Acid. Archives of Biochemistry and Biophysics **337:** 345-350

Eastmond PJ, Van Dijken AJH, Spielman M, Kerr A, Tissier AF, Dickinson HG, Jones JDG, Smeekens SC, Graham IA (2002) Trehalose-6-phosphate synthase 1, which catalyses the first step in trehalose synthesis, is essential for Arabidopsis embryo maturation. The Plant Journal **29:** 225-235

Efroni I, Blum E, Goldshmidt A, Eshed Y (2008) A Protracted and Dynamic Maturation Schedule Underlies Arabidopsis Leaf Development. The Plant Cell Online **20:** 2293-2306

Eichelmann H, Laisk A (1994) CO2 Uptake and Electron Transport Rates in Wild-Type and a Starchless Mutant of Nicotiana sylvestris (The Role and Regulation of Starch Synthesis at Saturating CO2 Concentrations). Plant Physiology **106:** 679-687

El-Bashiti T, HamamcI H, Öktem HA, Yücel M (2005) Biochemical analysis of trehalose and its metabolizing enzymes in wheat under abiotic stress conditions. Plant Science **169:** 47-54

Elberse IAM, Vanhala TK, Turin JHB, Stam P, Damme JMMv, van Tienderen PH (2004) Quantitative trait loci affecting growth-related traits in wild barley (Hordeum spontaneum) grown under different levels of nutrient supply. Heredity **93:** 22-33

Enquist BJ (2002) Universal scaling in tree and vascular plant allometry: toward a general quantitative theory linking plant form and function from cells to ecosystems. Tree Physiology **22:** 1045-1064
Enquist BJ, Kerkhoff AJ, Stark SC, Swenson NG, McCarthy MC, Price CA (2007) A general integrative model for scaling plant growth, carbon flux, and functional trait spectra. Nature **449:** 218-222
Enquist BJ, West GB, Charnov EL, Brown JH (1999) Allometric scaling of production and life-history variation in vascular plants. Nature **401:** 907-911
Escoubas JM, Lomas M, LaRoche J, Falkowski PG (1995) Light intensity regulation of cab gene transcription is signaled by the redox state of the plastoquinone pool. Proceedings of the National Academy of Sciences **92:** 10237-10241
Evans GC (1972) The quantitative analysis of plant growth, Vol Volume 1. Blackwell Scientific, Oxford
Evans J, Sharkey T, Berry J, Farquhar G (1986) Carbon Isotope Discrimination measured Concurrently with Gas Exchange to Investigate CO_2 Diffusion in Leaves of Higher Plants. Functional Plant Biology **13:** 281-292
Evans JR (2004) Developmental Constraints on Photosynthesis: Effects of Light and Nutrition

Photosynthesis and the Environment. *In* NR Baker, ed, Vol 5. Springer Netherlands, pp 281-304
Evans JR, Jakobsen I, Ögren E (1993) Photosynthetic light-response curves. Planta **189:** 191-200
Evans JR, Kaldenhoff R, Genty B, Terashima I (2009) Resistances along the CO2 diffusion pathway inside leaves. Journal of Experimental Botany **60:** 2235-2248
Evans JR, Poorter H (2001) Photosynthetic acclimation of plants to growth irradiance: the relative importance of specific leaf area and nitrogen partitioning in maximizing carbon gain. Plant Cell and Environment **24:** 755-767
Fahnenstich H, Saigo M, Niessen M, Zanor MI, Andreo CS, Fernie AR, Drincovich MF, Flügge U-I, Maurino VG (2007) Alteration of Organic Acid Metabolism in Arabidopsis Overexpressing the Maize C4 NADP-Malic Enzyme Causes Accelerated Senescence during Extended Darkness. Plant Physiology **145:** 640-652
Farquhar G, Richards R (1984) Isotopic Composition of Plant Carbon Correlates With Water-Use Efficiency of Wheat Genotypes. Functional Plant Biology **11:** 539-552
Farquhar GD, O'Leary MH, Berry JA (1982) On the Relationship Between Carbon Isotope Discrimination and the Intercellular Carbon Dioxide Concentration in Leaves. Functional Plant Biology **9:** 121-137
Fernandez O, Béthencourt L, Quero A, Sangwan RS, Clément C (2010) Trehalose and plant stress responses: friend or foe? Trends in Plant Science **15:** 409-417
Fey V, Wagner R, Bräutigam K, Pfannschmidt T (2005) Photosynthetic redox control of nuclear gene expression. Journal of Experimental Botany **56:** 1491-1498
Fieulaine S, Lunn JE, Ferrer J-L (2007) Crystal structure of a cyanobacterial sucrose-phosphatase in complex with glucose-containing disaccharides. Proteins: Structure, Function, and Bioinformatics **68:** 796-801
Fleming A (2002) The mechanism of leaf morphogenesis. Planta **216:** 17-22
Fleming A (2006) Metabolic aspects of organogenesis in the shoot apical meristem. Journal of Experimental Botany **57:** 1863-1870
Fleming AJ (2005) Formation of primordia and phyllotaxy. Current Opinion in Plant Biology **8:** 53-58
Fleming AJ (2006) The co-ordination of cell division, differentiation and morphogenesis in the shoot apical meristem: a perspective. Journal of Experimental Botany **57:** 25-32
Fleming AJ (2007) Cell Cycle Control During Leaf Development. *In* Annual Plant Reviews Volume 32: Cell Cycle Control and Plant Development. Blackwell Publishing Ltd, pp 203-226
Fleming AJ, McQueen-Mason S, Mandel T, Kuhlemeier C (1997) Induction of Leaf Primordia by the Cell Wall Protein Expansin. Science **276:** 1415-1418
Flexas J, Ortuño MF, Ribas-Carbo M, Diaz-Espejo A, Flórez-Sarasa ID, Medrano H (2007) Mesophyll conductance to CO2 in Arabidopsis thaliana. New Phytologist **175:** 501-511
Flexas J, Ribas-Carbo M, Diaz-Espej A, Galmes J, Medrano H (2008) Mesophyll conductance to CO2: current knowledge and future prospects. Plant Cell and Environment **31:** 602-621
Flis A (unpublished work). *In*,

Frechilla S, Talbott LD, Zeiger E (2002) The CO2 response of Vicia guard cells acclimates to growth environment. Journal of Experimental Botany **53:** 545-550
Frechilla S, Talbott LD, Zeiger E (2004) The Blue Light-Specific Response of Vicia faba Stomata Acclimates to Growth Environment. Plant and Cell Physiology **45:** 1709-1714
Friend D, Helson V, Fisher J (1962) Leaf growth in Marquis wheat, as regulated by temperature, light intensity and daylength. Canadian Journal of Botany **40:** 1299-1311
Frison M, Parrou JL, Guillaumot D, Masquelier D, Francois J, Chaumont F, Batoko H (2007) The Arabidopsis thaliana trehalase is a plasma membrane-bound enzyme with extracellular activity. Febs Letters **581:** 4010-4016
Gabriel KR (1971) The biplot graphic display of matrices with application to principal component analysis. Biometrika **58:** 453-467
Gaff D (1996) Tobacco-plant desiccation tolerance. Nature **382:** 502-502
Gehlen J, Panstruga R, Smets H, Merkelbach S, Kleines M, Porsch P, Fladung M, Becker I, Rademacher T, Häusler RE, Hirsch H-J (1996) Effects of altered phosphoenolpyruvate carboxylase activities on transgenic C3 plant Solanum tuberosum. Plant Molecular Biology **32:** 831-848
Genty B, Briantais J-M, Baker NR (1989) The relationship between the quantum yield of photosynthetic electron transport and quenching of chlorophyll fluorescence. Biochimica et Biophysica Acta (BBA) - General Subjects **990:** 87-92
Ghillebert R, Swinnen E, Wen J, Vandesteene L, Ramon M, Norga K, Rolland F, Winderickx J (2011) The AMPK/SNF1/SnRK1 fuel gauge and energy regulator: structure, function and regulation. FEBS Journal**:** no-no
Gibon Y, Bläsing OE, Palacios-Rojas N, Pankovic D, Hendriks JHM, Fisahn J, Höhne M, Günther M, Stitt M (2004) Adjustment of diurnal starch turnover to short days: depletion of sugar during the night leads to a temporary inhibition of carbohydrate utilization, accumulation of sugars and post-translational activation of ADP-glucose pyrophosphorylase in the following light period. The Plant Journal **39:** 847-862
Gibon Y, Pyl E-T, Sulpice R, Lunn JE, HÖHne M, GÜNther M, Stitt M (2009) Adjustment of growth, starch turnover, protein content and central metabolism to a decrease of the carbon supply when Arabidopsis is grown in very short photoperiods. Plant, Cell & Environment **32:** 859-874
Glinski M, Weckwerth W (2005) Differential Multisite Phosphorylation of the Trehalose-6-phosphate Synthase Gene Family in Arabidopsis thaliana. Molecular & Cellular Proteomics **4:** 1614-1625
Goddijn O, Verwoerd TC, Voogd E, Krutwagen R, de Graff P, Poels J, van Dun K, Ponstein AS, Damm B, Pen J (1997) Inhibition of Trehalase Activity Enhances Trehalose Accumulation in Transgenic Plants. Plant Physiology **113:** 181-190
Gomez LD, Baud S, Graham IA (2005) The role of trehalose-6-phosphate synthase in Arabidopsis embryo development, Vol 33. Portland Press, Colchester, ROYAUME-UNI
Gómez LD, Gilday A, Feil R, Lunn JE, Graham IA (2010) AtTPS1-mediated trehalose 6-phosphate synthesis is essential for embryogenic and vegetative growth and responsiveness to ABA in germinating seeds and stomatal guard cells. The Plant Journal **64:** 1-13
Gonzalez, Nathalie, Bodt D, Stefanie, Sulpice, Ronan, Jikumaru, Yusuke, Chae, Eunyoung, Dhondt, Stijn, Daele V, Twiggy, Milde D, Liesbeth, Weigel, Detlef, Kamiya, Yuji, Stitt, Mark, Beemster, S. GT, Inze, Dirk (2010) Increased Leaf Size: Different Means to an End, Vol 153. American Society of Plant Biologists, Rockville, MD, ETATS-UNIS
Gonzali S, Alpi A, Blando F, De Bellis L (2002) Arabidopsis (HXK1 and HXK2) and yeast (HXK2) hexokinases overexpressed in transgenic lines are characterized by different catalytic properties. Plant Science **163:** 943-954
Gordon SP, Heisler MG, Reddy GV, Ohno C, Das P, Meyerowitz EM (2007) Pattern formation during de novo assembly of the Arabidopsis shoot meristem. Development **134:** 3539-3548
Gorsuch PA, Pandey S, Atkin OK (2010) Temporal heterogeneity of cold acclimation phenotypes in Arabidopsis leaves. Plant, Cell & Environment **33:** 244-258
Graf A, Schlereth A, Stitt M, Smith AM (2010) Circadian control of carbohydrate availability for growth in Arabidopsis plants at night. Proceedings of the National Academy of Sciences **107:** 9458-9463

Granier C, Massonnet C, Turc O, Muller B, Chenu K, Tardieu F (2002) Individual Leaf Development in Arabidopsis thaliana: a Stable Thermal ‐ time ‐ based Programme. Annals of Botany **89:** 595-604
Granier C, Tardieu F (1998) Is thermal time adequate for expressing the effects of temperature on sunflower leaf development? Plant, Cell & Environment **21:** 695-703
Granier C, Turc O, Tardieu F (2000) Co-Ordination of Cell Division and Tissue Expansion in Sunflower, Tobacco, and Pea Leaves: Dependence or Independence of Both Processes? Journal of Plant Growth Regulation **19:** 45-54
Gray GR, Chauvin LP, Sarhan F, Huner N (1997) Cold Acclimation and Freezing Tolerance (A Complex Interaction of Light and Temperature). Plant Physiology **114:** 467-474
Groemping U (2006) Relative Importance for Linear Regression in R: The Package relaimpo. Journal of Statistical Software **17**
Grömping U (2006) Relative Importance for Linear Regression in R: The Package relaimpo. Journal of Statistical Software **17:** 1-27
Guedes Corrêa LG (2009) Evolutionary and functional analysis of transcription factors controlling leaf development. Universitaet Potsdam, Potsdma
Guo F-Q, Young J, Crawford NM (2003) The Nitrate Transporter AtNRT1.1 (CHL1) Functions in Stomatal Opening and Contributes to Drought Susceptibility in Arabidopsis. The Plant Cell Online **15:** 107-117
Hall AE, Richards RA, Condon AG, Wright GC, Farquhar GD (2010) Carbon Isotope Discrimination and Plant Breeding. *In* Plant Breeding Reviews. John Wiley & Sons, Inc., pp 81-113
Hamant O, Heisler MG, Jönsson H, Krupinski P, Uyttewaal M, Bokov P, Corson F, Sahlin P, Boudaoud A, Meyerowitz EM, Couder Y, Traas J (2008) Developmental Patterning by Mechanical Signals in Arabidopsis. Science **322:** 1650-1655
Hanson KR (1990) Steady-state and oscillating photosynthesis by a starchless mutant of Nicotiana sylvestris, Vol 93. American Society of Plant Biologists, Rockville, MD, ETATS-UNIS
Hanstein SM, Felle HH (2002) CO2-triggered chloride release from guard cells in intact fava bean leaves. Kinetics of the onset of stomatal closure. Plant Physiology **130:** 940-950
Harberd NP, Belfield E, Yasumura Y (2009) The Angiosperm Gibberellin-GID1-DELLA Growth Regulatory Mechanism: How an "Inhibitor of an Inhibitor" Enables Flexible Response to Fluctuating Environments. The Plant Cell Online **21:** 1328-1339
Hashimoto M, Negi J, Young J, Israelsson M, Schroeder JI, Iba K (2006) Arabidopsis HT1 kinase controls stomatal movements in response to CO2. Nat Cell Biol **8:** 391-397
Hauck J, Mika K (2003) Review: Different types of ordering. Crystal Research and Technology **38:** 831-846
Häusler RE, Schlieben NH, Nicolay P, Fischer K, Fischer KL, Flügge U-I (2000) Control of carbon partitioning and photosynthesis by the triose phosphate/phosphate translocator in transgenic tobacco plants (<i>Nicotiana tabacum</i> L.). I. Comparative physiological analysis of tobacco plants with antisense repression and overexpression of the triose phosphate/phosphate translocator. Planta **210:** 371-382
Hausmann NJ, Juenger TE, Sen S, Stowe KA, Dawson TE, Simms EL (2005) QUANTITATIVE TRAIT LOCI AFFECTING δ13C AND RESPONSE TO DIFFERENTIAL WATER AVAILIBILITY IN ARABIDOPSIS THALLANA. Evolution **59:** 81-96
Hawker JS (1967) Inhibition of sucrose phosphatase by sucrose. Biochemical Journal **102:** 401-406
Hedrich R, Marten I (1993) Malate-induced feedback regulation of plasma membrane anion channels could provide a CO[2] sensor to guard cells, Vol 12. Nature Publishing Group, London, ROYAUME-UNI
Hedrich R, Neimanis S, Savchenko G, Felle HH, Kaiser WM, Heber U (2001) Changes in apoplastic pH and membrane potential in leaves in relation to stomatal responses to CO₂, malate, abscisic acid or interruption of water supply. Planta **213:** 594-601
Heisler MG, Ohno C, Das P, Sieber P, Reddy GV, Long JA, Meyerowitz EM (2005) Patterns of Auxin Transport and Gene Expression during Primordium Development Revealed by Live Imaging of the Arabidopsis Inflorescence Meristem. Current Biology **15:** 1899-1911

Hendrickson L, Furbank R, Chow W (2004) A Simple Alternative Approach to Assessing the Fate of Absorbed Light Energy Using Chlorophyll Fluorescence. Photosynthesis Research **82:** 73-81

Hendriks JHM, Kolbe A, Gibon Y, Stitt M, Geigenberger P (2003) ADP-Glucose Pyrophosphorylase Is Activated by Posttranslational Redox-Modification in Response to Light and to Sugars in Leaves of Arabidopsis and Other Plant Species. Plant Physiology **133:** 838-849

Heraut-Bron V, Robin C, Varlet-Grancher C, Afif D, Guckert A (1999) Light quality (red : far-red ratio): does it affect photosynthetic activity, net CO2 assimilation, and morphology of young white clover leaves? Canadian Journal of Botany-Revue Canadienne De Botanique **77:** 1425-1431

Hetherington AM, Woodward FI (2003) The role of stomata in sensing and driving environmental change. Nature **424:** 901-908

Hieber AD, Kawabata O, Yamamoto HY (2004) Significance of the Lipid Phase in the Dynamics and Functions of the Xanthophyll Cycle as Revealed by PsbS Overexpression in Tobacco and In-vitro De-epoxidation in Monogalactosyldiacylglycerol Micelles. Plant and Cell Physiology **45:** 92-102

Hoffmann WA, Poorter H (2002) Avoiding Bias in Calculations of Relative Growth Rate. Annals of Botany **90:** 37-42

Holm S (1979) A Simple Sequentially Rejective Multiple Test Procedure. Scandinavian Journal of Statistics **6:** 65-70

Holmstrom K-O, Mantyla E, Welin B, Mandal A, Palva ET, Tunnela OE, Londesborough J (1996) Drought tolerance in tobacco. Nature **379:** 683-684

Horiguchi G, Ferjani A, Fujikura U, Tsukaya H (2006) Coordination of cell proliferation and cell expansion in the control of leaf size in Arabidopsis thaliana. Journal of Plant Research **119:** 37-42

Horiguchi G, Fujikura U, Ferjani A, Ishikawa N, Tsukaya H (2006) Large-scale histological analysis of leaf mutants using two simple leaf observation methods: identification of novel genetic pathways governing the size and shape of leaves. The Plant Journal **48:** 638-644

Hruz T, Laule O, Szabo G, Wessendorp F, Bleuler S, Oertle L, Widmayer P, Gruissem W, Zimmermann P (2008) Genevestigator V3: A Reference Expression Database for the Meta-Analysis of Transcriptomes. Advances in Bioinformatics **2008**

Hu H, Boisson-Dernier A, Israelsson-Nordstrom M, Bohmer M, Xue S, Ries A, Godoski J, Kuhn JM, Schroeder JI (2010) Carbonic anhydrases are upstream regulators of CO2-controlled stomatal movements in guard cells. Nat Cell Biol **12:** 87-93

Huber PJ (1964) Robust estimation of a location parameter. Annals of Mathematical Statistics **35:** 73-101

Hubick K, Farquhar G (1989) Carbon isotope discrimination and the ratio of carbon gained to water lost in barley cultivars. Plant, Cell & Environment **12:** 795-804

Humble G, Raschke K (1971) Stomatal opening quantitatively related to potassium transport. Evidence from electron probe analysis. Plant Physiology **48**

Huner NPA, Oquist G, Sarhan F (1998) Energy balance and acclimation to light and cold. Trends in Plant Science **3:** 224-230

Hunt R (1982) Plant growth curves: The functional approach to plant growth analysis. Arnold, London

Huxley J (1932) Problems of relative growth. *In*. Dial Press, New York

Ingram J, Bartels D (1996) The Molecular Basis of Dehydration Tolerance in Plants. Annual Review of Plant Physiology and Plant Molecular Biology **47:** 377-403

Inzé D, De Veylder L (2006) Cell Cycle Regulation in Plant Development1. Annual review of genetics **40:** 77-105

Iordachescu M, Imai R (2008) Trehalose Biosynthesis in Response to Abiotic Stresses. Journal of Integrative Plant Biology **50:** 1223-1229

Irihimovitch V, Shapira M (2000) Glutathione Redox Potential Modulated by Reactive Oxygen Species Regulates Translation of Rubisco Large Subunit in the Chloroplast. Journal of Biological Chemistry **275:** 16289-16295

Jacquot J-P, Lopez-Jaramillo J, Miginiac-Maslow M, Lemaire S, Cherfils J, Chueca A, Lopez-Gorge J (1997) Cysteine-153 is required for redox regulation of pea chloroplast fructose-1,6-bisphosphatase. Febs Letters **401:** 143-147

Jang I-C, Oh S-J, Seo J-S, Choi W-B, Song SI, Kim CH, Kim YS, Seo H-S, Choi YD, Nahm BH, Kim J-K (2003) Expression of a Bifunctional Fusion of the Escherichia coli Genes for Trehalose-6-Phosphate Synthase and Trehalose-6-Phosphate Phosphatase in Transgenic Rice Plants Increases Trehalose Accumulation and Abiotic Stress Tolerance without Stunting Growth. Plant Physiology **131:** 516-524

Jiang C, Wright RJ, Woo SS, DelMonte TA, Paterson AH (2000) QTL analysis of leaf morphology in tetraploid Gossypium (cotton). TAG Theoretical and Applied Genetics **100:** 409-418

Johnson K, Lenhard M (2011) Genetic control of plant organ growth. New Phytologist **191:** 319-333

Jones D, Nguyen C, Finlay R (2009) Carbon flow in the rhizosphere: carbon trading at the soil–root interface. Plant and Soil **321:** 5-33

Kaiser H (1958) The varimax criterion for analytic rotation in factor analysis. Psychometrika **23:** 187-200

Kaplan D, Hagemann W (1991) The relationship of cell and organism in vascular plants. BioScience **41:** 693-703

Kaplan F, Kopka J, Haskell DW, Zhao W, Schiller KC, Gatzke N, Sung DY, Guy CL (2004) Exploring the Temperature-Stress Metabolome of Arabidopsis. Plant Physiology **136:** 4159-4168

Karaba A, Dixit S, Greco R, Aharoni A, Trijatmiko KR, Marsch-Martinez N, Krishnan A, Nataraja KN, Udayakumar M, Pereira A (2007) Improvement of water use efficiency in rice by expression of HARDY, an Arabidopsis drought and salt tolerance gene. Proceedings of the National Academy of Sciences **104:** 15270-15275

Karim S, Aronsson H, Ericson H, Pirhonen M, Leyman B, Welin B, Mäntylä E, Palva E, Van Dijck P, Holmström K-O (2007) Improved drought tolerance without undesired side effects in transgenic plants producing trehalose. Plant Molecular Biology **64:** 371-386

Kawade K, Horiguchi G, Tsukaya H (2010) Non-cell-autonomously coordinated organ size regulation in leaf development. Development **137:** 4221-4227

Kay R, Chan A, Daly M, McPherson J (1987) Duplication of CaMV 35S Promoter Sequences Creates a Strong Enhancer for Plant Genes. Science **236:** 1299-1302

Kim G-T, Yano S, Kozuka T, Tsukaya H (2005) Photomorphogenesis of leaves: shade-avoidance and differentiation of sun and shade leaves. Photochemical & Photobiological Sciences **4:** 770-774

Kim J, Mayfield SP (2002) The Active Site of the Thioredoxin-Like Domain of Chloroplast Protein Disulfide Isomerase, RB60, Catalyzes the Redox-Regulated Binding of Chloroplast Poly(A)-Binding Protein, RB47, to the 5′ Untranslated Region of psbA mRNA. Plant and Cell Physiology **43:** 1238-1243

Kinoshita T, Doi M, Suetsugu N, Kagawa T, Wada M, Shimazaki K-i (2001) phot1 and phot2 mediate blue light regulation of stomatal opening. Nature **414:** 656-660

Kirkby EA, Knight AH (1977) Influence of the level of nitrate nutrition on ion uptake and assimilation, organic Acid accumulation, and cation-anion balance in whole tomato plants. Plant Physiology **60:** 349-353

Kleiman D, Aarssen LW (2007) The leaf size/number trade-off in trees. Journal of Ecology **95:** 376-382

Koerner C, Diemer M (1987) In situ Photosynthetic Responses to Light, Temperature and Carbon Dioxide in Herbaceous Plants from Low and High Altitude. Functional Ecology **1:** 179-194

Kofler H, Häusler RE, Schulz B, Gröner F, Flügge UI, Weber A (2000) Molecular characterisation of a new mutant allele of the plastid phosphoglucomutase in <i>Arabidopsis</i> , and complementation of the mutant with the wild-type cDNA. Molecular and General Genetics MGG **263:** 978-986

Kojima H, Suzuki T, Kato T, Enomoto K-i, Sato S, Kato T, Tabata S, Sáez-Vasquez J, Echeverría M, Nakagawa T, Ishiguro S, Nakamura K (2007) Sugar-inducible expression of the nucleolin-1 gene of Arabidopsis thaliana and its role in ribosome synthesis, growth and development. The Plant Journal **49:** 1053-1063

Kolbe A, Tiessen A, Schluepmann H, Paul M, Ulrich S, Geigenberger P (2005) Trehalose 6-phosphate regulates starch synthesis via posttranslational redox activation of ADP-glucose

pyrophosphorylase. Proceedings of the National Academy of Sciences of the United States of America **102:** 11118-11123

Koornneef M, Hanhart C, van Loenen-Martinet P, Blankestijn de Vries H (1995) The effect of daylength on the transition to flowering in phytochrome-deficient, late-flowering and double mutants of Arabidopsis thaliana. Physiologia Plantarum **95:** 260-266

Koornneef M, Hanhart CJ, Veen JH (1991) A genetic and physiological analysis of late flowering mutants in <i>Arabidopsis thaliana</i&gt. Molecular and General Genetics MGG **229:** 57-66

Kozuka T, Horiguchi G, Kim GT, Ohgishi M, Sakai T, Tsukaya H (2005) The different growth responses of the Arabidopsis thaliana leaf blade and the petiole during shade avoidance are regulated by Photoreceptors and sugar. Plant and Cell Physiology **46:** 213-223

Kramer D, Johnson G, Kiirats O, Edwards G (2004) New Fluorescence Parameters for the Determination of Q_A Redox State and Excitation Energy Fluxes. Photosynthesis Research **79:** 209-218

Krickerberg AL, Neuhaus HE, Feil R, Gottlieb LD, Stitt M (1989) Decreased-activity mutants of phosphoglucose isomerase in the cytosol and chloroplast of Clarkia xantiana: impact on mass-action and fluxes to sucrose and starch, and estimation of flux control coefficients and elasticity coefficients, Vol 261. Biochemical society, London, ROYAUME-UNI

Lake JA, Quick WP, Beerling DJ, Woodward FI (2001) Plant development - Signals from mature to new leaves. Nature **411:** 154-154

Lamoreaux R, Chaney W, KM B (1978) The plastochron index: a review after two decades of use. American Journal of Botany **65:** 586-593

Laporte MM, Shen B, Tarczynski MC (2002) Engineering for drought avoidance: expression of maize NADP‐malic enzyme in tobacco results in altered stomatal function. Journal of Experimental Botany **53:** 699-705

Lasceve G, Leymarie J, Vavasseur A (1997) Alterations in light-induced stomatal opening in a starch-deficient mutant of Arabidopsis thaliana L. deficient in chloroplast phosphoglucomutase activity. Plant, Cell & Environment **20:** 350-358

Latorre R, Olcese R, Basso C, Gonzalez C, Muñoz F, Cosmelli D, Alvarez O (2003) Molecular Coupling between Voltage Sensor and Pore Opening in the Arabidopsis Inward Rectifier K+ Channel KAT1. The Journal of General Physiology **122:** 459-469

Lau JA, Shaw RG, Reich PB, Shaw FH, Tiffin P (2007) Strong ecological but weak evolutionary effects of elevated CO2 on a recombinant inbred population of Arabidopsis thaliana. New Phytologist **175:** 351-362

Lee M, Choi Y, Burla B, Kim Y-Y, Jeon B, Maeshima M, Yoo J-Y, Martinoia E, Lee Y (2008) The ABC transporter AtABCB14 is a malate importer and modulates stomatal response to CO2. Nat Cell Biol **10:** 1217-1223

Lee Y, Lee D, Lim J, Yoon J, Bhoo S, Jeon J, Hahn T (2006) Carbon-partitioning in Arabidopsis is regulated by the fructose 6-phosphate, 2-kinase/fructose 2,6-bisphosphatase enzyme. Journal of Plant Biology **49:** 70-79

Leegood RC, Furbank RT (1986) Stimulation of photosynthesis by 2% oxygen at low temperatures is restored by phosphate. Planta **168:** 84-93

Leiber R-M, John F, Verhertbruggen Y, Diet A, Knox JP, Ringli C (2010) The TOR Pathway Modulates the Structure of Cell Walls in Arabidopsis. The Plant Cell Online **22:** 1898-1908

Leonhardt N, Kwak JM, Robert N, Waner D, Leonhardt G, Schroeder JI (2004) Microarray Expression Analyses of Arabidopsis Guard Cells and Isolation of a Recessive Abscisic Acid Hypersensitive Protein Phosphatase 2C Mutant. The Plant Cell Online **16:** 596-615

Leyman B, Van Dijck P, Thevelein JM (2001) An unexpected plethora of trehalose biosynthesis genes in Arabidopsis thaliana. Trends in Plant Science **6:** 510-513

Li B, Suzuki J-I, Hara T (1998) Latitudinal variation in plant size and relative growth rate in <i>Arabidopsis thaliana</i&gt. Oecologia **115:** 293-301

Li C, Potuschak T, Colón-Carmona A, Gutiérrez RA, Doerner P (2005) Arabidopsis TCP20 links regulation of growth and cell division control pathways. Proceedings of the National Academy of Sciences of the United States of America **102:** 12978-12983

Li P, Ma S, Bohnert HJ (2008) Coexpression characteristics of trehalose-6-phosphate phosphatase subfamily genes reveal different functions in a network context. Physiologia Plantarum **133:** 544-556

Li S, Assmann SM, Albert R (2006) Predicting Essential Components of Signal Transduction Networks: A Dynamic Model of Guard Cell Abscisic Acid Signaling. PLoS Biol **4:** e312
Li X-P, Gilmore AM, Caffarri S, Bassi R, Golan T, Kramer D, Niyogi KK (2004) Regulation of Photosynthetic Light Harvesting Involves Intrathylakoid Lumen pH Sensing by the PsbS Protein. Journal of Biological Chemistry **279:** 22866-22874
Li X-P, Müller-Moulé P, Gilmore AM, Niyogi KK (2002) PsbS-dependent enhancement of feedback de-excitation protects photosystem II from photoinhibition. Proceedings of the National Academy of Sciences **99:** 15222-15227
Lichtenthaler H, Buschmann C, Döll M, Fietz HJ, Bach T, Kozel U, Meier D, Rahmsdorf U (1981) Photosynthetic activity, chloroplast ultrastructure, and leaf characteristics of high-light and low-light plants and of sun and shade leaves. Photosynthesis Research **2:** 115-141
Lopez-Juez E, Bowyer JR, Sakai T (2007) Distinct leaf developmental and gene expression responses to light quantity depend on blue-photoreceptor or plastid-derived signals, and can occur in the absence of phototropins. Planta **227:** 113-123
López-Juez E, Paul Jarvis R, Takeuchi A, Page AM, Chory J (1998) New Arabidopsis cue Mutants Suggest a Close Connection between Plastid- and Phytochrome Regulation of Nuclear Gene Expression. Plant Physiology **118:** 803-815
Loveys BR, Scheurwater I, Pons TL, Fitter AH, Atkin OK (2002) Growth temperature influences the underlying components of relative growth rate: an investigation using inherently fast- and slow-growing plant species. Plant, Cell & Environment **25:** 975-988
Lu P, Outlaw Jr WH, Smith BG, Freed GA (1997) A New Mechanism for the Regulation of Stomatal Aperture Size in Intact Leaves (Accumulation of Mesophyll-Derived Sucrose in the Guard-Cell Wall of Vicia faba). Plant Physiology **114:** 109-118
Lu P, Zhang SQ, Outlaw WH, Riddle KA (1995) Sucrose: a solute that accumulates in the guard-cell apoplast and guard-cell symplast of open stomata. Febs Letters **362:** 180-184
Lu Y, Gehan JP, Sharkey TD (2005) Daylength and Circadian Effects on Starch Degradation and Maltose Metabolism. Plant Physiology **138:** 2280-2291
Lunn JE (2007) Gene families and evolution of trehalose metabolism in plants. Functional Plant Biology **34:** 550-563
Lunn JE, Ap Rees T (1990) Purification and properties of sucrose-phosphate synthase from seeds of Pisum sativum. Phytochemistry **29:** 1057-1063
Lunn JE, Ashton AR, Hatch MD, Heldt HW (2000) Purification, molecular cloning, and sequence analysis of sucrose-6F-phosphate phosphohydrolase from plants. Proceedings of the National Academy of Sciences **97:** 12914-12919
Lunn JE, Feil R, Hendriks JHM, Gibon Y, Morcuende R, Osuna D, Scheible WR, Carillo P, Hajirezaei MR, Stitt M (2006) Sugar-induced increases in trehalose 6-phosphate are correlated with redox activation of ADPglucose pyrophosphorylase and higher rates of starch synthesis in Arabidopsis thaliana. Biochemical Journal **397:** 139-148
Lunn JE, MacRae E (2003) New complexities in the synthesis of sucrose. Current Opinion in Plant Biology **6:** 208-214
Lytovchenko A, Bieberich K, Willmitzer L, Fernie A (2002) Carbon assimilation and metabolism in potato leaves deficient in plastidial phosphoglucomutase. Planta **215:** 802-811
Ma Y-Z, Holt NE, Li X-P, Niyogi KK, Fleming GR (2003) Evidence for direct carotenoid involvement in the regulation of photosynthetic light harvesting. Proceedings of the National Academy of Sciences **100:** 4377-4382
Marcotrigiano M (2010) A role for leaf epidermis in the control of leaf size and the rate and extent of mesophyll cell division. American Journal of Botany **97:** 224-233
Martins M (2011) What are the downstream targets of trehalose-6-phosphate in plants ? Universitaet Potsdam, Potsdam
Masle J, Gilmore SR, Farquhar GD (2005) The ERECTA gene regulates plant transpiration efficiency in Arabidopsis. Nature **436:** 866-870
Maxwell DP, Laudenbach DE, Huner N (1995) Redox Regulation of Light-Harvesting Complex II and cab mRNA Abundance in Dunaliella salina. Plant Physiology **109:** 787-795
McLaren JS, Smith H (1978) Phytochrome control of the growth and development of Rumex obtusifolius under simulated canopy light environments*. Plant, Cell & Environment **1:** 61-67
McWatters HG, Devlin PF (2011) Timing in plants - A rhythmic arrangement. Febs Letters **585:** 1474-1484

Melzer E, O'Leary MH (1987) Anapleurotic CO[2] fixation by phosphoenolpyruvate carboxylase in C[3] plants, Vol 84. American Society of Plant Biologists, Rockville, MD, ETATS-UNIS
Méndez-Vigo B, de Andrés MT, Ramiro M, Martínez-Zapater JM, Alonso-Blanco C (2010) Temporal analysis of natural variation for the rate of leaf production and its relationship with flowering initiation in Arabidopsis thaliana. Journal of Experimental Botany **61:** 1611-1623
Messinger SM, Buckley TN, Mott KA (2006) Evidence for Involvement of Photosynthetic Processes in the Stomatal Response to CO2. Plant Physiology **140:** 771-778
Micol JL (2009) Leaf development: time to turn over a new leaf? Current Opinion in Plant Biology **12:** 9-16
Milla R, Reich PB (2007) The scaling of leaf area and mass: the cost of light interception increases with leaf size. Proceedings of the Royal Society B: Biological Sciences **274:** 2109-2115
Miranda J, Avonce N, Suárez R, Thevelein J, Van Dijck P, Iturriaga G (2007) A bifunctional TPS–TPP enzyme from yeast confers tolerance to multiple and extreme abiotic-stress conditions in transgenic <i>Arabidopsis</i&gt. Planta **226:** 1411-1421
Miyazawa SI, Makino A, Terashima I (2003) Changes in mesophyll anatomy and sink–source relationships during leaf development in Quercus glauca, an evergreen tree showing delayed leaf greening. Plant, Cell & Environment **26:** 745-755
Mizukami Y, Fischer RL (2000) Plant organ size control: AINTEGUMENTA regulates growth and cell numbers during organogenesis. Proceedings of the National Academy of Sciences **97:** 942-947
Montané M-H, Tardy F, Kloppstech K, Havaux M (1998) Differential Control of Xanthophylls and Light-Induced Stress Proteins, as Opposed to Light-Harvesting Chlorophyll a/bProteins, during Photosynthetic Acclimation of Barley Leaves to Light Irradiance. Plant Physiology **118:** 227-235
Moore B, Zhou L, Rolland F, Hall Q, Cheng W-H, Liu Y-X, Hwang I, Jones T, Sheen J (2003) Role of the Arabidopsis Glucose Sensor HXK1 in Nutrient, Light, and Hormonal Signaling. Science **300:** 332-336
Morcuende R, Pérez P, Martínez-Carrasco R (1997) Short-term feedback inhibition of photosynthesis in wheat leaves supplied with sucrose and glycerol at two temperatures. Photosynthetica **33:** 179-188
Mott KA, Michaelson O (1991) Amphistomy as an adaptation to high light intensity in Ambrosia cordifolia (compositae), Vol 78. Botanical Society of America, Ithaca, NY, ETATS-UNIS
Mullineaux P, Rausch T (2005) Glutathione, photosynthesis and the redox regulation of stress-responsive gene expression. Photosynthesis Research **86:** 459-474
Munekage Y, Hojo M, Meurer J, Endo T, Tasaka M, Shikanai T (2002) PGR5 Is Involved in Cyclic Electron Flow around Photosystem I and Is Essential for Photoprotection in Arabidopsis. Cell **110:** 361-371
Mustilli A-C, Merlot S, Vavasseur A, Fenzi F, Giraudat J (2002) Arabidopsis OST1 Protein Kinase Mediates the Regulation of Stomatal Aperture by Abscisic Acid and Acts Upstream of Reactive Oxygen Species Production. The Plant Cell Online **14:** 3089-3099
Nagel OW, Lambers H (2002) Changes in the acquisition and partitioning of carbon and nitrogen in the gibberellin-deficient mutants A70 and W335 of tomato (Solanum lycopersicum L.). Plant, Cell & Environment **25:** 883-891
Nakaya M, Tsukaya H, Murakami N, Kato M (2002) Brassinosteroids Control the Proliferation of Leaf Cells of Arabidopsis thaliana. Plant and Cell Physiology **43:** 239-244
Narang RA, Bruene A, Altmann T (2000) Analysis of Phosphate Acquisition Efficiency in Different Arabidopsis Accessions. Plant Physiology **124:** 1786-1799
Negi J, Matsuda O, Nagasawa T, Oba Y, Takahashi H, Kawai-Yamada M, Uchimiya H, Hashimoto M, Iba K (2008) CO2 regulator SLAC1 and its homologues are essential for anion homeostasis in plant cells. Nature **452:** 483-486
Niinemets Ü, Díaz-Espejo A, Flexas J, Galmés J, Warren CR (2009) Importance of mesophyll diffusion conductance in estimation of plant photosynthesis in the field. Journal of Experimental Botany **60:** 2271-2282
Niinemets Ü, Díaz-Espejo A, Flexas J, Galmés J, Warren CR (2009) Role of mesophyll diffusion conductance in constraining potential photosynthetic productivity in the field. Journal of Experimental Botany **60:** 2249-2270

Niinemets Ü, Portsmuth A, Tena D, Tobias M, Matesanz S, Valladares F (2007) Do we Underestimate the Importance of Leaf Size in Plant Economics? Disproportional Scaling of Support Costs Within the Spectrum of Leaf Physiognomy. Annals of Botany **100:** 283-303
Niklas KJ (1994) Plant allometry: The scaling of form and process. University of Chicago Press, Chicago
Niklas KJ (2004) Plant allometry: is there a grand unifying theory? Biological Reviews **79:** 871-889
Nordhausen M (1903) Über Sonnen- und Schattenblätter. Berichte der Deutschen Botanischen Gesellschaft **XXI:** 30-45
O'Leary MH (1981) Carbon isotope fractionation in plants. Phytochemistry **20:** 553-567
O'Leary MH (1982) Phosphoenolpyruvate Carboxylase: An Enzymologist's View. Annual Review of Plant Physiology **33:** 297-315
Ogawa K (2008) The leaf mass/number trade-off of Kleiman and Aarssen implies constancy of leaf biomass, its density and carbon uptake in forest stands: scaling up from shoot to stand level. Journal of Ecology **96:** 188-191
Ögren E, Evans JR (1993) Photosynthetic light-response curves. Planta **189:** 182-190
Oguchi R, Hikosaka K, Hirose T (2003) Does the photosynthetic light-acclimation need change in leaf anatomy? Plant Cell and Environment **26:** 505-512
Ohto M-a, Onai K, Furukawa Y, Aoki E, Araki T, Nakamura K (2001) Effects of Sugar on Vegetative Development and Floral Transition in Arabidopsis. Plant Physiology **127:** 252-261
Okushima Y, Mitina I, Quach HL, Theologis A (2005) AUXIN RESPONSE FACTOR 2 (ARF2): a pleiotropic developmental regulator. The Plant Journal **43:** 29-46
Olsen RL, Pratt RB, Gump P, Kemper A, Tallman G (2002) Red light activates a chloroplast-dependent ion uptake mechanism for stomatal opening under reduced CO2 concentrations in Vicia spp. New Phytologist **153:** 497-508
Oster U, Brunner H, Rüdiger W (1996) The greening process in cress seedlings. V. Possible interference of chlorophyll precursors, accumulated after thujaplicin treatment, with light-regulated expression of Lhc genes. Journal of Photochemistry and Photobiology B: Biology **36:** 255-261
Osuna D, Usadel B, Morcuende R, Gibon Y, Blasing OE, Hohne M, Gunter M, Kamlage B, Trethewey R, Scheible WR, Stitt M (2007) Temporal responses of transcripts, enzyme activities and metabolites after adding sucrose to carbon-deprived Arabidopsis seedlings. Plant Journal **49:** 463-491
Oswald O, Martin T, Dominy PJ, Graham IA (2001) Plastid redox state and sugars: Interactive regulators of nuclear-encoded photosynthetic gene expression. Proceedings of the National Academy of Sciences **98:** 2047-2052
Outlaw W (2003) Integration of cellular and physiological functions of guard cells. Critical Reviews in Plant Sciences **22:** 503-529
Outlaw W, Manchester J (1979) Guard Cell Starch Concentration Quantitatively Related to Stomatal Aperture. Plant Physiology **64:** 79-82
Outlaw WH, De Vlieghere-He X (2001) Transpiration Rate. An Important Factor Controlling the Sucrose Content of the Guard Cell Apoplast of Broad Bean. Plant Physiology **126:** 1716-1724
Outlaw WH, Du Z, Xia Meng F, Aghoram K, Riddle KA, Chollet R (2002) Requirements for activation of the signal-transduction network that leads to regulatory phosphorylation of leaf guard-cell phosphoenolpyruvate carboxylase during fusicoccin-stimulated stomatal opening. Archives of Biochemistry and Biophysics **407:** 63-71
Outlaw WH, Lowry OH (1977) Organic acid and potassium accumulation in guard cells during stomatal opening. Proceedings of the National Academy of Sciences **74:** 4434-4438
Palatnik JF, Allen E, Wu X, Schommer C, Schwab R, Carrington JC, Weigel D (2003) Control of leaf morphogenesis by microRNAs. Nature **425:** 257-263
Pandey S, Wang X-Q, Coursol SA, Assmann SM (2002) Preparation and applications of Arabidopsis thaliana guard cell protoplasts. New Phytologist **153:** 517-526
Paul M (2007) Trehallose 6-phosphate. Current Opinion in Plant Biology **10:** 303-309
Paul M, Pellny T, Goddijn O (2001) Enhancing photosynthesis with sugar signals. Trends in Plant Science **6:** 197-200
Paul MJ, Jhurreea D, Zhang Y, Primavesi LF, Delatte T, Schluepmann H, Wingler A (2010) Up-regulation of biosynthetic processes associated with growth by trehalose 6-phosphate. Plant Signaling & Behavior **5:** 386-392

Pearson CK, Wilson SB, Schaffer R, Ross AW (1993) NAD turnover and utilisation of metabolites for RNA synthesis in a reaction sensing the redox state of the cytochrome b6f complex in isolated chloroplasts. European Journal of Biochemistry **218:** 397-404

Pellny TK, Ghannoum O, Conroy JP, Schluepmann H, Smeekens S, Andralojc J, Krause KP, Goddijn O, Paul MJ (2004) Genetic modification of photosynthesis with E. coli genes for trehalose synthesis. Plant Biotechnology Journal **2:** 71-82

Peterson RB, Hanson KR (1991) Changes in photochemical and fluorescence yields in leaf tissue from normal and starchless Nicotiana sylvestris with increasing irradiance. Plant Science **76:** 143-151

Pfaffl MW, Horgan GW, Dempfle L (2002) Relative expression software tool (REST©) for group-wise comparison and statistical analysis of relative expression results in real-time PCR. Nucleic Acids Research **30:** e36

Pfannschmidt T (2003) Chloroplast redox signals: how photosynthesis controls its own genes. Trends in Plant Science **8:** 33-41

Pfannschmidt T, Nilsson A, Allen JF (1999) Photosynthetic control of chloroplast gene expression. Nature **397:** 625-628

Pien S, Wyrzykowska J, Fleming AJ (2001) Novel marker genes for early leaf development indicate spatial regulation of carbohydrate metabolism within the apical meristem. The Plant Journal **25:** 663-674

Pien S, Wyrzykowska J, McQueen-Mason S, Smart C, Fleming A (2001) Local expression of expansin induces the entire process of leaf development and modifies leaf shape. Proceedings of the National Academy of Sciences **98:** 11812-11817

Pigliucci M, Kolodynska A (2002) Phenotypic plasticity to light intensity in *Arabidopsis thaliana*: invariance of reaction norms and phenotypic integration. Evolutionary Ecology **16:** 27-47

Pilon-Smits EAH, Terry N, Sears T, Hyeong K, Zayed A, Seongbin H, Van Dun K, Voogd E, Verwoerd TC, Krutwagen RWHH, Goddijn OJM (1998) Trehalose-producing transgenic tobacco plants show improved growth performance under drought stress, Vol 152. Elsevier, Munich, ALLEMAGNE

Piques M, Schulze WX, Hohne M, Usadel B, Gibon Y, Rohwer J, Stitt M (2009) Ribosome and transcript copy numbers, polysome occupancy and enzyme dynamics in Arabidopsis. Mol Syst Biol **5**

Poethig RS (2003) Phase Change and the Regulation of Developmental Timing in Plants. Science **301:** 334-336

Poethig RS (2009) Small RNAs and developmental timing in plants. Current Opinion in Genetics & Development **19:** 374-378

Poffenroth M, Green DB, Tallman G (1992) Sugar concentrations in guard cells of Vicia faba illuminated with red or blue light : analysis by high performance liquid chromatography, Vol 98. American Society of Plant Biologists, Rockville, MD, ETATS-UNIS

Poorter H (1994) Construction costs and payback time of biomass: a whole plant perspective. *In* JG Roy, E, ed, A Whole Plant Perspective on Carbon-Nitrogen Interactions. SPB Academic Publishing, The Hague, pp 111-127

Poorter H, Garnier E (1996) Plant growth analysis: an evaluation of experimental design and computational methods. Journal of Experimental Botany **47:** 1343-1351

Poorter H, Nagel O (2000) The role of biomass allocation in the growth response of plants to different levels of light, CO_2, nutrients and water: a quantitative review. Functional Plant Biology **27:** 1191-1191

Poorter H, Niinemets Ü, Poorter L, Wright IJ, Villar R (2009) Causes and consequences of variation in leaf mass per area (LMA): a meta-analysis. New Phytologist **182:** 565-588

Poorter H, Remkes C (1990) Leaf area ratio and net assimilation rate of 24 wild species differing in relative growth rate. Oecologia **83:** 553-559

Poorter H, Remkes C, Lambers H (1990) Carbon and Nitrogen Economy of 24 Wild Species Differing in Relative Growth Rate. Plant Physiology **94:** 621-627

Poorter H, Rijn C, Vanhala T, Verhoeven K, Jong Y, Stam P, Lambers H (2005) A genetic analysis of relative growth rate and underlying components in Hordeum spontaneum. Oecologia **142:** 360-377

Poorter H, van de Vijver C, Boot R, Lambers H (1995) Growth and carbon economy of a fast-growing and a slow-growing grass species as dependent on nitrate supply. Plant and Soil **171:** 217-227

Poorter H, van der Werf A (1998) Is inherent variation in RGR determined by LAR at low irradiance and by NAR at high irradiance? A review of herbaceous species. *In* H Lambers, H Poorter, M Van Vuuren, eds, Inherent variation in plant growth. Physiological mechanisms and ecological consequences. Backhuys Publishers, Leiden

Porter MA, Stringer CD, Hartman FC (1988) Characterization of the regulatory thioredoxin site of phosphoribulokinase. Journal of Biological Chemistry **263:** 123-129

Pouteau S, Ferret V, Gaudin V, Lefebvre D, Sabar M, Zhao G, Prunus F (2004) Extensive Phenotypic Variation in Early Flowering Mutants of Arabidopsis. Plant Physiology **135:** 201-211

Radoglou KM, Jarvis PG (1990) Effects of CO2 Enrichment on Four Poplar Clones. I. Growth and Leaf Anatomy. Annals of Botany **65:** 617-626

Raines C, Paul M (2006) Products of leaf primary carbon metabolism modulate the developmental programme determining plant morphology. J. Exp. Bot. **57:** 1857-1862

Ramon M, De Smet I, Vandesteene L, Naudts M, Leyman B, Van Dijck P, Rolland F, Beeckman T, Thevelein JM (2009) Extensive expression regulation and lack of heterologous enzymatic activity of the Class II trehalose metabolism proteins from Arabidopsis thaliana. Plant Cell and Environment **32:** 1015-1032

Raschke K (1987) Action of Abscisic Acid on Guard Cells. *In* E Zeiger, G Farquhar, I Cowan, eds, Stomatal Function. Stanford University Press, Stanford, pp 253-281

Raschke K, Schnabl H (1978) Availability of chloride affects the balance between potassium chloride and potassium malate in guard cells of Vicia faba L. Journal Name: Plant Physiol.; (United States); Journal Volume: 62**:** Medium: X; Size: Pages: 84-87

Raschke K, Schnabl H (1978) Availability of chloride affects the balance between potassium chloride and potassium malate in guard cells of *Vicia faba* L. Plant Physiology **62:** 84-87

Rasse DP, Tocquin P (2006) Leaf carbohydrate controls over Arabidopsis growth and response to elevated CO2: an experimentally based model. New Phytologist **172:** 500-513

Reckmann U, Scheibe R, Raschke K (1990) Rubisco Activity in Guard Cells Compared with the Solute Requirement for Stomatal Opening. Plant Physiology **92:** 246-253

Reddy GV, Heisler MG, Ehrhardt DW, Meyerowitz EM (2004) Real-time lineage analysis reveals oriented cell divisions associated with morphogenesis at the shoot apex of Arabidopsis thaliana. Development **131:** 4225-4237

Rees M, Osborne Colin P, Woodward FI, Hulme Stephen P, Turnbull Lindsay A, Taylor Samuel H (2010) Partitioning the Components of Relative Growth Rate: How Important Is Plant Size Variation? The American Naturalist **176:** E152-E161

Reich PB, Tjoelker MG, Walters MB, Vanderklein DW, Buschena C (1998) Close association of RGR, leaf and root morphology, seed mass and shade tolerance in seedlings of nine boreal tree species grown in high and low light. Functional Ecology **12:** 327-338

Reich PB, Walters MB, Ellsworth DS (1997) From tropics to tundra: Global convergence in plant functioning. Proceedings of the National Academy of Sciences **94:** 13730-13734

Reinhardt D, Pesce E-R, Stieger P, Mandel T, Baltensperger K, Bennett M, Traas J, Friml J, Kuhlemeier C (2003) Regulation of phyllotaxis by polar auxin transport. Nature **426:** 255-260

Ren M, Qiu S, Venglat P, Xiang D, Feng L, Selvaraj G, Datla R (2011) Target of Rapamycin Regulates Development and Ribosomal RNA Expression through Kinase Domain in Arabidopsis. Plant Physiology **155:** 1367-1382

Renton M, Poorter H (2011) Using log–log scaling slope analysis for determining the contributions to variability in biological variables such as leaf mass per area: why it works, when it works and how it can be extended. New Phytologist **190:** 5-8

Reymond M, Svistoonoff S, Loudet O, Nussaume L, Desnos T (2006) Identification of QTL controlling root growth response to phosphate starvation in Arabidopsis thaliana. Plant, Cell & Environment **29:** 115-125

Richard C, Lescot M, Inzé D, De Veylder L (2002) Effect of auxin, cytokinin, and sucrose on cell cycle gene expression in *Arabidopsis thaliana* cell suspension cultures. Plant Cell, Tissue and Organ Culture **69:** 167-176

Ridley JN (1982) Packing efficiency in sunflower heads. Mathematical Biosciences **58:** 129-139
Riou-Khamlichi C, Huntley R, Jacqmard A, Murray JAH (1999) Cytokinin Activation of Arabidopsis Cell Division Through a D-Type Cyclin. Science **283:** 1541-1544
Ritte G, Rosenfeld J, Rohrig K, Raschke K (1999) Rates of Sugar Uptake by Guard Cell Protoplasts of Pisum sativum L. Related to the Solute Requirement for Stomatal Opening. Plant Physiology **121:** 647-656
Roderick ML, Berry SL, Noble IR, Farquhar GD (1999) A theoretical approach to linking the composition and morphology with the function of leaves. Functional Ecology **13:** 683-695
Rodermel S (2001) Pathways of plastid-to-nucleus signaling. Trends in Plant Science **6:** 471-478
Roelfsema MRG, Hanstein S, Felle HH, Hedrich R (2002) CO2 provides an intermediate link in the red light response of guard cells. The Plant Journal **32:** 65-75
Roeske CA, O'Leary MH (1984) Carbon isotope effects on enzyme-catalyzed carboxylation of ribulose bisphosphate. Biochemistry **23:** 6275-6284
Romero C, Bellés J, Vayá J, Serrano R, Culiáñez-Macià F (1997) Expression of the yeast trehalose-6-phosphate synthase gene in transgenic tobacco plants: pleiotropic phenotypes include drought tolerance. Planta **201:** 293-297
Rook F, Gerrits N, Kortstee A, Van Kampen M, Borrias M, Weisbeek P, Smeekens S (1998) Sucrose-specific signalling represses translation of the Arabidopsis ATB2 bZIP transcription factor gene. The Plant Journal **15:** 253-263
Rose KE, Atkinson RL, Turnbull LA, Rees M (2009) The costs and benefits of fast living. Ecology Letters **12:** 1379-1384
Ryan P, Delhaize E, Jones D (2001) Function and mechanism of organic anion exudation from plant roots. Annual Review of Plant Physiology and Plant Molecular Biology **52:** 527-560
Sage HF (1990) A model describing the regulation of ribulose-1,5-bisphospate carboxylase, electron transport, and triose phosphate use in respone to light intensity and CO[2] in C[3] plants, Vol 94. American Society of Plant Biologists, Rockville, MD, ETATS-UNIS
Sajitz-Hermstein M, Nikoloski Z (2010) A novel approach for determining environment-specific protein costs: the case of Arabidopsis thaliana. Bioinformatics **26:** i582-i588
Satoh-Nagasawa N, Nagasawa N, Malcomber S, Sakai H, Jackson D (2006) A trehalose metabolic enzyme controls inflorescence architecture in maize. Nature **441:** 227-230
Savitch LV, Maxwell DP, Huner N (1996) Photosystem II Excitation Pressure and Photosynthetic Carbon Metabolism in Chlorella vulgaris. Plant Physiology **111:** 127-136
Scheibe R (1990) Light/dark modulation: regulation of chloroplast metabolism in a new light, Vol 103. Thieme, Stuttgart, ALLEMAGNE
Schluepmann H, Pellny T, van Dijken A, Smeekens S, Paul M (2003) Trehalose 6-phosphate is indispensable for carbohydrate utilization and growth in Arabidopsis thaliana. Proceedings of the National Academy of Sciences of the United States of America **100:** 6849-6854
Schmidt H-L (2003) Fundamentals and systematics of the non-statistical distributions of isotopes in natural compounds. Naturwissenschaften **90:** 537-552
Schroeder JI, Allen GJ, Hugouvieux V, Kwak JM, Waner D (2001) Guard Cell Signal Transduction. Annual Review of Plant Physiology and Plant Molecular Biology **52:** 627-658
Seo HS, Koo YJ, Lim JY, Song JT, Kim CH, Kim JK, Lee JS, Choi YD (2000) Characterization of a Bifunctional Enzyme Fusion of Trehalose-6-Phosphate Synthetase and Trehalose-6-Phosphate Phosphatase of Escherichia coli. Appl. Environ. Microbiol. **66:** 2484-2490
Sharkey TD, Stitt M, Heineke D, Gerhardt R, Raschke K, Heldt HW (1986) Limitation of photosynthesis by carbon metabolism. II: O[2]-insensitive CO[2] uptake results from limitation of triose phosphate utilization, Vol 81. American Society of Plant Biologists, Rockville, MD, ETATS-UNIS
Sharkey TD, Vanderveer PJ (1989) Stromal phosphate concentration is low during feedback limited photosynthesis, Vol 91. American Society of Plant Biologists, Rockville, MD, ETATS-UNIS
Sharpe P, Wu H, Spence R (1987) Stomatal Mechanics. *In* E Zeiger, G Farquhar, I Cowan, eds, Stomatal Function. Stanford University Press, Stanford, pp 91-115
Shimazaki K-I, Zeiger E (1985) Cyclic and noncyclic photophosphorylation in isolated guard cell chloroplasts from Vicia faba L, Vol 78. American Society of Plant Biologists, Rockville, MD, ETATS-UNIS
Shipley B (2006) Net assimilation rate, specific leaf area and leaf mass ratio: which is most closely correlated with relative growth rate? A meta-analysis. Functional Ecology **20:** 565-574

Shipley B, Lechowicz MJ, Wright I, Reich PB (2006) Fundamental Trade-Offs Generating The Worldwide Leaf Economics Spectrum. Ecology **87:** 535-541
Sidak Z (1967) Rectangular Confidence Regions for the Means of Multivariate Normal Distributions. Journal of the American Statistical Association **62:** 626-633
Sivak MN, Walker DA (1986) Photosynthesis in vivo can be limited by phosphate supply, Vol 102. Blackwell, Oxford, ROYAUME-UNI
Smart LB, Nall NM, Bennett AB (1999) Isolation of RNA and Protein from Guard Cells of Nicotiana glauca. Plant Molecular Biology Reporter **17:** 371-383
Smeekens S, Ma J, Hanson J, Rolland F (2010) Sugar signals and molecular networks controlling plant growth. Current Opinion in Plant Biology **13:** 273-278
Smith AM, Stitt M (2007) Coordination of carbon supply and plant growth. Plant, Cell & Environment **30:** 1126-1149
Sparla F, Costa A, Lo Schiavo F, Pupillo P, Trost P (2006) Redox Regulation of a Novel Plastid-Targeted β-Amylase of Arabidopsis. Plant Physiology **141:** 840-850
Speer M, Kaiser WM (1991) Ion relations of symplastic and apoplastic space in leaves from Spinacia oleracea L. and Pisum sativum L. under salinity, Vol 97. American Society of Plant Biologists, Rockville, MD, ETATS-UNIS
Stahl I (1880) Über dem Einfluss der Lichtintensität auf Struktur und Anordnung des Assimilationsparenchyms. Botanische Zeitung **51**
Steer BT, Hocking PJ (1983) Leaf and Floret Production in Sunflower (Helianthus annuus L.) as Affected by Nitrogen Supply. Annals of Botany **52:** 267-277
Stewart GR, Gracia CA, Hegarty EE, Specht RL (1990) Nitrate reductase activity and chlorophyll content in sun leaves of subtropical Australian closed-forest (rainforest) and open-forest communities. Oecologia **82:** 544-551
Stiller I, Dulai S, Kodrak M, Tarnai R, Szabo L, Toldi O, Banfalvi Z (2008) Effects of drought on water content and photosynthetic parameters in potato plants expressing the trehalose-6-phosphate synthase gene of Saccharomyces cerevisiae. Planta **227:** 299-308
Stitt M (1990) Fructose-2,6-Bisphosphate as a Regulatory Molecule in Plants. Annual Review of Plant Physiology and Plant Molecular Biology **41:** 153-185
Stitt M, Gibon Y, Lunn JE, Piques M (2007) Multilevel genomics analysis of carbon signalling during low carbon availability: coordinating the supply and utilisation of carbon in a fluctuating environment. Functional Plant Biology **34:** 526-549
Stitt M, Hurry V (2002) A plant for all seasons: alterations in photosynthetic carbon metabolism during cold acclimation in Arabidopsis. Current Opinion in Plant Biology **5:** 199-206
Stitt M, Lilley RM, Gerhardt R, Heldt HW (1989) [32] Metabolite levels in specific cells and subcellular compartments of plant leaves. *In* BF Sidney Fleischer, ed, Methods in Enzymology, Vol Volume 174. Academic Press, pp 518-552
Stitt M, Schulze D (1994) Does Rubisco control the rate of photosynthesis and plant growth? An exercise in molecular ecophysiology. Plant, Cell & Environment **17:** 465-487
Sulpice R, Pyl E-T, Ishihara H, Trenkamp S, Steinfath M, Witucka-Wall H, Gibon Y, Usadel B, Poree F, Piques MC, Von Korff M, Steinhauser MC, Keurentjes JJB, Guenther M, Hoehne M, Selbig J, Fernie AR, Altmann T, Stitt M (2009) Starch as a major integrator in the regulation of plant growth. Proceedings of the National Academy of Sciences **106:** 10348-10353
Sulpice R, Trenkamp S, Steinfath M, Usadel B, Gibon Y, Witucka-Wall H, Pyl E-T, Tschoep H, Steinhauser MC, Guenther M, Hoehne M, Rohwer JM, Altmann T, Fernie AR, Stitt M (2010) Network Analysis of Enzyme Activities and Metabolite Levels and Their Relationship to Biomass in a Large Panel of Arabidopsis Accessions. The Plant Cell Online **22:** 2872-2893
Sun J, Gibson KM, Kiirats O, Okita TW, Edwards GE (2002) Interactions of Nitrate and CO2 Enrichment on Growth, Carbohydrates, and Rubisco in Arabidopsis Starch Mutants. Significance of Starch and Hexose. Plant Physiology **130:** 1573-1583
Sun J, Okita TW, Edwards GE (1999) Modification of Carbon Partitioning, Photosynthetic Capacity, and O2 Sensitivity in Arabidopsis Plants with Low ADP-Glucose Pyrophosphorylase Activity. Plant Physiology **119:** 267-276
Syvertsen JP, Lloyd J, McConchie C, Kriedemann PE, Farquhar GD (1995) On the relationship between leaf anatomy and CO2 diffusion through the mesophyll of hypostomatous leaves. Plant, Cell & Environment **18:** 149-157

Szakonyi D, Byrne ME (2011) Ribosomal protein L27a is required for growth and patterning in Arabidopsis thaliana. The Plant Journal **65:** 269-281
Takizawa K, Kanazawa A, Kramer DM (2008) Depletion of stromal Pi induces high 'energy-dependent' antenna exciton quenching (qE) by decreasing proton conductivity at CFO-CF1 ATP synthase. Plant, Cell & Environment **31:** 235-243
Talbott LD, Shmayevich IJ, Chung Y, Hammad JW, Zeiger E (2003) Blue Light and Phytochrome-Mediated Stomatal Opening in the npq1 and phot1 phot2 Mutants of Arabidopsis. Plant Physiology **133:** 1522-1529
Talbott LD, Zeiger E (1993) Sugar and Organic-Acid Accumulation in Guard-Cells of Vicia-Faba in Response to Red and Blue-Light. Plant Physiology **102:** 1163-1169
Talbott LD, Zeiger E (1993) Sugar and Organic Acid Accumulation in Guard Cells of Vicia faba in Response to Red and Blue Light. Plant Physiology **102:** 1163-1169
Talbott LD, Zeiger E (1996) Central Roles for Potassium and Sucrose in Guard-Cell Osmoregulation. Plant Physiology **111:** 1051-1057
Talbott LD, Zeiger E (1998) The role of sucrose in guard cell osmoregulation. Journal of Experimental Botany **49:** 329-337
Tan W, Bögre L, López-Juez E (2008) Light fluence rate and chloroplasts are sources of signals controlling mesophyll cell morphogenesis and division. Cell Biology International **32:** 563-565
Tardieu F, Granier C, Muller B (1999) Modelling leaf expansion in a fluctuating environment: are changes in specific leaf area a consequence of changes in expansion rate? New Phytologist **143:** 33-43
Tcherkez G, Mauve C, Lamothe M, Le Bras C, Grapin A (2011) The 13C/12C isotopic signal of day-respired CO2 in variegated leaves of Pelargonium × hortorum. Plant, Cell & Environment **34:** 270-283
Terashima I, Araya T, Miyazawa S-I, Sone K, Yano S (2005) Construction and Maintenance of the Optimal Photosynthetic Systems of the Leaf, Herbaceous Plant and Tree: an Eco-developmental Treatise. Annals of Botany **95:** 507-519
Terashima I, Hanba YT, Tazoe Y, Vyas P, Yano S (2006) Irradiance and phenotype: comparative eco-development of sun and shade leaves in relation to photosynthetic CO2 diffusion. Journal of Experimental Botany **57:** 343-354
Terashima I, Miyazawa S-I, Hanba YT (2001) Why are Sun Leaves Thicker than Shade Leaves? — Consideration based on Analyses of CO_2 Diffusion in the Leaf. Journal of Plant Research **114:** 93-105
Tesfaye M, Temple SJ, Allan DL, Vance CP, Samac DA (2001) Overexpression of Malate Dehydrogenase in Transgenic Alfalfa Enhances Organic Acid Synthesis and Confers Tolerance to Aluminum. Plant Physiology **127:** 1836-1844
Thayer SS, Björkman O (1992) Carotenoid distribution and deepoxidation in thylakoid pigment-protein complexes from cotton leaves and bundle-sheath cells of maize. Photosynthesis Research **33:** 213-225
Thiele A, Herold M, Lenk I, Quail PH, Gatz C (1999) Heterologous Expression of Arabidopsis Phytochrome B in Transgenic Potato Influences Photosynthetic Performance and Tuber Development. Plant Physiology **120:** 73-82
Tholen D, Boom C, Noguchi KO, Ueda S, Katase T, Terashima I (2008) The chloroplast avoidance response decreases internal conductance to CO2 diffusion in Arabidopsis thaliana leaves. Plant, Cell & Environment **31:** 1688-1700
Thomas PW, Woodward FI, Quick WP (2004) Systemic irradiance signalling in tobacco. New Phytologist **161:** 193-198
Tisné S, Reymond M, Vile D, Fabre J, Dauzat M, Koornneef M, Granier C (2008) Combined Genetic and Modeling Approaches Reveal That Epidermal Cell Area and Number in Leaves Are Controlled by Leaf and Plant Developmental Processes in Arabidopsis. Plant Physiology **148:** 1117-1127
Tschoep H, Gibon Y, Carillo P, Armengaud P, Szecowka M, Nunes-Nesi A, Fernie AR, Koehl K, Stitt M (2009) Adjustment of growth and central metabolism to a mild but sustained nitrogen-limitation in Arabidopsis. Plant, Cell & Environment **32:** 300-318
Tsukaya H (1997) Determination of the unequal fate of cotyledons of a one-leaf plant, Monophyllaea. Development **124:** 1275-1280

Tsukaya H (2003) Organ shape and size: a lesson from studies of leaf morphogenesis. Current Opinion in Plant Biology **6:** 57-62
Tsukaya H, Beemster G (2006) Genetics, cell cycle and cell expansion in organogenesis in plants. Journal of Plant Research **119:** 1-4
Vahisalu T, Kollist H, Wang Y-F, Nishimura N, Chan W-Y, Valerio G, Lamminmaki A, Brosche M, Moldau H, Desikan R, Schroeder JI, Kangasjarvi J (2008) SLAC1 is required for plant guard cell S-type anion channel function in stomatal signalling. Nature **452:** 487-491
Valerio C, Costa A, Marri L, Issakidis-Bourguet E, Pupillo P, Trost P, Sparla F (2011) Thioredoxin-regulated β-amylase (BAM1) triggers diurnal starch degradation in guard cells, and in mesophyll cells under osmotic stress. Journal of Experimental Botany **62:** 545-555
van Dijken AJH, Schluepmann H, Smeekens SCM (2004) Arabidopsis trehalose-6-phosphate synthase 1 is essential for normal vegetative growth and transition to flowering. Plant Physiology **135:** 969-977
Van Kirk C, Raschke K (1978) Presence of chloride reduces malate production in epidermis during stomatal opening. Plant Physiology **61:** 361-364
Van Kirk CA, Raschke K (1978) Presence of chloride reduces malate production in epidermis during stomatal opening. Journal Name: Plant Physiol.; (United States); Journal Volume: 61:3**:** Medium: X; Size: Pages: 361-364
Vandesteene L, Ramon M, Le Roy K, Van Dijck P, Rolland F (2010) A Single Active Trehalose-6-P Synthase (TPS) and a Family of Putative Regulatory TPS-Like Proteins in Arabidopsis. Molecular Plant **3:** 406-419
Vavasseur A, Raghavendra AS (2005) Guard cell metabolism and CO2 sensing. New Phytologist **165:** 665-682
Venables WN, Ripley BD (2002) Modern Applied Statistics with S, Ed Fourth Edition. Springer, New York
Vert G, Walcher CL, Chory J, Nemhauser JL (2008) Integration of auxin and brassinosteroid pathways by Auxin Response Factor 2. Proceedings of the National Academy of Sciences **105:** 9829-9834
Vile D, Garnier E, Shipley B, Laurent G, Navas ML, Roumet C, Lavorel S, Diaz S, Hodgson JG, Lloret F, Midgley GF, Poorter H, Rutherford MC, Wilson PJ, Wright IJ (2005) Specific leaf area and dry matter content estimate thickness in laminar leaves. Annals of Botany **96:** 1129-1136
Vogel G, Aeschbacher RA, Müller J, Boller T, Wiemken A (1998) Trehalose-6-phosphate phosphatases from Arabidopsis thaliana: identification by functional complementation of the yeast tps2 mutant. The Plant Journal **13:** 673-683
Vogel G, Fiehn O, Jean‐Richard‐dit‐Bressel L, Boller T, Wiemken A, Aeschbacher RA, Wingler A (2001) Trehalose metabolism in Arabidopsis: occurrence of trehalose and molecular cloning and characterization of trehalose‐6‐phosphate synthase homologues. Journal of Experimental Botany **52:** 1817-1826
von Caemmerer S, Lawson T, Oxborough K, Baker NR, Andrews TJ, Raines CA (2004) Stomatal conductance does not correlate with photosynthetic capacity in transgenic tobacco with reduced amounts of Rubisco. Journal of Experimental Botany **55:** 1157-1166
Vu JCV, Allen Jr LH, Bowes G (1989) Leaf ultrastructure, carbohydrates and protein of soybeans grown under CO2 enrichment. Environmental and Experimental Botany **29:** 141-147
Walter A, Silk WK, Schurr U (2009) Environmental Effects on Spatial and Temporal Patterns of Leaf and Root Growth. Annual Review of Plant Biology **60:** 279-304
Walters RG, Shephard F, Rogers JJM, Schwarzenegger A, Rolfe SA, Horton P (2003) Identification of Mutants of Arabidopsis Defective in Acclimation of Photosynthesis to the Light Environment. Plant Physiology **131:** 472-481
Wang J-W, Schwab R, Czech B, Mica E, Weigel D (2008) Dual Effects of miR156-Targeted SPL Genes and CYP78A5/KLUH on Plastochron Length and Organ Size in Arabidopsis thaliana. The Plant Cell Online **20:** 1231-1243
Warner JR (1999) The economics of ribosome biosynthesis in yeast. Trends in Biochemical Sciences **24:** 437-440
Webb A, Hetherington AM (1997) Convergence of the Abscisic Acid, CO2, and Extracellular Calcium Signal Transduction Pathways in Stomatal Guard Cells. Plant Physiology **114:** 1557-1560

Welham T, Pike J, Horst I, Flemetakis E, Katinakis P, Kaneko T, Sato S, Tabata S, Perry J, Parniske M, Wang TL (2009) A cytosolic invertase is required for normal growth and cell development in the model legume, Lotus japonicus. Journal of Experimental Botany **60:** 3353-3365

Werner T, Motyka V, Laucou V, Smets R, Van Onckelen H, Schmülling T (2003) Cytokinin-Deficient Transgenic Arabidopsis Plants Show Multiple Developmental Alterations Indicating Opposite Functions of Cytokinins in the Regulation of Shoot and Root Meristem Activity. The Plant Cell Online **15:** 2532-2550

West GB, Brown JH, Enquist BJ (1999) The Fourth Dimension of Life: Fractal Geometry and Allometric Scaling of Organisms. Science **284:** 1677-1679

Westoby M, Falster DS, Moles AT, Vesk PA, Wright IJ (2002) Plant ecological strategies : some leading dimensions of variation between species. *In*,

Westoby M, Wright IJ (2003) The leaf size - twig size spectrum and its relationship to other important spectra of variation among species. Oecologia **135:** 621-628

Weston E, Thorogood K, Vinti G, Lopez-Juez E (2000) Light quantity controls leaf-cell and chloroplast development in Arabidopsis thaliana wild type and blue-light-perception mutants. Planta **211:** 807-815

White J, Gould S (1965) Interpretation of the coefficient in the allometric equation. The American Naturalist **99:** 5-18

Whitman T, Aarssen LW (2010) The leaf size/number trade-off in herbaceous angiosperms. Journal of Plant Ecology **3:** 49-58

Wiese A, Christ MM, Virnich O, Schurr U, Walter A (2007) Spatio-temporal leaf growth patterns of Arabidopsis thaliana and evidence for sugar control of the diel leaf growth cycle. New Phytologist **174:** 752-761

Wiese A, Elzinga N, Wobbes B, Smeekens S (2004) A Conserved Upstream Open Reading Frame Mediates Sucrose-Induced Repression of Translation. The Plant Cell Online **16:** 1717-1729

Willmer CM, Rutter JC (1977) Guard cell malic acid metabolism during stomatal movements. Nature **269:** 327-328

Wingler A (2002) The function of trehalose biosynthesis in plants. Phytochemistry **60:** 437-440

Woodson JD, Chory J (2008) Coordination of gene expression between organellar and nuclear genomes. Nat Rev Genet **9:** 383-395

Woodward FI (1987) Stomatal numbers are sensitive to increases in CO2 from pre-industrial levels. Nature **327:** 617-618

Wright G, Hubick K, Farquhar G (1988) Discrimination in Carbon Isotopes of Leaves Correlates With Water-Use Efficiency of Field-Grown Peanut Cultivars. Functional Plant Biology **15:** 815-825

Wright IJ, Reich PB, Cornelissen JHC, Falster DS, Garnier E, Hikosaka K, Lamont BB, Lee W, Oleksyn J, Osada N, Poorter H, Villar R, Warton DI, Westoby M (2005) Assessing the generality of global leaf trait relationships. New Phytologist **166:** 485-496

Wright IJ, Reich PB, Flexas J, Garnier E, Groom PK, Gulias J, Hikosaka K, Lamont BB, Lee T, Lee W, Lusk C, Midgley JJ, Westoby M, Ackerly DD, Baruch Z, Bongers F, Cavender-Bares J, Chapin T, Cornelissen JHC, Diemer M (2005) The Worldwide leaf economics spectrum. *In*,

Wright IJ, Westoby M (1999) Differences in seedling growth behaviour among species: trait correlations across species, and trait shifts along nutrient compared to rainfall gradients. Journal of Ecology **87:** 85-97

Wright IJ, Westoby M (2000) Cross-species relationships between seedling relative growth rate, nitrogen productivity and root vs leaf function in 28 Australian woody species. Functional Ecology **14:** 97-107

Wright IJ, Westoby M (2001) Understanding seedling growth relationships through specific leaf area and leaf nitrogen concentration: generalisations across growth forms and growth irradiance. Oecologia **127:** 21-29

Wu G, Park MY, Conway SR, Wang J-W, Weigel D, Poethig RS (2009) The Sequential Action of miR156 and miR172 Regulates Developmental Timing in Arabidopsis. Cell **138:** 750-759

Wu G, Poethig RS (2006) Temporal regulation of shoot development in Arabidopsis thaliana by miR156 and its target SPL3. Development **133:** 3539-3547

Wu X, Dabi T, Weigel D (2005) Requirement of Homeobox Gene STIMPY/WOX9 for Arabidopsis Meristem Growth and Maintenance. Current Biology **15:** 436-440
Yadav U (2009) Sucrose and Trehalose-6-phosphate Signalling in Arabidopsis thaliana. Universitaet Potsdam, Potsdam
Yamamoto HY (1979) Biochemistry of the violaxanthin cycle in higher plants. Pure and Applied Chemistry **51:** 639-648
Yang D, Li G, Sun S (2008) The Generality of Leaf Size versus Number Trade-off in Temperate Woody Species. Annals of Botany **102:** 623-629
Yano S, Terashima I (2001) Separate localization of light signal perception for sun or shade type chloroplast and palisade tissue differentiation in Chenopodium album. Plant and Cell Physiology **42:** 1303-1310
Yano S, Terashima I (2004) Developmental process of sun and shade leaves in Chenopodium album L. Plant, Cell & Environment **27:** 781-793
Yazdanbakhsh N, Fisahn J (2009) High throughput phenotyping of root growth dynamics, lateral root formation, root architecture and root hair development enabled by PlaRoM. Functional Plant Biology **36:** 938-946
Yazdanbakhsh N, Fisahn J (2011) Mutations in leaf starch metabolism modulate the diurnal root growth profiles of Arabidopsis thaliana. Plant Signal. Behav. **6:** 995-998
Yin X, Kropff MJ, Stam P (1999) The role of ecophysiological models in QTL analysis: the example of specific leaf area in barley. Heredity **82:** 415-421
Yoo CY, Pence HE, Hasegawa PM, Mickelbart MV (2009) Regulation of Transpiration to Improve Crop Water Use. Critical Reviews in Plant Sciences **28:** 410-431
Young JJ, Mehta S, Israelsson M, Godoski J, Grill E, Schroeder JI (2006) CO2 signaling in guard cells: Calcium sensitivity response modulation, a Ca2+-independent phase, and CO2 insensitivity of the gca2 mutant. Proceedings of the National Academy of Sciences **103:** 7506-7511
Zeeman SC, Rees TA (1999) Changes in carbohydrate metabolism and assimilate export in starch-excess mutants of Arabidopsis. Plant, Cell & Environment **22:** 1445-1453
Zeeman SC, Smith SM, Smith AM (2007) The diurnal metabolism of leaf starch. Biochem J **401:** 13-28
Zeiger E, Hepler P (1976) Production of guard cell protoplast/s from onion and tobacco. Plant Physiology **58:** 492-498
Zeiger E, Talbott LD, Frechilla S, Srivastava A, Zhu J (2002) The guard cell chloroplast: a perspective for the twenty-first century. New Phytologist **153:** 415-424
Zell MB, Fahnenstich H, Maier A, Saigo M, Voznesenskaya EV, Edwards GE, Andreo C, Schleifenbaum F, Zell C, Drincovich MF, Maurino VG (2010) Analysis of Arabidopsis with Highly Reduced Levels of Malate and Fumarate Sheds Light on the Role of These Organic Acids as Storage Carbon Molecules. Plant Physiology **152:** 1251-1262
Zhang N, Kallis RP, Ewy RG, Portis AR (2002) Light modulation of Rubisco in Arabidopsis requires a capacity for redox regulation of the larger Rubisco activase isoform. Proceedings of the National Academy of Sciences **99:** 3330-3334
Zhang SQ, Outlaw Jr WH, Chollet R (1994) Lessened malate inhibition of guard-cell phosphoenolpyruvate carboxylase velocity during stomatal opening. Febs Letters **352:** 45-48
Zhang YH, Primavesi LF, Jhurreea D, Andralojc PJ, Mitchell RAC, Powers SJ, Schluepmann H, Delatte T, Wingler A, Paul MJ (2009) Inhibition of SNF1-Related Protein Kinase1 Activity and Regulation of Metabolic Pathways by Trehalose-6-Phosphate. Plant Physiology **149:** 1860-1871
Zhao ZX, Zhang W, Stanley BA, Assmann SM (2008) Functional Proteomics of Arabidopsis thaliana Guard Cells Uncovers New Stomatal Signaling Pathways. Plant Cell **20:** 3210-3226
Zimmermann P, Hirsch-Hoffmann M, Hennig L, Gruissem W (2004) GENEVESTIGATOR. Arabidopsis Microarray Database and Analysis Toolbox. Plant Physiology **136:** 2621-2632